

# For Reference

---

**NOT TO BE TAKEN FROM THIS ROOM**

For Reference

NOT TO BE TAKEN FROM THIS ROOM

Ex LIBRIS  
UNIVERSITATIS  
ALBERTAENSIS









thesis  
1963(F)  
#6 D



Digitized by the Internet Archive  
in 2018 with funding from  
University of Alberta Libraries

<https://archive.org/details/Green1963>

THE UNIVERSITY OF ALBERTA

HYDRODYNAMIC AND OPTICAL ROTATORY DISPERSION

STUDIES ON FETUIN

by

WILLIAM A. GREEN

A THESIS

SUBMITTED TO THE FACULTY OF GRADUATE STUDIES

IN PARTIAL FULFILMENT OF THE REQUIREMENTS FOR THE DEGREE  
OF DOCTOR OF PHILOSOPHY

DEPARTMENT OF BIOCHEMISTRY

EDMONTON, ALBERTA

AUGUST, 1963



## ABSTRACT

A general background of glycoprotein structure is presented and some recent work described in greater detail in order that the findings of workers concerned with the calf fetal blood glycoprotein, fetuin, may be better integrated. Although in some instances, the physiological function may be recognized for certain blood glycoproteins, little information of structure in relation to function is at present available. In particular, to what extent the presence of specific carbohydrate moieties may influence the secondary structure and confer the conjugated protein with certain properties is not known. Reference is made to a variety of findings which suggest that terminal sialic acid groups attached to the carbohydrate moiety may have a special significance. This appears to be the case whether or not a protein occurs as a separate entity as in blood plasma, or incorporated as an integral part of the cellular architecture. The major part of the investigation described in this study is concerned with the physical characterization of fetuin aimed at a better understanding of the behaviour of the molecule in solution and of its secondary structure. Since two of the methods described in the literature for its preparation, viz., salt fractionation and the more recent ethanol method of Spiro, influence the behaviour of the protein in solution, material obtained by both methods was investigated. In order to facilitate the presentation of the results and their discussion, a section covering the theoretical background of the hydrodynamic





and optical rotatory techniques used is included in the introduction.

The central theme of the investigation is the observation of fetuin in buffered media in two distinct pH ranges: the pH region 7-8, where the molecule is monomeric, and in the isoelectric region, pH 2-4, where it associates. The results are presented and separately discussed in three sections. The first deals with the behaviour of the molecule in aqueous buffers, and the second, on the influence of certain organic solvents added to the buffered systems. The third section deals with the stability of fetuin with regard to proteolytic attack and the influence on the molecule of its sialic acid content, following complete or partial removal by neuraminidase. The results demonstrate that the properties of the hydrodynamic unit are markedly dependent on both the ionic composition of the aqueous system and its content of organic solvent in the pH range 7-8. The optical rotatory properties further suggest that the secondary structure is likewise dependent on the composition of the system. Although in the isoelectric region the extent of association is not markedly influenced by organic reagents, this property is closely related to the sialic acid content of the molecule. In this case, the secondary structure appears to depend on the stabilizing influence of the terminal sialic acid residues. An attempt is made in the final conclusion section to integrate these findings with the plausibility of a hydrodynamic model in terms of the known composition of the molecule.



## Dedication

To my wife, Margaret, whose trust, encouragement and  
patience has provided a foundation for this volume.



## ACKNOWLEDGMENTS

I would like, first of all, to express my sincere thanks to my thesis supervisor, Dr. C. M. Kay, for his guidance and generous help throughout this work. I also wish to extend my gratitude to Dr. J. S. Colter and members of the Biochemistry Department who have all, at one time or another, helped me with my problems both real and imaginary. In particular, I wish to thank Dr. M. S. Spencer, who encouraged my interest in subcellular structure, and Dr. B. G. Lane for numerous discussions and help during my attempt to learn a little of protein biosynthesis. I would also like to thank Drs. G. R. Freeman, H. B. Dunford, and C. C. Bigelow for help in physical chemistry. I am indebted to Mr. R. Swindlehurst, also from the Department of Chemistry, for the optical rotatory data.

A special thanks to Mr. J. Durgo for his enthusiastic help at all times and for his skillful contribution in preparing the graphs, illustrations and photographs. Thanks also to Mr. T. Keri for several pH stat experiments and general technical help, and to Mr. K. Oikawa for additional technical assistance.

The formidable task of converting the rough draft into a finished manuscript was undertaken by Mrs. L. Randall. Only by her skill and effort am I able to submit a coherent account of my investigations. For this I am most grateful.

Financial assistance in the form of a Fellowship from the Canadian Muscular Dystrophy Association and a Scholarship from the University of Alberta is gratefully acknowledged.





# TABLE OF CONTENTS

	<u>Page</u>
Abstract . . . . .	iii
Acknowledgments . . . . .	vi
List of Illustrations and Tables . . . . .	x
List of Abbreviations . . . . .	xiii
I. INTRODUCTION . . . . .	1
Occurrence and Composition of Carbohydrate Containing Proteins . . . . .	1
Some Aspects of Structure and Behaviour . . . . .	2
Fetal Blood and Passive Immunity. . . . .	5
Fetuin . . . . .	7
II. THEORETICAL BACKGROUND . . . . .	23
Chain Conformation in Polypeptides and Proteins .	23
Gross Structure Based on Hydrodynamic Considera- tions . . . . .	25
Chain Conformation Based on Optical Rotatory Measurements . . . . .	34
The Drude Equation . . . . .	36
The Moffitt Equation . . . . .	37
Partial Helical Content . . . . .	38
III. METHODS . . . . .	43
Isolation of Protein . . . . .	43
Commercial Preparations . . . . .	44
Enzymatic Modifications . . . . .	45
Thiobarbituric Acid Assay of Sialic Acid . . . . .	46
Buffer Systems . . . . .	48
Determination of Concentration . . . . .	49



### III. METHODS (continued)

Partial Specific Volume . . . . .	50
Sedimentation Velocity . . . . .	51
Sedimentation Approach to Equilibrium . . . . .	53
Kinematic Viscosity . . . . .	56
Diffusion . . . . .	57
Optical Rotatory Dispersion . . . . .	59

### IV. RESULTS

Part 1. Molecular Properties of Fetuin at pH 7-8, pH 2-4 and Some Correlation Checks between Different Preparations . . . . .	67
Molecular Properties of Monomeric Fetuin .	68
Molecular Properties of Associated Fetuin.	72
Discussion . . . . .	74
Part 2. The Influence of Some Organic Solvents on Salt Precipitated Fetuin at pH 7-8 and pH 2.4 . . . . .	106
Discussion . . . . .	109
Part 3. A. Stability of Fetuin . . . . .	123
Discussion . . . . .	124
B. Sialic Acid Content of Fetuin and Its Removal by Neuraminidase . . . . .	128
Discussion . . . . .	130

V. CONCLUSIONS . . . . .	143
Peptide Chain Length . . . . .	145
Carbohydrate Moiety . . . . .	146
Secondary Structure . . . . .	147



V.	CONCLUSIONS (Continued)	
	Stability and Associative Properties . . . . .	150
	Suggestions for Further Investigation . . . . .	151
VI.	BIBLIOGRAPHY . . . . .	153
VII.	APPENDICES . . . . .	160





# LIST OF ILLUSTRATIONS AND TABLES

## Chapters I - III

	<u>Page</u>
Figure A. Structures of Common Sugars in Carbohydrate Containing Proteins . . . . .	15
B(a) (b) (c). Recognized Carbohydrate Peptide Linkages . . . . .	16
B(d). Disaccharide from Bovine Submaxillary Gland . . . . .	17
C. Suggested Terminal Sequence of Carbohydrate Residues of Fetuin . . . . .	18
D. Plots Utilized in Optical Rotatory Dispersion.	41
E. Disposition of Moffitt Plot for Standard Polypeptide Chain Conformations. . . . .	42
F. Salt Fractionation of Calf Fetal Blood . . . .	60
G. Ethanol Fractionation of Calf Fetal Blood. . .	61
H. Warren Method for Sialic Acid Determination. .	62
I. Kraemer Plot for the Determination of Partial Specific Volume . . . . .	63
J. Concentration Gradient Curves Observed During Sedimentation. . . . .	64
K. Concentration Gradient Curve and Plot Utilized in Diffusion . . . . .	65
Table I. Chemistry and Properties of Well-Characterized Serum Glycoproteins. . . . .	19
II. Carbohydrate Content and Physical Parameters of Fetuin . . . . .	20
III. Amino Acid Analysis of Fetuin (Spiro) . . . .	21
IV. Amino Acid Analysis of Fetuin (Fisher) . . . .	22
V. Buffer Systems . . . . .	66

## Chapters IV - VI

Figures 1 - 5. Sedimentation and Viscosity Characteristics of Commercial Monomeric Fetuin in Tris, Phosphate, Borate and Acetate Buffers . . . . .	78
6 - 7. Optical Rotatory Dispersion Characteristics of Commercial Monomeric Fetuin in Borate Buffers	83



Figures 8 - 9. Sedimentation and Viscosity Characteristics of Monomeric Ethanol Prepared Fetuin in Phosphate and Borate Buffers . . . . .	85
10 - 11. Optical Rotatory Dispersion Characteristics of Commercial and Ethanol Prepared Monomeric Fetuin in Phosphate and Borate Buffers . . . . .	87
12 - 14. Diffusion Characteristics of Commercial and Ethanol Prepared Monomeric Fetuin in Phosphate and Borate Buffers . . . . .	89
15. Kraemer Plots for Partial Specific Volumes of Commercial and Ethanol Prepared Monomeric Fetuin in Phosphate and Borate Buffers . . . . .	92
16 - 17. Sedimentation and Viscosity Characteristics as a Function of pH for Associated Commercial and Ethanol Prepared Fetuin in Glycine/HCl Buffer. . . . .	93
18 - 19. Sedimentation and Viscosity Correlation for Different Preparations of Monomeric Fetuin . . . . .	95
20. Correlation of Optical Rotatory Dispersion Characteristics for Different Preparations of Monomeric Fetuin . . . . .	97
21. Moffitt Plot for Evaluation of $\lambda_0$ . . . . .	98
22 - 29. Sedimentation, Viscosity and Optical Rotatory Dispersion Characteristics for Commercial Fetuin in Formamide, Dioxane and Ethylene Glycol Phosphate Buffered Systems . . . . .	113
30. Tryptic Attack of Commercial and Ethanol Prepared Fetuin . . . . .	133
31 - 32. Influence of Ionic Strength on Optical Rotatory Dispersion Characteristics of Commercial Fetuin . . . . .	134
33. Release of Sialic Acid from Fetuin During Neuraminidase Treatment . . . . .	136
34 - 35. Optical Rotatory Dispersion Characteristics of Sialic Acid Free Fetuin in Phosphate and Acetate Buffers . . . . .	137



	<u>Page</u>
Table 1. Molecular Properties of Commercial Fetuin . . .	99
2. Molecular Properties of Ethanol Fractionated Fetuin . . . . .	100
3. Optical Rotatory Dispersion Data on Commercial Fetuin in the Presence of Organic Solvents. . .	121
4. Sedimentation Values Obtained at pH 2.4 in the Presence of Organic Solvents . . . . .	122
5. Molecular Weight Studies of Fetuin . . . . .	139
6. Sialic Acid Content of Fetuin . . . . .	140
7. Neuraminidase Treated Commercial Fetuin: Molecular Characteristics . . . . .	141
Plate A. Electrophoresis of Commercial and Ethanol Prepared Monomeric Fetuin . . . . .	101
B. Diffusion of Commercial and Ethanol Prepared Monomeric Fetuin. . . . .	102
C. Sedimentation Velocity of Commercial and Ethanol Prepared Monomeric Fetuin . . . . .	103
D. Sedimentation Approach to Equilibrium for Commercial Monomeric Fetuin . . . . .	104
E. Sedimentation Approach to Equilibrium for Associated Ethanol Prepared Fetuin . . . . .	105
F. Sedimentation Approach to Equilibrium for Neuraminidase Treated Fetuin . . . . .	142





# LIST OF ABBREVIATIONS

		<u>Units</u>
$S_{20,w}$	Sedimentation coefficient in water at 20°C.	Svedbergs
$S_{20,w}^0$	" " " " (at infinite dilution)	"
$D_{20,w}$	Diffusion coefficient in water at 20°C.	$\text{cm}^2 \text{sec}^{-1}$
$D_{20,w}^0$	" " " " (at infinite dilution)	"
$\eta_{\text{red}}$	Reduced viscosity	ml./gm.
$[\eta]$	Intrinsic viscosity	"
$\checkmark$	Viscosity increment	-
$p$	Axial ratio of ellipsoidal particle	-
$V_e$	Effective volume of ellipsoidal particle	cu. Å
$f/f_0$	Frictional ratio	-
$\beta$	Scheraga Mandelkern function	-
$E_{1\text{cm}}^{1\%}$	Extinction coefficient of protein	-
$M$	Molecular weight of anhydrous particle	-
$c_0$	Total concentration of macromolecule (Archibald)	$\text{cm}^2$
$\frac{dc}{dx}$	Concentration gradient (Archibald)	cm.
$\bar{v}$	Partial specific volume of anhydrous particle	ml./gm.
$[\alpha]_\lambda$	Specific rotation at wavelength $\lambda$	degrees
$\lambda_c$	Critical wavelength Yang/Doty plot	mμ
$[m^1]_\lambda$	Reduced residue rotation at wavelength $\lambda$	degrees
$\lambda_0$	Dispersion parameter Moffitt plot	mμ
$a_0$	Ordinate intercept Moffitt plot	degrees
$b_0$	Slope Moffitt plot	degrees



## I. INTRODUCTION

Fetuin is a glycoprotein isolated from calf fetal serum. As such, it is to be expected that it will exhibit similarities in structure and behaviour to other glycoproteins, and that the methods which have given useful information about such molecules will be applicable to fetuin. Investigations of a glycoprotein include the application of methods peculiar to the carbohydrate moiety in addition to the usual macromolecular techniques of physical characterization such as hydrodynamic and optical rotatory measurements. Before giving an account of investigations carried out by various workers on fetuin, some considerations relevant to our purpose will be drawn from the general area of carbohydrate-containing proteins. Since the physical investigations recorded later in this report, on solutions of the protein, are aimed at providing a better understanding of the conformational and associative properties of fetuin, some consideration will be given to primary structure, for the better this is understood the better we may be able to interpret behaviour in solution under a variety of conditions. Blood serum from mammals is a rich source of many glycoproteins and, as in the case of fetuin, provides a convenient system from which these molecules may be isolated. For this reason, much of our information is derived from this area.

### Occurrence and composition

Proteins to which a carbohydrate moiety is attached have a wide distribution. They have been identified in bacterial cell walls (1), the erythrocyte membrane (2), and appear to be distributed



throughout the subcellular fractions of tissues including the microsomes and mitochondria (3). They are found in salivary secretion (4,5) and in great variety in mammalian blood (6). Included in the latter are such transport proteins as transferrin and ceruloplasmin (7), the gonadotropic hormones (8), and the  $\gamma$ -globulins (9). Some enzymes too contain appreciable quantities of carbohydrate (10,11). The amount and composition of the carbohydrate attached to the polypeptide chain show considerable diversity. This is illustrated in Table I in which the carbohydrate content and some physical parameters of a number of plasma proteins are given (12). Figure A presents the structures of the common sugars and sugar derivatives found in the oligosaccharide chains which form the prosthetic group of this type of conjugated protein.

#### Some aspects of structure and behaviour

A considerable portion of the more recent investigations on glycoproteins and mucoproteins deals with the structure of the carbohydrate moiety and its mode of attachment to the peptide chain. One approach is to reduce the molecule to several glycopeptides by proteolytic attack, and by continued degradation of the peptide chain (if necessary) to try and determine the amino acid involved in the attachment to the sugar. Ovalbumin was investigated in this manner and the linkage was found to be through aspartic acid (13,14,15). The present view is that the reducing end group of the oligosaccharide is attached by a glycosylamine bond to the amide of aspartic acid (16,17,18,19) (see Figure B(a)). From human  $\gamma$ -globulin three glycopeptides were obtained which on further treatment with carboxypeptidase and leucine amino peptidase gave a product in which only aspartic acid was attached to carbohydrate (20,21). Similar





findings were recorded for rabbit and bovine  $\gamma$ -globulin (22,23).

A series of investigations on bovine and ovine submaxillary gland mucoprotein demonstrated that in each case, following treatment of the protein with mild alkali, a compound, 6 $\alpha$ -D N acetyl neuraminy-N-acetyl galactosamine, was liberated. (See Figure B(d)). Ion exchange resins were used to effect the separation. Further, it was demonstrated in each case using the method of reductive cleavage ( $\text{LiBH}_4$  in tetra hydro furan) that about 80% of the prosthetic groups are involved in glycosidic-ester linkage to the free-carboxyl groups of  $\beta$ -aspartyl and  $\gamma$ -glutamyl residues. After 4 hr. heating in 0.01 N NaOH, 18% of the total N-acetyl neuraminic acid remained bound to the glycoprotein which suggested that this part of the carbohydrate was attached by an alkali stable O-glycosidic linkage (24,25) involving serine and/or threonine (see Figure B(b) (c)).

It is also of interest that treatment of the ovine preparation with neuraminidase resulted in a viscosity drop, which may also be observed on lowering the pH from 7.8 to 1.7. Seventy-five per cent of this drop occurs in the pH region from 4.4 - 1.6 corresponding to the range in which the sialic acid carboxyl groups lose their charge ( $\text{pK}_a = 2.6$ ). It would appear that the removal of these groups, on their deionization, results in a more compact conformation (26). This implies a molecule of considerable flexibility with little internal constraint. Increasing interest in the possible role of the sialic acid residues in glycoproteins is reflected in the literature. Investigation of the thyroxine binding properties of bovine  $M_2$  glycoprotein showed that only 33% of its sialic acid content is removed by neuraminidase and that this





removable part is not involved in the hormone binding property (27). Other examples include studies on fibrinogen which demonstrate that the release of sialic acid by neuraminidase produces a molecule with an increased ability to clot (28). A similar observation is illustrated with prothrombin, the enzymatic inactivity of which--prior to its conversion to thrombin--is greatly influenced by the presence of its sialic acid content. Neuraminidase liberates two-thirds of the sialic acid residues and its rate of conversion to thrombin is greatly increased (29).

The decrease in electric charge of the erythrocyte on neuraminidase treatment is due to release of N acyl or N, O-acyl neuraminic acid (30). Restoration of the normal respiratory response of cerebral tissue kept in the cold, by certain fractions of blood plasma proteins has been correlated with their content of neuraminic acid derivatives (31). Finally, it has been shown that there appears to be no significant difference in hexosamine or sialic acid content between certain tumor cells (including HeLa and C3H ascitic hepatomas of different types) and non-malignant cells from liver tissue (32). If, as suggested by Sjostrand (33), glycoprotein may be a constituent of the membranous material of the mitochondria, it is likely that sialic acid containing glycoproteins may be of considerable importance as universal constituents of cellular architecture. If, in fact, the observations cited above with regard to tumor tissue are true, it would strengthen the concept that the rise in sialic acid containing plasma glycoproteins observed in neoplasia is not specifically related to the malignant process. This is not unexpected since it is well-recognized that similar alterations in plasma proteins occur in other diseased states (34,35).



Another aspect of glycoproteins is the resistance that some exhibit to proteolytic attack. Specific inhibitors of trypsin and chymotrypsin have been isolated from both human serum (36) and bovine serum (37,38). They are both glycoproteins and form complexes with either enzyme. The protein from bovine serum has a carbohydrate composition which resembles ovomucoid. Of particular interest is the  $\alpha_1$ -acid glycoprotein (orosomucoid) with its isoelectric point of 2.7 due largely to the sixteen moles of sialic acid which it contains. The molecule is very resistant to proteolytic digestion (39,40,41) and for this reason some workers have introduced HCl gas into solution to bring about cleavage (39). If, however, the molecule is treated with neuraminidase or mild acid, all of the sixteen terminal sialic acid groups are removed and the remainder of the molecule is readily attacked by trypsin. The nature of the bond split is believed to be glycosidic between the sialic acid reducing carbon and the hydroxyl group of an adjacent sugar (42). Additional characterization data for the  $\alpha_1$ -acid glycoprotein has been reported (43,44,45,46). Glycoprotein from equine plasma (47), the  $M_2$  glycoprotein from normal bovine plasma (48) and a zinc (precipitable)  $\alpha_2$ -glycoprotein from human plasma (49) have also been characterized.

#### Fetal blood and passive immunity

Little information is at present available as to the changes in composition of the serum proteins during the development of the fetus and in the young mammal immediately following birth. One well-recognized species difference is the time at which passive immunity is transferred from the mother to her young, as shown by a relatively large  $\gamma$ -globulin content in the serum of the offspring.





In the case of man (and the rabbit and guinea pig) such transfer is prenatal whereas for the ox, goat, sheep, pig and horse, it is postnatal. Others seem to combine both processes in which part transfer occurs prior to birth and part afterwards. The dog, mouse and rat come in this category. Postnatal transfer occurs in suckling animals by absorption of proteins from colostrum and milk, when the gut has a transient high permeability for native protein. This phase is short and varies from 36 hours to about 20 days depending on the specie in question (50). In the case of the ox, in which transfer is believed to be entirely postnatal, the gut loses the capacity for protein absorption at the end of the 36-hour period. The blood picture of the calf at birth is characterized by little or no  $\gamma$ -globulin, small amounts of  $\beta$ -globulin but large amounts of  $\alpha$ -globulin and albumin. During the suckling period, up to 36 hours after birth there is a rapid increase in  $\gamma$ -globulin with a concomitant fall in  $\alpha$ -globulin and albumin levels (51,52,53). This is accompanied by a transient proteinuria in which presumably the excess amounts of albumin and  $\alpha$ -globulin are excreted, little change in the  $\beta$ -globulin level being observed. Since the amount of  $\alpha$ -globulin in the calf fetus may be as high as 40% of the total serum proteins, it provides a rich source for isolation. Its accumulation in the fetus is probably a reflection of the complexity of the placenta in this mammal, since exchange with the maternal system does not appear to occur. The possible role of this fraction in the development of the fetus is open to speculation and gives additional interest. It is from this fraction that the glycoprotein fetuin is isolated. For a review, see Kekwick (54).





## Fetuin

The normal globulin present in calf blood of sedimentation coefficient 7S was observed by Pedersen to be difficult to detect until after the calf was about three weeks old. Up to this time also the sedimentation coefficient of the albumin was abnormally low (55,56,57). By means of ammonium sulfate precipitation a protein fraction containing two components was obtained. One, which amounted to 90% of the fraction had a sedimentation coefficient  $S_{20w}$  of about 3S and the remainder an  $S_{20w}$  of about 20S. Accurate measurements of sedimentation as a function of concentration gave extrapolated values of  $S_{20,w}^{\circ}$  of 3.28 and 3.16S for the slower component, isolated from blood of the newborn calf and fetal calf, respectively. Pedersen gave the name fetuin to this material. By combining this data with measurements of diffusion, a molecular weight of 50,600 was obtained for calf fetuin, and 48,700 for calf fetal fetuin.

A different preparative procedure was followed by Deutsch (58). If an equal volume of 10% sodium trichloroacetate is added to calf fetal serum and the pH adjusted to 3.5 with 10% trichloroacetic acid, most of the serum proteins are precipitated, leaving the fetuin in solution. About half of the protein in the  $\alpha$ -globulin region is fetuin. Ammonium sulfate precipitation followed by ethanol fractionation gave a single component at pH 7 during electrophoresis and ultracentrifugation. Heterogeneity at pH 3.0 was observed. Centrifugation gave rise to several peaks and two peaks were obtained during electrophoresis at this pH. The latter technique indicated that about two-thirds of the preparation was iso-electric at pH 3.4 while the remainder was iso-electric at pH 4.4. From



sedimentation diffusion at pH 7.0 Deutsch estimated a molecular weight close to 45,000. He also recognized the presence of approximately 18% carbohydrate.

The carbohydrate content of a preparation made according to the same isolation procedure, by Klenk and Stoffel in 1955 (59) gave a content of 5.3% hexose, 9.9% hexosamine, and 6.0% neuraminic acid. Also isolated from the preparation was methoxyneuraminic acid identical with that obtained from bovine submaxillary mucin. When Deutsch applied the same procedure to adult ox serum, he was unable to recover any mucoprotein. The immunological heterogeneity of fetuin was also demonstrated by Myers and Deutsch in 1955 (60) using purified  $\gamma$ -globulin from rabbit-immune serum. Using the agar gel diffusion technique of Oudin (61), fetuin gave six precipitin bands. As little as 3% of the antigen in the antigen-antibody mixture was carried down at the point of maximum precipitation, and it was observed that the glucosamine content of the precipitated fraction was appreciably higher than that of the entire preparation.

The biological function of fetuin in calf fetal serum is not known, but it exhibits activity as a growth supplement for S3 HeLa cells (63). This is not unique to fetuin since a variety of sera from different mammalian sources show a similar activity and which is associated with a macromolecular fraction of the added serum (62). Fisher et al. in 1958 (63) showed that the growth of S3 HeLa cells occurs only in media from which cell attachment and stretching to a clean glass surface occurs when the latter is placed in contact with a non-agitated suspension of cells. Further, a different degree of stretching of glass-attached cells was observed depending on the origin of the serum, and at least two protein constituents were





actively involved in the in vitro cell growth. One was serum albumin, acting perhaps as a carrier of essential small molecules and an  $\alpha$ -globulin which is involved in the attachment of the cells to the glass surface. Both fetuin and material isolated from normal human, bovine, or equine sera exhibit a strong antitryptic action. The method of fractionation of blood serum employed for both normal and fetal sera (Fisher et al.) was essentially that of Pedersen used originally for the isolation of fetuin. Essentially the method uses ammonium sulfate precipitation, the final  $\alpha_1$  globulin fraction--with which the stretching and growth promoting activity is associated--being obtained from the product at 45% saturation of the salt. The results of Fisher et al. showed further that the "stretching" factor from fetal serum is much higher than that obtained from normal sera. The attachment activity of fetuin requires divalent cations and  $10^{-3}$ M versene inhibits attachment. Mg at a concentration of  $3 \times 10^{-4}$ M is maximally active and Ca is less active. Since mammalian cells grown in vitro are strongly proteolytic (64) and fetuin prepared by salt fractionation acts as a trypsin inhibitor (58), these workers suspected that this latter property of fetuin might be related to the stretching and attachment activity described above. Trypsin will liberate glass-attached cells and both fetuin and the less pure  $\alpha_1$  globulin from adult normal horse serum are effective in blocking this tryptic effect.

In summary the product from salt fractionated fetal serum exhibits stretching and growth promoting activities for HeLa cells and this function appears to depend on the presence of an anti-tryptic activity of the macromolecules and the presence of certain cations such as  $Mg^{++}$  or  $Ca^{++}$ . It is unfortunate that the material consisting



of  $\alpha_1$ -globulin was not homogeneous but contained the 18S component (ca. 5%) which is precipitated with the fetuin proper under the conditions of salt fractionation. In an attempt to isolate a homogeneous fraction exhibiting the biological activity, Lieberman et al. in 1959 (65) applied the material obtained by ammonium sulfate fractionation to a DEAE cellulose column. That the activity resides in the precipitated fraction was confirmed, but following the chromatographic procedure less than half the total activity was recovered. However, of this, by far the greatest amount appeared in the 4th eluate which contained about 11% of the total protein applied to the column. Two components were observed on centrifugation, one with an  $S_{20,w}$  of about 3 and the other which moved more rapidly. Other eluates showing little activity also gave a component with a sedimentation coefficient corresponding to fetuin. This work emphasizes the heterogeneity of this protein fraction demonstrated by Myers and Deutsch (60), but does not prove conclusively that the growth promoting activity is not associated with a component of  $S_{20,w}^0$  of about 3 corresponding to fetuin.

In an attempt to prepare a fetuin from calf fetal serum sufficiently homogeneous for reliable analysis and characterization, a method involving the use of ethanol fractionation at low temperature in the presence of zinc and barium acetate, was devised by R. G. Spiro in 1960 (66). The product obtained, while lacking the ability to promote attachment and stretching of HeLa cells, was undoubtedly of high purity, being homogeneous by both ultracentrifugation and electrophoresis from pH 1.1 - 11.2. It also appeared to consist of one component on the basis of immunochemical studies. The chemical composition and physicochemical properties of this preparation as





reported by this worker, are given in Table II. It is noteworthy that no heterogeneity or association of the molecule was observed in the region of its isoelectric point and that unlike the material obtained by the salting out procedure, no 18S component was present separately in the material isolated with ethanol. The molecular weight of 48,400 is in good agreement with Pedersen (57) but higher than other workers (58,67).

The second publication of Spiro (68) dealt with the nature of the carbohydrate units. Ethanol prepared fetuin was found to be susceptible to extensive degradation by numerous proteolytic enzymes including trypsin, pepsin, papain, and subtilisin. This is of considerable interest since, as pointed out by Spiro, the  $\alpha_1$ -acid glycoprotein, with similarities to fetuin including a large number of terminal sialic acid groups, is not so attacked, unless the sialic acid groups have been removed (39,40,41). Furthermore, fetuin prepared by salt fractionation exhibits antitryptic properties (58,63). In view of this, however, a convenient means was available for degradation and following proteolysis, glycopeptides were obtained which were nondialyzable and which contained up to 80% carbohydrate. Their composition reflected the same sugar ratios exhibited by the native protein and in conjunction with molecular weight measurements, allowing for the attached peptide content, it was concluded that fetuin contains three similar carbohydrate moieties, each attached at different points to the peptide chain. Again, as discussed by Spiro, the presence of these large heteropolysaccharide units in fetuin is quite different from the case of submaxillary gland mucoprotein in which a large number of disaccharide units are believed to be attached to the peptide chain (24,25).



Ovalbumin resembles fetuin in having a single complex polysaccharide unit of about 1200 molecular weight (fetuin has three complex units) but which consists only of a combination of mannose and glucosamine (69). Studies of human  $\gamma$ -globulin indicate that it too contains a single heteropolysaccharide unit of about 3500 molecular weight (21). It is to be noted that the amino acid composition of the glycopeptides obtained from fetuin containing on the average about seven residues was similar. Those appearing in significant amounts most frequently were aspartic acid, alanine, serine and proline.

A continued investigation of carbohydrate units in fetuin was carried out by Spiro (70). By following the order of release of the monosaccharides by graded acid hydrolysis and by selective cleavage of sugar residues using glycosidase and neuraminidase, a better understanding of the sequential arrangement was obtained. From partial hydrolysates of the protein, two disaccharides were identified: 4-O- $\beta$ -D-galactopyranosyl-D-glucosamine and its N-acetyl derivative. It was shown that the sialic acid residues are terminal and that galactose is the adjacent internal sugar. A number of the hexosamine residues are attached to galactose, while the remainder of the hexosamine and the mannose residues appear to occupy internal positions in the sugar sequence. Spiro suggests that in accordance with the results obtained, the carbohydrate moieties might consist of a branched structure in which the terminal sialic acid is linked by a ketosidic bond to galactose, which is linked to the 4 position of N-acetylhexosamine by a  $\beta$ -glycosidic bond (see Figure C). These residues would be attached to the internal portion of the carbohydrate chain consisting of the mannose and the additional hexosamine residues.





The amino acid composition of the protein has been reported by Spiro (71) and by H. W. Fisher et al. (72) (see Tables III and IV, respectively). On the basis of  $\mu$ moles of amino acid per mg. of protein, the agreement is generally good. In particular, the aromatic amino acids are almost identical so that differences in extinction coefficient are not to be expected. Some deviation in threonine and arginine is, however, observed. Another discrepancy between these workers lies in the values of sialic acid reported. On the basis of a molecular weight of 45,000 the number of moles of N-acetyl neuraminic acid reported by Fisher et al. per mole of protein is close to nine. The Spiro figure is close to twelve. The hexose and hexosamine content are in good agreement for this molecular weight and give values of twenty and fourteen residues per mole, respectively.

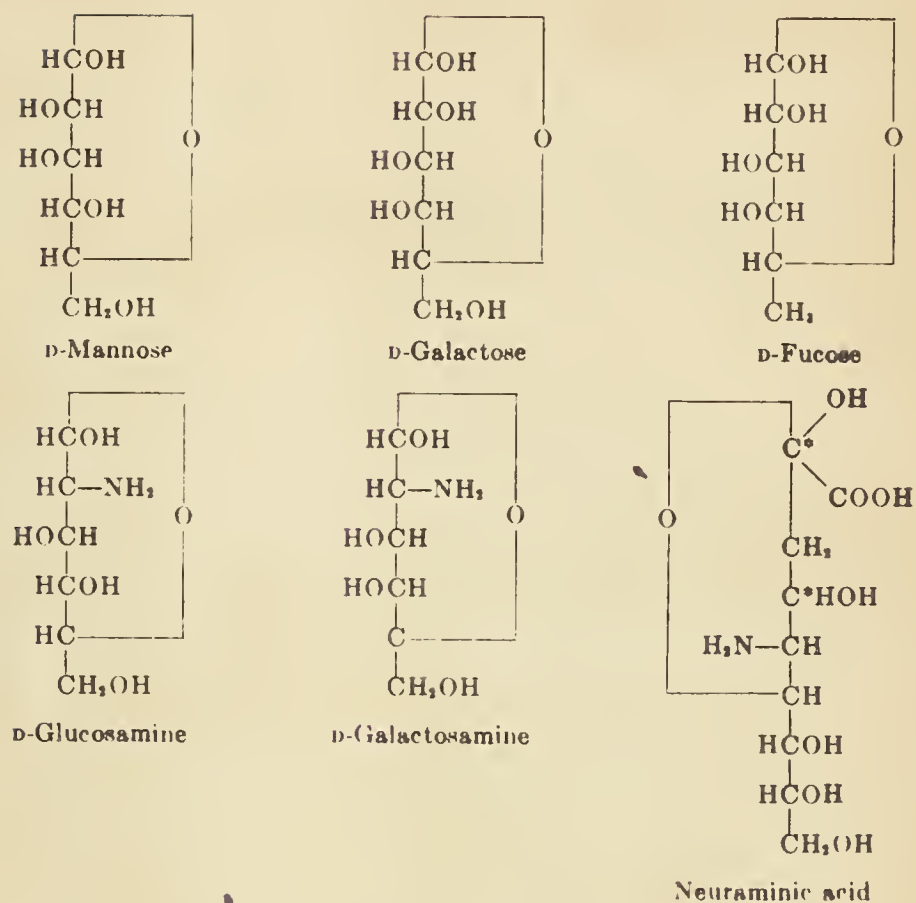
Further studies on fetuin have been reported by Spiro (73) in which, on the basis of hydrodynamic measurements on oxidized and reduced alkylated fetuin, it is suggested that fetuin contains only a single peptide chain. A drop in  $S_{20,w}$  and concomitant increase in  $\eta_{red}$  on performic oxidized material is indicative of a shape change resulting from rupture of the disulfide bridges. Using the dinitrofluorobenzene and the Edman phenylisothiocyanate methods, a single amino terminal residue was identified as isoleucine. By means of hydrazinolysis and carboxypeptidase digestion, isoleucine was again identified as the single-COOH terminal amino acid. As pointed out by Spiro in his discussion, the identification of an  $NH_2$  terminal amino acid in fetuin is contrary to reports on other glycoproteins in which free terminal  $NH_2$  residues have not been detected. This includes ovalbumin, the  $\alpha_1$ -acid glycoprotein and the zinc  $\alpha_2$ -glycoprotein from human serum (74,75,76); alternatively the barium





$\alpha_2$ -glycoproteins do, like fetuin, have free  $\text{NH}_2$  terminal residues (77). Another group of workers, A. G. M. Marr et al. (78) using the isolation method described by Fisher, Puck and Sato (63) obtained from calf fetal serum a preparation containing fetuin and a macroglobulin; further, these workers claimed that both proteins showed tissue culture growth activity. An examination of the chemical composition of the macroglobulin suggested strongly that the latter is neither an aggregate of fetuin nor formed from it by any simple chemical process. This latter point is disputed by K. J. Turner (79) who also reports some physical data on both fetuin and the macroglobulin. The findings are in keeping with the results of earlier publications (57,58).





From Putnam, "The Plasma Proteins", p. 312.

Figure A  
Structures of Common Sugars in Carbohydrate  
Containing Proteins



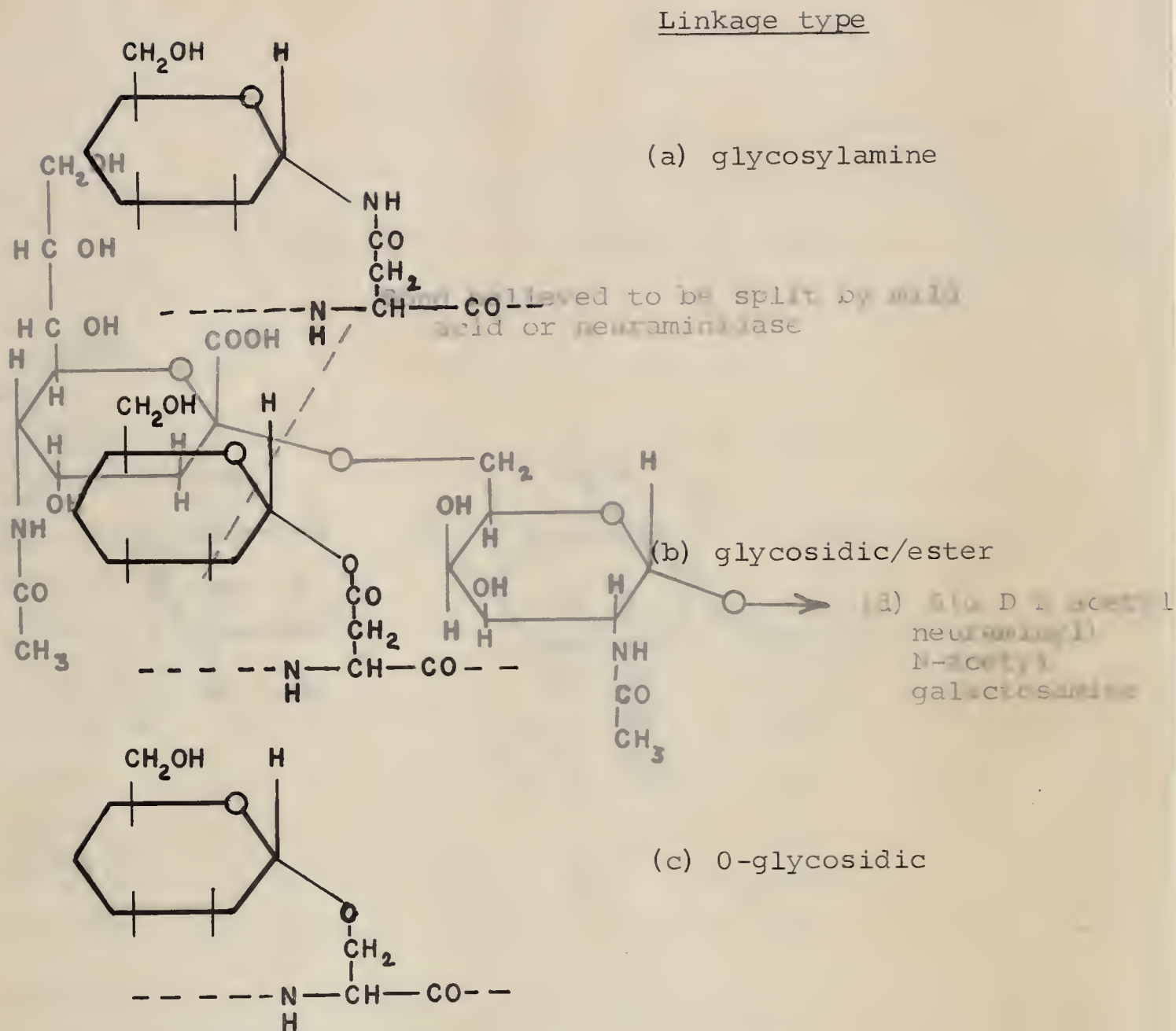


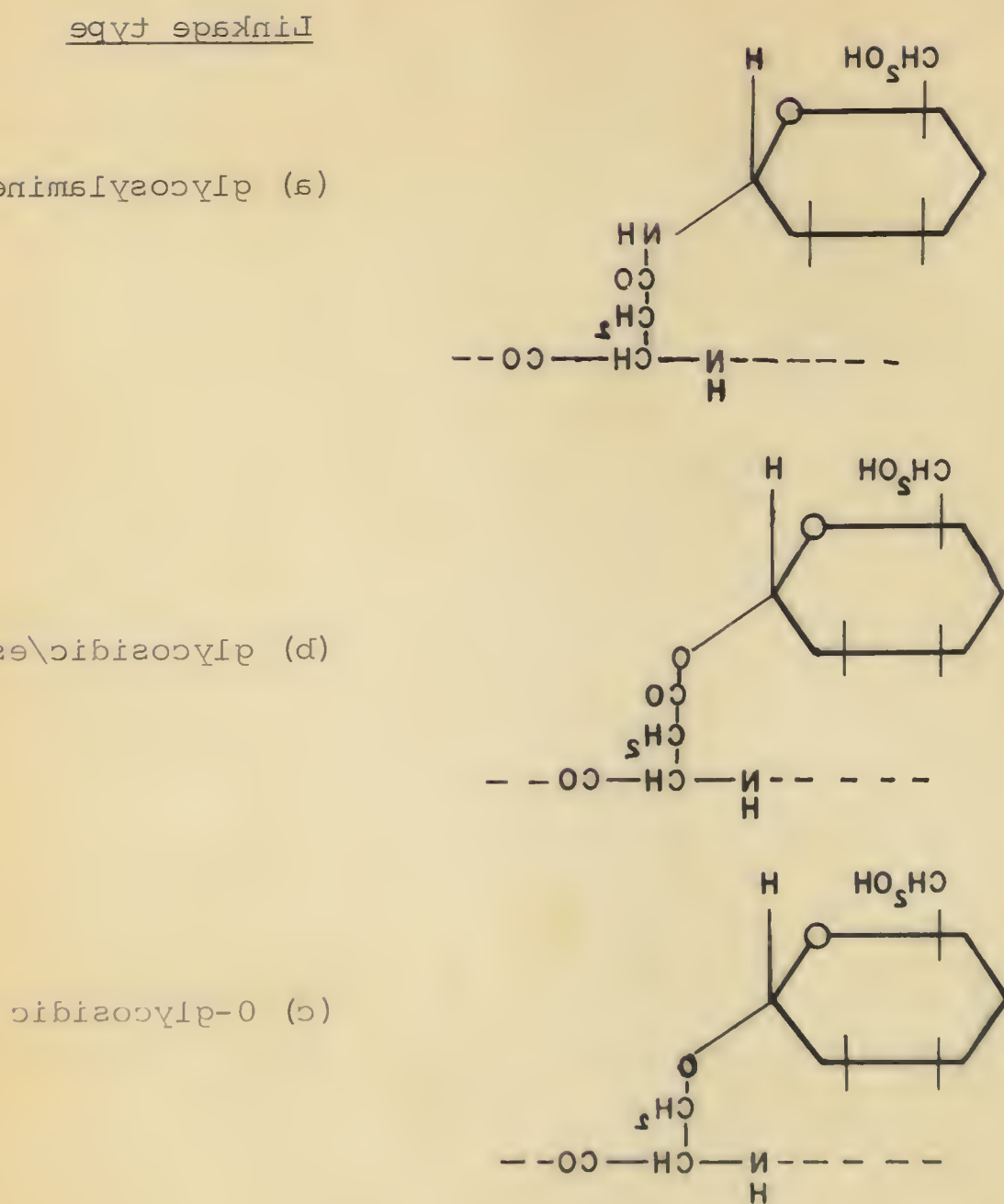
Figure B (a) (b) (c)

Linkages recognized in glycoproteins connecting the carbohydrate moieties with the peptide chain.

Disaccharide from bovine submaxillary gland

Linkages recognized in glycoproteins connecting the  
carbohydrate molecule with the peptide chain.

Figure B (a) (b) (c)



Linkage type



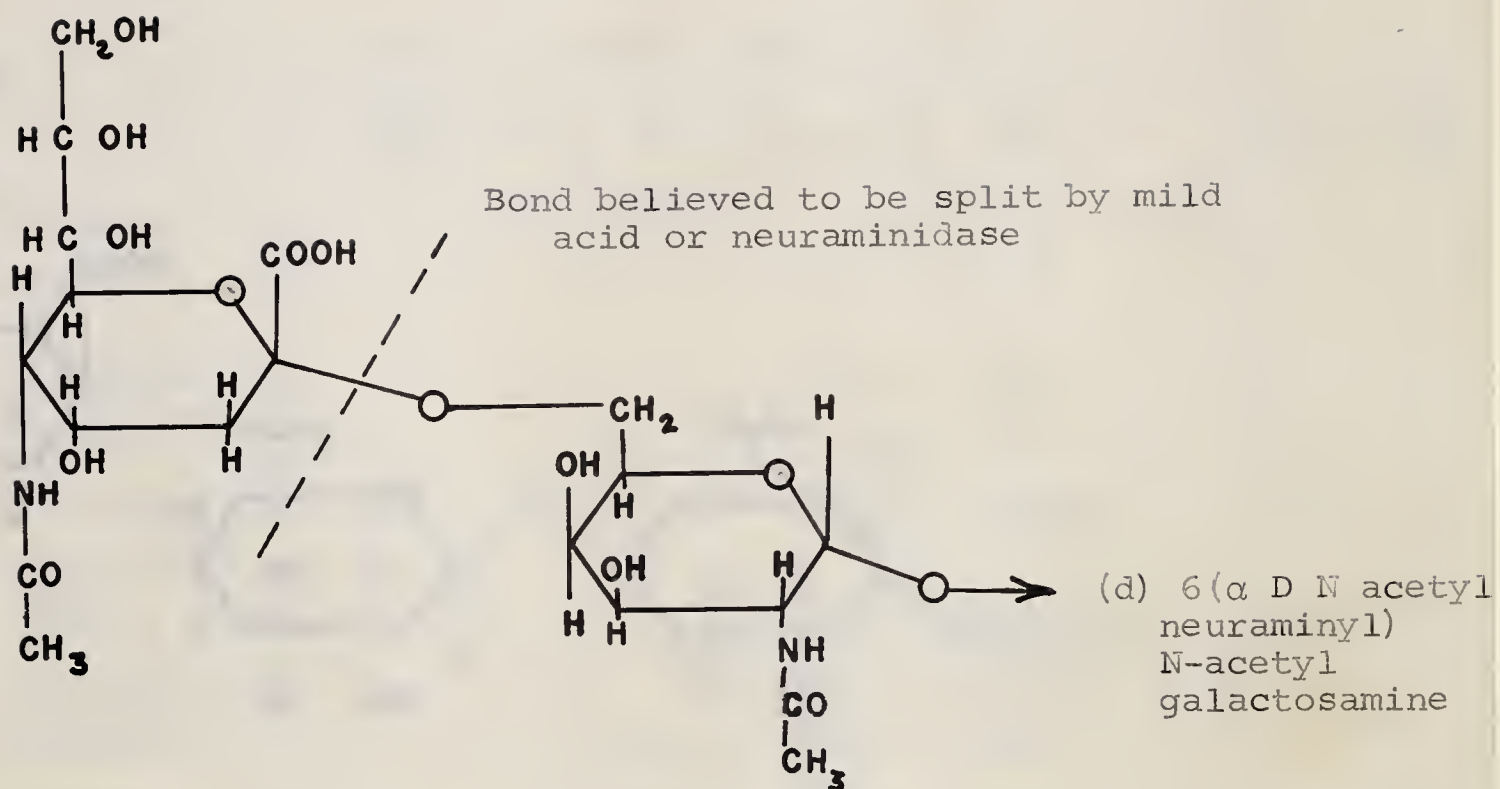


Figure B (d)

Disaccharide from bovine submaxillary gland

Chemical structure of the compound is shown below.

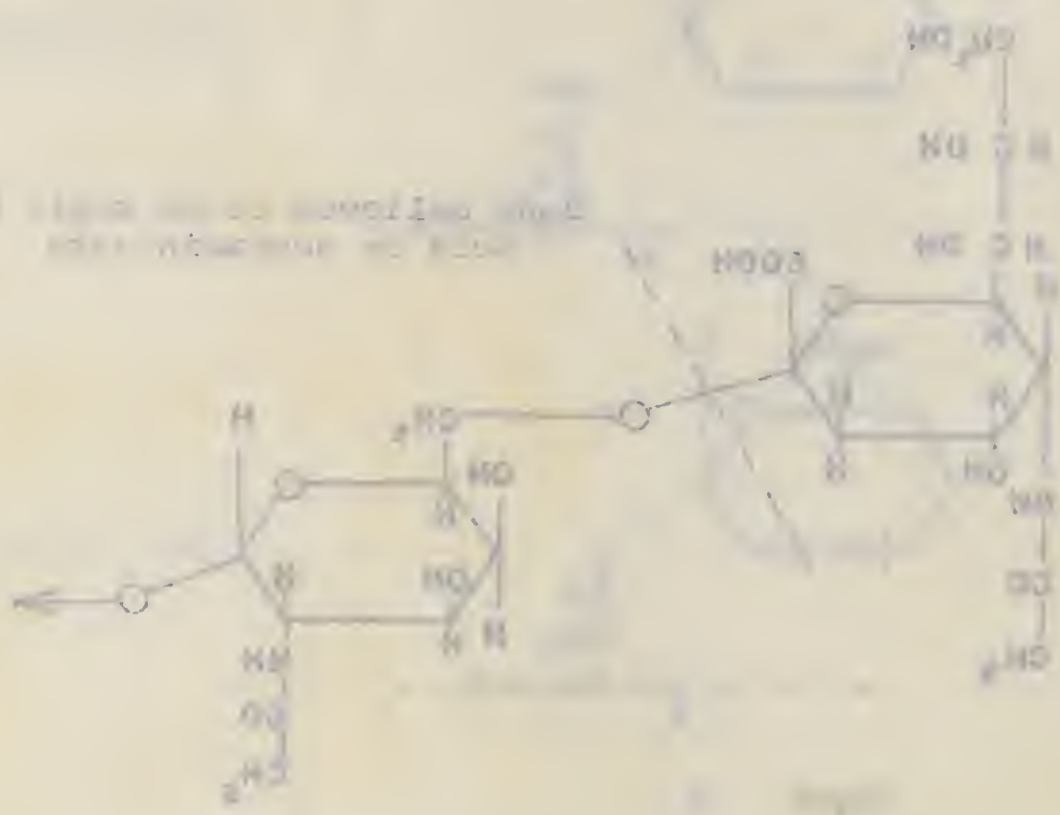


Figure 1. Chemical structure of the compound.

Table I

CHEMISTRY AND PROPERTIES OF WELL CHARACTERIZED SERUM GLYCOPROTEINS

	Hexose (%)	Glucosamine (%)	Hexosamine (%)	Sialic acid (%)	Fucose (%)	Total sugar <sup>a</sup> (%)	Nitro- gen (%)	"Blue" Protein (g) 100 g protein	Molecular weight or $\bar{M}_n$	pI	Mobility at pH 4.6 ( $\times 10^4$ cm/sec/volt)	Amount in serum (mg/100 ml)
Pre-albumin	1.1	—	0.15	0	0	1.3	—	96	61,000	—	9.0	—
Orosomucoid	15.0 <sup>b</sup>	2	12.0 <sup>b</sup>	12 <sup>b</sup>	1.0 <sup>b</sup>	41.0 <sup>b</sup>	10.1	63 <sup>b</sup>	41,000	1.8-2.7 <sup>d</sup>	5.1	75
$\alpha_1$ -Glycoprotein	6.8	—	3.6	3.3	—	13.7 <sup>c</sup>	13.3	84	54,000	—	5.0	30
Ceruloplasmin	—	2	1.9	2	0.18	—	13.8	95	151,000	4.4	4.6	30
Haptoglobins	—	—	5.7	5.5	0.18	—	12.9	83	95,000 and 170,000	4.1	3.3 (pH 4.6)	100
$\alpha_2$ -Macroglobulin (Brown)	—	—	3.8	—	—	—	—	85	$\bar{M}_n = 16.3$	—	—	240
(Schultze)	—	—	2.3	1.8	0.12	7.8	14	92	$\bar{M}_n = 19$ (100,000)	—	—	240
(Müller-Eberhard)	4.8	—	2.7	2.3	—	9.8 <sup>c</sup>	12.2	—	$\bar{M}_n = 19$	—	—	—
Small $\alpha_2$ -Globulin	5.0	—	3.5	7.0	—	15.5 <sup>c</sup>	12.6	80	$\bar{M}_n = 2.6$	3.85	4.2	—
Prothrombin (beef)	4.6	2	2.3	4.2	0.09	11.2	12.7	85	62,000	5	4	—
Transferrin	2.4	2	1.6	1.4	0.07	5.5	15.3	96	88,000	5.9	3.1	400
$\beta_{2A}$ -Globulin	4.9	—	3.7	—	—	—	16.2	—	$\bar{M}_n = 7$	—	—	—
Fibrinogen (human)	3.2	1	1.0	0.8	0	5.0	16.7	—	340,000	—	2.1	—
Fibrinogen (beef)	1.0	0.43-5	0.7	0.6	0	2.3	—	92	350,000	—	—	300
$\gamma$ -Globulins (7 S)	1.2	0.43-5	1.4 <sup>c</sup>	0.22	0.29	3.1	15.64	97	157,000	—	1.2	1000
$\gamma$ -Globulins (19 S)	5.2	—	2.9	1.7	0.62	10.4	14.57	—	$\bar{M}_n = 19$	—	—	—

<sup>a</sup> Sum of hexose, glucosamine, sialic acid, and fucose.

<sup>b</sup> Composite of several published figures.

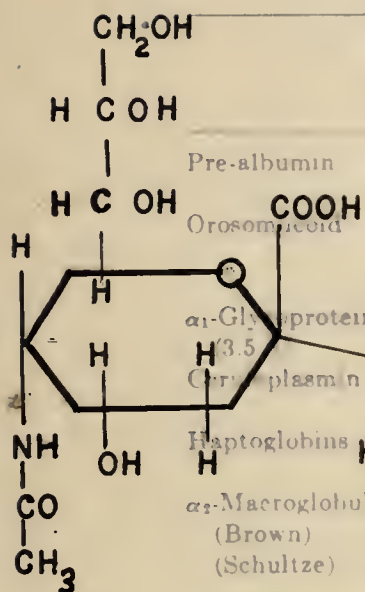
<sup>c</sup> Solely glucosamine.

<sup>d</sup> Depending on buffer.

<sup>e</sup> Not including fucose.

Figure C

From Putnam, "The Plasma Proteins", p. 319-320.  
Suggested terminal sequence of carbohydrate residues of  
fetuin according to R. G. Spiro



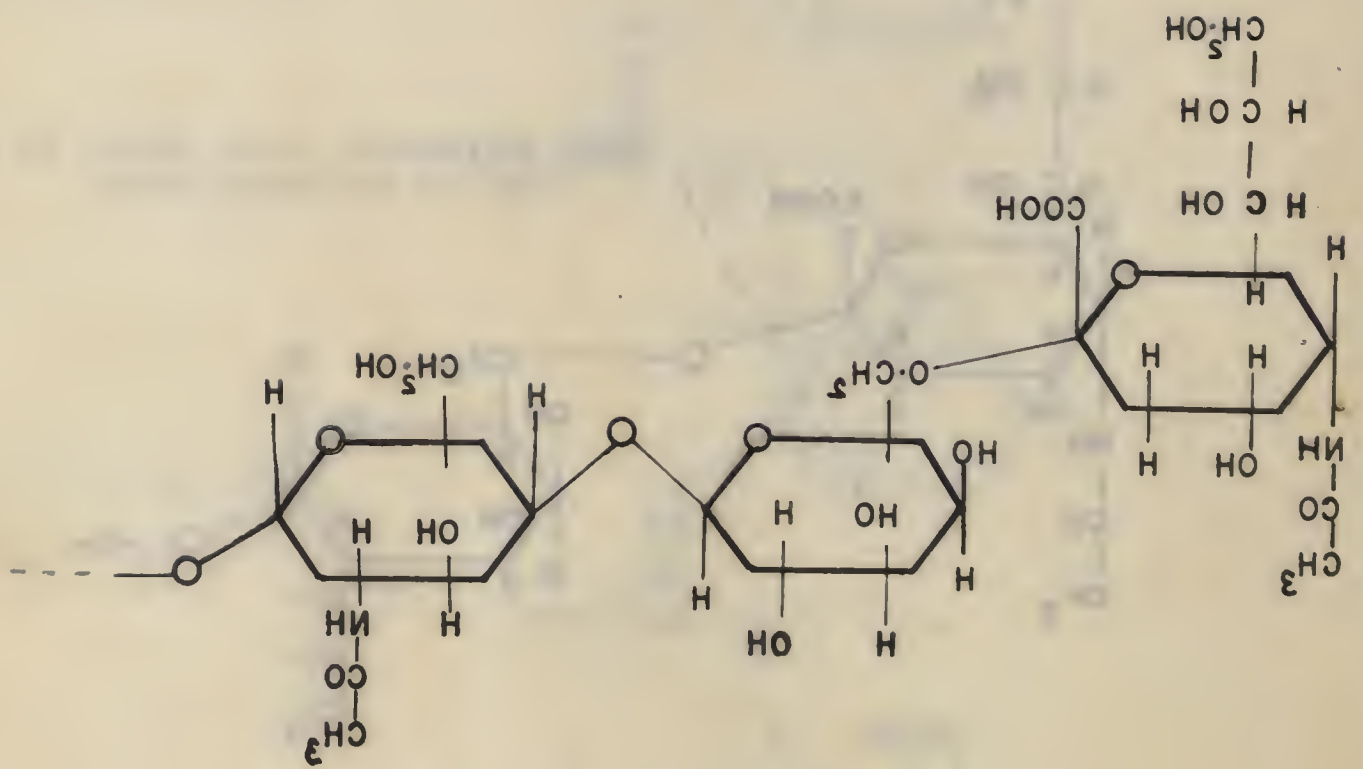


Figure C  
Suggested terminal sequence of oligosaccharide residues of  
fetuin according to R. G. Spiro

Table I

CHEMISTRY AND PROPERTIES OF WELL-CHARACTERIZED SERUM GLYCOPROTEINS

	Hexose (%)	Galactose-Mannose Ratio	Hexosamine (%)	Sialic acid (%)	Fucose (%)	Total sugar <sup>a</sup> (%)	Nitrogen (%)	"Biuret" Protein (%)	Molecular weight or $s_{20}$	pI	Mobility at pH 8.6 ( $\times 10^4$ cm <sup>2</sup> /sec/volt)	Amount in serum (mg/100 ml)
Pre-albumin	1.1	—	0.15	0	0	1.3	—	96	61,000	—	9.0	30
Orosomucoid	15.0 <sup>b</sup>	2	12.0 <sup>b</sup>	12 <sup>b</sup>	1.0 <sup>b</sup>	41.0 <sup>b</sup>	10.1	63 <sup>b</sup>	41,000	1.8-2.7 <sup>d</sup>	5.1	75
$\alpha_1$ -Glycoprotein (3.5 S)	6.8	—	3.6	3.3	—	13.7 <sup>c</sup>	13.3	84	54,000	—	5.0	30
Ceruloplasmin	3.0	2	1.9	2	0.18	7.1	13.8	95	151,000	4.4	4.6	30
Haptoglobins	11.3	1	5.7	5.5	0.18	22.7	12.9	83	85,000 and 170,000	4.1	3.3 (at pH 7.6)	100
$\alpha_2$ -Macroglobulins (Brown)	5.3	—	3.8	—	—	—	—	98	$s_{20} = 16.3$	—	3.9	240
(Schultze)	3.6	1	2.3	1.8	0.12	7.8	14.8	92	$s_{20} = 19$ (850,000)	—	4.2	240
(Müller-Eberhard)	4.8	—	2.7	2.3	—	9.8 <sup>c</sup>	14.2	—	$s_{20} = 19$	—	—	—
Small $\alpha_2$ -Globulin	5.0	—	3.5	7.0	—	15.5 <sup>c</sup>	12.6	80	$s_{20} = 2.6$	3.85	4.2	—
Prothrombin (beef)	4.6	2	2.3	4.2	0.09	11.2	14.7	85	62,000	5	4.	—
Transferrin	2.4	2	1.6	1.4	0.07	5.5	15.4	96	88,000	5.9	3.1	400
$\beta_{2A}$ -Globulin	4.9	—	3.7	—	—	—	16.2	—	$s_{20} = 7$	—	—	—
Fibrinogen (human)	3.2	1	1.0	0.8	0	5.0	16.7	—	340,000	—	2.1	—
Fibrinogen (beef)	1.0	0.43-5	0.7	0.6	0	2.3	—	92	350,000	—	—	300
$\gamma$ -Globulins (7 S)	1.2	0.43-5	1.4 <sup>c</sup>	0.22	0.29	3.1	15.64	97	157,000	—	1.2	1480
$\gamma$ -Globulins (19 S)	5.2	—	2.9	1.7	0.62	10.4	14.57	—	$s_{20} = 19$	—	—	—

<sup>a</sup> Sum of hexose, hexosamine, sialic acid, and fucose.

<sup>b</sup> Composite of several published figures.

<sup>c</sup> Solely glucosamine.

<sup>d</sup> Depending on buffer.

<sup>e</sup> Not including fucose.

From Putnam, "The Plasma Proteins", p. 318-319.







Table II

Carbohydrate Content and Physical Parameters  
of Fetuin According to Spiro (66).

	Content <sup>a</sup> %	Residues <sup>b</sup> per mole
Polypeptide	74	
Hexose	8.3	
Galactose	4.6	12.4
Mannose	3.0	8.1
Hexosamines <sup>c</sup>	5.5	
Glucosamine	4.9	13.2
Galactosamine	0.6	1.6
Sialic acids <sup>d</sup>	8.7	13.6
Nitrogen	12.2	
Sulfur	0.83	
Phosphorus	0	
Ash	<0.5	

<sup>a</sup> Expressed as percentage of the deionized, moisture-free protein.

<sup>b</sup> Calculated on the basis of a molecular weight of 48,400.

<sup>c</sup> Expressed as the free base. If expressed as the *N*-acetyl hexosamines, the value would be 6.8%.

<sup>d</sup> Expressed as *N*-acetylneuraminic acid. Approximately 7% of the sialic acid is *N*-glycolylneuraminic acid.

*Physicochemical properties of fetuin*

$s_{20,w}^0$	3.47 S
$D_{20,w}^0$	$5.73 \times 10^{-7}$ cm <sup>2</sup> per second
$V_{20}$	0.696 ml per g
Molecular weight	48,400
$f/f_0$	1.58
$[\eta]_{20}$	7.8 ml per g
$pI$	11.2
Isoelectric point	pH 3.3
Isoionic point	pH 4.0
Electrophoretic mobility pH 8.6, barbital-citrate, ionic strength, 0.1	5.6 cm <sup>2</sup> per volt second
$E_{1\text{ cm}}^{1\%}$ (278 mμ)	4.10



Table III

Amino Acid Analysis of Fetuin According to Spiro (71).

Component	Average amount per 100 mg of protein	Average no. of residues per mole	Residue weight per 100 g of protein	No. of residues per mole to nearest integer *
	$\mu$ moles		g	
Aspartic acid	68.1	33.0	7.84	33
Threonine	51.4	24.9	5.20	25
Serine	54.1	26.2	4.71	26
Glutamic acid	70.0	33.9	9.04	34
Proline	69.6	33.7	6.76	34
Glycine	50.0	24.2	2.85	24
Alanine	69.1	33.4	4.91	33
Valine	83.2	40.3	8.24	40
Isoleucine	30.8	14.9	3.49	15
Leucine	55.4	26.8	6.27	27
Tyrosine	14.0	6.8	2.28	7
Phenylalanine	22.4	10.8	3.30	11
Lysine	34.0	16.5	4.36	16
Histidine	21.1	10.2	2.89	10
Arginine	24.3	11.8	3.79	12
Half-cystine	25.0	12.1	2.55	12
Tryptophan	4.6	2.2	0.86	2
Amide N	49.2	23.8	(0.69)	(24)
Sialic acids		13.6	8.20	
Hexosamines		17.1	7.20	
Galactose		12.4	4.15	
Mannose		8.1	2.70	
			101.59	361

\* Calculated from the molecular weight of fetuin of 48,400



Table IV

Amino Acid Analysis of Fetuin According to Fisher et al. (72)

Residue	Micromoles/mg. protein				Calculated No. of resi- dues/mole protein	Nearest integral number	Calculated molecular weight
	16-hr. hydrolysis	24-hr. hydrolysis	72-hr. hydrolysis	Final or extrapolated value			
1. Aspartic	0.52	0.52	0.60	0.60	26.8	27	45,000
2. Threonine	0.32	0.29	0.33	0.36	16.0	16	44,750
3. Serine	0.40	0.31	0.37	0.46	20.6	21	45,600
4. Glutamic	0.59	0.62	0.69	0.69	30.8	31	44,800
5. Proline	0.64	0.61	0.75	0.78	34.9	35	44,800
6. Glycine	0.35	0.37	0.41	0.41	18.3	18	44,000
7. Alanine	0.54	0.55	0.62	0.62	27.7	28	45,200
8. Valine	0.55	0.67	0.73	0.73	32.6	33	45,200
9. Isoleucine	0.23	0.24	0.27	0.27	12.1	12	44,300
10. Leucine	0.54	0.45	0.53	0.62	27.7	28	45,200
11. Tyrosine	0.17	0.15	0.15	0.17	7.6	8	47,000
12. Phenylalanine	0.20	0.20	0.21	0.21	9.4	9	42,800
13. Lysine	0.31	0.30	0.34	0.35	15.6	16	45,800
14. Histidine	0.20	0.16	0.20	0.24	10.7	11	46,000
15. Arginine	0.26	0.20	0.29	0.35	15.6	16	45,800
16. Tryptophan	—	—	—	0.042	1.9	2	47,000
17. $\frac{1}{2}$ -Cystine	—	—	—	(0.40)	< (17.9)	< (18)	(44,900)
18. Methionine	0.012	0.007	0.004	0.012	0.54	(Probably 0)	—
19. Ammonia	0.90	1.03	1.2	(1.2)	—	—	—
20. Hexosamine	—	—	—	0.301	13.5	14	46,300
21. Hexose	—	—	—	0.443	19.8	20	45,200
22. N-Acetylneuraminic acid	—	—	—	0.191	8.6	9	46,800





## II. THEORETICAL BACKGROUND

### Chain conformation in polypeptides and proteins

A variety of methods is available for the study of chain conformation (80). These include x-ray diffraction and electron microscopy, infra red spectroscopy, light scattering and optical rotatory dispersion, and a range of hydrodynamic techniques of which the measurements of sedimentation and viscosity are among the most frequently used. Only one of these methods, namely, x-ray diffraction, can specify the relative disposition of atoms in a molecule, and is therefore able to detect the presence of  $\alpha$ -helices and  $\beta$  structure. In order to make such measurements, it is necessary to prepare the material in crystalline form (81,82,83). Although infra red spectroscopy has the advantage that it is able to discriminate in solution between hydrogen bonds involved in helices and the extended ( $\beta$ ) form (84), it cannot accurately distinguish the form of the random coil, nor the alternative types of helices that have been proposed (85). It follows then that much of the evidence that has been obtained to distinguish between one conformation and another has its origin in light scattering and hydrodynamics. More recently, optical rotatory parameters have been correlated with different aspects of secondary structure, percent helix and so forth, but the justification for such correlation rests on conclusions drawn from the currently more familiar hydrodynamic methods. Furthermore, many of the studies on conformation have been carried out on synthetic polymers of amino acids in a variety of media varied in a



systematic manner so as to induce alterations in secondary structure. While the similarity of polymers of this nature and proteins is self-evident, it is equally obvious that proteins are more complex in that in addition to being composed of 20-odd amino acids, cross chain linkages such as the disulfide bridge restrict the extent of deformation that the molecule may undergo. For the influence of solvent composition on chain conformation, see [Singer] (86). In globular proteins, in particular, the peptide chain may exist in nearly equal amounts of helical and disordered regions, and yet, because of a series of folds in the chain, this results in a very compact structure which hydrodynamically exhibits a behaviour consistent with a near spherical unit. In addition to the basic differences in the polypeptide structure, many proteins contain appreciable quantities of non-peptide moieties as integral parts of their molecules. A good example exists in the group of well-known carbohydrate containing proteins whose composition may include up to 50% carbohydrate (87). For a comprehensive review of optical rotation in relation to chain conformation, see Urnes and Doty (1961) (88).

On the basis of the comments above, it is evident that any investigations aimed at obtaining information on conformation or changes therein should be supported by several techniques offering independent evidence which may be integrated to reach some reasonable conclusion. In addition, these methods also are capable of providing additional means whereby a macromolecule may be characterized.

The main theme throughout this work is based on the hydrodynamic methods of sedimentation and viscosity for molecular characterization in conjunction with inferences drawn, from parallel





measurements of optical rotatory dispersion, with regard to secondary structure. The underlying basis for the expression of gross size and shape in terms of the measurable hydrodynamic quantities of effective volume ( $V_e$ ) and axial ratio ( $p$ ) will be discussed first of all. This will be followed by an outline of the optical rotatory method whereby in conjunction with the hydrodynamic picture, some conclusions may be drawn about the underlying secondary structure of the protein molecule.

#### Gross structure based on hydrodynamic considerations

On dissolving a polyamino acid or protein in a suitable solvent, the volume taken up by the solvated molecule and the conformation adopted by the peptide chain will depend in large measure on the affinity of the solvent for the polymer--or parts of it--and the affinities between different sections of the polymer itself. In addition, for proteins, internal constraints such as the disulfide bridge will limit the extent of a preferred conformation, perhaps favoring one form over another under a given set of circumstances. Since the hydrodynamic properties of a molecule are largely dependent on its gross structure, or more specifically on its effective volume, which reflects its bulk, and on its asymmetry, which reflects its shape, sedimentation and viscosity measurements carried out on solutions of proteins give useful information on the extent of folding, or otherwise, of the peptide chain. Although certain generalizations are possible, exact interpretation is not easy largely because the interpretation of hydrodynamic data involves the use of models and the extent to which a model is representative for a given molecular species is often in doubt. In practice, finite concentrations of protein have to be used and in order to eliminate





the effects of disturbance in solvent flow around the macromolecule due to the proximity of another macromolecule, the parameters measured are extrapolated to infinite dilution. This gives rise to the well-known intrinsic values of viscosity and sedimentation which in conjunction with other parameters, find applicability in the Scheraga-Mandelkern function. This function enables deductions to be made in terms of a hydrodynamically equivalent ellipsoid based on the measurements made with the protein solution (89).

The hydrodynamic theories give rise to three quantities: the intrinsic viscosity  $[\eta]$ , the translational frictional coefficient  $f$ , and the rotational frictional coefficient  $\int$ . The experimental method chosen enables one of these quantities to be computed. Since each of these depends on two parameters, that is, the bulk size and shape, two of the quantities must be measured. In terms of an equivalent ellipsoid model, the computation of its effective volume and axial ratio would be possible from viscosity measurements which would give  $[\eta]$  and sedimentation measurements which would give  $f$ . Since these are the methods used in this work, no further reference will be made to techniques such as flow birefringence which enables the computation of the rotational frictional coefficient.

A brief outline will now be given of the essential equations involved and the underlying steps taken which lead to the derivation of the Scheraga-Mandelkern relation. For treatment in detail, see Scheraga (90).

In the absence of solute-solute interaction, the specific viscosity  $\eta_{sp}$  of a solution of ellipsoidal particles may be expressed as the product of three terms.



$$\eta_{sp} = \frac{(\eta - \eta_o)}{\eta_o} = (n) (V_e) (\gamma) \quad (1)$$

where  $\eta$  is the coefficient of viscosity of the solution of particles,

$\eta_o$  is the coefficient of viscosity of the pure solvent,

$n$  is the number of particles/ml.,

$V_e$  is the effective volume of an individual particle,

$\gamma$  is a function only of the axial ratio.

This may be rewritten as follows:

$$\left( \frac{\eta_{sp}}{c} \right)_{\text{Lt. } c \rightarrow 0} = [\eta] = \left( \frac{N}{100} \right) \left( \frac{V_e}{M} \right) \gamma \quad (2)$$

where  $c$  is the dry weight concentration in grams/100 mls.,

$M$  is the anhydrous molecular weight,

$N$  is Avagadro's number.

$\gamma$  has been computed by Simha for zero-velocity gradient as a function of axial ratio for the ellipsoidal forms (91).

Let us now consider the frictional coefficient  $f$ . This also is dependent both on  $V_e$  and the axial ratio  $p$ . This was treated by Perrin (92) who introduced the concept of the frictional ratio  $\frac{f}{f_o}$  where  $f_o$  is the frictional coefficient of a sphere whose volume is the same as the equivalent ellipsoid  $V_e$ . It follows that  $\frac{f}{f_o}$  is independent of  $V_e$  and depends on the axial ratio only. In this way, he derived an expression for  $\left( \frac{f}{f_o} \right)$  in terms of  $p$  for the two cases: (a) the prolate ellipsoid, (b) the oblate ellipsoid; i.e.

$$\frac{f}{f_o} = f(p).$$

Since, from Stokes law,

$$f_o = 6 \pi \eta_o r_o \quad (3)$$



where  $r_o$  is the radius of the sphere.

$$f = 6\pi\eta_o r_o \left( \frac{f}{f_o} \right)$$

Further,  $r_o = \left( \frac{3}{4\pi} \right)^{\frac{1}{3}} V_e^{\frac{1}{3}}$ .

Hence,  $f = (162\pi^2)^{\frac{1}{3}} (V_e)^{\frac{1}{3}} \eta_o \frac{f}{f_o}$  (4)

From equations (2) and (4),  $V_e$  may be eliminated and since both  $\gamma$  and  $\frac{f}{f_o}$  have been derived for an ellipsoid,  $p$  may be computed. By substitution,  $V_e$  may also be found.

Experimentally,  $f$  may be determined either from diffusion or sedimentation measurements.

For translational diffusion:

$$f = \frac{kT}{D}$$
 (5)

where  $k$  = the Boltzmann constant,

$T$  is the absolute temperature,

$D$  is the diffusion coefficient.

For sedimentation velocity in a binary solution at infinite dilution:

$$f = \frac{M(1 - \bar{v}\rho)}{NS}$$
 (6)

where  $M$  is the molecular weight of the anhydrous particle,

$\bar{v}$  is the partial specific volume of the anhydrous particle,

$\rho$  is the density of solvent.

By elimination of  $V_e$  from equations (2) (4) and combination with (5) we arrive at the  $\beta$  function of Scheraga and Mandelkern:

$$\beta = \frac{D[\eta]^{1/3} M^{1/3} \eta_o}{kT} = \frac{N^{1/3}}{(16,200\pi^2)^{1/3}} \cdot \frac{\gamma^{1/3}}{\left( \frac{f}{f_o} \right)} \quad (7)$$





Combination with equation (6) gives the alternative form of the function:

$$\beta = \frac{NS [\eta]^{1/3} \eta_o}{M^{2/3} (1-\bar{v}\rho)} = \frac{N^{1/3}}{(16,200 \pi^2)^{1/3}} \cdot \frac{\gamma^{1/3}}{\left(\frac{f}{f_o}\right)} \quad (8)$$

As a function of  $\gamma$  and  $\left(\frac{f}{f_o}\right)$   $\beta$  depends only on the axial ratio. It can be determined experimentally and calculated from the theory outlined above in which the model used is the ellipsoid. Tables (90) have been drawn up on the theoretical basis described which then enables a protein molecule to be described in terms of its equivalent hydrodynamic ellipsoid. Once  $\beta$  has been evaluated,  $\gamma$  and  $\left(\frac{f}{f_o}\right)$  can be immediately obtained and from equation (1)  $V_e$  may also be found.

References to such tables reveal that the  $\beta$  values for the oblate case are almost independent of the axial ratio. Further, since the volume of an ellipsoid is given by  $V_e = 4/3 \pi ab^2$ , the semi major and minor axes  $a$ ,  $b$ , respectively, are calculable.

In order to evaluate the Scheraga-Mandelkern expression, additional parameters are required. One of these, the molecular weight, has to be determined by an independent method. One possibility is from sedimentation diffusion measurements by use of the Svedberg equation (93):

$$M = \frac{RTS}{D(1-\bar{v}\rho)} \quad (9)$$

Another frequently used method is the sedimentation equilibrium or approach to equilibrium system using the ultracentrifuge. Since a true equilibrium condition of centrifugation may take days to achieve, the approach method, which takes only a few hours, is



preferable. The equation due to Archibald is as follows (94):

$$M_m = \frac{RT}{\omega^2 (1 - \bar{v} \rho)} \frac{\left( \frac{dc}{dx} \right)_m}{x_m c_m} \quad (10)$$

where  $M_m$  is the molecular weight at the meniscus,

$c_m$  is the protein concentration at the meniscus,

$x_m$  is the distance of the meniscus from the axis of rotation,

$\frac{dc}{dx}$  is the concentration gradient at the meniscus,

$\omega$  is the angular velocity of rotation.

Here also, as in some of the expressions above, the partial specific volume  $\bar{v}$  appears. It is necessary to determine this quantity by measurements of density on a series of concentrations of protein dissolved in the appropriate solvent; details of this procedure are given in Experimental Methods, following the procedure of Kraemer (95).

In order to determine  $c_m$  it is necessary to know the total quantity of protein in the solution and this is obtained from a separate run at high speed. Details of the method and the Archibald calculation are given in (96).

Although in this discussion, first mention of molecular weight has come about through its participation in the Scheraga-Mandelkern relation, it is, per se, probably the most important single parameter in the characterization of any macromolecule. Apart from the expression of conformation by means of equivalent ellipsoids, certain generalizations may be drawn from sedimentation and viscosity measurements in conjunction with determinations of molecular weight.

Let us suppose that under certain conditions a given protein



molecule may undergo some conformational change and under other distinct conditions may associate, or perhaps dissociate, into small units. If the molecule were to become more compact, then, because of a decrease in the frictional coefficient the viscosity might be expected to decrease and the sedimentation velocity to increase. A constant value of the molecular weight would support this. If, on the other hand, an increase in sedimentation were accompanied by an increase in molecular weight, the viscosity would be expected to increase also, due to the larger effective volume of the associated particle. Such considerations then enable one to distinguish between extremes in which systems exhibit conformational changes or associative properties. By computing such conformational changes through the Scheraga-Mandelkern equation, expression is given in more quantitative terms, as emphasized above, by the concept of a hydrodynamically equivalent model.

Up to this point, little attention has been given to the nature of the hydrodynamic unit, the macromolecule being visualized as behaving somewhat as a rigid particle with a more or less regular geometric form. Any interaction between the components of the suspending medium has been ignored as has the effect of electrostatic potential gradients on a molecule possessing an electric charge. Brief consideration will be given to these points since, in practice, the simplest systems used generally involve the use of a buffer pair to maintain a constant pH and furthermore, a protein will always carry some residual charge due to the ionization of groups attached to its side chains, except at its isoelectric point. Additional complications may be introduced when, as is often the case, organic solvents are deliberately used in







order to induce molecular changes. The subject is a complicated one and not entirely understood. A summary only of the general ideas will be attempted here. Consideration to these and other aspects of hydrodynamics is given in Schachman (97).

The effect of solvation on a molecule moving through a fluid under the influence of a centrifugal field will depend on how solvation will influence the effective mass,  $m(1-\bar{v}\rho)$  and the frictional coefficient. If a molecule has a mass  $m$  and a volume  $v$ , and it combines with a volume  $h$  of solvent of density  $d$ , the mass of the hydrodynamic unit is  $(m + hd)$ . This solvated particle will have an effective volume  $(v + h)$ , and will therefore displace a mass of fluid  $(v + h)\rho$  where  $\rho$  is the density of the solution. The effective mass of the molecule then becomes  $m + hd - (v + h)\rho$ . It follows that in a binary system, e.g. protein in water,  $d = \rho$  and the solvation term cancels. In more complex systems, if there is any selective binding this term does not cancel and the effective mass will change. This is illustrated in the modified sedimentation equation:

$$S = \frac{M}{Nf} \left\{ 1 - \bar{v}\rho + \frac{h}{m} (d - \rho) \right\} \quad (11)$$

Only if the interaction between solvent and protein does not exist, i.e.  $h = 0$ , or if  $d = \rho$  will the sedimentation coefficient be unchanged because of effective mass. As mentioned earlier, the frictional coefficient depends on the volume and asymmetry of the hydrodynamic unit. It follows that any solvation which would result in an increase in effective volume would increase the frictional coefficient. This would then affect the viscosity of the solution directly and the sedimentation indirectly through the frictional



term. From these considerations alone, it is evident that in multi-component systems interpretation may be tentative.

If a protein molecule is being examined at a pH significantly removed from its isoelectric point, it will carry an appreciable charge. In viscosity measurements the electroviscous effect, that is, contributions to the viscosity due to the relative motion of the charged macromolecule through electric fields in the medium, is generally regarded as being very small. This may not, however, be the case in ultracentrifugation. Two effects are recognized and are called, respectively, the primary and secondary charge effects.

When a macro-ion sediments away from its (small) counterions, an electric field is created between the large ion and the counterions. This will result in a decrease in sedimentation of the macro-ion. This is called the primary charge effect. If differences should exist in the sedimentation of positively and negatively charged ions of the supporting electrolyte, an electric field will be set up, the direction of which will depend on which of the supporting ions sediments at the greater rate. This may increase or decrease the sedimentation of the macro-ion depending on the sign of its resultant charge. This is referred to as the secondary charge effect. The primary charge effect does not usually present a problem in most experiments, since among other factors which influence its magnitude, it is found to vary inversely with the conductivity of the solution so that even at ionic strengths of about 0.1 its effect is usually negligible. The secondary charge effect is not so straightforward but as indicated above, will be operative only if the rates of sedimentation of the oppositely charged ions in the solution differ appreciably. If





this is believed to be causing interference, a different choice of supporting electrolyte would be desirable.

#### Chain conformation based on optical rotatory measurements

It is the spatial disposition of the peptide bonds in the chain structure of polypeptides and proteins that is largely responsible for the rotatory properties of these polymers. It is to be expected that optical measurements reflecting such disposition do in fact give information about the secondary structure of the molecule. Since alterations in secondary structure involve reorientation of the polymer chain, measurements of optical rotation reflect chain conformation much as hydrodynamic measurements reflect gross size and shape. Further, since in general, significant alterations in secondary structure result in changes in gross size and shape, it is possible to obtain correlation of one in terms of the other. The aim, ultimately, is to be able to define secondary structure of protein molecules by measurement and analysis of optical rotatory properties. Much of the background for this approach has been obtained by studies on different systems of polyamino acids in solution, and a brief summary of some essential findings will now be attempted. It is appropriate at this point to mention that while the origins of the Drude and Moffitt equations (see below) are well-established in vibration theory and quantum mechanics (98), their application to chain conformation is largely a phenomenological process.

#### Expressions used to describe optical rotation of polyamino acid and protein molecules

The specific rotation  $[\alpha]_{\lambda}^T$  at a given wavelength  $\lambda$  and temperature  $T$  is given by:





$$[\alpha]_{\lambda}^T = \left( \frac{100}{dc} \right) \alpha_{\lambda} \quad (12)$$

where  $\alpha_{\lambda}$  is the observed rotation through  $d$  (decimeters) of solution containing  $c$  grams of polymer/100 mls. at a wavelength  $\lambda$  and temperature  $T$ .

In order to make rotational comparisons between one molecule and another, rotations have to be placed on a common basis. The optical rotatory power of a polymer is largely a function of the independent residues (rather than molecular weight). Since both molecular weight and the amino acid composition vary from one poly-amino acid (or protein) to the next, the mean residue weight (MRW) is used as a basis for comparison.

The mean residue rotation  $[m]_{\lambda}$  is defined as:

$$[m]_{\lambda} = \frac{(\text{MRW})}{100} [\alpha]_{\lambda} \quad (13)$$

The dimensions of  $[m]_{\lambda}$  are degrees  $\text{cm}^2/\text{decimole}$ .

Since in proteins the molecular weights are usually close to 115, specific rotations are comparable at a given wavelength. Optical rotation is also dependent on refractive index of the solvent and the Lorentz correction is used to reduce the value to that approximating vacuum conditions. When organic solvents are used, this correction may be considerable. The reduced mean residue rotation  $[m^1]_{\lambda}$  is given by the expression:

$$[m^1]_{\lambda} = \left( \frac{3}{n^2+2} \right) \frac{(\text{MRW})}{100} [\alpha]_{\lambda} \quad (14)$$

where  $n$  is the refractive index of the medium.

#### Rotatory dispersion curves

When the rotation of an (L) polyamino acid or protein is observed as a function of wavelength in the visible range from



circa 300-650mμ the plot appears as illustrated in Figure D(1):

Such a curve is relatively featureless and two equations have been developed, the first by Drude, the second by Moffitt, which when plotted in a suitable manner will lead to linear relationships for certain systems. From measurements of the slope and intercepts conclusions may be drawn with regard to secondary structure.

#### The Drude equation

This may be expressed as follows for a given system:

$$[m^1]_{\lambda} = \text{constant } [\alpha]_{\lambda} = \frac{a \lambda_c^2}{\lambda^2 - \lambda_c^2} \quad (15)$$

where  $\lambda$  is the wavelength of measurement and  $a$  and  $\lambda_c$  are constants for a given system. If this relationship is plotted according to the method of Yang and Doty (99) and if the system follows what is called simple dispersion, a linear plot is obtained from the slope of which the critical wavelength  $\lambda_c$  may be calculated. It has been shown that this parameter is related to the conformation of the peptide chain. In general, the property of simple dispersion is shown by the random coil form of polyamino acids and globular proteins in which the extent of helix does not exceed about 40%. If the helical content exceeds this amount, distinct curvature of the plot at higher wavelengths is observed. It follows that the optical rotatory dispersion of the rod-like form of polyamino acids which results when they assume a helical form, or that of proteins which contain larger amounts of helix, cannot be expressed by the Drude equation to give a linear relation.

The Yang-Doty plot expressed by  $\lambda^2 [\alpha]_{\lambda}$  vs.  $[\alpha]_{\lambda}$ , as shown in Figure D(2).



Much of the usefulness of polyamino acids in the study of optical rotation and conformation arises from the property they exhibit of being able to exist in the extreme forms approaching 100% helix on the one hand and the random coil on the other. Transition from one form to the other is readily inducible by changing the polarity of the solvent in the system. For example, poly- $\gamma$ -benzyl-L-glutamate in m-cresol exhibits the helical form while in dichloroacetic acid it has the properties of a random coil (99). Such properties have been deduced by independent methods such as viscosity, sedimentation and light scattering. In the former solvent, the affinity of the polymeric units in forming intra H bonds exceeds the attraction between solvent and polymer. In the polar solvent dichloroacetic acid, these forces are overcome by solvent interaction with the polymer and a random disposition results.

#### The Moffitt equation

The so-called complex dispersion which results when a polyamino acid forms a helical conformation, or the dispersion exhibited by a protein containing larger amounts of helix, i.e. more than 40%, is a distinct result of the helix itself. A linear relation between rotation and wavelength is expressed by the Moffitt equation when treated in a suitable manner. The equation due to Moffitt is:

$$[\alpha]_{\lambda}^H = \frac{a_o^H \lambda_o^2}{\lambda^2 - \lambda_o^2} + \frac{b_o^H \lambda_o^4}{(\lambda^2 - \lambda_o^2)^2} \quad (16)$$

A convenient method of treatment of this relationship is due to Urnes and Doty(100). For plot, see Figure D(3). Symbols: The index H refers to the helical form,  $a_o^H$  and  $b_o^H$  are constants for a given system. Both are related to the macromolecular conformation.







In the Moffitt equation  $\lambda_0$  is a constant and for a given system its choice must result in linearity if any significance is to be attributed to the  $a_0$  and  $b_0$  terms in the expression. Frequently, its value, consonant with this condition, is close to 212 m $\mu$  and as this value for  $\lambda_c$  is frequently exhibited by the random coil form of polyamino acids and unfolded proteins, it has additional significance. This point will emerge more clearly in the general application of the Moffitt form given below. However, in many instances, values of  $\lambda_0$  both higher and lower than this value have to be chosen.

Up to this point, we have concerned ourselves with the dispersion properties of polyamino acids in the extreme states of random coil and near 100% helix. The counterpart to these states is exhibited by proteins which have completely unfolded (for example, by suitable heat treatment) and by the fibrous type proteins, respectively. We now have to consider how both the Drude and Moffitt functions may be combined to give expression to partial helical content as shown by a typical globular protein in which sections of the peptide chain consist of helices interspersed with regions devoid of obvious order. We must also bear in mind that other ordered structures such as helices of opposite sense and the extended  $\beta$  structure may be present.

#### Partial helical content

The basic premise underlying this treatment is that the rotations at a given wavelength, due to the helical regions and the random regions are additive in a proportional manner (101). If we consider a long polypeptide chain whose mean reduced residue rotation in the disordered form is  $[m^L]_{\lambda}^D$  and in the helical form is



$[m^1]_{\lambda}^H$  we assume that the mean reduced residue rotation of the molecule  $[m^1]_{\lambda}$  in which a fraction  $f_H$  is helical and a fraction  $f_D$  is random coil is given by the expression:

$$[m^1]_{\lambda} = f_D [m^1]_{\lambda}^D + f_H [m^1]_{\lambda}^H \quad (17)$$

If the Drude equation for the disordered form is introduced for  $[m^1]_{\lambda}^D$  and the Moffitt equation for  $[m^1]_{\lambda}^H$ , it follows:

$$[m^1]_{\lambda} = f_D \left( \frac{a_o^D \lambda_c^2}{\lambda^2 - \lambda_c^2} \right) + f_H \left\{ \frac{a_o^H \lambda_o^2}{\lambda^2 - \lambda_o^2} + \frac{b_o^H \lambda_o^4}{(\lambda^2 - \lambda_o^2)^2} \right\} \quad (18)$$

By making the additional assumption that  $\lambda_o$  in the Moffitt term is equal to  $\lambda_c$  for the random coil and replacing  $f_D$  by its equivalent  $(1-f_H)$ , we arrive at the expression for  $[m^1]_{\lambda}$ :

$$[m^1]_{\lambda} = \frac{(a_o^D + f_H a_o^{H-D}) \lambda_o^2}{(\lambda^2 - \lambda_o^2)} + \frac{f_H b_o^H \lambda_o^4}{(\lambda^2 - \lambda_o^2)^2} \quad (19)$$

In these expressions the indices D and H refer to the disordered form and the helical form of the entire molecule, respectively, while H-D refers only to the helix itself.

It is to be noted that the basic form of the Moffitt equation still persists upon replacing  $(a_o^D + f_H a_o^{H-D})$  by  $a_o^{obs}$  and  $f_H b_o^H$  by  $b_o^{obs}$ . In this situation we have:

$$[m^1]_{\lambda} = \frac{a_o^{obs} \lambda_o^2}{(\lambda^2 - \lambda_o^2)} + \frac{b_o^{obs} \lambda_o^4}{(\lambda^2 - \lambda_o^2)^2} \quad (20)$$

Treatment of the rotatory data according to Urnes and Doty enables  $b_o^{obs}$  to be obtained directly from the slope of the plot. Since  $b_o^{obs} = f_H b_o^H$  it is directly proportional to helical content,  $f_H$ .



Provided then that independent considerations show that helices of opposite sense are absent and no appreciable content of the  $\beta$  form is present, we have a method whereby helical content can be estimated and changes in helix observed. It has been shown that like the right-handed  $\alpha$  helix, the rotational characteristics of the  $\beta$  form results in a less negative rotation (102) but, unlike the right-handed  $\alpha$  helix, in positive  $b_0$  values. Further, the greater the extent of random coil content, the greater the negative values of rotation and provided the helical content does not exceed 40%, the Yang-Doty plot for the Drude equation must be linear. Obviously this plot must give values for  $\lambda_c$  greater than the random value if any helix is present at all. Finally, under extreme denaturing conditions  $\lambda_c$  must approach a value for the disordered state and an independent criterion is available for  $\lambda_0$  other than linearity in the Moffitt equation (see Figure E).

From such considerations and supported by measurements of sedimentation and viscosity, some insight into secondary structure may be achieved.

In this investigation, both Yang-Doty and Urnes-Doty plots are interpreted in conjunction with the Scheraga-Mandelkern treatment of sedimentation and viscosity data. Alternatively, provided a constant molecular weight has been established, inverse shifts in sedimentation and viscosity, being a reflection of changes in shape or effective volume, may be correlated with changes in  $\lambda_c$  from the Drude relation or  $b_0$  from the Moffitt equation.







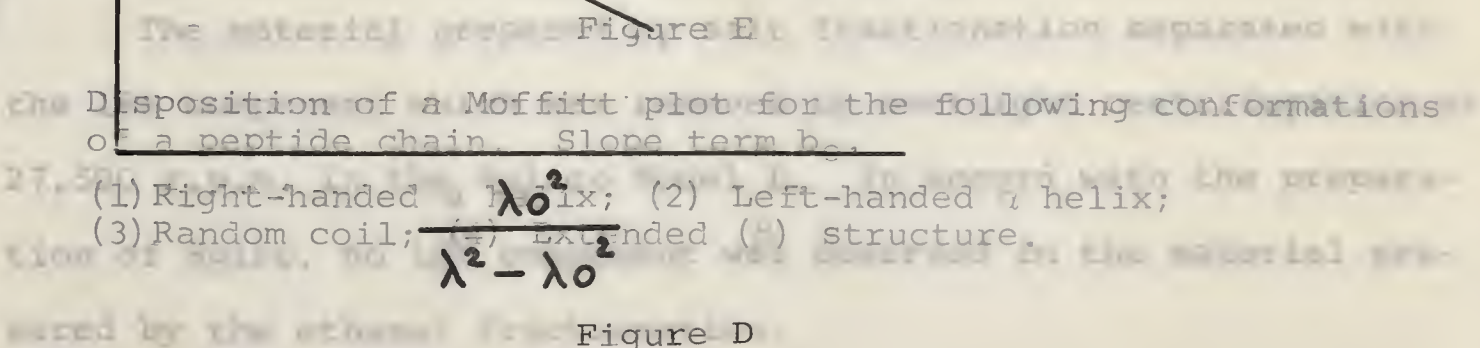
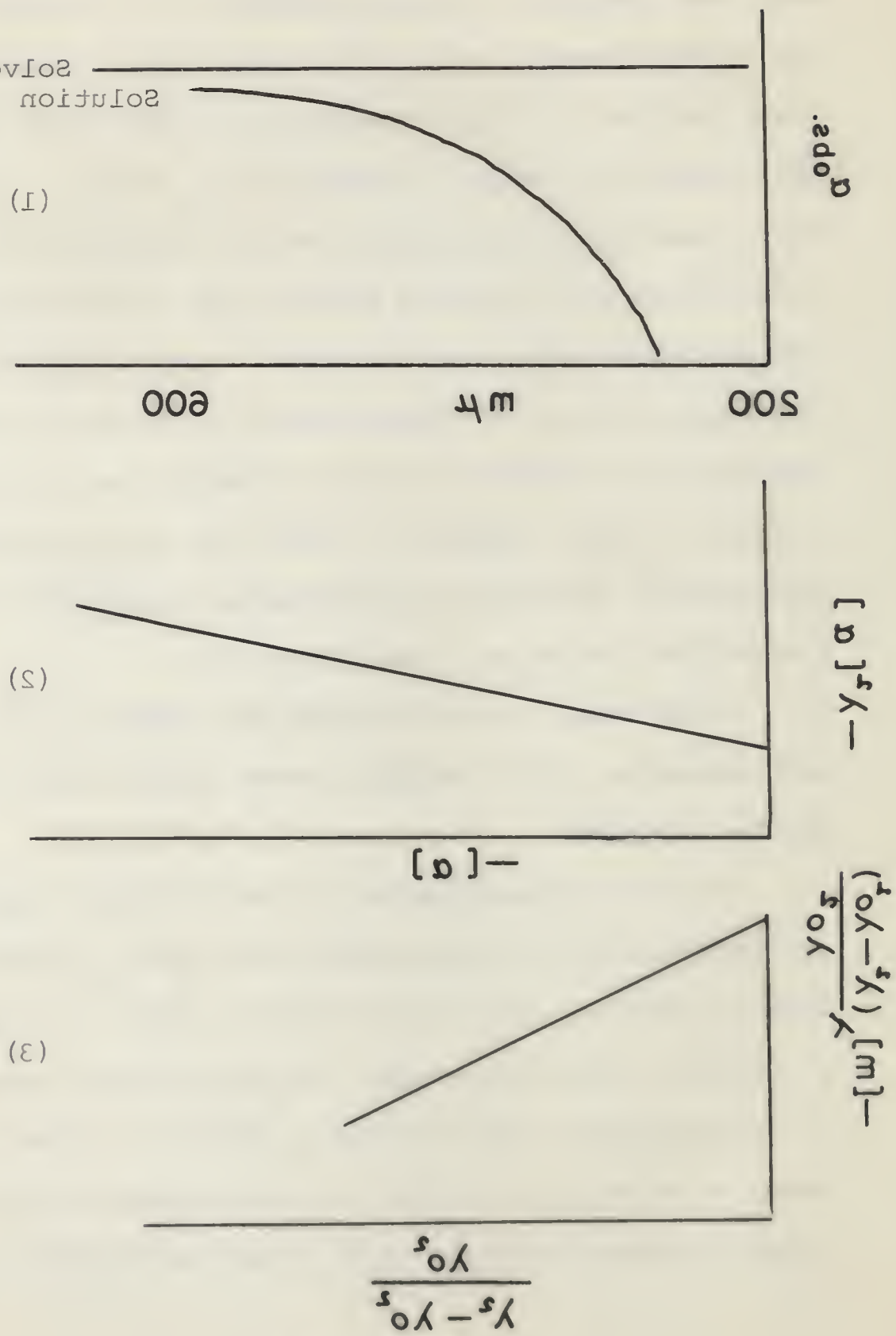


Figure D

(1) OR dispersion curve; (2) Yang-Doty plot; (3) Moffitt plot.

(1) OR dispersion curve; (2) Yand-Doyle plot; (3) Mott plot.

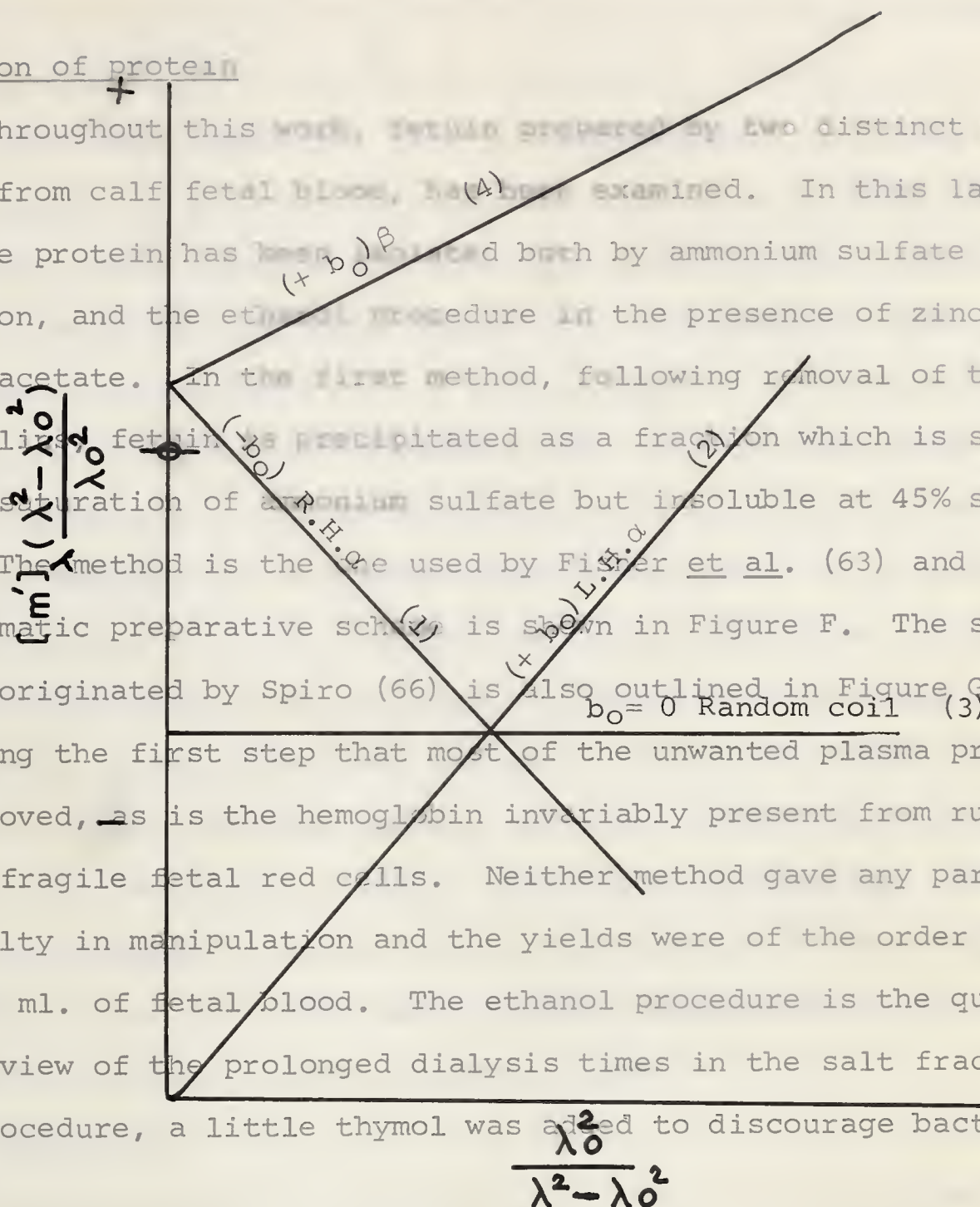
Figure D



# III. METHODS

## Isolation of protein

Throughout this work, protein prepared by two distinct procedures, from calf fetal blood, has been examined. In this laboratory the protein has been isolated both by ammonium sulfate fractionation, and the ethanol procedure in the presence of zinc and barium acetate. In the first method, following removal of the  $\gamma$ -globulins, fetal serum is precipitated as a fraction which is soluble in 40% saturation of ammonium sulfate but insoluble at 45% saturation. The method is the one used by Fisher et al. (63) and a diagrammatic preparative scheme is shown in Figure F. The second method originated by Spiro (66) is also outlined in Figure G. It is during the first step that most of the unwanted plasma proteins are removed, as is the hemoglobin invariably present from rupture of the fragile fetal red cells. Neither method gave any particular difficulty in manipulation and the yields were of the order of 0.5 gm./100 ml. of fetal blood. The ethanol procedure is the quicker and in view of the prolonged dialysis times in the salt fractionation procedure, a little thymol was added to discourage bacterial growth.



The material prepared by salt fractionation separated with

the Disposition of a Moffitt plot for the following conformations of a peptide chain. Slope term  $b_0$ .  
 27,500 r.p.m. in the Spinco Model L. In accord with the preparation of Spiro, no 185 component was observed in the material prepared by the ethanol fractionation.



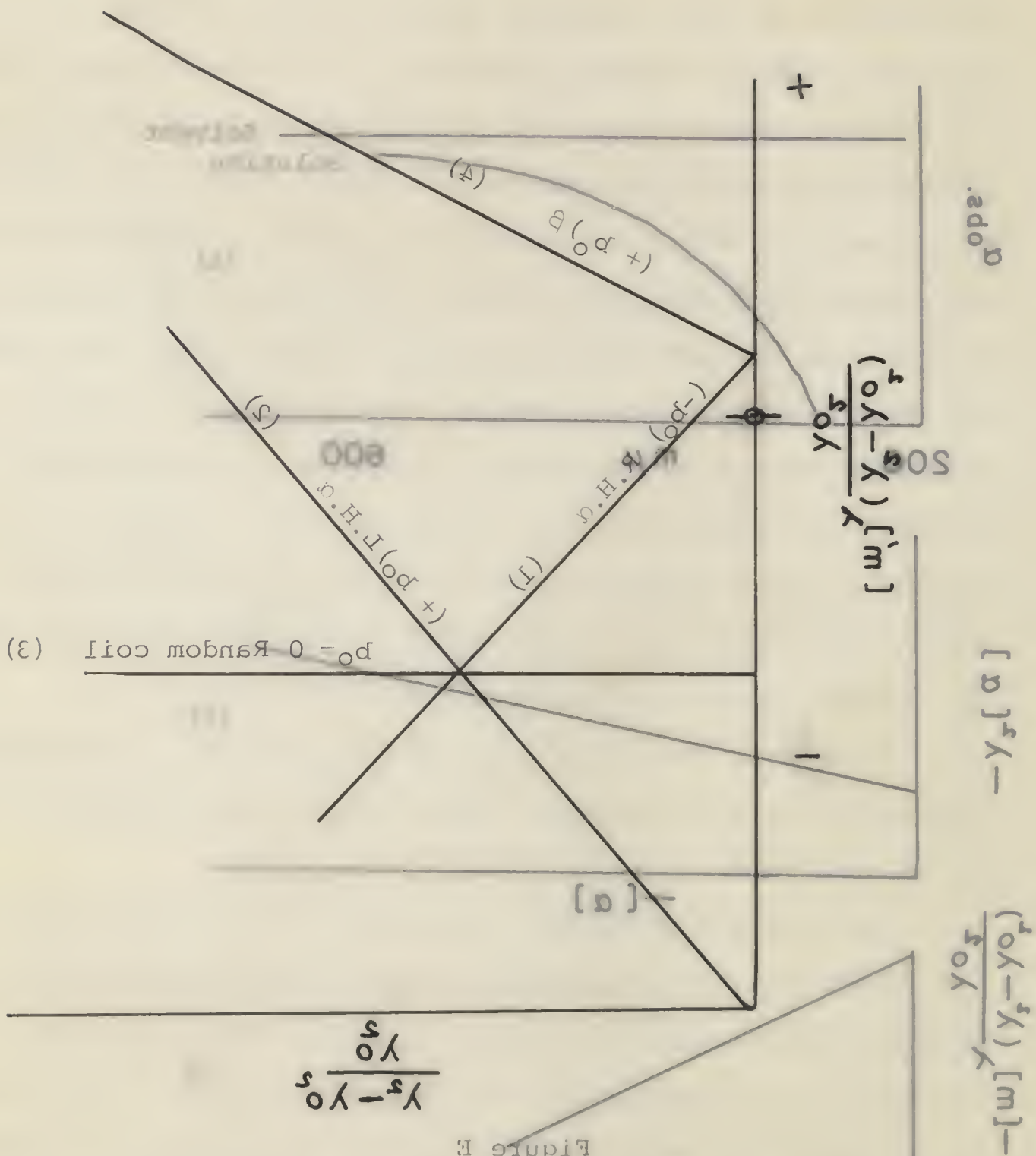
(1) On a coordinate system the following conformations

Figure 5

- (1) Right-handed helix; (2) Left-handed helix; (3) Random coil; (4) Extended structure.

Disposition of a Mollif plot for the following conformations of a peptide chain. Slope term  $p_0$ .

Figure 6



### III. METHODS

#### Isolation of protein

Throughout this work, fetuin prepared by two distinct procedures, from calf fetal blood, has been examined. In this laboratory the protein has been isolated both by ammonium sulfate fractionation, and the ethanol procedure in the presence of zinc and barium acetate. In the first method, following removal of the  $\gamma$ -globulins, fetuin is precipitated as a fraction which is soluble in 40% saturation of ammonium sulfate but insoluble at 45% saturation. The method is the one used by Fisher et al. (63) and a diagrammatic preparative scheme is shown in Figure F. The second method originated by Spiro (66) is also outlined in Figure G. It is during the first step that most of the unwanted plasma proteins are removed, as is the hemoglobin invariably present from rupture of the fragile fetal red cells. Neither method gave any particular difficulty in manipulation and the yields were of the order of 0.5 gm./100 ml. of fetal blood. The ethanol procedure is the quicker and in view of the prolonged dialysis times in the salt fractionation procedure, a little thymol was added to discourage bacterial growth.

The material prepared by salt fractionation separated with the 18S component which was removed by overnight centrifugation at 27,500 r.p.m. in the Spinco Model L. In accord with the preparation of Spiro, no 18S component was observed in the material prepared by the ethanol fractionation.





### Commercial preparations

Much of the characterization of salt prepared fetuin was carried out on material supplied by the Colorado Serum Company. This product was also prepared by the method of Fisher, outlined above (63). The commercial material was packaged in 500 mg. lots, under vacuum, as a lyophilized powder which contained the 18S component. This required the overnight centrifugation (about 18 hours) to separate the heavy contaminant. Usually the 500 mg. of protein was dissolved in 3 x 9 ml. buffer in which the examination was to proceed (e.g. phosphate, pH 7.7, ionic strength 0.16). At the completion of the centrifugation the top 6 ml. of each of the three samples was carefully withdrawn by means of a pipette. The concentration of the supernatant varied from about 1-1.2%. If the solid protein was required, a similar procedure was followed, using water as the suspension medium. In order to remove traces of salt, 24-hour dialysis against deionized water was carried out prior to freeze-drying. Another commercial preparation, obtained from the Commonwealth Serum Laboratories in Australia was also examined. This also contained the 18S component which was removed in similar fashion to that described above.

### Homogeneity

Routine checks for homogeneity at pH 7-8 relied primarily on (a) the absence of any visible fast sedimenting component in the ultracentrifuge at 59,780 r.p.m., using a sample from the supernatant following the 18 hours preparative spin, (b) a molecular weight determination on such a sample. In the early stages of the investigation, samples were also checked by free boundary electrophoresis using the Perkin Elmer Model 38A. Subsequent determinations



of sedimentation and viscosity as a function of concentration showed these parameters to be closely reproducible from one preparation to the next.

### Enzymatic modifications

#### Proteolysis of fetuin

The rate of proteolytic attack of fetuin by the enzymes trypsin and  $\alpha$ -chymotrypsin was followed in the pH stat at pH 8.0 and 25°C. The fetuin was dissolved in a solution of 0.1M NaCl and a quantity of the enzyme, dissolved in  $10^{-3}$ M HCl, added to give an enzyme/substrate ratio of 1/45. The rate of proton release was recorded as equivalents of standard base added during the reaction (103).

#### Removal of sialic acid from commercial fetuin by means of neuraminidase

The enzyme was kindly supplied by Professor H. E. Schultze of Behringwerke, in sealed tubes in a 0.05M acetate buffer solution, pH 5.5, containing 0.9 g/dl NaCl + 0.1 g/dl  $\text{CaCl}_2$ . The sample of commercial fetuin was dissolved in buffer of the same composition (500 mg. of protein in 32 ml. of buffer). This was centrifuged for approximately 18 hr. at 27,500 r.p.m. in the Spinco Model L centrifuge using the 40,000 head, to remove the 18S component.\* The top 75% by volume was carefully withdrawn by means of a pipette. The solution of monomeric fetuin thus obtained was a little over 1% in concentration and 24 mls. in volume. The concen-

---

\* Alternatively, protein from which the 18S component had been previously removed and subsequently obtained in solid form by freeze drying, was dissolved in the acetate buffer and the neuraminidase added.





tration was determined exactly, the solution placed in a dialysis bag along with 1.5 ml. of the neuraminidase solution and immersed in 230 ml. of the buffer. A few drops of toluene were added and the solution gently agitated at room temperature using a magnetic stirrer. These quantities were so chosen that total release of the sialic acid would approximate a concentration of  $0.05 \mu\text{M}$  of N-acetyl neuraminic acid in 0.2 ml. of dialysate. The course of the reaction could be followed directly on 0.2 ml. samples withdrawn from the dialysate, using the thiobarbituric assay method of Warren (104). No further liberation of sialic acid occurred after 48 hrs. The dialysis bag was removed and dialyzed against deionized water for three days and the contents lyophilized. Slight enzyme contamination of the product does occur but estimates based on the specified activity of the preparations and examination of the neuraminidase solution in the centrifuge suggested that the extent of contamination was not greater than 1%.

#### Thiobarbituric acid assay of sialic acids

This method devised by Warren (104) measures unbound sialic acid. The free sialic acid is oxidized at room temperature with sodium periodate with the formation of  $\beta$ -formyl pyruvic acid. Excess periodate is inactivated with sodium arsenite and the periodate oxidation product coupled with thiobarbituric acid. The product is coloured pink and the intensity is increased by extraction with cyclohexanone. There is a linear relation between colour and the concentration of N-acetyl neuraminic acid over a concentration range of the latter from  $0.01$ - $0.06 \mu\text{mole}/0.2\text{ml}$ . Molecular extinction coefficient is 57,000 measured at a wavelength of 549 m $\mu$ .





If the total volume of 4.3 ml. of aqueous solution is extracted with 4.3 ml. of cyclohexanone (see Figure H), the following equation for measuring unbound sialic acid may be used.

$$\mu\text{moles (N-acetyl neuraminic)} = \frac{4.3 \times (\text{OD})_{549=\lambda}}{57} \quad (21)$$

In order to check the method, a solution containing .0039 gm. in 50 ml. of water was prepared. This corresponds to .0505  $\mu\text{moles/}$  0.2 ml. Determinations were carried out on 0.2 ml. of this solution and on 0.2 ml. of a 50:50 dilution. The values obtained were 0.0426 and 0.0217  $\mu\text{M}$ , respectively. In view of the small quantities used and the fact that no correction for moisture content was made, these figures are regarded as indicative that the method is satisfactory for our purposes.

#### Release of sialic acid from protein

Hydrolysis of fetuin using 0.1N  $\text{H}_2\text{SO}_4$  (in a boiling water bath for 1 hour) has been recommended by Spiro (66) to remove the sialic acid. Colorado material in the amount of 3.3 mg. was digested for 1 hour with 1 ml. of 0.1N  $\text{H}_2\text{SO}_4$ ; this was then diluted to a volume of 5 ml. and 0.2 ml. was used for the determination. A value of 6.6% for the sialic acid content of the Colorado sample was obtained. This is equivalent to 9.4 moles of N-acetyl neuraminic acid/mole of fetuin based on a molecular weight for the latter of 44,000. This is approximate and assumes 10% moisture content for the fetuin sample used. Figures obtained by other workers (recalculated to 44,000) gave 8.5 moles by Fisher et al. (72) and 12.4 moles by Spiro (71).

On the basis of the foregoing, the methods are considered adequate to follow the release of sialic acid by means of neuro-



minidase and to check the product for sialic acid content.

#### Buffer systems

Two regions of pH have been consistently used in this investigation. The first, in the pH range 7-8 where the properties of the molecule are insensitive to pH changes, and the second pH range of 1.5-4 where, because of varying extents of association the hydrodynamic parameters are critically dependent on this factor. The compositions of the buffer systems are shown in Table V.

For experiments in which organic solvents were added to buffered systems, constant ionic strength was maintained by using quantities of buffer solution, of double strength, in which the protein was dissolved. An equal volume of diluent was added to give the correct ionic strength. By variation of the solvent/H<sub>2</sub>O ratio of the diluent, a possible 0-50% solvent by volume could be obtained in the final solution while maintaining constant protein and ionic composition. Measurement of pH was made on the final solution, prior to examination and, in general, little variation in pH from that of the buffer system itself was observed. The standard procedure was followed using either a Beckman instrument (Model G) or the pH stat radiometer equipment adapted for pH measurement. Prior standardization in the appropriate range was observed using commercial buffer standards.

#### Determination of concentration

The procedure adopted throughout was by measurement of optical density in the ultraviolet region at a wavelength of 278mμ. Depending on the approximate concentration of protein solution, an amount, accurately measured by means of a micro pipette, of 250-500λ





was added to 3 ml. of buffer in a cuvette tube. The calculation based on a knowledge of the extinction coefficient  $E_{1\text{cm}}^{1\%}$  (see below) is as follows, using a 250  $\lambda$  sample of protein solution.

$$\% \text{ fetuin concentration} = \frac{\text{O.D.} \times 3.25 \times 100}{E_{1\text{cm}}^{1\%} \times 100 \times .25} \quad (22)$$

The instrument used was the DU Beckman spectrophotometer.

Extinction coefficient  $E_{1\text{cm}}^{1\%}$

The procedure is the same as described above for concentration measurement except that in this case the percent protein in the buffer solution is accurately known. The basis for this is the preparation of a solution on a dry weight basis of protein, and it is therefore necessary a priori to determine the moisture content of the pure protein. Samples used were of the solid preparation obtained by freeze-drying, and which had been exhaustively dialyzed against deionized water. Moisture content was determined by drying known weights of the protein from a sufficient sample, part of which was also used to make up a solution on a weight basis. Drying was achieved at 95°C. in a vacuum oven for 18 hrs. At the end of this period the weighing bottles and contents were immediately placed in a desiccator over phosphorous pentoxide and allowed to cool to room temperature. The weighing bottles had previously been so treated before the introduction of protein. From the weight of moist protein used and the loss in weight, the percentage of moisture was calculated. It was then possible to make a correction to the amount weighed for the optical density measurement. By slight transposition of the above equation,  $E_{1\text{cm}}^{1\%}$  was determined.



### Partial specific volume

The experimental procedure requires the accurate measurement by means of a sensitive balance, of the mass of a fixed volume of protein solution for a series of known concentrations of protein. The method follows the usual scheme used in measurements of density. A 10 ml. capped pycnometer of known volume is filled to such a level with protein solution that after equilibration in a thermostatically controlled waterbath, the insertion of the ground glass seal causes a slight overflow of solution. This insures that the container is completely full, and care must be taken that no air bubbles are included in the solution. The side arm is capped, the whole carefully wiped dry and immediately weighed. The concentration of the solution is determined by optical density measurement, and knowing the volume of the pycnometer the mass of the protein can be calculated. The mass of the solution is immediately available and the weight (or mass) fraction  $w_1$  can be found. This is given by the expression

$$w_1 = \frac{\text{mass of protein}}{\text{mass of solution}} .$$

By plotting mass content of pycnometer versus weight fraction according to the equation of Kraemer, the partial specific volume  $\bar{v}$  may be found (95). (See Figure I).

$$(1 - \bar{v}\rho) = \frac{(1 - w_1)}{m} \cdot \frac{dm}{dw_1} \quad (23)$$

The slope of the plot,  $\frac{dm}{dw_1}$  may be obtained and a check is available since the ordinate intercept, known as the solvent point, should give the mass content of the pycnometer filled with pure solvent. The measurements were made at 20°C. in all cases, using



a pycnometer of approximately 10 ml. capacity on fetuin dissolved in phosphate or borate buffer, pH 7.7. Concentrations of the protein used were from circa 0.4-1.5% and the weighings were made to five places using a semi-micro Sartorius balance.

### Sedimentation velocity

The Model L Spinco ultracentrifuge was used at a speed of 59,780 r.p.m. for measurement of this parameter. The temperature of 20°C. (or close to it) was maintained automatically by the temperature control equipment. In most cases, pictures were taken at 16 minute intervals over a period of 64 minutes. For solvents of high viscosity such as 50% ethylene glycol or 80% formamide, the picture interval was increased to 32 minutes. The distance of the concentration gradient peak from the reference line was measured on a Gaertner two-dimensional comparator. The distance of the reference line from the axis of rotation is 5.70 cm. An additional 0.02 cms. is added to this to allow for the expansion of the rotor at high speed. Having divided the measured distances on the plates by the magnification factor of the schlieren optical system (2.138), each distance is added on to the value of 5.72 to give the distance of the gradient from the axis of rotation in cm. The sedimentation coefficient  $S$  of the sedimenting molecule is given by the relation (105) :

$$S = \frac{\frac{dx}{dt}}{\omega^2 x} \quad (24)$$

where  $\frac{dx}{dt}$  = rate of migration at distance  $x$  from axis of rotation,  
 $\omega$  = angular velocity.





Integration of this expression gives:

$$S(t_1 - t_2) = \frac{1}{\omega^2} \left\{ \log_e x_1 - \log_e x_2 \right\}$$

or

$$S = \frac{2.303}{\omega^2 (t_1 - t_2)} \left\{ \log_{10} x_1 - \log_{10} x_2 \right\} \quad (25)$$

where the concentration gradient is a distance  $x$  cms. from the axis of rotation at time  $t$ , and correspondingly  $x_2$  at time  $t_2$ . In order to determine  $S$  (at a fixed temperature  $T$  at the prevailing concentration of protein)  $\log_{10} x$  is plotted vs. time  $t$ , from which the slope  $\frac{\log_{10} x_1 - \log_{10} x_2}{(t_1 - t_2)}$  is readily obtained.

The term  $\left( \frac{2.303}{\omega^2} \right) = 9.786 \times 10^{-10}$  for a speed of 59,780 r.p.m. and multiplication of the slope by this factor gives the sedimentation coefficient under the conditions of the experiment. It is usual to reduce this to  $S_{20,w}$  that is, the value for  $S$  which would be obtained if the temperature of the experiment were  $20^\circ\text{C}$ . and the viscosity and density of the supporting medium were equal to water at this temperature. The equation for this correction is as follows (106):

$$S_{20,w} = S \left( \frac{\eta^\circ_T}{\eta^\circ_{20}} \right) \left( \frac{\eta}{\eta^\circ} \right)_T \frac{(1 - \bar{v} \rho^\circ)_{20w}}{(1 - \bar{v} \rho)_T} \quad (26)$$

The first term in brackets represents the ratio of the viscosity of water at temperature  $T$  of the experiment to that of water at  $20^\circ\text{C}$ ., and constitutes the temperature correction. The second term is the ratio of the viscosity of the supporting medium to that of water at temperature  $T$  and is the viscosity correction. The density correction of the medium is given by the last term where  $\bar{v}$  is the partial



specific volume of the protein in the medium at 20°C. (slight changes in  $\bar{v}$  with temperature are ignored) and  $\rho$  and  $\rho^\circ$  are densities of the medium and water, respectively. The measurement of  $\bar{v}$  has been discussed above and density measurements were either obtained from tables or measured at 20°C. by means of a pycnometer. Throughout this work the value for  $\bar{v}$  measured at pH 7-8 in phosphate or borate buffer has been assumed to be unchanged by pH and solvent composition. This is probably untrue (107). However, provided that selective binding does not occur by one of the components of the system, the differences are likely to be small. Solvent viscosities were usually obtained from the solvent runs of the kinematic determinations of reduced viscosity described below.

#### Sedimentation approach to equilibrium

This method was used throughout for the determination of molecular weight. It involves two distinct runs on the ultracentrifuge, one at 59,780 r.p.m. (as in the normal sedimentation velocity method) and a run at a lower speed usually in the range of 10,000-16,000 r.p.m. in which only after prolonged running does the protein entirely leave the meniscus. The purpose of the first run is to obtain an area which is proportional to the total concentration of protein in the solution ( $c_0$ ) and the purpose of the second is to determine how much has left the meniscus position when running at a constant (lower) speed. For the  $c_0$  value the area is determined directly by use of the two-dimensional comparator by measuring values of ordinates for a fixed increment in abscissa  $dx$ . The area





in "sq. cms." is given by\*

$$\text{Area} = \frac{\sum y dx}{(2.138)^2} \quad (27)$$

On the approach run, ordinates are measured at regular increments from the meniscus and their distance from the base line determined. From these measurements a somewhat lengthy calculation is required in order to calculate  $c_m$  the protein concentration at the meniscus. The ordinate intercept at the meniscus gives the value for  $\frac{dc}{dx}$  also required in the Archibald equation. It is essential that the same bar angle of the schlieren optical system be the same for each run. An angle of  $75^\circ$  was usually used in this work. In measuring the ordinate intercept at the meniscus the picture chosen was the one in which the gradient line appeared to intercept as a straight line projection. If it is curved, the value of  $\frac{dc}{dx}$  may be seriously in error. Similar measurements can be made at the cell bottom but due to uncertainties in measuring the ordinate intercept, these were usually omitted (see Figure J).

The Archibald equation is given by:

$$M_m = \frac{RT}{\omega^2 (1 - \bar{v}\rho)} \cdot \frac{\frac{dc}{dx}}{x_m c_m} \quad (10)$$

and

$$c_m = c_o - \frac{1}{x_n^2} \cdot \frac{dx}{2.138} \cdot \sum z_n x_n^2 \quad (10a)$$

R is the gas constant, and T is the absolute temperature.

---

\*For convenience, all measurements are converted to cm. and sq. cm. The magnification in the  $\frac{dc}{dx}$  dimension is taken as equal to 2.138, the same as for the x direction. This is arbitrary since in the final equation the factor for  $\frac{dc}{dx}$  cancels. This has the advantage that for a given bar angle, protein concentration may be compared on the basis of area.



Details of the method are given in Schachman (96).

Difficulty in measuring the  $c_0$  from the area beneath the gradient curve from the high speed run is sometimes encountered, due to the uncertainty of the true position of the base line. Usually the gradient curve intersects the meniscus a little above the level of the line towards the cell bottom. The base line for measurements of the ordinates is taken at the mid-position (see Figure J). When organic solvents such as formamide are introduced, the intersection at the meniscus appears to be artificially raised. The choice of a "mid" position or the use of a sloping base line, as frequently used in the graphical procedure gives an area which is too small for the concentration of protein. The latter may be evaluated from a separate run in which the organic solvent is absent. It appears that the reliable index for the positioning of the base line is the gradient curve minimum towards the cell bottom rather than the "mid" position. By positioning the horizontal cross line of the comparator above the minimum of the gradient curve and at a distance equal to its thickness, consistent values are obtained. This, in general, corresponds to the "mid" position chosen previously, in the absence of organic solvents, for an ionic strength of 0.16 and a protein concentration of 0.5-0.7%. The ultimate justification for this rests on the fact that over a range of concentrations from 0.5-0.7% of protein in different media, molecular weights for the monomeric material appear to be reproducible within  $\pm 1500$  and that an independent check using sedimentation diffusion also agreed quite closely with the values obtained by the approach to equilibrium method.





### Kinematic viscosity

During a series of measurements the viscometer was left overnight filled with a dilute solution of detergent. Prior to use the detergent was removed and the viscometer washed several times with distilled water. A water pump was used to pull the liquid through the capillary. This was followed by several treatments with acetone, after which it was allowed to dry thoroughly as air is pulled through the capillary by means of the pump. Since all preparations of the protein during preparation had been subjected to an overnight centrifugation at 27,500 r.p.m. to remove the 18S component, additional clarification was not required. The usual procedure was to start with a solution of about 1.2% protein and to make a series of dilutions, the concentration of each being measured by means of the spectrophotometer. The times of flow of each solution was determined in addition to that of the solvents both at the beginning and end of the experiment. For solutions of protein in aqueous buffers, a 5 ml. viscometer of flow time for water of about 9 minutes was used. For solutions to which organic solvents had been added, a 0.5 ml. viscometer was used, with a flow time for water of about 3 min. In either case, a solution flow time of about 10-12 min. was measured. Accurate temperature control was maintained at 20°C. by immersing the viscometer in a thermostated bath (produced by the Scientific Development Company, State College, Pennsylvania). Deviations in flow time for a given solution seldom exceeded 0.3 seconds. Contribution of the protein to density difference between solution and solvent was ignored. From the time of flow of the solvent alone, knowing the calibration constant of the viscometer,





the solvent viscosity required for the sedimentation correction could also be obtained. From the times of flow of solution and solvent the specific viscosity could be obtained and knowing the concentration, the reduced viscosity. This was then plotted as a function of concentration, and by extrapolation to zero concentration, the intrinsic value  $[\eta]$ , evaluated (108).

#### Diffusion measurements

A Spinco Model H electrophoresis diffusion unit was used for this purpose. Prior to use, the protein solution is dialyzed against the buffer solution overnight. The cell is immersed in the temperature controlled bath at 1°C. and following introduction of the protein solution, the buffer is carefully layered on top. This process requires extreme care. Sharpening of the boundary is achieved by positioning the needle used for solution transfer in the appropriate position as viewed through the optical system and making a small withdrawal. The procedure followed is described in detail in Schachman (109). Since protein concentrations used were from circa 0.4-1.0% the areas obtained from the schlieren optical system were conveniently treated by the maximum ordinate method. This involved the use of the two-dimensional comparator much as described under the approach method for molecular weight measurements. The total area beneath two gradient curves was measured and averaged to give an area proportional to the concentration. The maximum ordinate for each picture, taken at a recorded time, was also measured. The data was then treated as follows. Following the calculation of the square of the ordinates, the reciprocals of the squares are plotted vs. time (see Figure K, ordinates in cm.,



time in sec.). The concentration gradient  $\frac{dc}{dx}$  is obtained from the solution to the diffusion equation. The expression is given by (110):

$$\frac{dc}{dx} = \frac{c_o \cdot e^{-\frac{x^2}{4Dt}}}{2\sqrt{\pi Dt}} \quad (28)$$

At  $x = 0$ , i.e.  $\frac{dc}{dx}$  = maximum ordinate, this reduces to

$$\left(\frac{dc}{dx}\right)_{x=0} = \frac{c_o}{2\sqrt{\pi Dt}} = \frac{\int_0^n \left(\frac{dc}{dx}\right) x \, dx}{2\sqrt{\pi Dt}} \quad (29)$$

where  $c_o$  is the concentration of protein in the solution and  $D$  is the diffusion coefficient. It follows that the expression for  $t$  may be written  $t = \frac{A^2}{4\pi D(y_m)^2}$  where\*  $A$  is proportional to  $c_o$

and  $y_m$  to  $\left(\frac{dc}{dx}\right)_{x=0}$ .

From the plot of  $t$  vs.  $\frac{1}{(y_m)^2}$ , the slope  $\frac{A^2}{4\pi D}$  may be obtained from which, knowing  $A$ , the diffusion coefficient  $D$  may be found under the prevailing conditions of temperature and solvent. This apparent  $D$  is then corrected to the value for water at  $20^\circ\text{C}$ . by means of the equation (109):

$$D_{20,w} = D_{\text{Meas.}} \left(\frac{293}{273+T}\right) \left(\frac{\eta}{\eta^\circ}\right)_T \left(\frac{\eta^\circ_T}{\eta^\circ_{20}}\right) \quad (31)$$

---

\*The linear magnification in the  $x$  direction is unity. The  $\frac{dc}{dx}$  factor is taken (arbitrary) equal to this also, since the dimensions of  $\frac{dc}{dx}$  cancel in the final equation.





By plotting  $D_{20,w}$  as a function of concentration, the extrapolated value  $D_{20,w}^{\circ}$  is obtained.

### Optical rotatory dispersion

Values of optical rotation for all protein preparations in the appropriate system was measured as a function of wavelength. A Rudolph Model 260 automatic recording spectropolarimeter was used. The wavelength range covered was 300-650 mμ, using a Xenon compact arc lamp as the light source. Generally a concentration of fetuin from 0.5-0.8% in the various solvent media were examined in 5 cm. path length cells. A symmetrical angle of 5° was used throughout the measurements. The Yang-Doty plot of  $-\lambda^2 [\alpha]$  versus  $-\lambda [\alpha]$ , according to the Drude one term equation, gave linear relations, as is to be expected for a molecule of low helical content. The value of  $\lambda_c$  was determined from the square root of the slope of the function (99). The generalized Moffitt treatment of the optical rotatory data involved the plotting of  $[m^1]_{\lambda}[(\lambda^2 - \lambda_o^2) / \lambda_o^2]$  vs.  $\lambda^2 / (\lambda^2 - \lambda_o^2)$  (100). The mean residue rotation,  $[m^1]$ , was computed on the basis of a mean residue weight of 110 and a refractive index of 1.33. Values for  $a_o$  and  $b_o$  were obtained in the usual fashion from the ordinate intercept and slope, respectively. A value of  $\lambda_o = 205$  mμ was chosen since this gives a linear plot as distinct from a value of 212 mμ, the use of which introduces distinct curvature. (See Results, Part I)



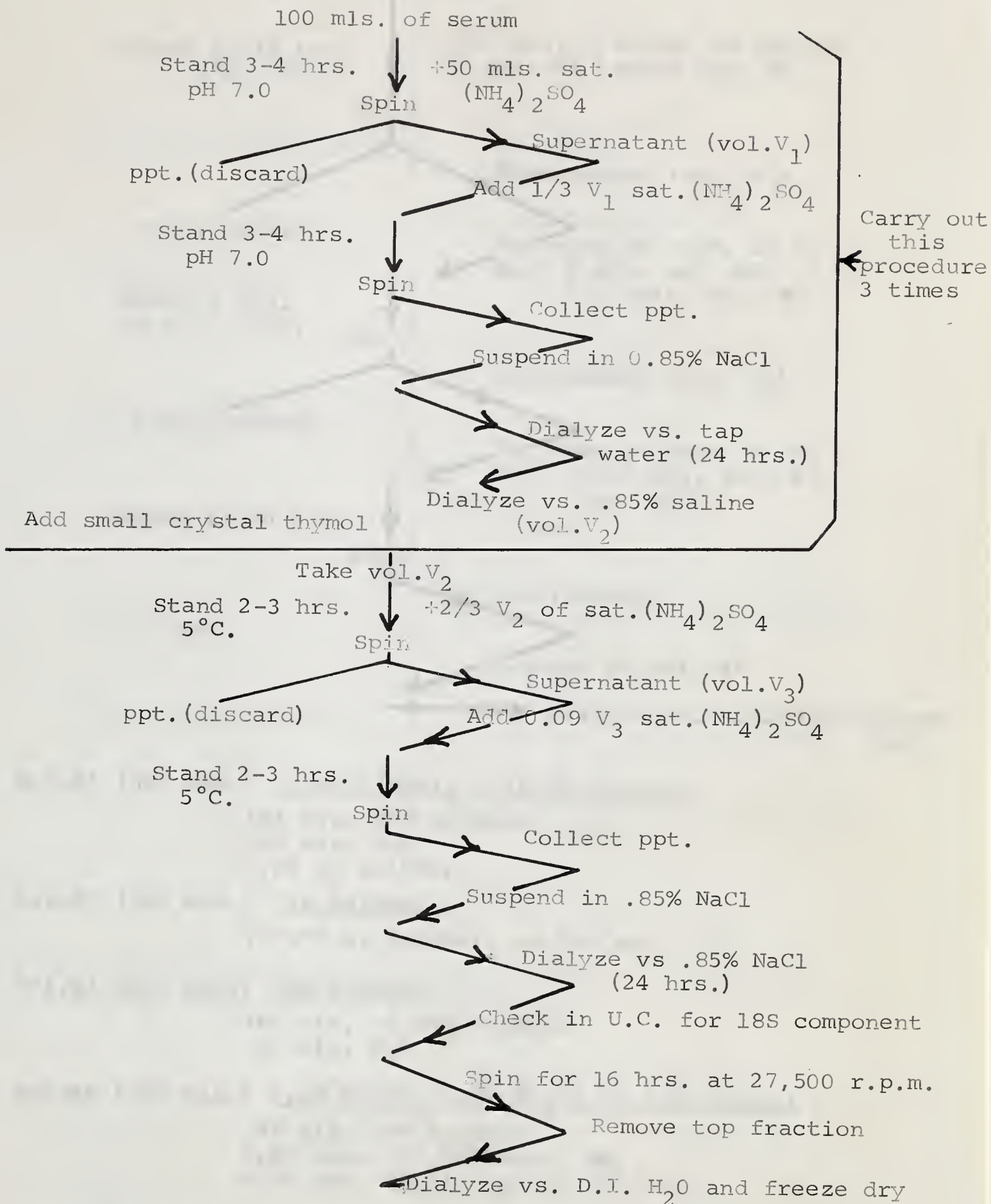
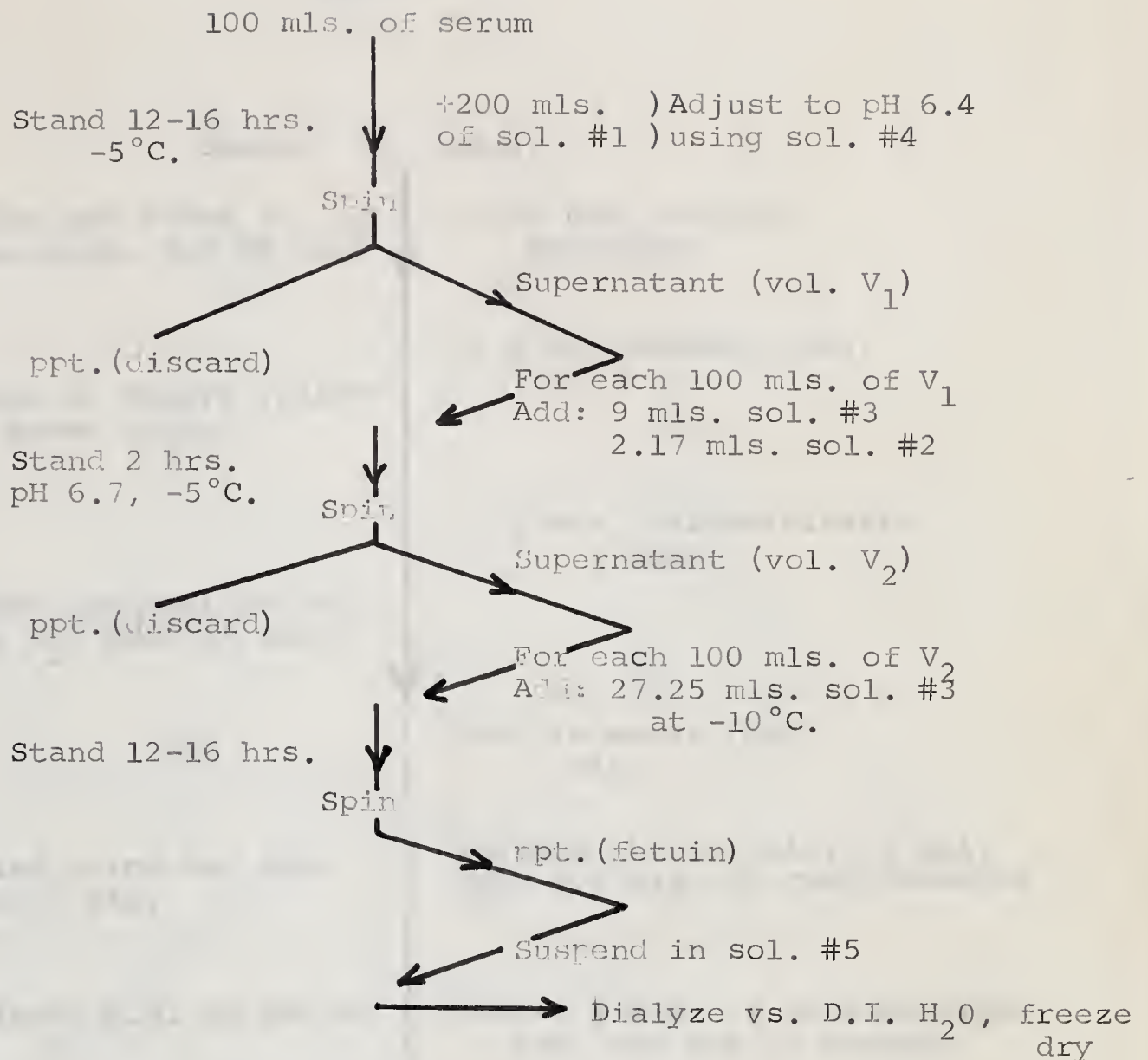


Figure F

$(\text{NH}_4)_2\text{SO}_4$  Fractionation







Sol.#1 (500 mls.) .03M  $Zn(OAc)_2$  + 28.5% ethanol

144 mls. 99% ethanol

356 mls.  $H_2O$

3.29 g.  $Zn(OAc)_2$

Sol.#2 (500 mls.) 1M  $Ba(OAc)_2$

127.75 g.  $Ba(OAc)_2$  to 500 mls.  $H_2O$

Sol.#3 (500 mls.) 95% ethanol

480 mls. of 99% ethanol

20 mls.  $H_2O$

Sol.#4 (250 mls.) 0.5M  $NH_4OH$ , 0.5M  $NH_4Cl$  in 19% ethanol

48 mls. 99% ethanol

7.45 mls. (28.5%) conc.  $NH_3$

6.69 gms.  $NH_4Cl$ ,  $H_2O$  to 250 mls.

Sol.#5 (200 mls.) 0.1M tri Na citrate

6.96 gms. with  $H_2O$  to 200 mls.

Figure G

Ethanol Fractionation



100 ml. of water

4.0 ml. of 10% (A) to 100 ml. of 1% (B) sol. #4

20 ml. of 1% (A) to 100 ml. of 1% (B) sol. #4

20 ml. of 1% (A) to 100 ml. of 1% (B) sol. #4

For each 100 ml. of 1% (A) to 100 ml. of 1% (B) sol. #4

20 ml. of 1% (A) to 100 ml. of 1% (B) sol. #4

20 ml. of 1% (A) to 100 ml. of 1% (B) sol. #4

20 ml. of 1% (A) to 100 ml. of 1% (B) sol. #4

20 ml. of 1% (A) to 100 ml. of 1% (B) sol. #4

For each 100 ml. of 1% (A) to 100 ml. of 1% (B) sol. #4

20 ml. of 1% (A) to 100 ml. of 1% (B) sol. #4

20 ml. of 1% (A) to 100 ml. of 1% (B) sol. #4

20 ml. of 1% (A) to 100 ml. of 1% (B) sol. #4

20 ml. of 1% (A) to 100 ml. of 1% (B) sol. #4

20 ml. of 1% (A) to 100 ml. of 1% (B) sol. #4

20 ml. of 1% (A) to 100 ml. of 1% (B) sol. #4

20 ml. of 1% (A) to 100 ml. of 1% (B) sol. #4

20 ml. of 1% (A) to 100 ml. of 1% (B) sol. #4

20 ml. of 1% (A) to 100 ml. of 1% (B) sol. #4

20 ml. of 1% (A) to 100 ml. of 1% (B) sol. #4

20 ml. of 1% (A) to 100 ml. of 1% (B) sol. #4

20 ml. of 1% (A) to 100 ml. of 1% (B) sol. #4

20 ml. of 1% (A) to 100 ml. of 1% (B) sol. #4

20 ml. of 1% (A) to 100 ml. of 1% (B) sol. #4

20 ml. of 1% (A) to 100 ml. of 1% (B) sol. #4

20 ml. of 1% (A) to 100 ml. of 1% (B) sol. #4

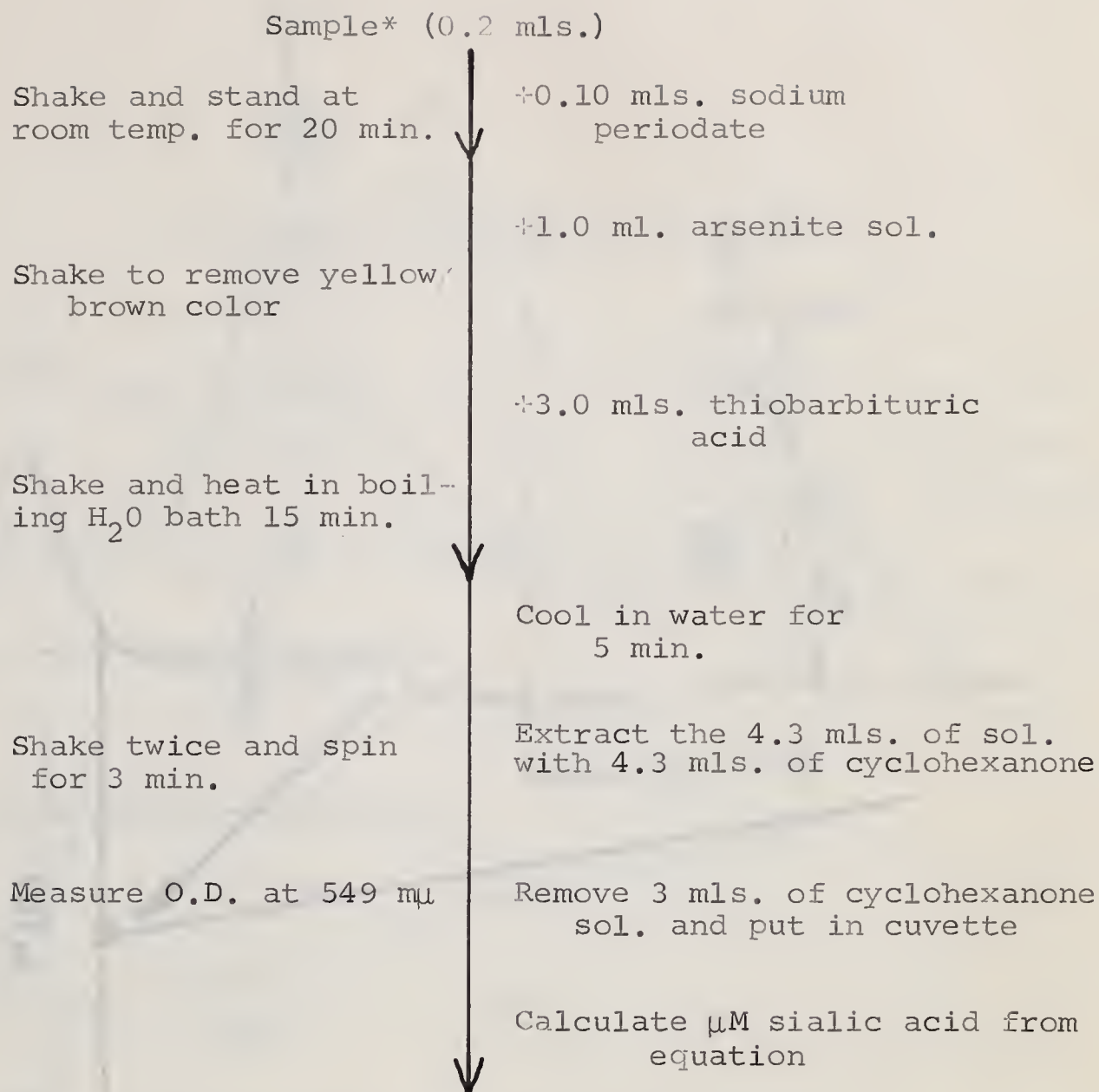
20 ml. of 1% (A) to 100 ml. of 1% (B) sol. #4

20 ml. of 1% (A) to 100 ml. of 1% (B) sol. #4

20 ml. of 1% (A) to 100 ml. of 1% (B) sol. #4

20 ml. of 1% (A) to 100 ml. of 1% (B) sol. #4

20 ml. of 1% (A) to 100 ml. of 1% (B) sol. #4



\*The initial sample should contain from 0.01-0.06  $\mu M$  of N acetyl neuraminic acid/0.2 mls.

Figure H

Analytic scheme for sialic acid (free)

Sample (1) (ml.)

4.15 ml. solution  
added

Shake and allow to  
room temp. for 30 min.

4.15 ml. solution added

Shake to remove yellow  
brown color

4.80 ml. third solution  
added

Shake and wait in dark  
for 20 min. 15 min.

Cool in water for  
5 min.

Shake twice and spin  
for 5 min.

Washed with 4.3 ml. of water  
with 4.2 ml. of cyclohexane

Remove 3 ml. of cyclohexane  
sol. and use for analysis

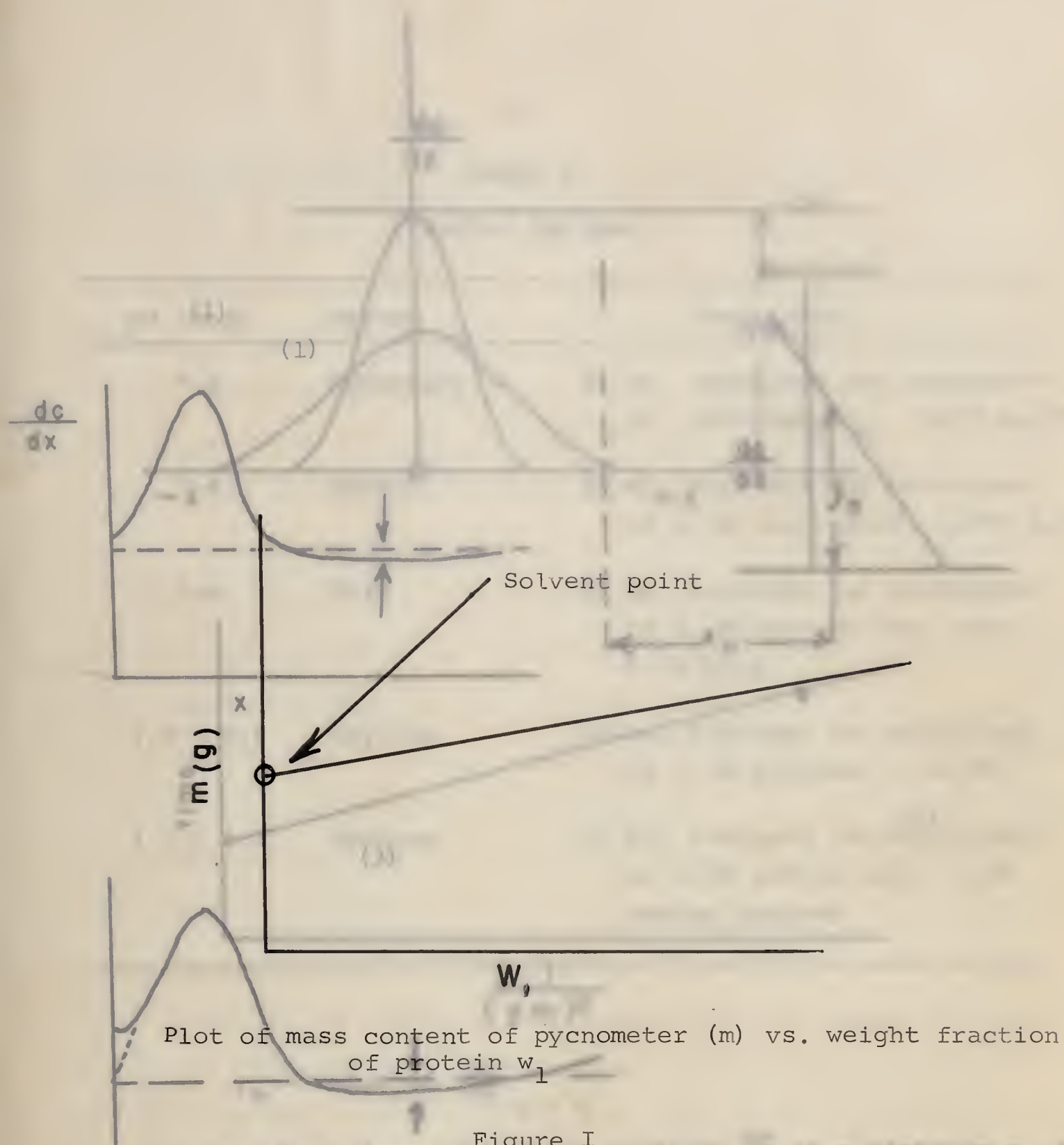
Measure 0.5 ml. of 243 ml

Calculate the amount of  
solution

The initial amount would contain from 0.01-0.05 ml of  
a highly concentrated solution.

Figure 11

Analysis of solution for nitric acid (1957)



Plot of mass content of pycnometer (m) vs. weight fraction of protein  $w_1$

Figure I

$z_n$  = value of concentration at which the curve crosses the y-axis  
 Illustration of Kraemer plot for the determination of partial specific volume.

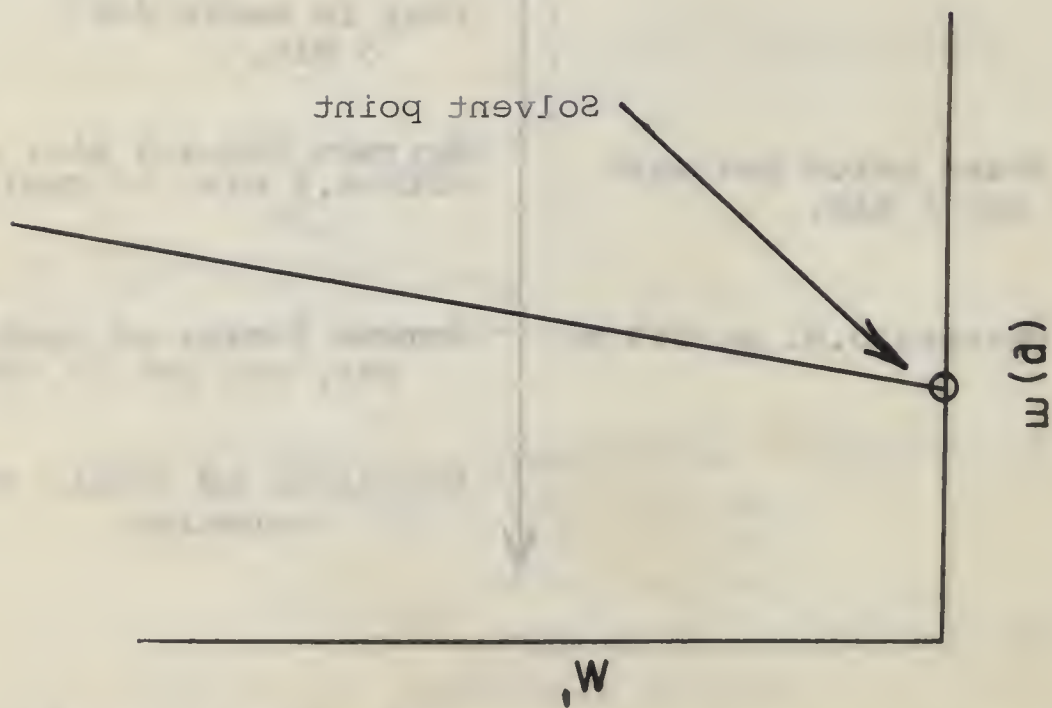
Illustration of the Kraemer plot method for the determination of partial specific volume by the Schlieren method. The plot shows the relationship between the concentration of the solution and the partial specific volume. The curve is a straight line passing through the origin. The slope of the line is the partial specific volume. The y-intercept is the value of the concentration at which the curve crosses the y-axis. (1) High speed centrifugation sometimes leads to the formation of organic solvents during high speed runs.



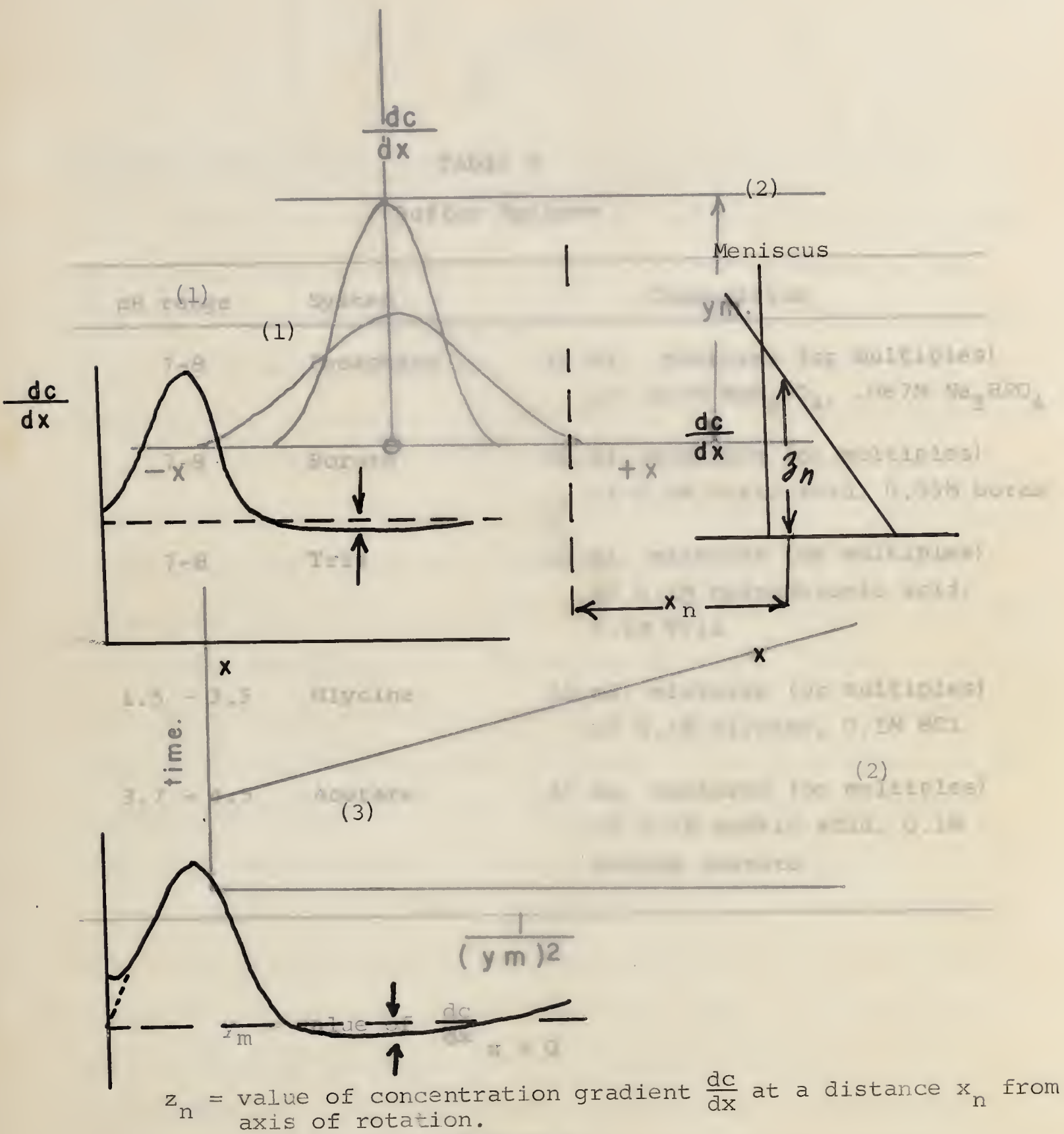
Illustration of Kraemer plot for the determination of partial specific volume.

Figure 1

Plot of mass content of pycnometer (m) vs. weight fraction of protein  $w_1$







- Illustration of the concentration gradient curves produced by the schlieren optical system during the approach to equilibrium method for molecular weight determination.
- (1) High speed run for c; (2) Approach run; (3) Meniscus distortion sometimes encountered in the presence of organic solvents during high speed run.

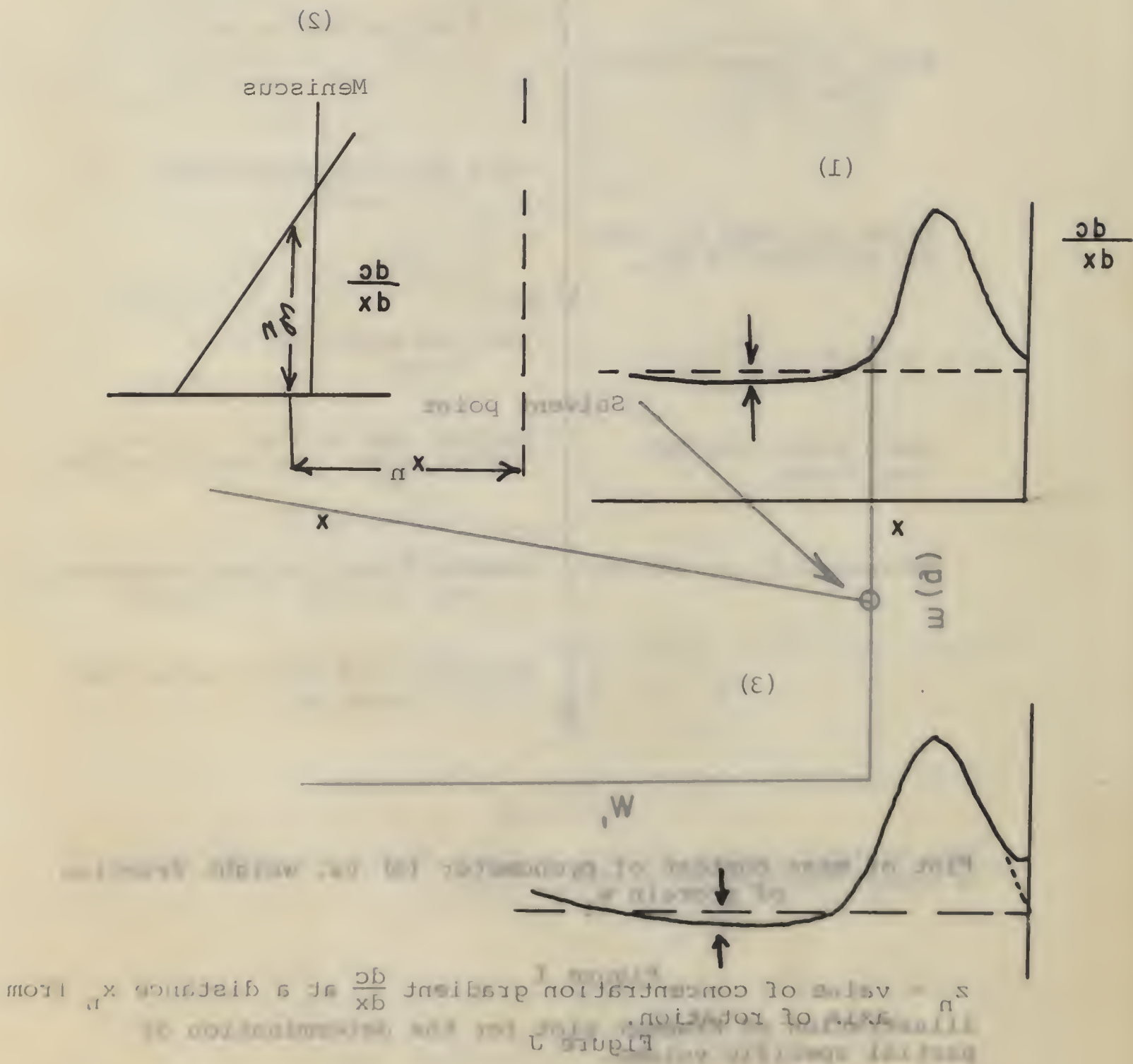
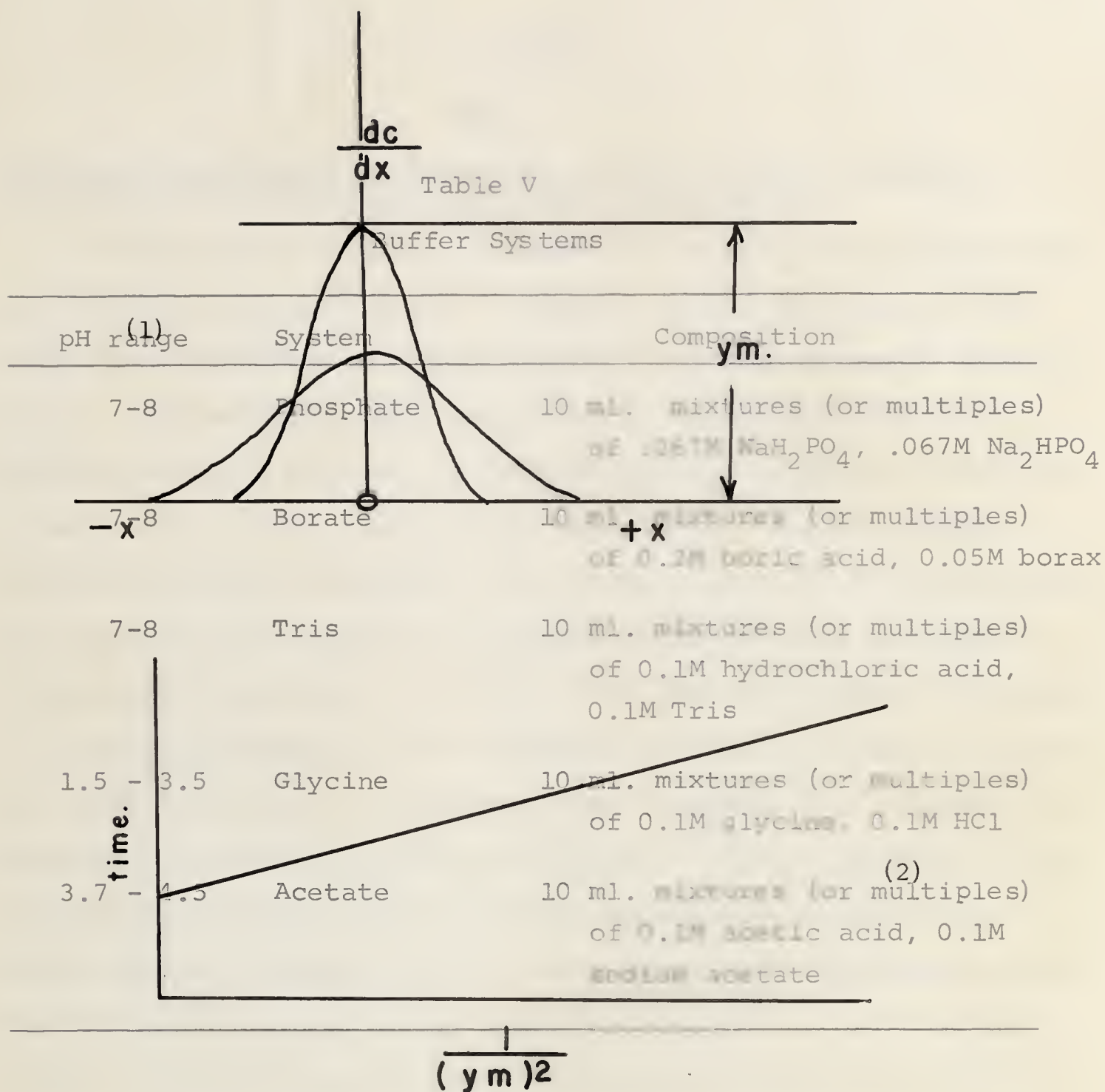


Illustration of the concentration gradient curves produced by the schlieren optical system during the approach to equilibrium method for molecular weight determination. (1) High speed run for  $c$ ; (2) Approach run; (3) Meniscus distortion sometimes encountered in the presence of organic solvents during high speed run.



$$y_m = \text{value of } \frac{dc}{dx} \text{ at } x = 0$$

Figure K

- Illustration of the concentration gradient curves produced
- (1) by the schlieren optical system during diffusion;
  - (2) Plot of maximum ordinate method for determination of the diffusion coefficient.



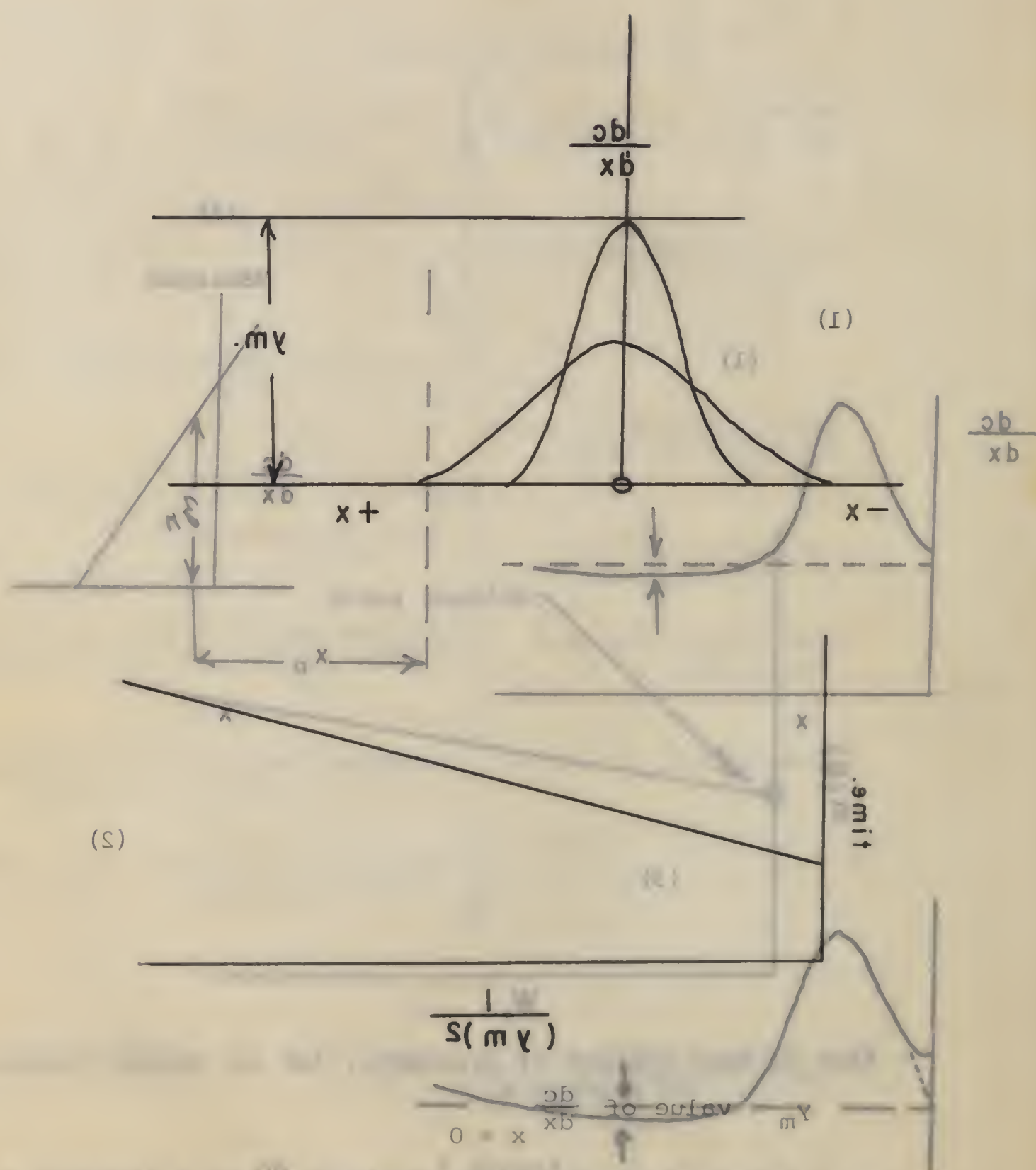


Figure K

Illustration of the concentration gradient method for determination of the diffusion coefficient. (1) Plot of maximum ordinate method for determination of the diffusion coefficient. (2) Plot of concentration gradient method for determination of the diffusion coefficient.

Table V  
Buffer Systems

pH range	System	Composition
7-8	Phosphate	10 ml. mixtures (or multiples) of .067M $\text{NaH}_2\text{PO}_4$ , .067M $\text{Na}_2\text{HPO}_4$
7-8	Borate	10 ml. mixtures (or multiples) of 0.2M boric acid, 0.05M borax
7-8	Tris	10 ml. mixtures (or multiples) of 0.1M hydrochloric acid, 0.1M Tris
1.5 - 3.5	Glycine	10 ml. mixtures (or multiples) of 0.1M glycine, 0.1M HCl
3.7 - 4.5	Acetate	10 ml. mixtures (or multiples) of 0.1M acetic acid, 0.1M sodium acetate





## IV. RESULTS

### Part I

#### Molecular properties of fetuin at pH 7-8, pH 2-4, and some correlation checks between different preparations

This section gives an account of the behaviour of both salt and ethanol prepared fetuin in certain buffer systems, pH 7-8, from the standpoint of hydrodynamic and optical rotatory measurements. Sedimentation and viscosity in conjunction with the determination of partial specific volume and molecular weight are interpreted through the Scheraga Mandelkern relation. This enables the size and shape of the protein molecule to be expressed in terms of the effective volume and axial ratio of its hydrodynamically equivalent ellipsoid. The optical rotatory dispersion is treated according to the Yang-Doty method for simple dispersion and from the values of the dispersion constant,  $\lambda_c$ , inferences are made with regard to secondary structure. This is extended by the generalized Moffitt treatment where alterations in secondary structure are reflected in the slope term,  $b_0$ . Additional hydrodynamic measurements in the isoelectric region of both preparations (ca. pH 2-4) confirm the associative properties of the molecule. In addition to the commercial (salt precipitated) material used for much of the initial characterization, two preparations of salt fractionated and three of ethanol fetuin were prepared from fetal blood. Checks of molecular weight and



sedimentation were used routinely on the different preparations and usually the preparations behaved in similar fashion. Included in this first section are some additional checks on the overall reproducibility observed throughout this work. Photographs from runs of electrophoresis, diffusion, sedimentation velocity and approach data for commercial and ethanol fetuin are shown in Plates A to E.

#### Molecular properties of monomeric fetuin

That the  $S_{20,w}$  values of the commercial preparation of fetuin are influenced by the composition of the buffer medium at pH 7-8 is shown in Figures 1 and 2 which present the  $S_{20,w}$  versus  $c$  plots in the four buffer systems: tris, phosphate, borate, and borate + calcium acetate. Figure 1 also includes a plot in acetate, pH 5.5. Noteworthy is the increased slope in the borate system which may reflect an increased asymmetry in this medium. Addition of certain salts to the borate system results in a decreased slope and an increase in intrinsic sedimentation; of the various salts tested, the most effective in this regard was calcium acetate at approximately 0.1 M. A similar effect is shown in Figure 3 for fetuin in tris buffer where a maximum  $S_{20,w}$  is observed at 0.1 M addition of calcium chloride.

The equations for  $\eta_{red}$  in the case of commercial fetuin are as follows: for the phosphate,  $6.0 + 0.6 c$  (ml./gm.) and borate + 0.1 M calcium acetate system,  $6.0 + 0.8 c$  (ml./gm.) where  $c$  is in gm./100 ml.), and for the tris and borate systems,  $\eta_{red} = 7.3 + 0.8 c$  (Figures 4 and 5). The effect of added





calcium acetate to the borate system indicates a drop in viscosity to that comparable with phosphate. The influence of the addition of calcium chloride to the tris system on the reduced viscosity is also shown in Figure 3, where a minimum  $\eta_{\text{red}}$  is obtained with 0.1 M calcium chloride.

On the assumption that the molecular weight of the particle does not change, these differences in  $S_{20,w}$  and  $\eta_{\text{red}}$  may be interpreted as the result of a change in shape of the molecule in the different media. That no gross change in molecular weight occurs is demonstrated by essentially constant values obtained from sedimentation approach to equilibrium studies in each of the buffer systems (see Table 1). In particular, in the borate and borate +  $\text{CaAc}_2$  systems where the greatest changes in  $S_{20,w}^\circ$  and  $[\eta]$  are observed, the molecular weight appears to be constant within experimental error. Values obtained in the two systems are  $44,320 \pm 1500$  and  $43,420 \pm 1500$ , respectively, which are rather lower than some published measurements for this protein (66,57) but in good agreement with the values of Deutsch (58) and Kay and Marsh (67).

Table 1 summarizes the intrinsic values observed from the above experiments and records the values for frictional and axial ratios according to the Scheraga Mandelkern relation (89). Values of axial ratio thus calculated vary from unity to about 6:1. Estimates of effective volume from this data indicate that the value of this parameter in phosphate buffer, viz., 2.4 ml./gm. is  $\sim$  double that in the other systems. Additional parameters



determined on the commercial material are also included in Table 1. Further evidence that some type of conformational change occurs on the addition of calcium acetate to fetuin in the borate system is illustrated in Figure 6, by the difference in slope obtained in the Yang-Doty plot for these media. The addition of the salt to the borate system lowers  $\lambda_c$  from 230 to 216 m $\mu$ . This is reflected in a change of  $b_0$  in the Moffitt treatment, where this quantity increases from  $-102^\circ$  to  $-42^\circ$  (Figure 7).

Results of sedimentation checks in the phosphate and borate systems on fetuin isolated from the same sample of blood serum by the  $(\text{NH}_4)_2\text{SO}_4$  and ethanol methods show that the material isolated by the former method behaved as expected, i.e. in the same manner as the commercial material prepared in the same way (see Table 1, asterisk values). The phosphate values appeared to be a little low for some reason, although the borate values fell on the plot of the commercial material (Figure 18). The difference in slope in the two buffer systems was also exhibited by the ethanol separated material (Figure 8). It may be noted that our value of 3.10S for  $S_{20,w}^\circ$  in phosphate buffer, ionic strength 0.16, for ethanol prepared material is lower than the 3.47S reported by Spiro, in which his supporting medium consisted of 80% NaCl (66).

Subsequent preparations of ethanol material from fresh samples of blood serum were used for the determination of additional parameters, and these are included in Table 2. For ethanol material in borate,  $\eta_{red} = 8.0 + 1.0 c$  while in phosphate,  $\eta_{red} = 6.65 + 1.35 c$  (Figure 9). The substitution of





80% NaCl in the latter system to maintain an ionic strength of 0.16 did not influence the viscosity from that in the buffer composed entirely of the buffering ions (Figure 19). Further, the intrinsic values of  $\eta_{\text{red}}$  appear to be a little higher than the corresponding values for commercial fetuin. Addition of calcium acetate to the borate system produced a drop in  $\eta_{\text{red}}$  as noted previously (Figure 19).

The value of  $\eta_{\text{red}}$  in phosphate, 6.65 ml./gm., is lower than that of 7.8 quoted by Spiro (66). The values of  $\beta$  calculated from the Scheraga Mandelkern relation were correspondingly lower, giving in our case a frictional ratio close to unity. Extinction coefficients for fetuin prepared by both methods gave for  $E_{1\text{cm}}^{1\%}$  a value close to 4.5 in each case. As in the case of commercial fetuin, ethanol prepared fetuin appears to give reproducible Yang-Doty plots from optical rotatory measurements (Figure 20). The ethanol material gives lower values for  $\lambda_c$  and higher values for (negative) specific rotation (Figure 10). The difference in optical rotatory behaviour between commercial and ethanol material is brought out more clearly by the Moffitt treatment (Figure 11). In phosphate buffer a value of  $-120.5^\circ$  for  $b_0$  is recorded for the former material while the latter gives a value of only  $-61.0^\circ$ , suggesting that ethanol treatment may have resulted in partial denaturation of the molecule. The Kraemer plots of partial specific volume for commercial fetuin in phosphate and ethanol in borate are also shown (Figure 15). Values close to 0.70 ml./gm. were obtained in each case.





### Molecular properties of associated fetuin

Plots of  $S_{20,w}$  as a function of pH for the two preparations of protein are shown in Figure 16 and plots of  $\eta_{red}$  versus pH in Figure 17. The measurements were carried out in glycine/HCl buffer over the pH range 1.5-4.0. Maxima occur for both preparations in the curves of sedimentation and viscosity at approximately pH 2.5 and pH 2.0, respectively. The simultaneous increase in sedimentation and viscosity is indicative of an increase in molecular weight above that at pH 7-8. This is in contrast to the effect noted earlier on the addition of calcium acetate to the borate system, where a shape change was inferred as a result of these parameters shifting in opposite directions. The maxima for  $\eta_{red}$  and  $S_{20,w}$  using commercial fetuin are 11 ml./gm. and 4S, respectively. Confirmation of this observation was achieved by the Archibald method which gave a molecular weight average of  $118,300 \pm 3000$  at pH 3.0. Although the ethanol preparation also showed an increase in molecular weight to  $70,850 \pm 1500$  at pH 3.5 (compared with 94,850 under the same conditions for the salted out material), its behaviour was different, consistently lower values of sedimentation being obtained. Noteworthy, however, is that at pH 2.3 corresponding to the pH where a maximum  $S_{20,w}$  was obtained for this preparation, the molecular weight increased to a value comparable with salt fractionated material. At pH 3.5, the association is a reversible process for the commercial material, at least, and may be generally true; dialysis with the appropriate buffer at pH 7-8 will restore sedimentation values



to those characteristic of the latter pH. While as a rule only one peak is observed in the concentration gradient curve on ultracentrifugation, skewing is occasionally encountered, and doubtless reflects a generally inhomogeneous product at pH values in the proximity of the isoelectric point. Some weight average molecular weights as determined by the Archibald method for the two preparations in the isoelectric region are summarized in Tables 1 and 2 in addition to molecular weights determined for monomeric material at pH 7-8.

As a check on the values of molecular weight obtained at pH 7-8 by the Archibald method, the diffusion coefficient was determined at two concentrations, in borate buffer, pH 8.0, for commercial material. The maximum ordinate plots of  $\frac{1}{y^2}$  vs. time for the two runs are shown in Figures 12 and 13. Also shown in Figure 14 are the coefficients corrected to water at 20°C. and the plot extrapolated to infinite dilution. An extrapolation of two points cannot be considered very accurate. However, for the value of  $D_{20,w}^{\circ}$  of  $6.07 \times 10^{-7}$  obtained with commercial material in borate and the corresponding  $S_{20,w}^{\circ}$  of 3.30, the molecular weight of 44,050 obtained is in good agreement with the Archibald values. Of the two points used in the phosphate plot, the one at 1% concentration is for commercial material, the other at 0.3% is ethanol material. Other than as an approximate check, there is no real justification for extrapolation of these values. Since, however, the sedimentation viscosity behaviour of commercial and ethanol material is very similar, it is to be expected that the diffusion values would be similar. It is not, therefore,





surprising that the extrapolated value of  $5.78 \times 10^{-7}$  obtained for  $D_{20,w}^{\circ}$  in phosphate and an average value of 3.10 for  $S_{20,w}^{\circ}$ , gives a molecular weight of 43,280, also in good agreement with the other values. Further, the marked concentration dependency of the borate plot as distinct from the low slope obtained in the phosphate case confirms the picture obtained by sedimentation and viscosity methods. It also discounts the likelihood of secondary charge effects in centrifugation due to a negative electrostatic potential gradient set up by sedimentation of the  $B_4O_7^{=}$  ion which appears to be the one responsible for the steep slope of the sedimentation plot in the borate system.

### Discussion

A comparison of the hydrodynamic parameters of salt fractionated fetuin with those of the protein prepared by the ethanol method indicates a close similarity. In particular, the differences observed from one buffer system to another are duplicated irrespective of the method of preparation. If, from these differences, conformational changes are inferred, then such changes are apparently exhibited by either material. In the borate system, numerous salts added to concentrations between 0.1 and 0.5 M will influence the sedimentation behaviour; of the ones tested, calcium acetate or  $CaCl_2$  appears to be most effective in decreasing the slope, in part, to that found in the phosphate system, sodium acetate exerting an intermediate effect. This effect appears to be similar to the observed behaviour of fetuin in tris buffer, on the addition of  $CaCl_2$  or  $MgCl_2$  at approximately 0.1 M, in that an increase in  $S_{20,w}$  is accompanied



by a decrease in  $\eta_{red}$ . Of interest also is that in acetate buffer alone, the  $s$  vs.  $c$  plot closely parallels that in borate +  $CaAc_2$ . In this case, however, the addition of calcium salts has no effect. Such behaviour suggests that the presence of certain ions induces a more compact conformation, either by a decrease in axial ratio or a decrease in effective volume. Treatment of the data according to the Scheraga Mandelkern  $\beta$  function shows that the equivalent hydrodynamic ellipsoid does not exhibit a change in axial ratio on addition of calcium acetate to the borate system. It does, however, show a decrease in effective volume from 1.34 to 0.99 ml./gm., suggesting that possibly the molecule has lost part of its bound water. This might result from a reorientation of charge on the external sialic acid groups, believed to bind anions (66), due to the presence of the added salt.

While the behaviour in tris buffer parallels that in borate the application of Scheraga Mandelkern treatment gives a  $\beta$  value in phosphate for the equivalent hydrodynamic ellipsoid of 2.02, somewhat less than the minimum value of 2.12 expected for an equivalent sphere. Furthermore, the effective volume has increased considerably from a value of 1.34 (in tris and borate) to 2.4 ml./gm. in the phosphate buffer. Values of  $\beta$  less than 2.12 are not unknown and may be interpreted as due either to experimental errors in the measured parameters (109) or to limitations in the validity of the Scheraga Mandelkern relation for low axial ratios of the equivalent ellipsoid (111).





In phosphate then, the results suggest a more symmetrical conformation of the fetuin molecule resulting from, or at least accompanied by a considerable increase in hydration. Other experiments implicate the  $B_4O_7^{=}$  ion as being involved in the increased concentration dependency of sedimentation in the borate system, suggesting that while the molecule shows exceptional behaviour in phosphate, this may in fact be more representative of the natural conformation of the native molecule in the absence of added ions.

The parameters arising from the optical rotatory dispersion measurements are of interest since the changes in effective volume  $V_e$ , parallel the changes in  $b_o$  and  $a_o$  derived from the Moffitt treatment. Values close to 230  $m\mu$  obtained from the Yang-Doty plots for commercial material suggest a content of about .15% helix which is compatible with  $b_o$  values of about  $-120^\circ$ , when a value of  $\lambda_o = 205 m\mu$  is used to describe the Moffitt plot. Although the choice of this value of  $\lambda_o$  was based on a requirement for linearity (Figure 21), implicit in the treatment of molecules showing simple Drude dispersion, by the Moffitt plot, is that  $\lambda_o$  should be the value of  $\lambda_c$  for the disordered chain. A  $\lambda_c$  value of  $206 \pm 2 m\mu$  for sialic acid free material has in fact been obtained (see Part III) and which gives a  $b_o$  term sensibly equal to zero. It is not therefore unreasonable to regard changes in  $b_o$  as representative of changes in secondary structure and that these changes are concomitant with alterations in effective volume. If, however, as may be the case, changes in  $V_e$  are a result of changes in hydration, it is not impossible



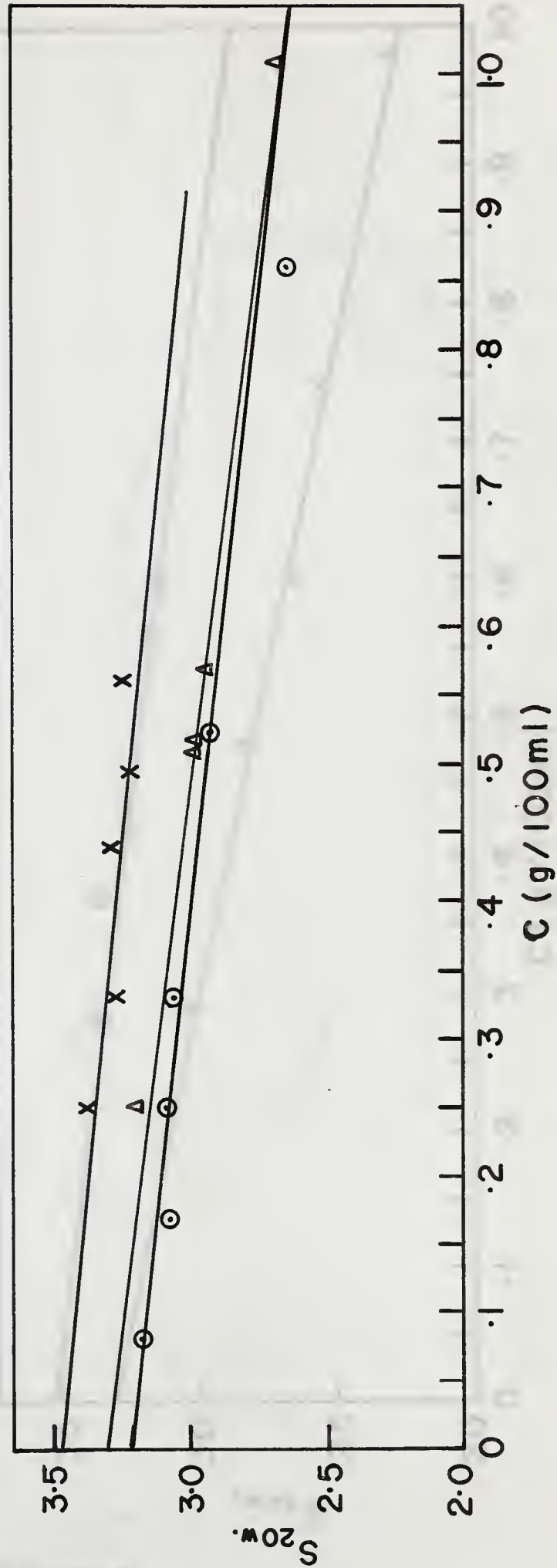


that variations in solvent interaction with the molecule could cause changes in rotation, resulting in different  $b_o$  values, which are not expressions of changes in % helix.

It is also evident from the lower (-ve) values of  $b_o$  and higher (-ve) values of  $a_o$  exhibited by ethanol prepared fetuin in both the phosphate and borate systems that this material is markedly different from the salt prepared protein. Of interest is that although the  $V_e$  decreases with  $-b_o$ , it does not bear any absolute relationship with the values for salt prepared fetuin. This suggests that while the effective volume is probably related to  $b_o$ , this parameter is not an expression of  $V_e$  due to variable solvation, but does in fact represent a measure of helical content. If this is so, we have the attractive picture of a molecule which can exhibit changes in shape and effective volume in the presence of certain ions while exhibiting concomitant changes in secondary structure.

With regard to hydrodynamic measurements of both preparations in the isoelectric region these confirm the earlier reports that association takes place; the increase in both  $S$  and  $\eta$ , supported by measurements of molecular weight, suggest possible dimers and trimers as the associating units. Here again, the ethanol material differs from the other material in that different values of molecular weight are obtained at a given pH, suggesting that whatever structural difference exists between these two preparations, it alters the pH dependency of this process. The associative capacity of ethanol material is unchanged, however, since a molecular weight of ca. 120,000 is obtained at the lower pH of 2.3 corresponding to a maximum value of  $S_{20,w}$  for this material.

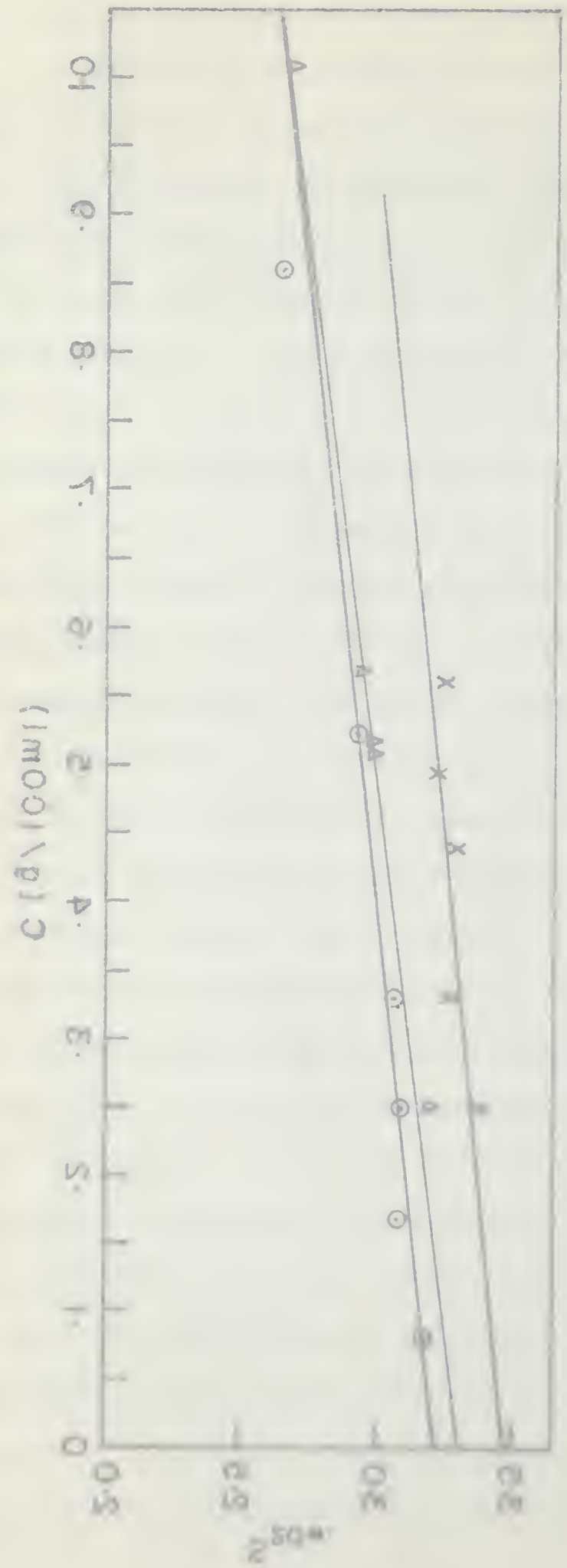




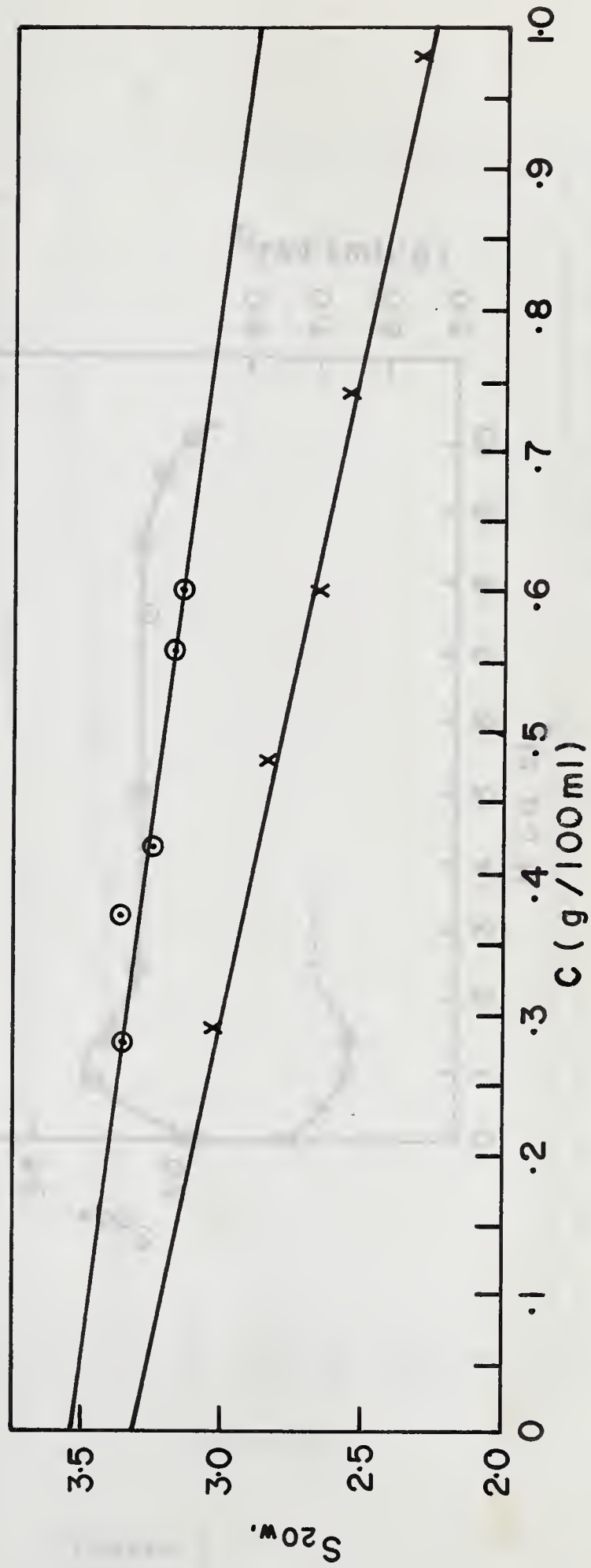
$S_{20,w}$  vs. concentration of commercial (Colorado) fetuin in Tris buffer, pH 8.0,  $\mu = 0.1$  ( $\Delta$ ); phosphate buffer, pH 7.9,  $\mu = 0.16$  ( $\odot$ ); acetate buffer, pH 5.5,  $\mu = 0.1$  ( $x$ ).

Figure 1

Fig. 1. Dependence of the rate of polymerization on the concentration of the monomer. The reaction was carried out at 25°C. The data were obtained from the experiments of [1].







$S_{20,w}$  vs. concentration of commercial (Colorado) fetuin in Borate buffer, pH 8.0,  $\mu = 0.16$  (x); borate + 0.1 M calcium acetate, pH 8.0 (O).

Figure 2

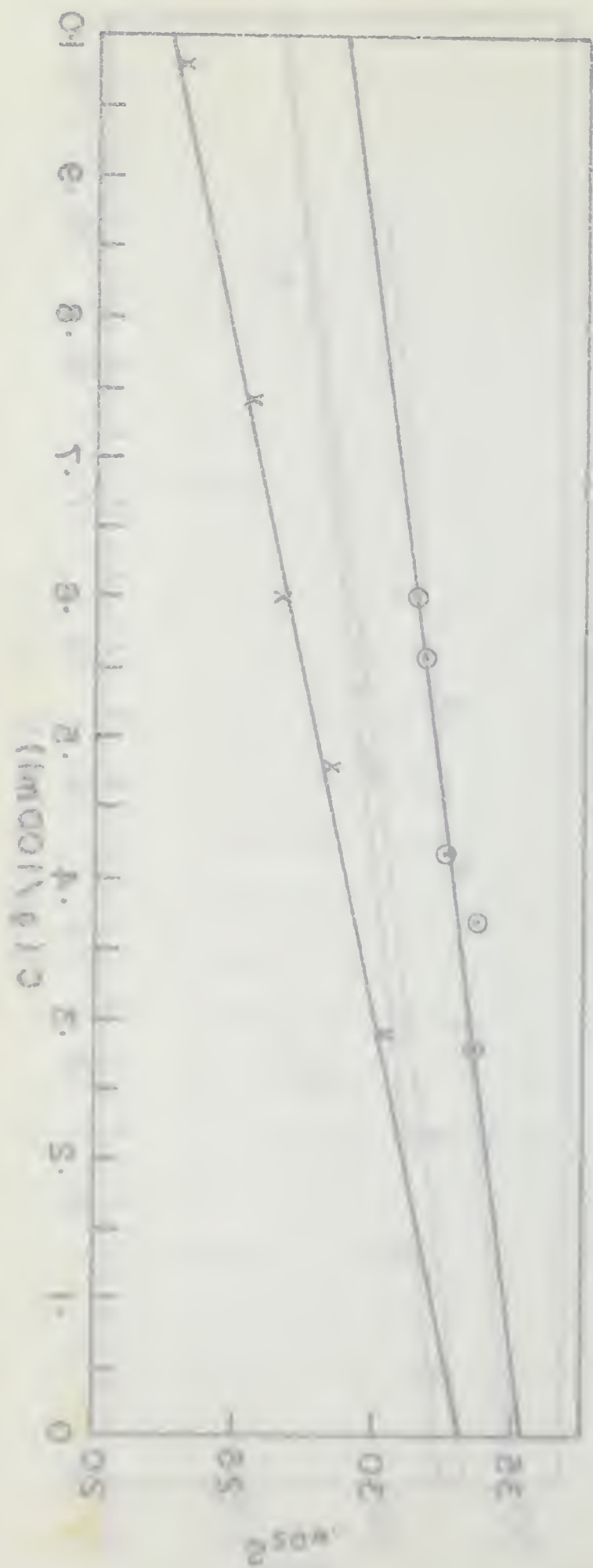
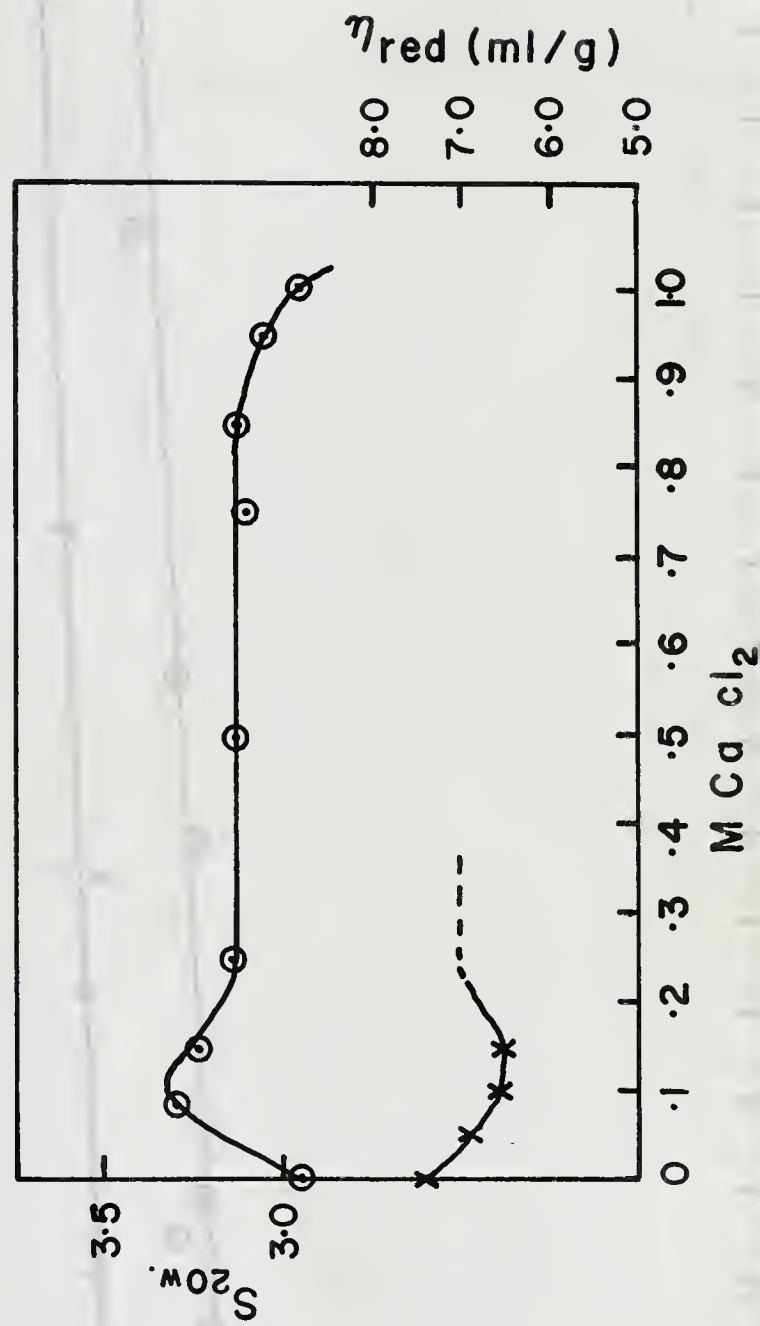


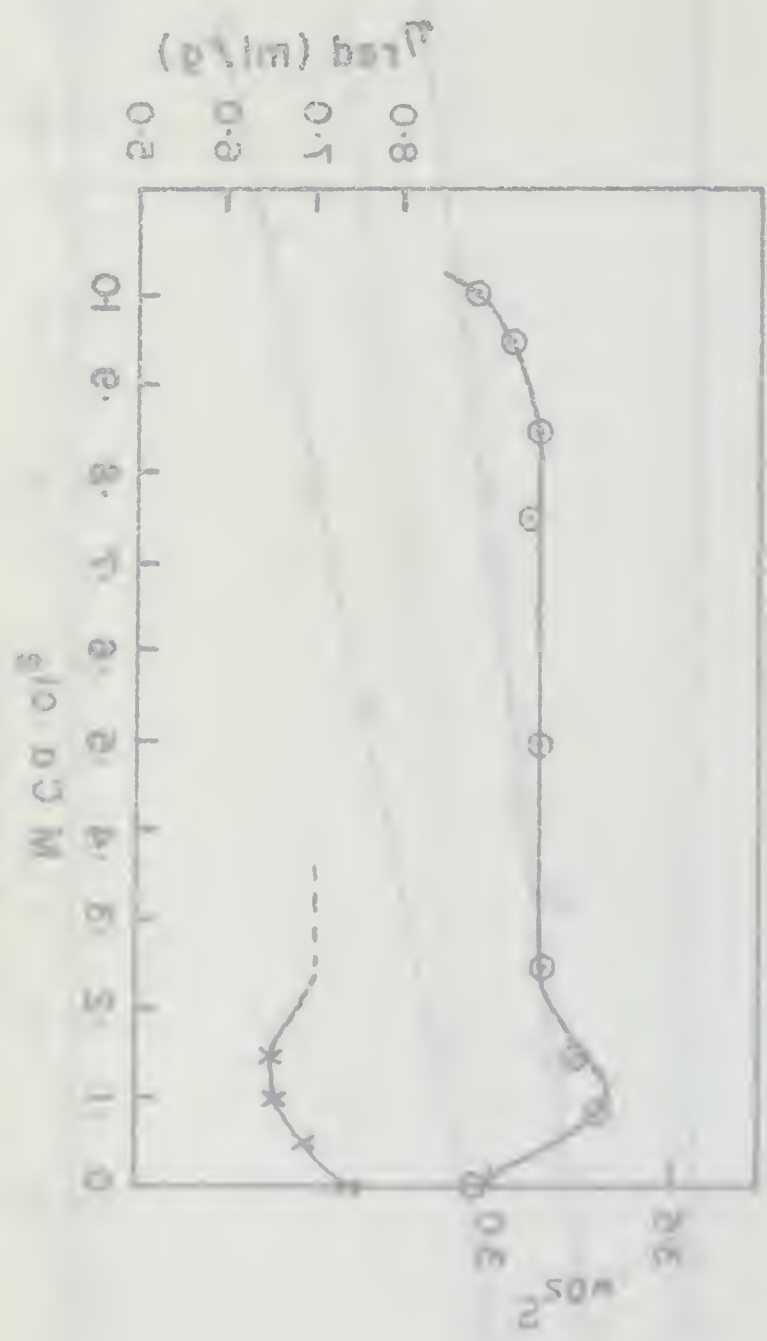
Fig. 1. Logarithm of the rate constant ( $\log k$ ) versus the inverse of temperature ( $1/T$ ) for the reaction of nitrobenzene with sodium hydroxide. (a)  $0.1 \text{ mole/l}$ ; (b)  $0.2 \text{ mole/l}$ ; (c)  $0.5 \text{ mole/l}$ .

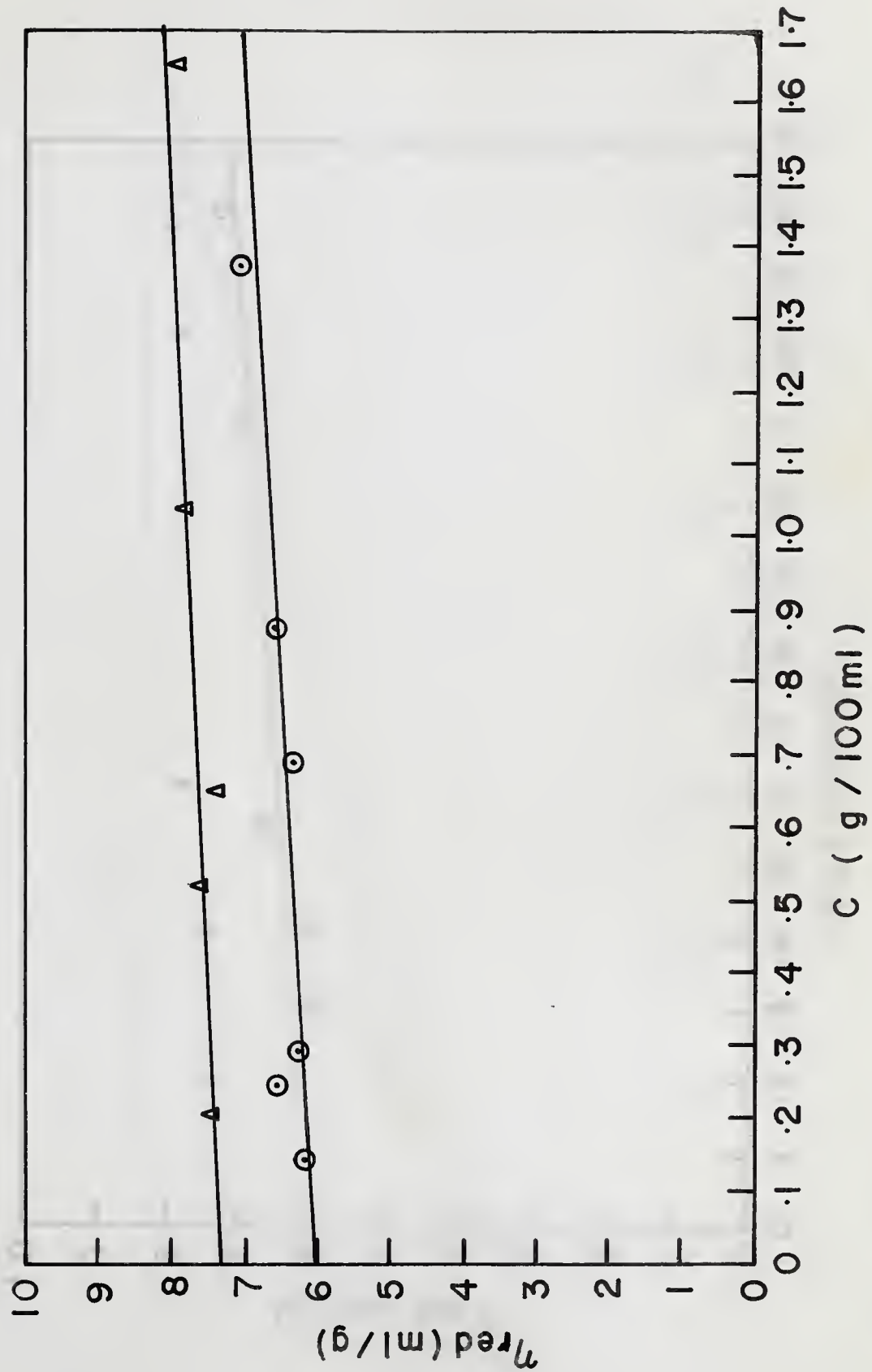


$S_{20,w}$  vs. concentration of calcium chloride for commercial (Colorado) fetuin, 0.51% in Tris buffer, pH 8 (O); and  $\eta_{red}$  values for 0.66% fetuin (x).

Figure 3

(2)  $\mu$  (cm<sup>2</sup>/V-sec) vs.  $\log C$  (mole/l) for the system  $\text{H}_2\text{O} - \text{H}_2\text{SO}_4$  at 25°C. The values of  $\mu$  are given in Table I. The values of  $\mu$  are given in Table I.



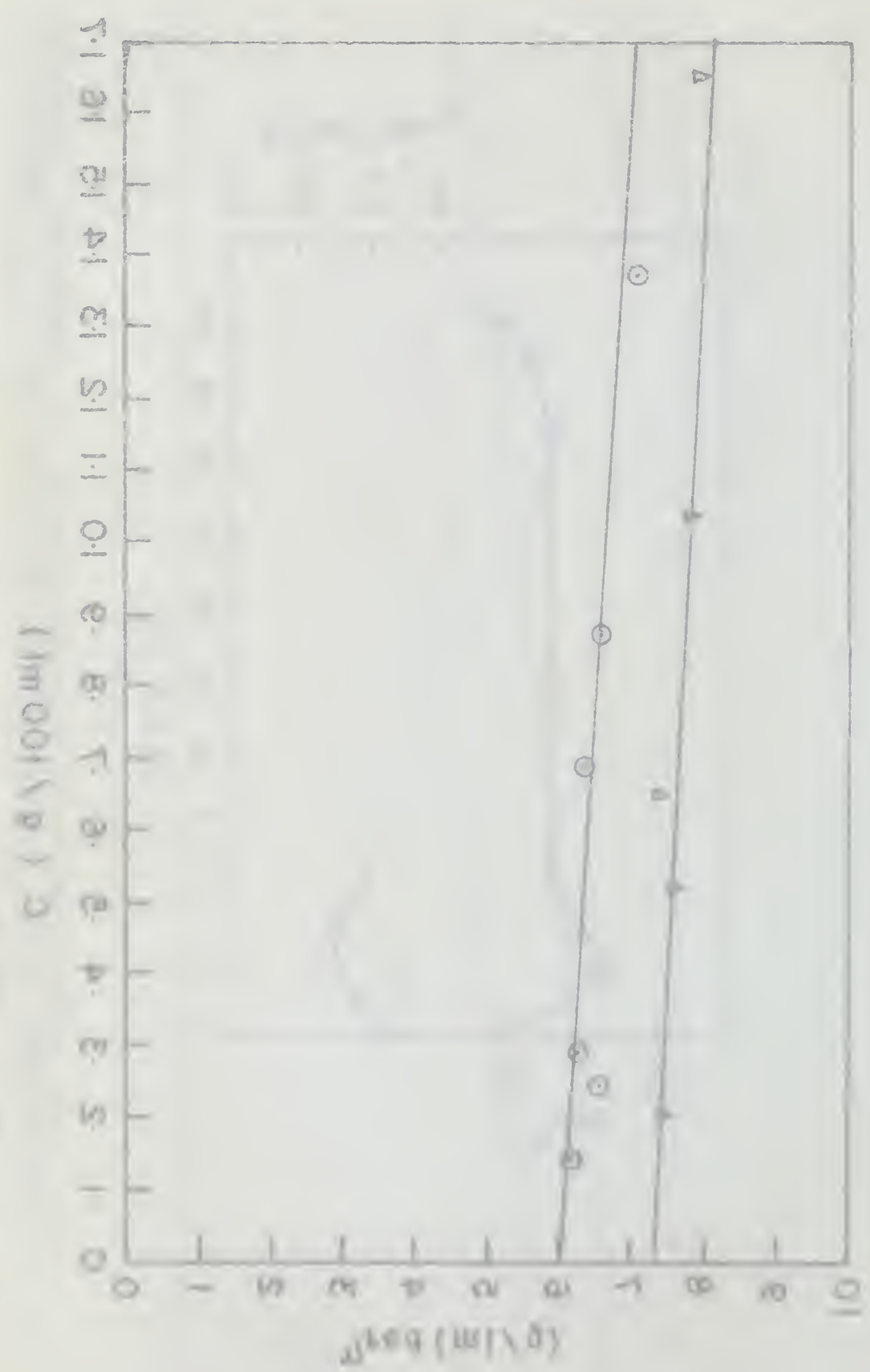


$\eta_{red}$  vs. concentration of commercial (Colorado) fetuin in Tris buffer, pH 8.0,  $\mu = 0.1$  ( $\Delta$ ); phosphate buffer, pH 7.9,  $\mu = 0.16$  ( $\odot$ ).

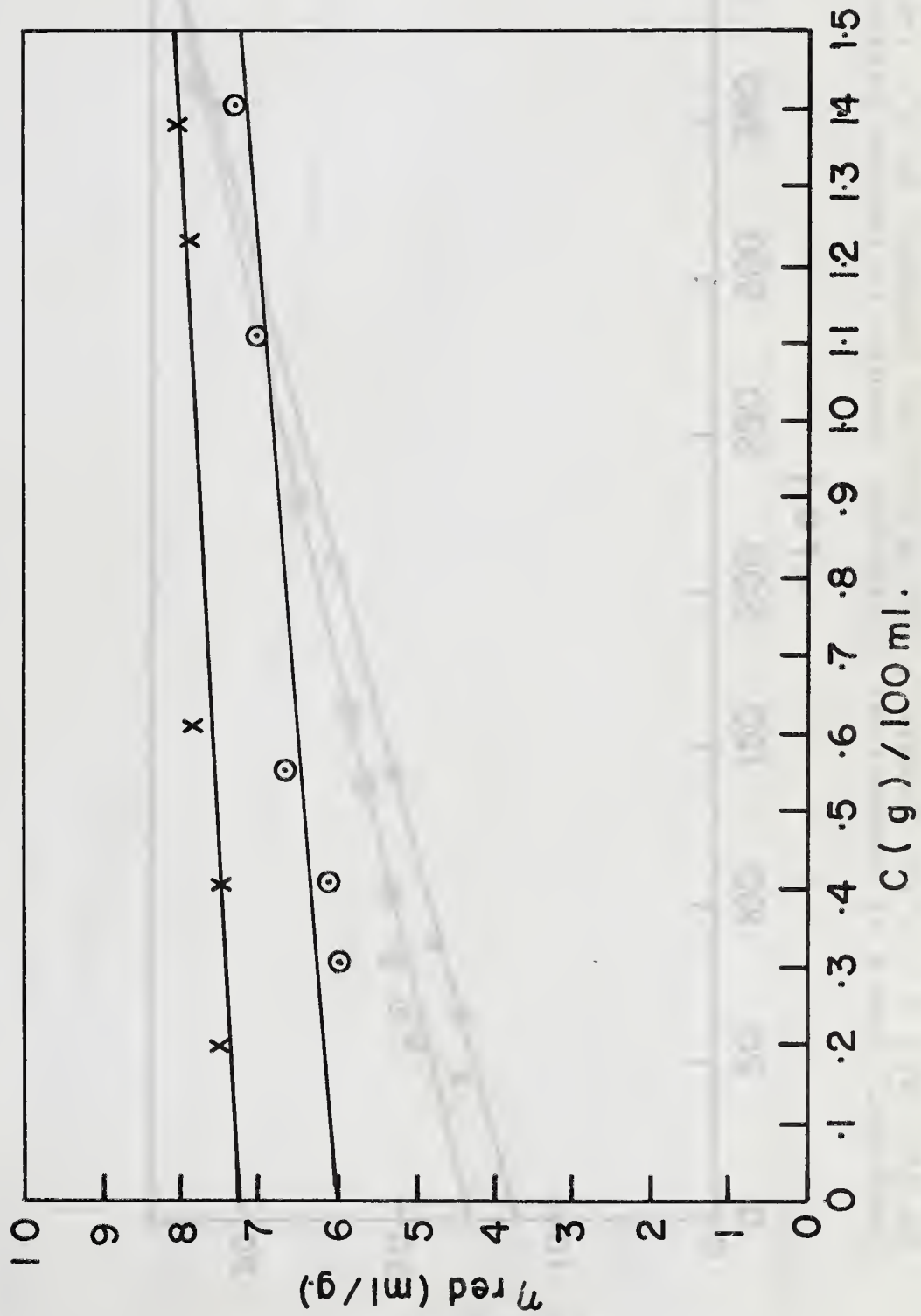
Figure 4



Figure 2

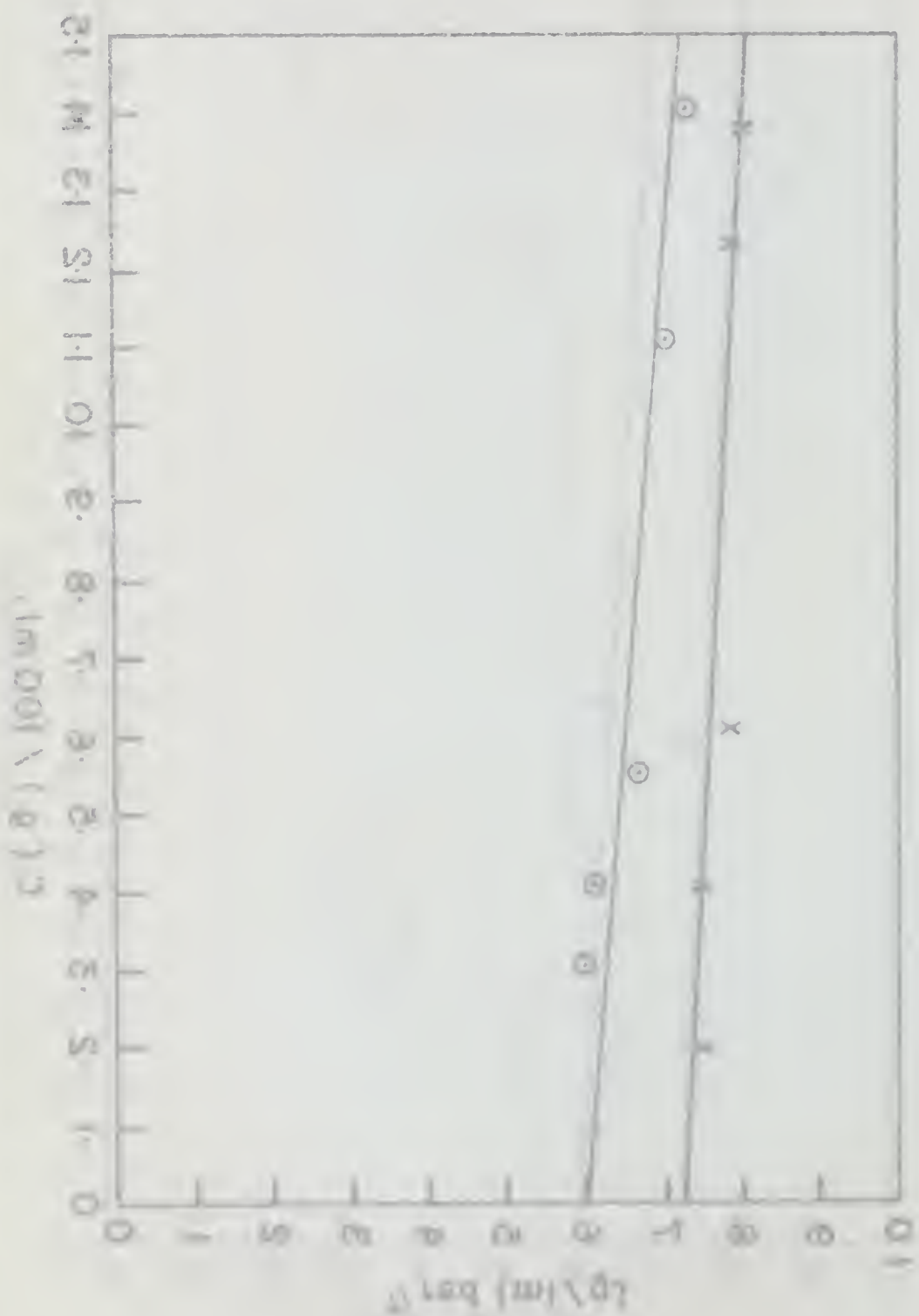


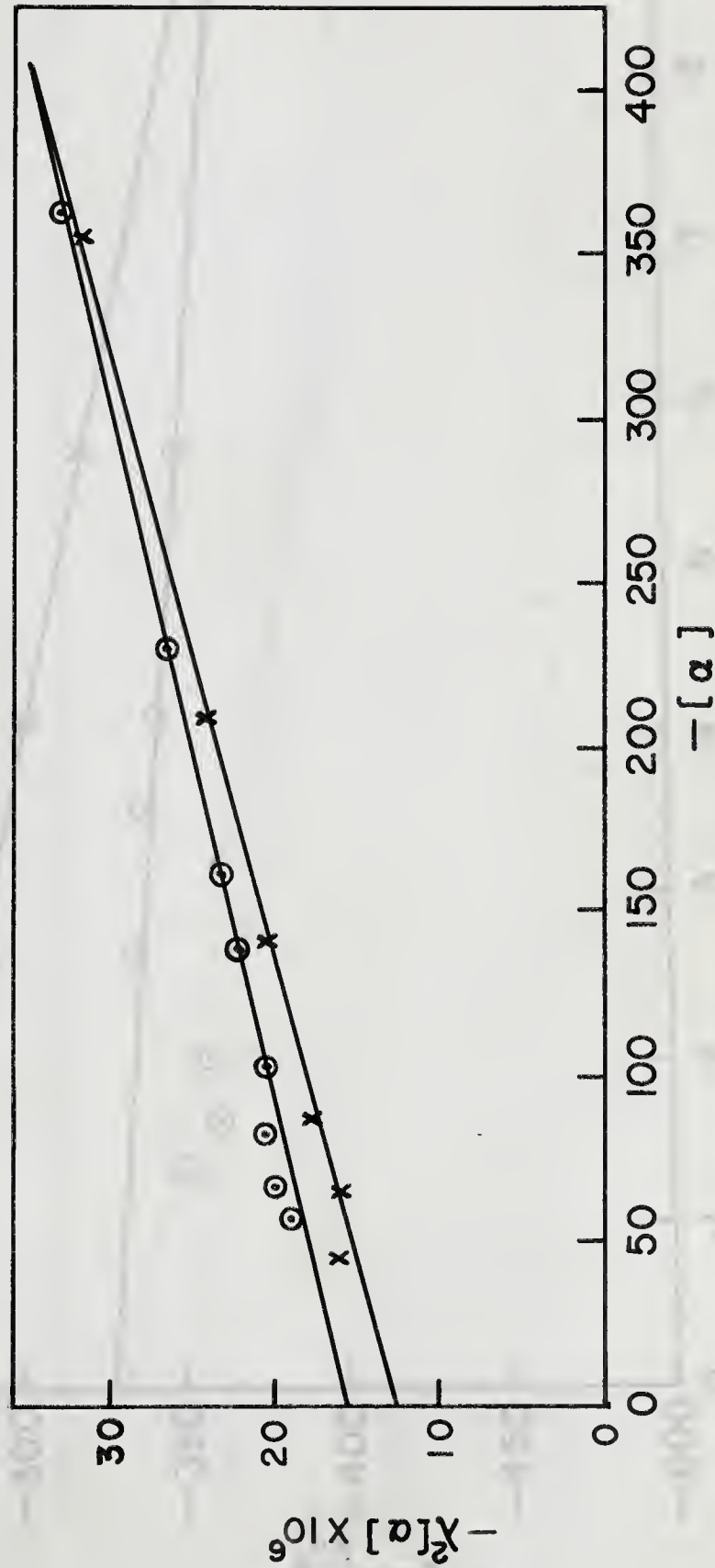
Values of  $\log V(m) \bar{V}^0$  for series A and B are plotted against concentration  $C$  (mole/l) in Figure 2. The values of  $\log V(m) \bar{V}^0$  for series A and B are 7.5 and 5.5 respectively at  $C = 0$ .



$\eta_{red}$  vs. concentration of commercial (Colorado) fetuin in borate buffer, pH 8.0,  $\mu = 0.16$  (x); borate + 0.1 M calcium acetate, pH 8.0 (o).

Figure 5

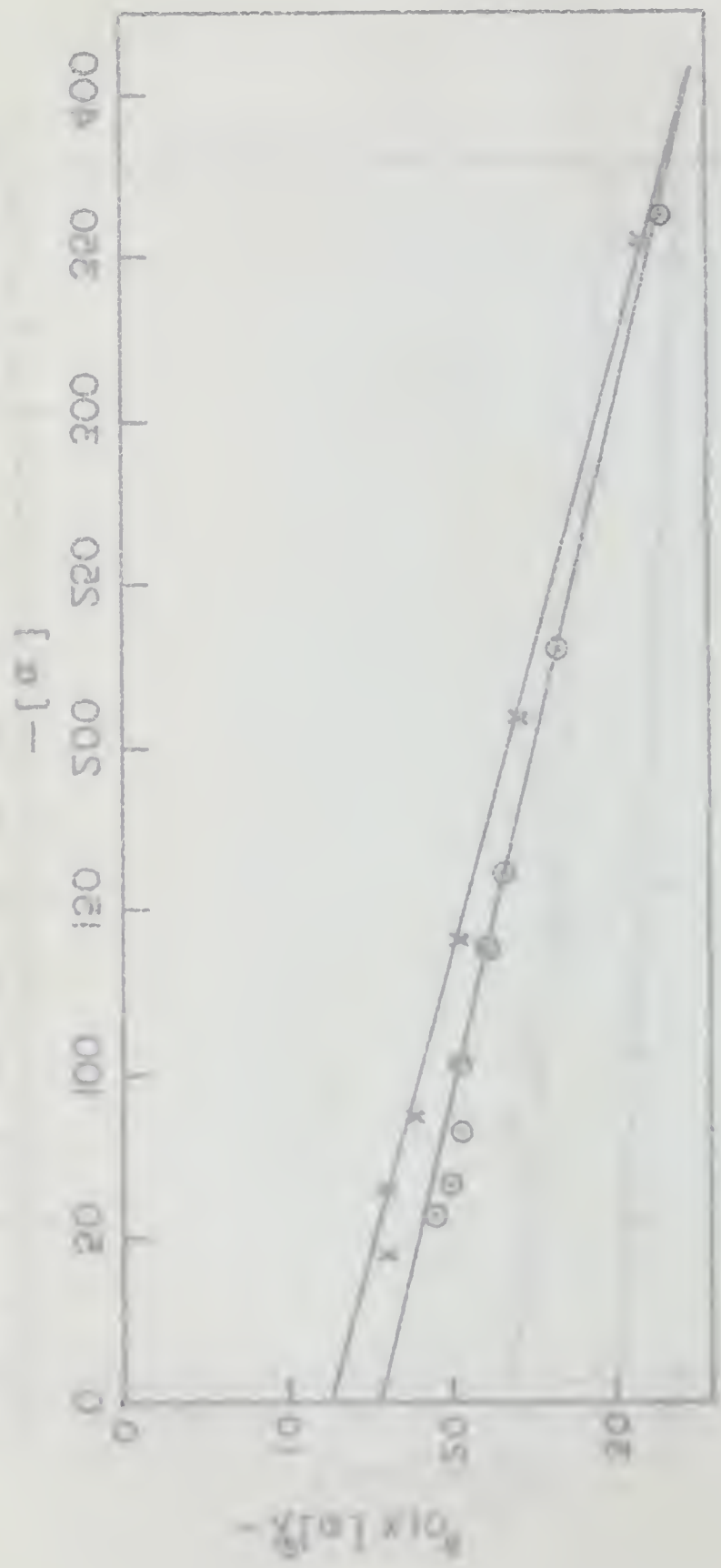




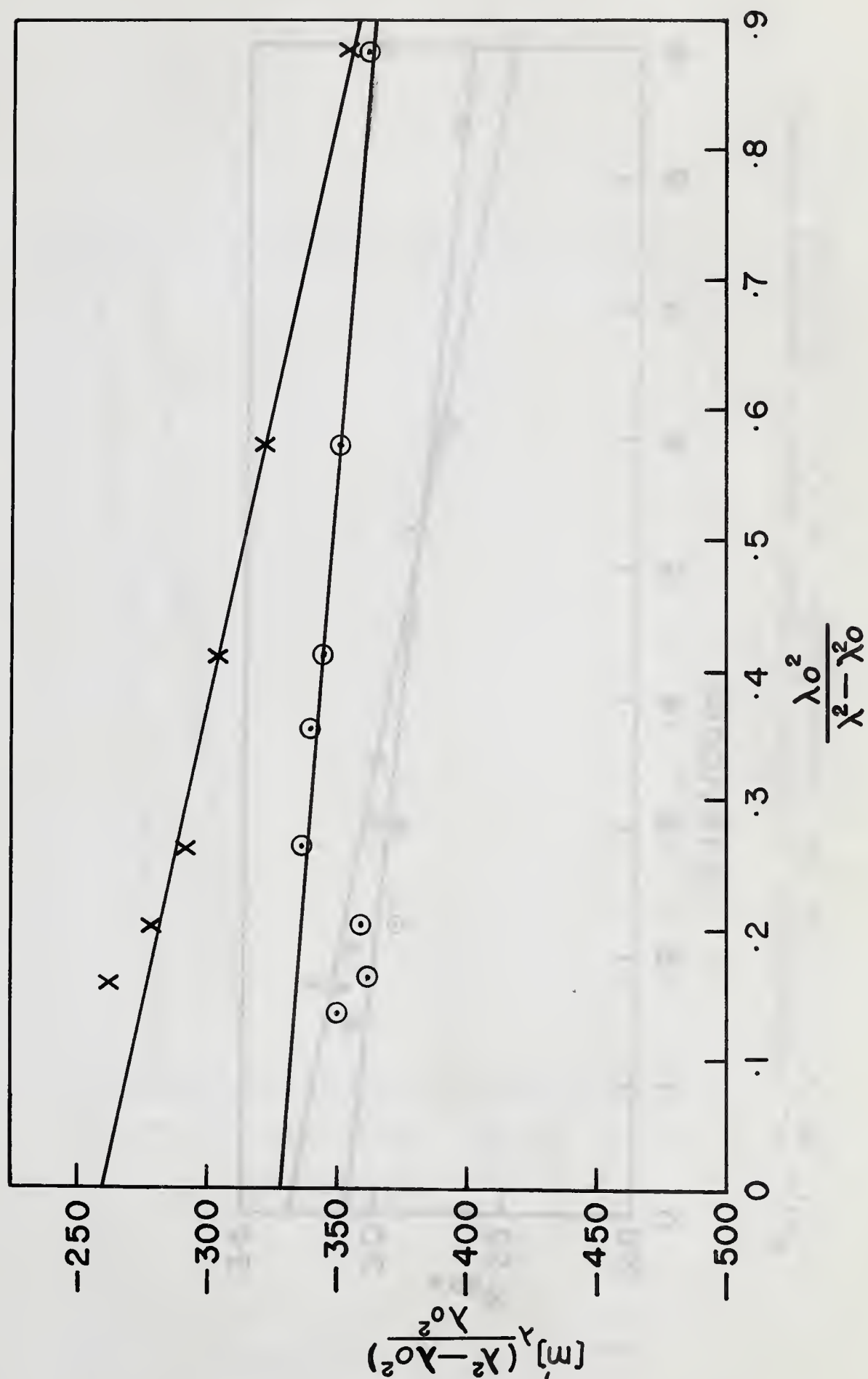
Yang-DoTy plots of commercial (Colorado) fetuin in borate buffer, pH 8.0 (x);  $\mu = 0.16$ ; borate + 0.1 M calcium acetate, pH 8.0 (o).

Figure 6

Fig. 2.  $\log \eta = 0.751 \log \eta_0 + 0.171 W$  (calculated according to eq. 2.0) for  
 various values of concentration (concentration is given in percent by weight).



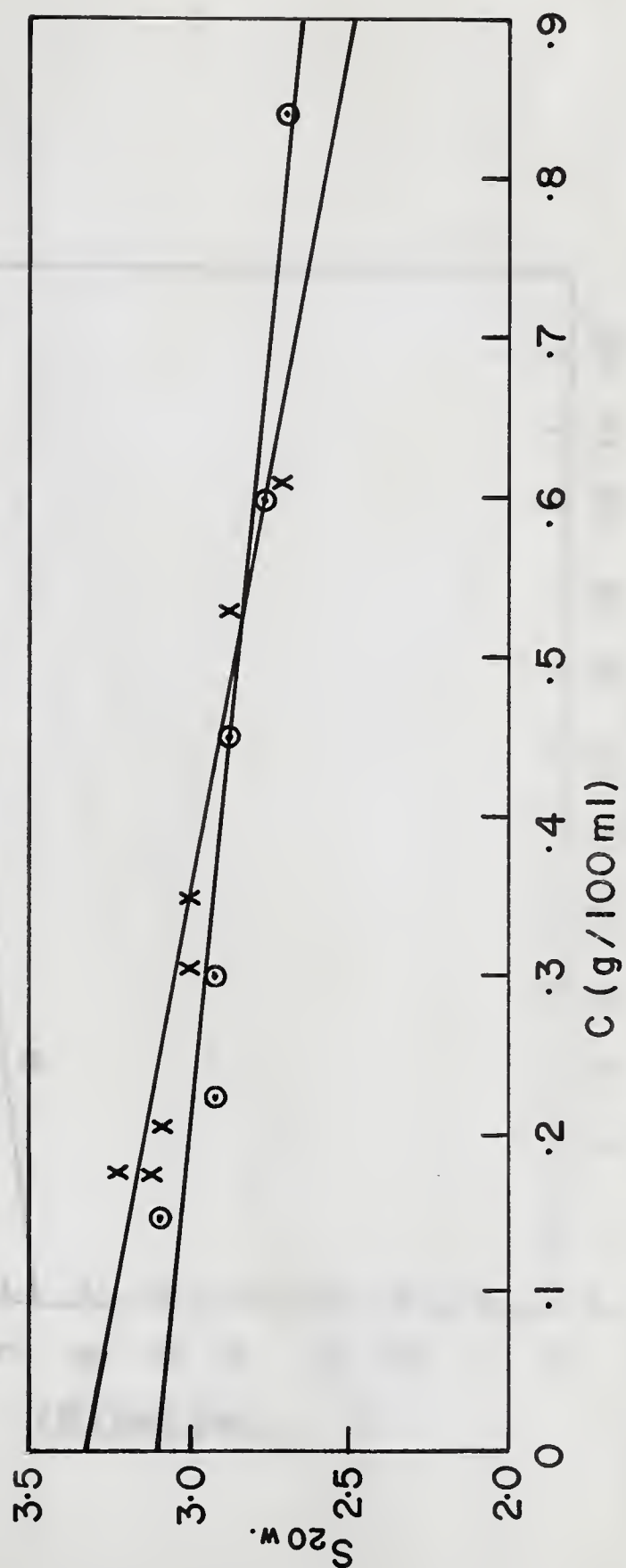




Moffitt plots corresponding to Figure 6, commercial (Colorado) fetuin in borate buffer, pH 8.0,  $\mu = 0.16$  (x); borate + 0.1 M calcium acetate, pH 8.0 (o).

Figure 7





$S_{20,w}$  vs. concentration of ethanol prepared fetuin in phosphate buffer, pH 7.7,  $\mu = 0.16$  (o); borate buffer, pH 8.0,  $\mu = 0.16$  (x).

Figure 8

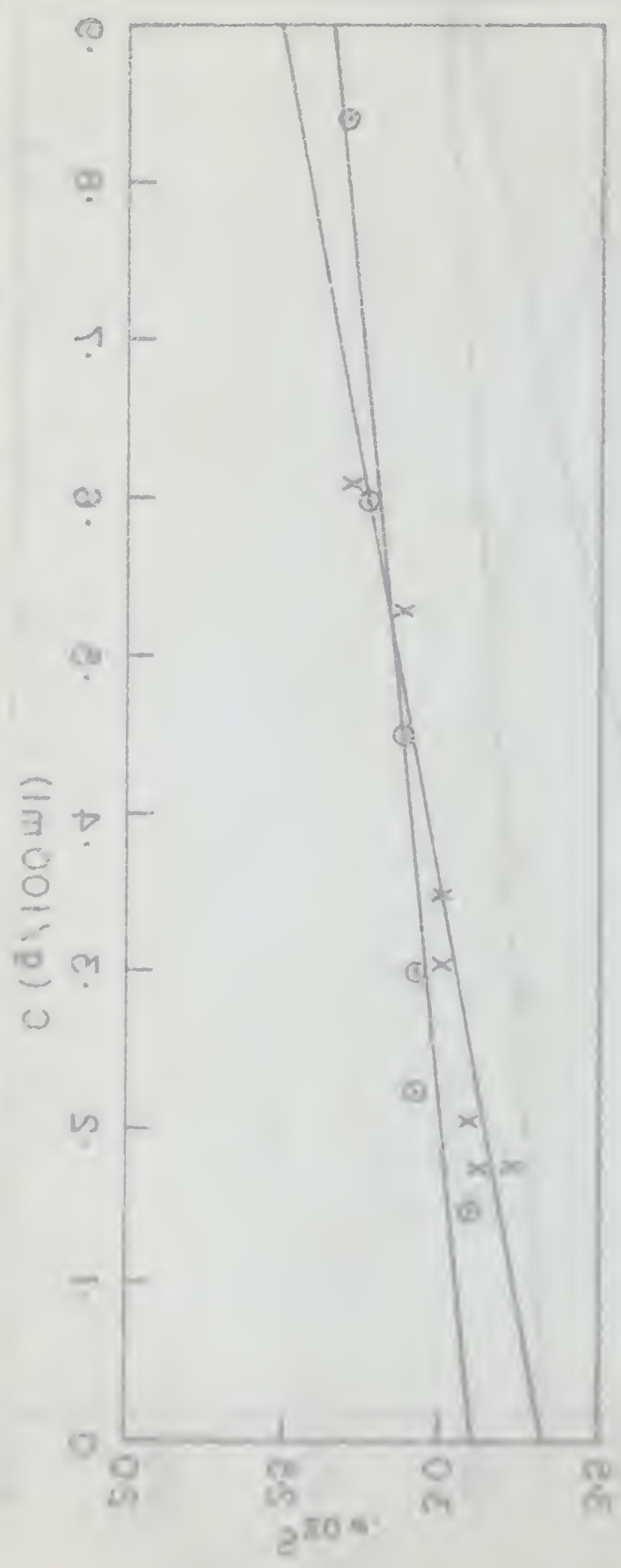
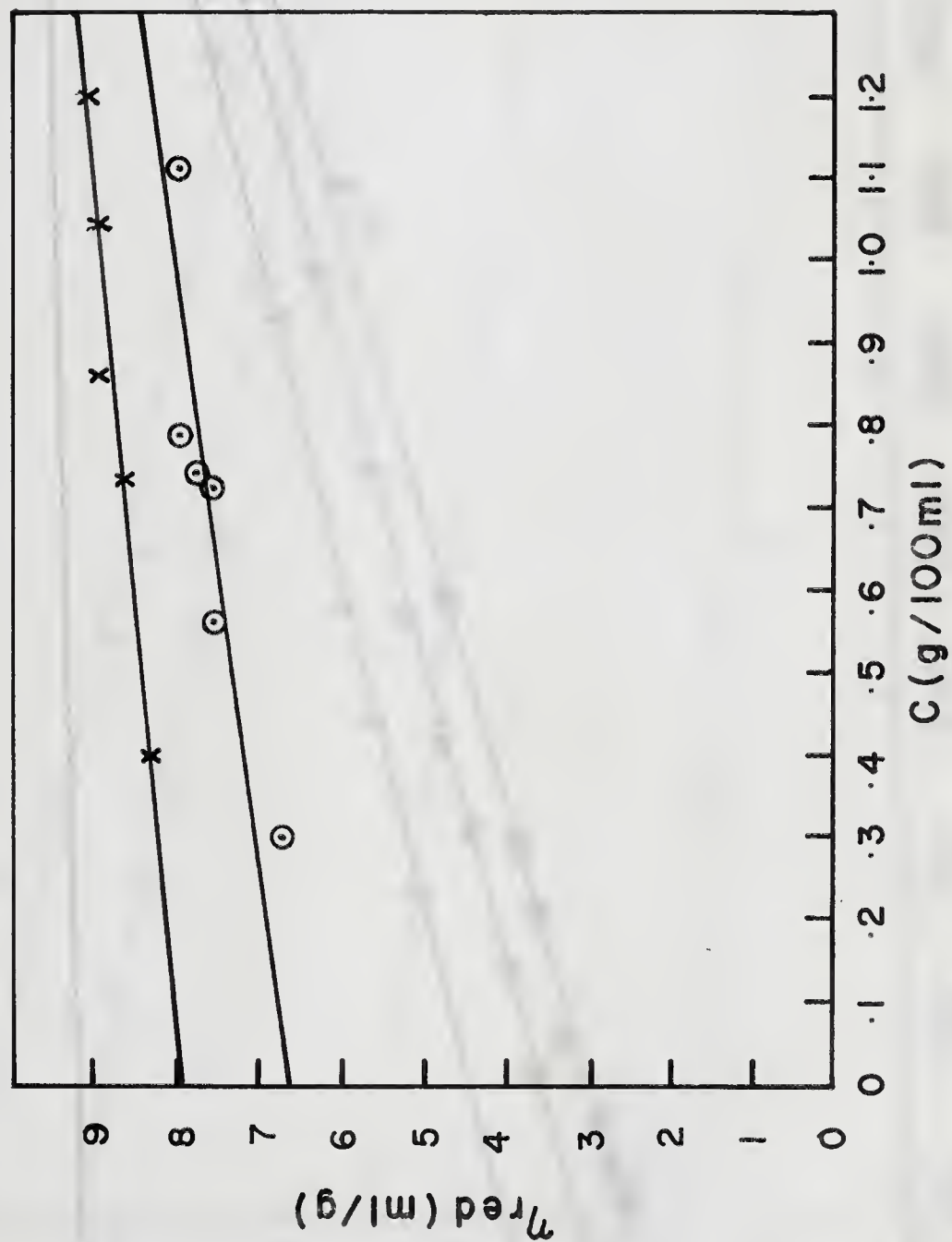


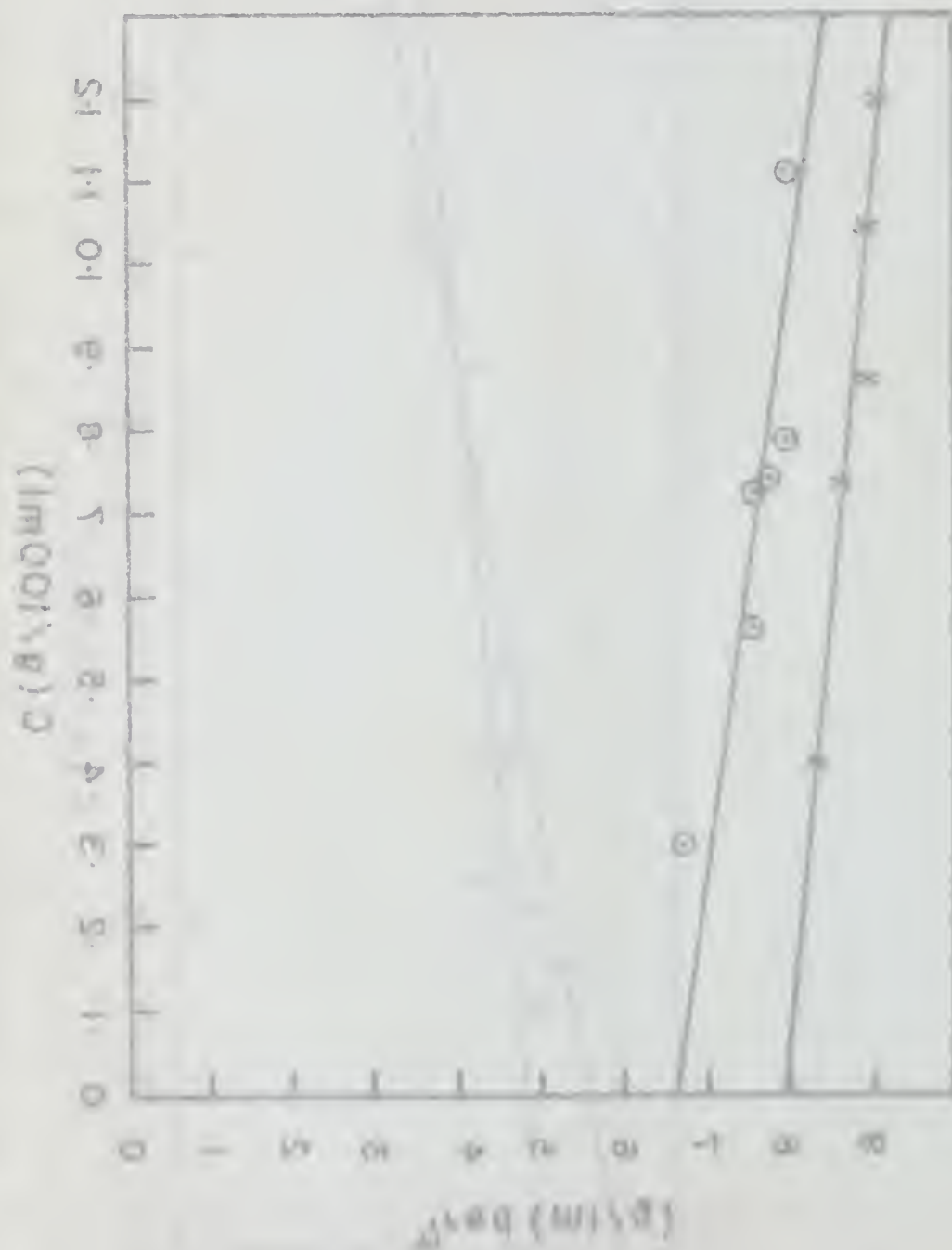
Figure 11. Relationship between  $\log_{10} K$  and  $(mCO_1/p) C$  for the reaction  $CO + H_2O \rightleftharpoons CO_2 + H_2$  at 1000°C. (O)  $p_{CO} = 0.8$  atm,  $p_{H_2O} = 0.2$  atm. (X)  $p_{CO} = 0.4$  atm,  $p_{H_2O} = 0.1$  atm.

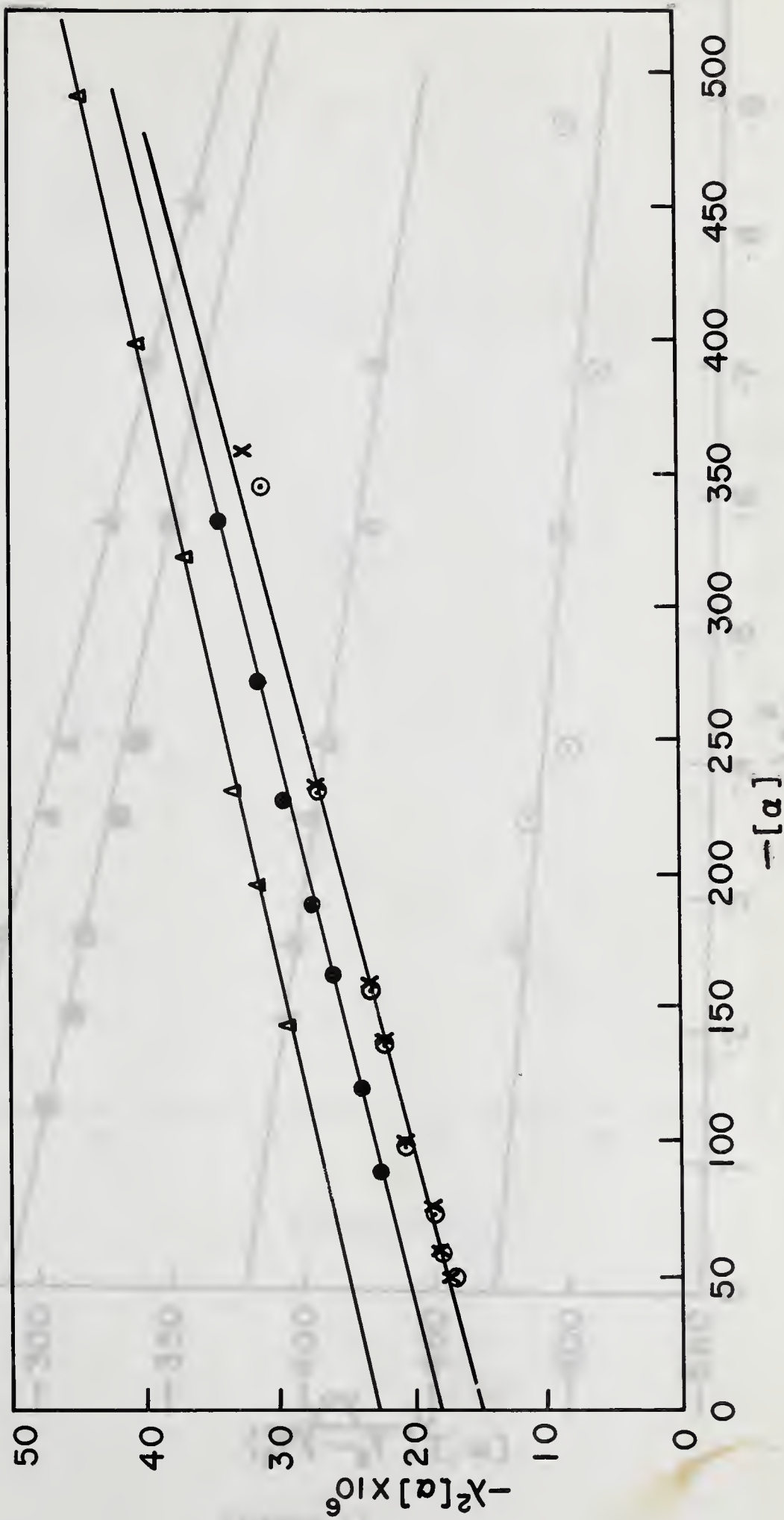


$\eta_{red}$  vs. concentration of ethanol prepared fetuin in phosphate buffer, pH 7.7,  $\mu = 0.16$  (●); borate buffer, pH 7.9,  $\mu = 0.16$  (x).

Figure 9







Yang-Doty plots for (1) commercial (Colorado) fetuin in phosphate buffer, pH 7.9,  $\mu = 0.16$  ( $\circ$ ); borate buffer, pH 8.0  $\mu = 0.16$  (x); (2) ethanol prepared fetuin in phosphate ( $\bullet$ ); borate ( $\Delta$ ).

Figure 10

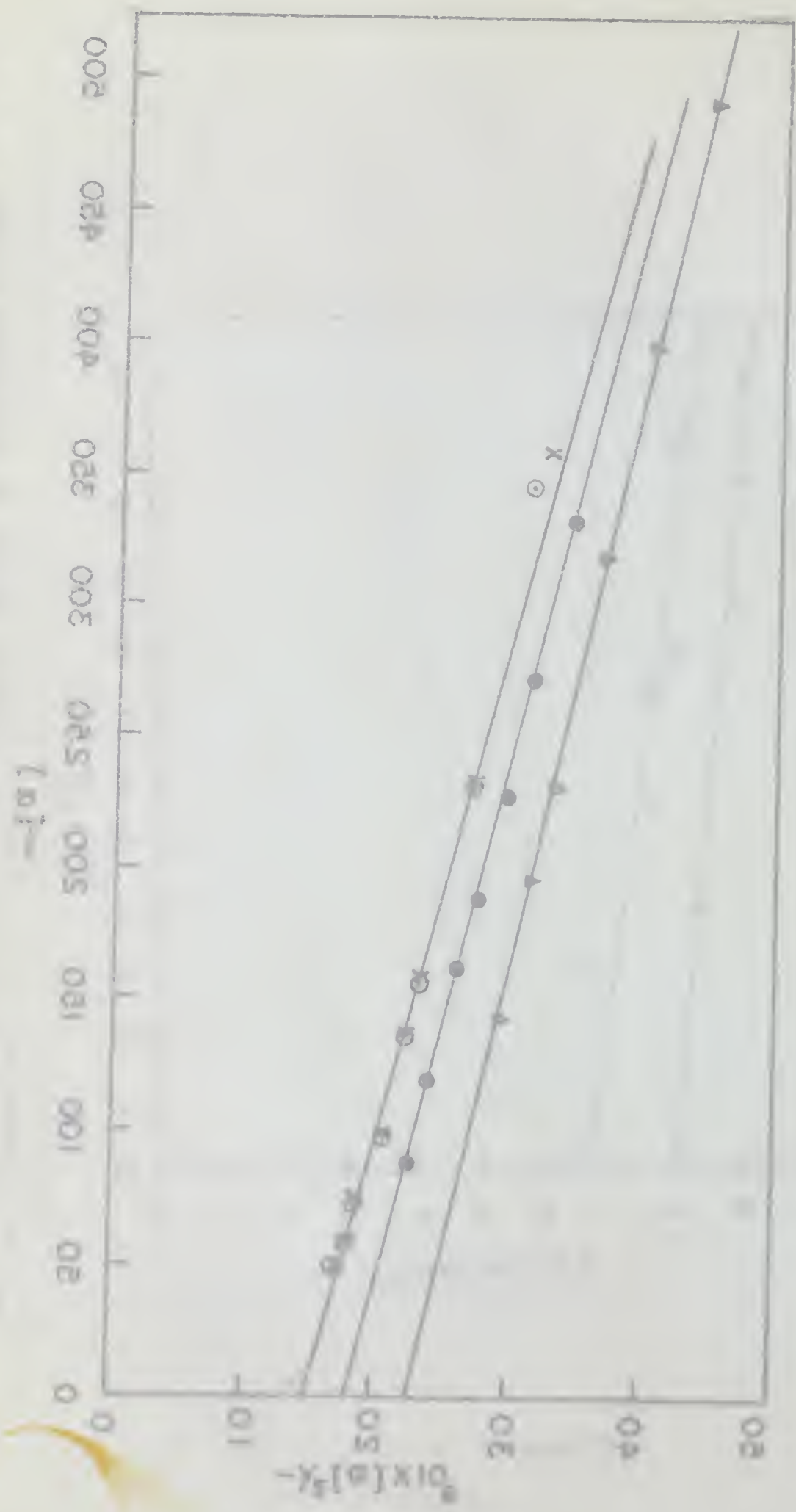


Fig. 10. Logarithmic relationship of  $\log(x)$  and  $\log(x_0)$  for various values of  $\alpha$  and  $\beta$ . The curves are calculated for  $\alpha = 0.1$  and  $\beta = 0.1$ . The symbols are: (1)  $\circ$  for  $\alpha = 0.1$  and  $\beta = 0.1$ ; (2)  $\Delta$  for  $\alpha = 0.1$  and  $\beta = 0.2$ ; (3)  $\square$  for  $\alpha = 0.1$  and  $\beta = 0.3$ .

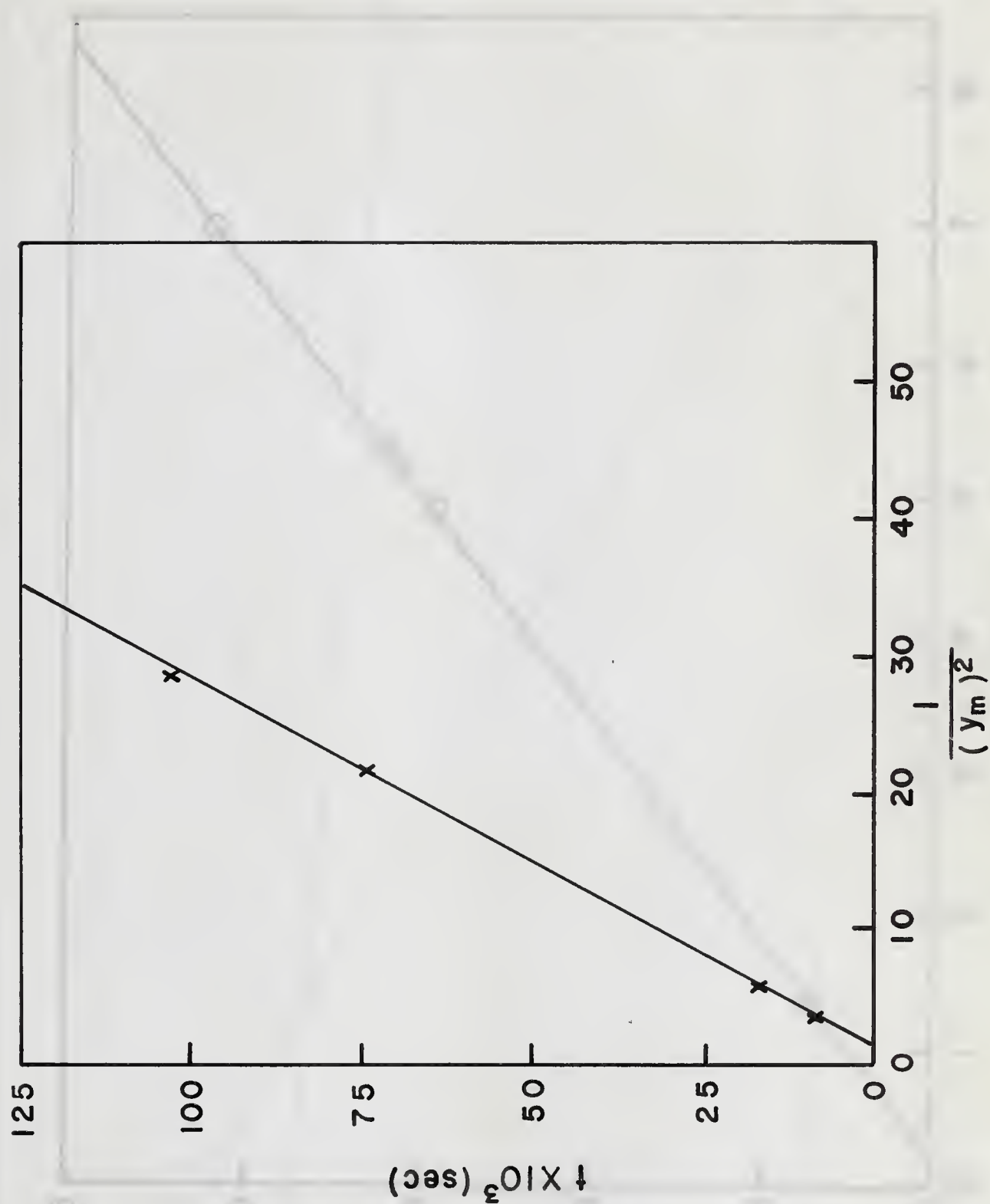


Figure 11

Moffitt plots corresponding to Figure 10: Colorado in phosphate (▲), Colorado in borate (●); ethanol in phosphate (Δ); ethanol in borate (⊙).







Diffusion of 0.3% commercial (Colorado) fetuin in borate buffer, pH 8.0,  $\mu = 0.16$ ,  $\frac{1}{y_m^2}$  vs. time.

Figure 12

Figure 1. Dependence of the rate of polymerization on the concentration of the initiator. The reaction was carried out at 50°C in a 0.5 M solution of the monomer. The concentration of the initiator was varied from 0.01 to 0.1 M. The rate of polymerization was determined by the method of titration with a solution of potassium permanganate.

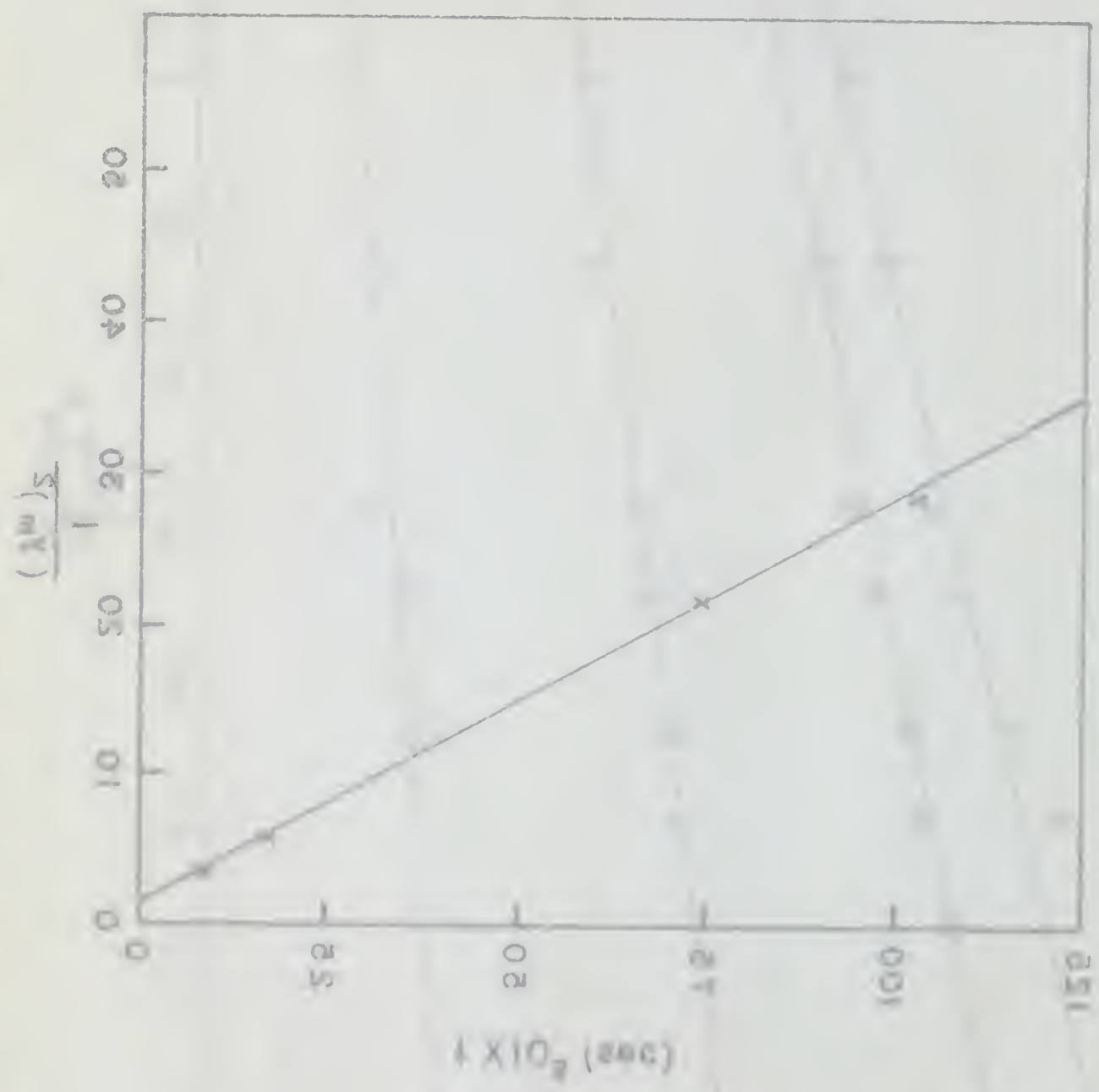


Figure 1

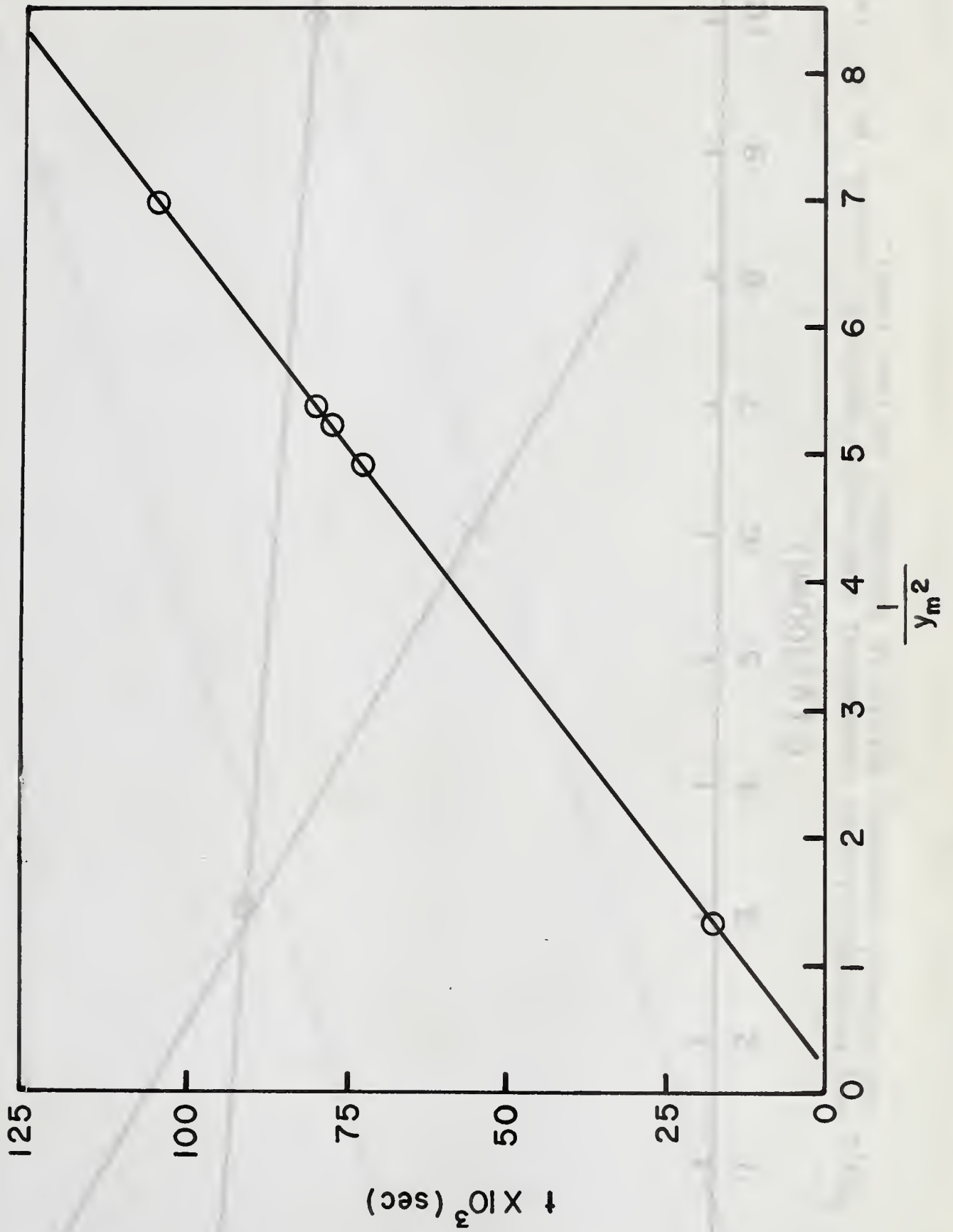
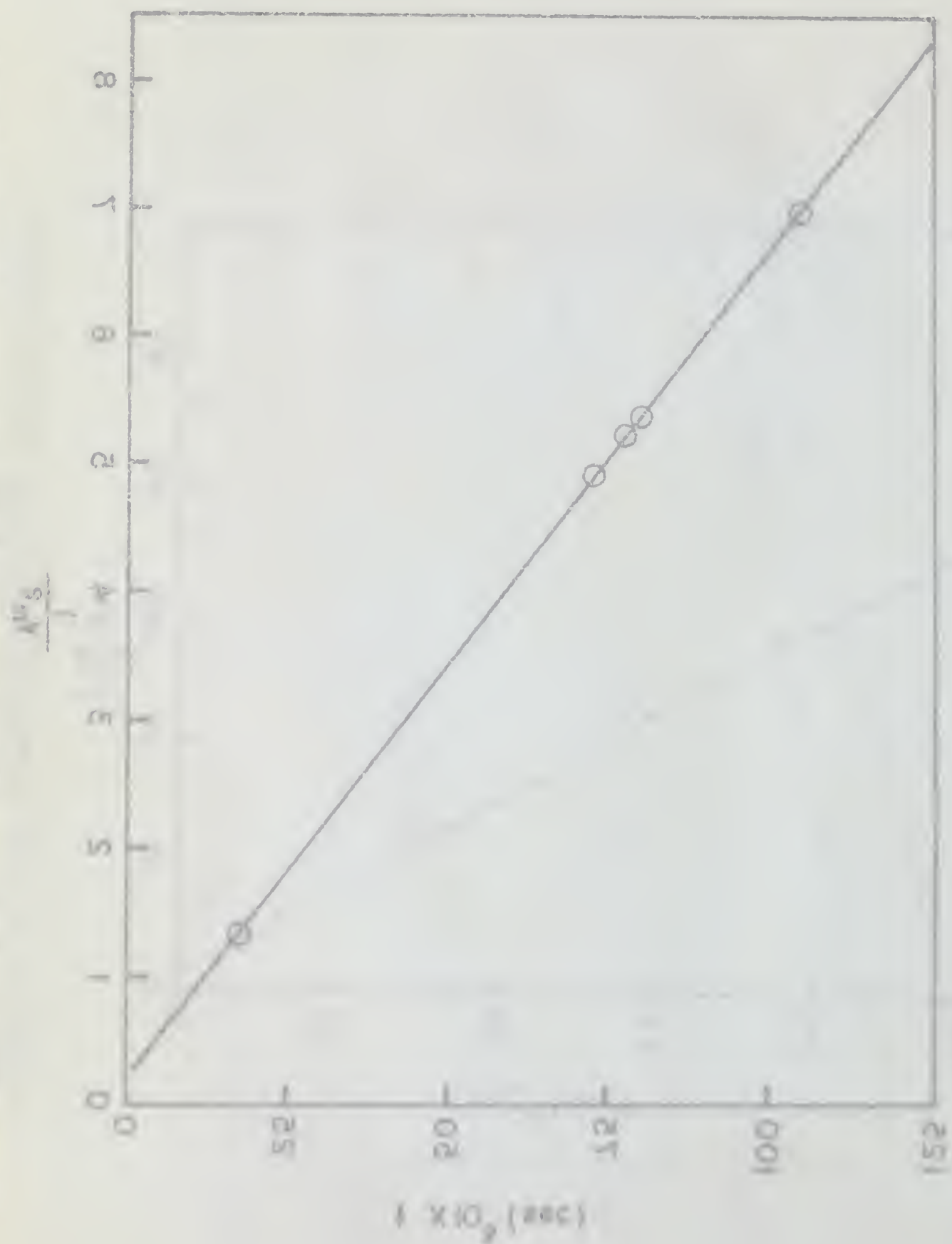
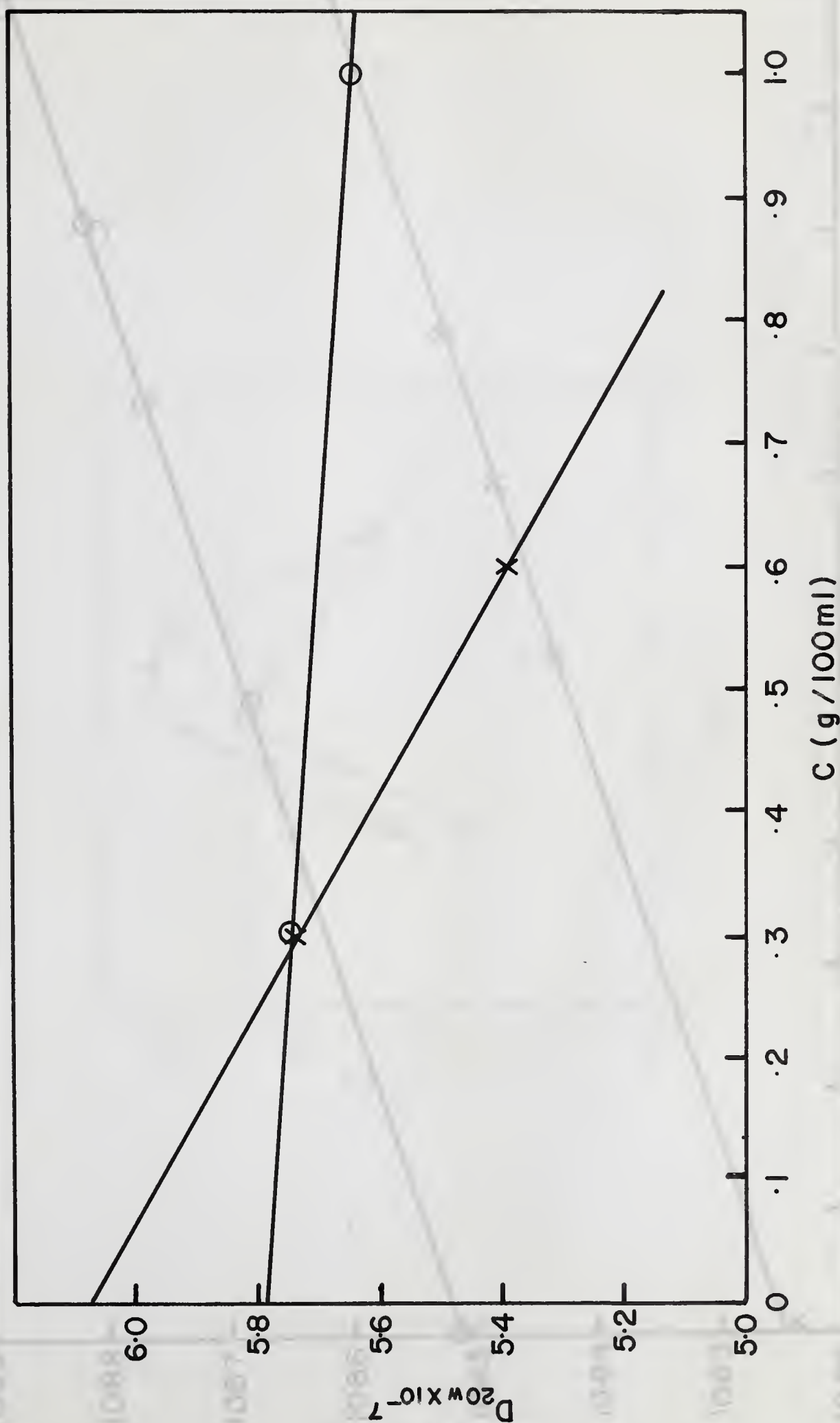


Figure 13

Diffusion of 0.60% commercial (Colorado) fetuin in borate buffer, pH 8.0,  
 $\mu = 0.16$ ,  $\frac{l^2}{y_m^2}$  vs. time (o).



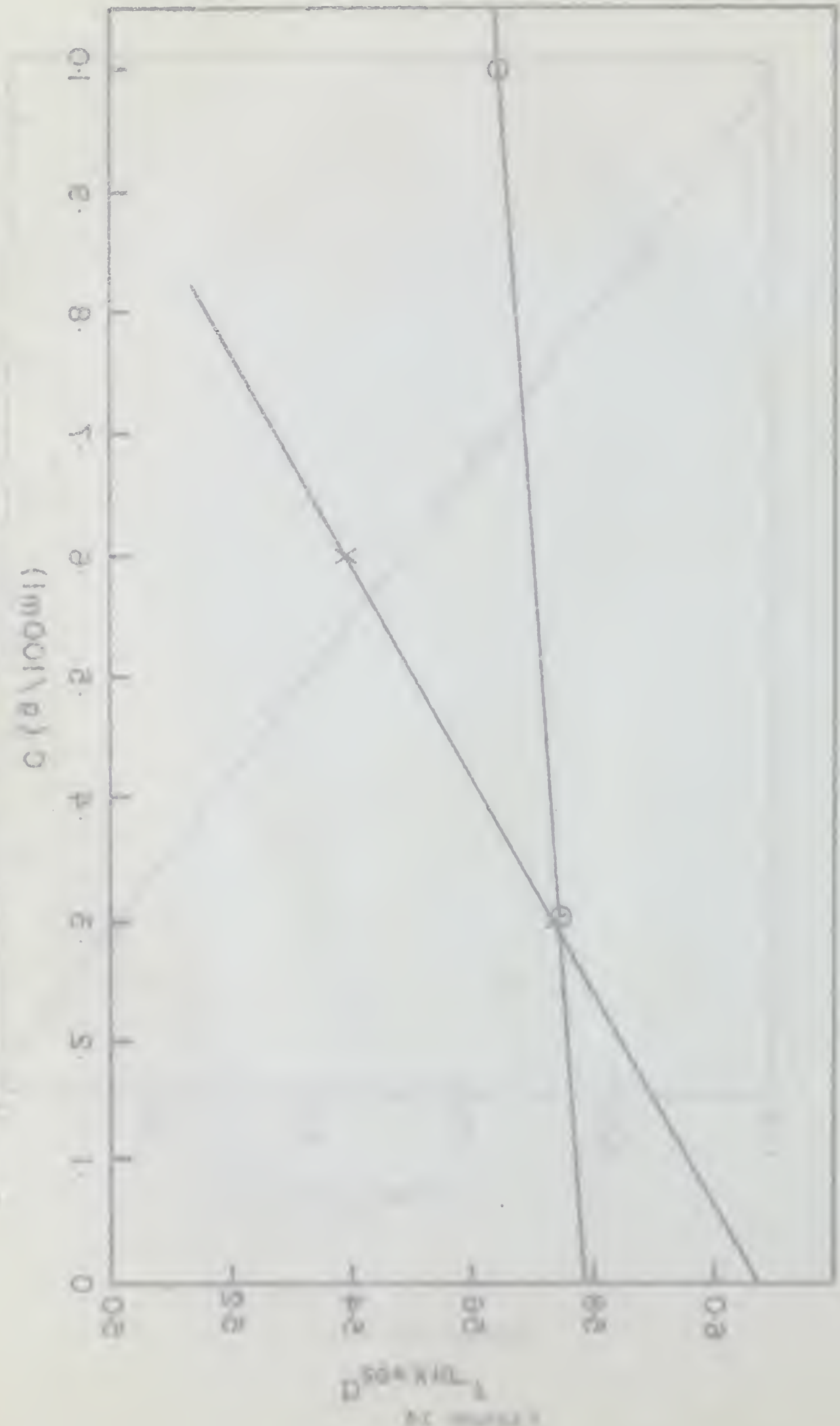


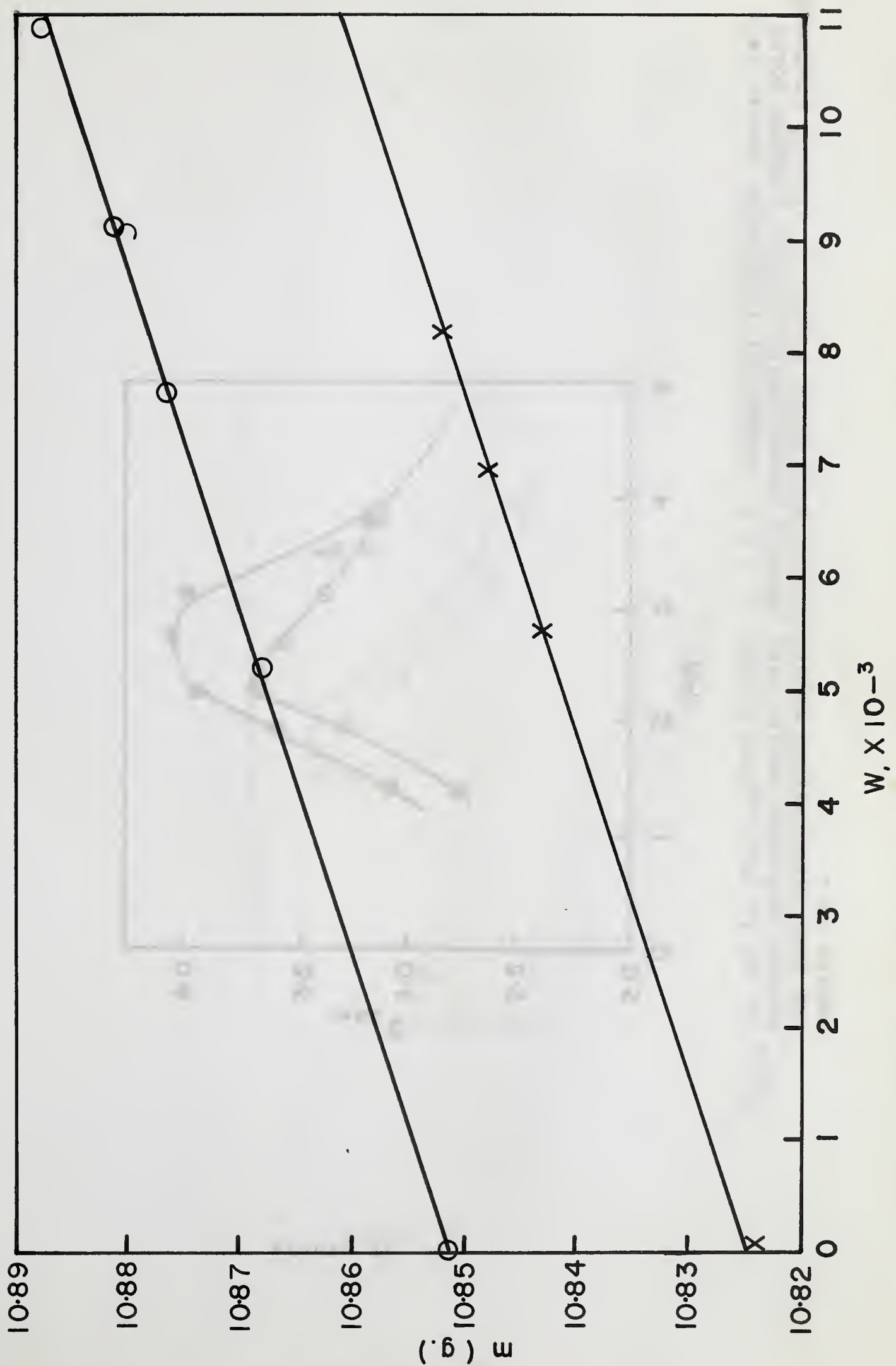
$D_{20,w}$  vs. concentration of commercial (Colorado) fetuin in borate, pH 8.0 (x); and ethanol prepared fetuin in phosphate (o) (see text).

Figure 14



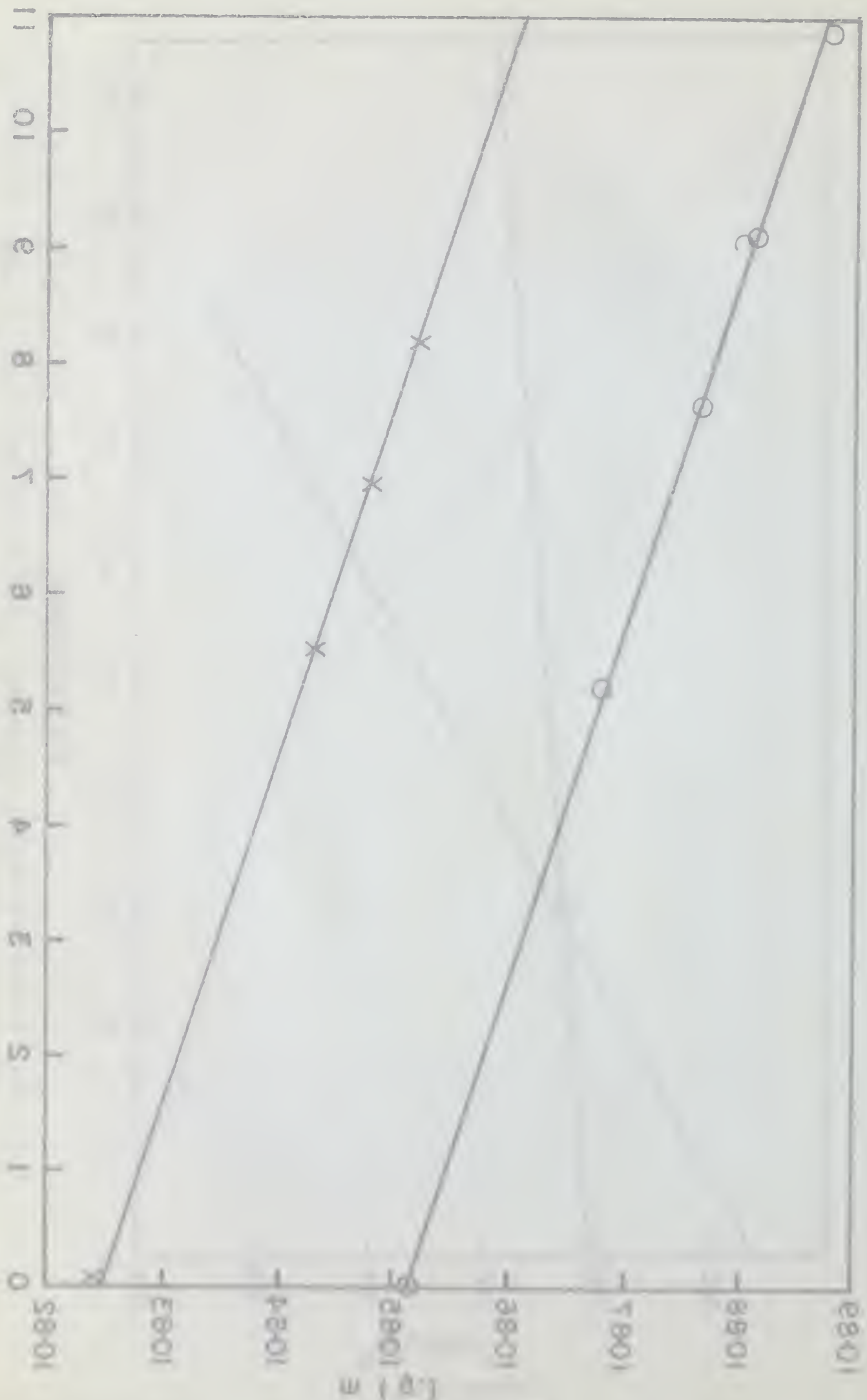
Fig. 1. Dependence of the concentration of the monomer on the concentration of the initiator. (x) 0.1 M; (o) 0.2 M; (x) 0.3 M; (o) 0.4 M; (x) 0.5 M; (o) 0.6 M; (x) 0.7 M; (o) 0.8 M; (x) 0.9 M; (o) 1.0 M.



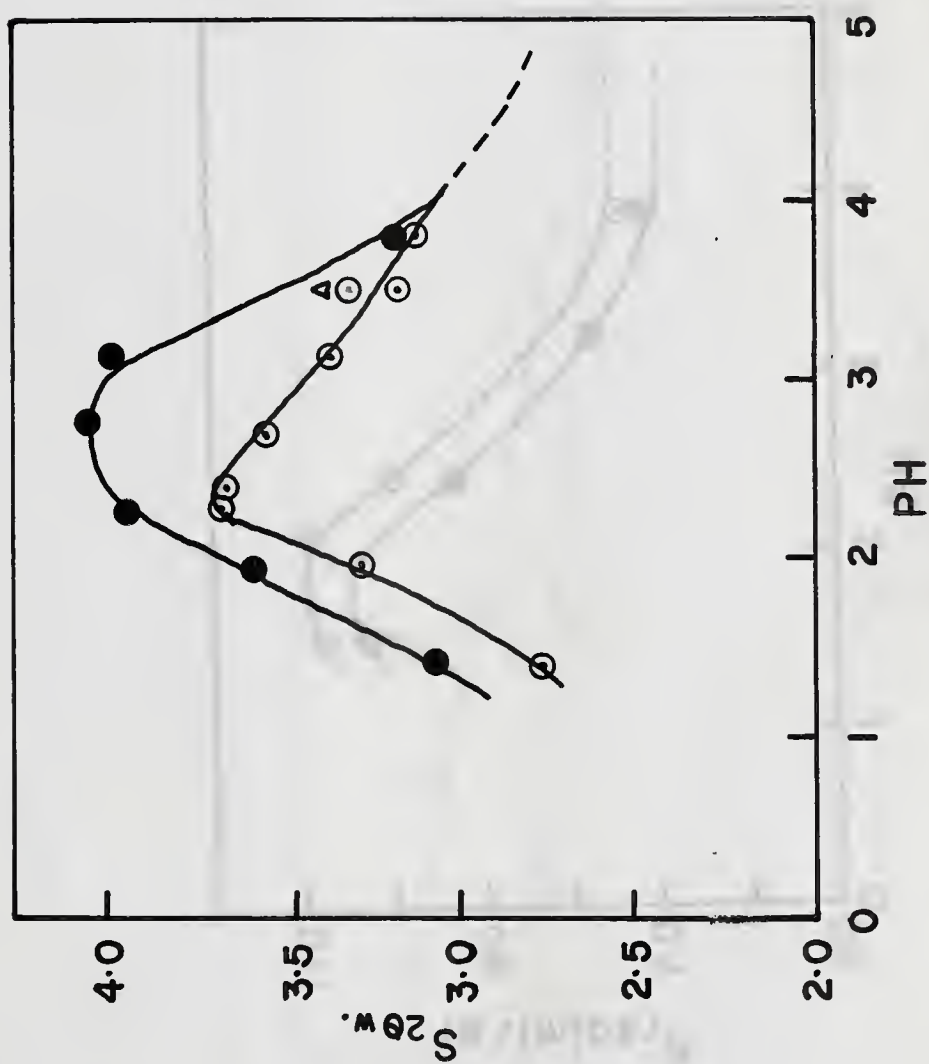


Kraemer plots for partial specific volume, Colorado in phosphate, pH 7.7 (O); ethanol in borate, pH 8.0 (x).

Figure 15



For the (0) T. I. for, starting with the same value, the only difference is the C.P. for, which is not



$S_{20,w}$  vs. pH in glycine/HCl buffer,  $\mu = 0.1$ : commercial (Colorado) fetuin (●); ethanol prepared fetuin (○), protein concentration 0.65%; a check point for salt fractionated material from same blood sample as ethanol prepared fetuin (△).

Figure 16

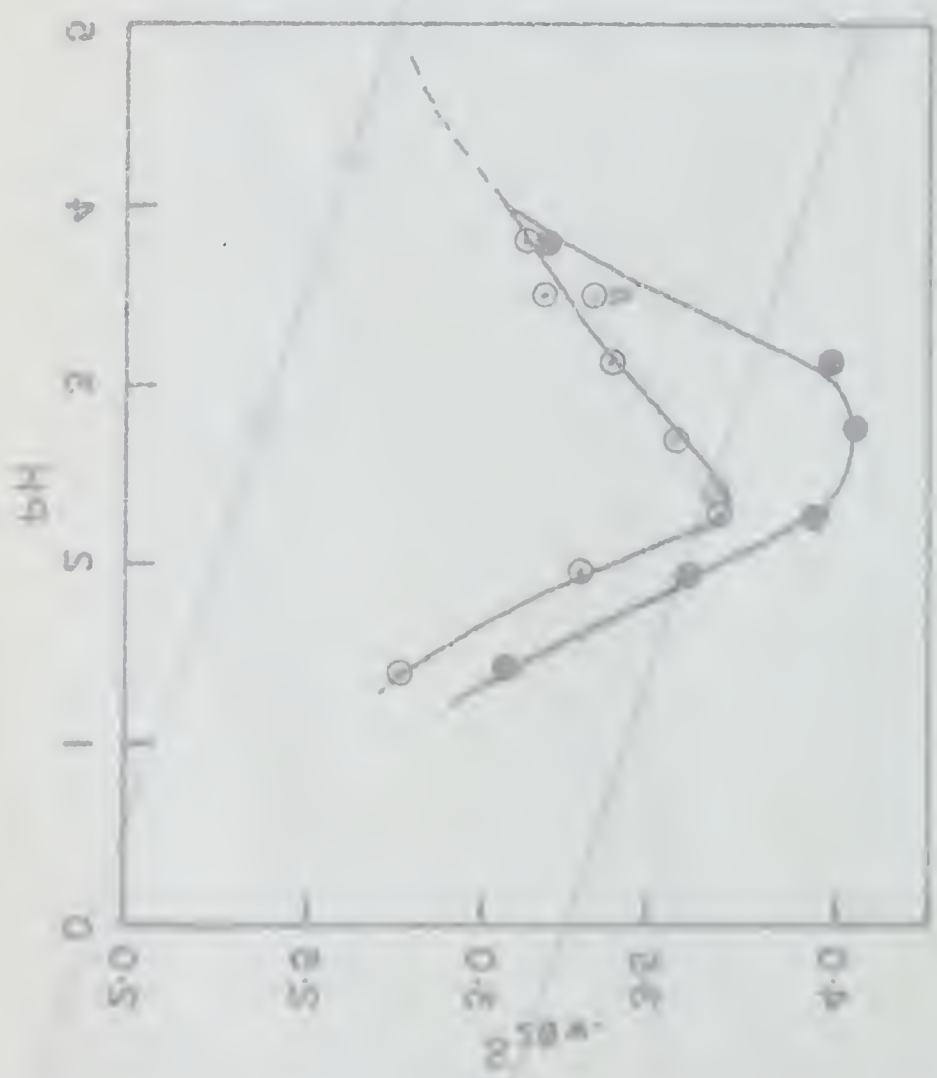
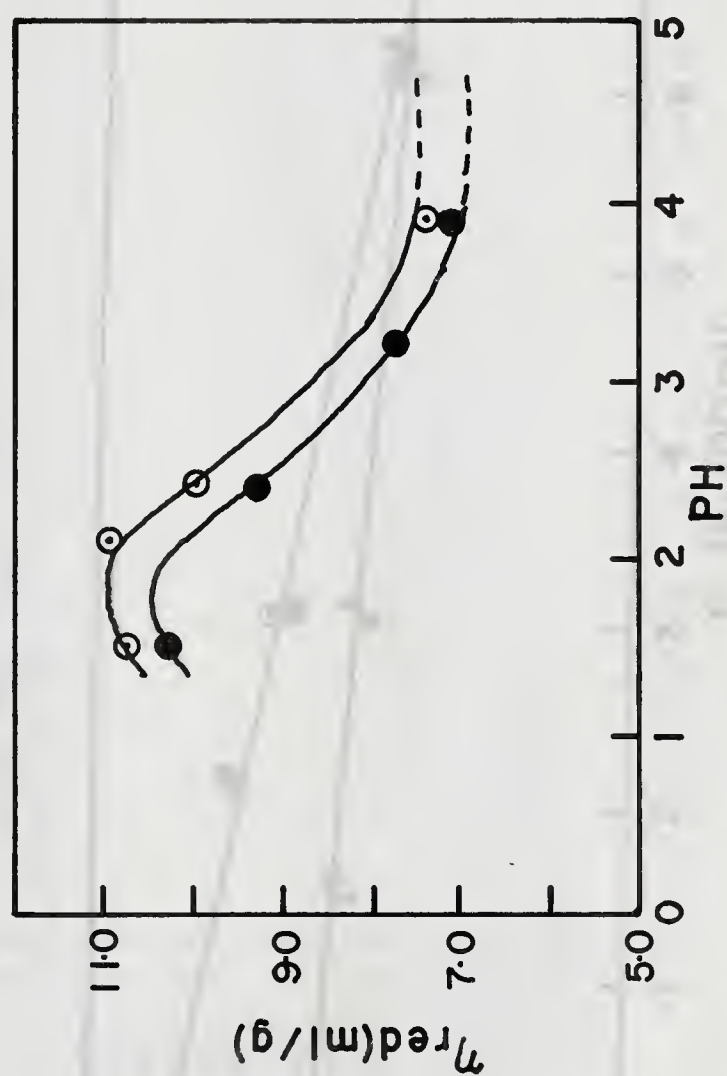


Fig. 1. Dependence of the factor  $Hq$  on the parameter  $\alpha$  for different values of  $\beta$ . The solid circles correspond to  $\beta = 0.5$  and the open circles to  $\beta = 1.0$ . The dashed line represents the theoretical curve for  $\beta = 0.5$  and  $\alpha = 0$ .

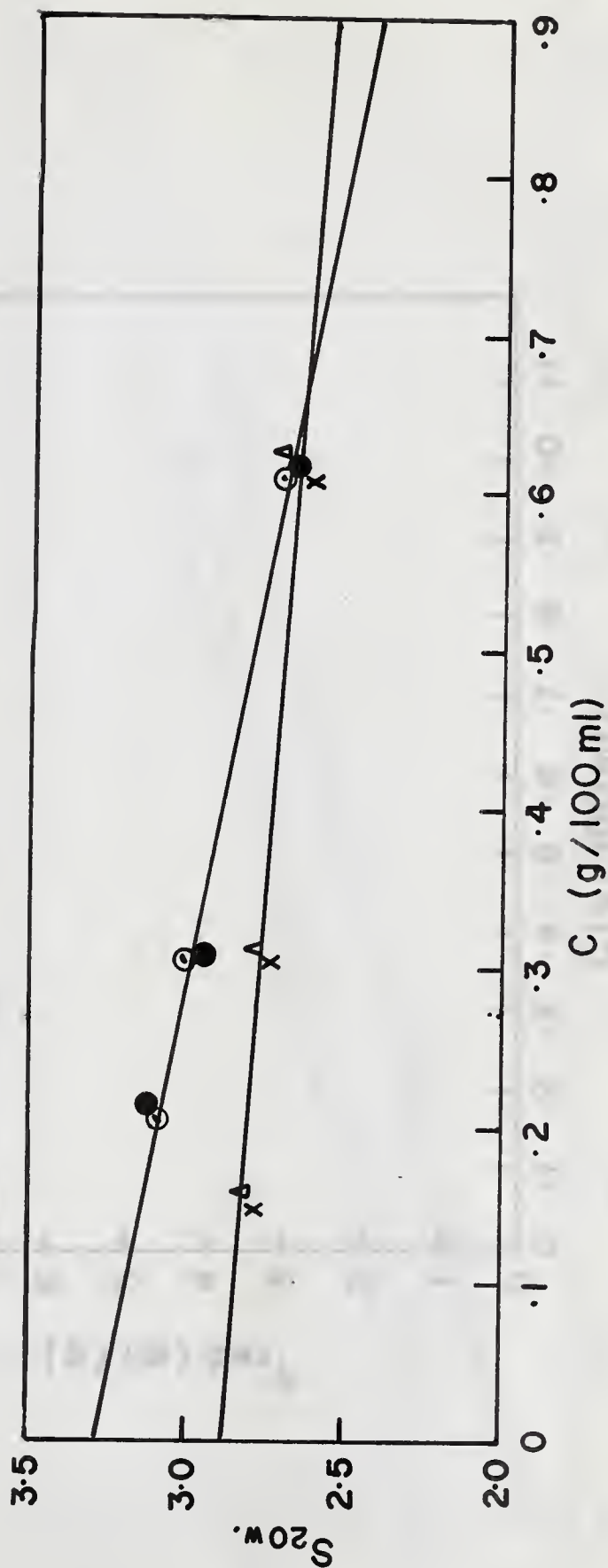




$\eta_{red}$  vs. pH in glycine/HCl buffer,  $\mu = 0.1$ : commercial (Colorado) fetuin (●); ethanol prepared fetuin (○), protein concentration for commercial fetuin 0.80%, for ethanol prepared fetuin 0.67%.

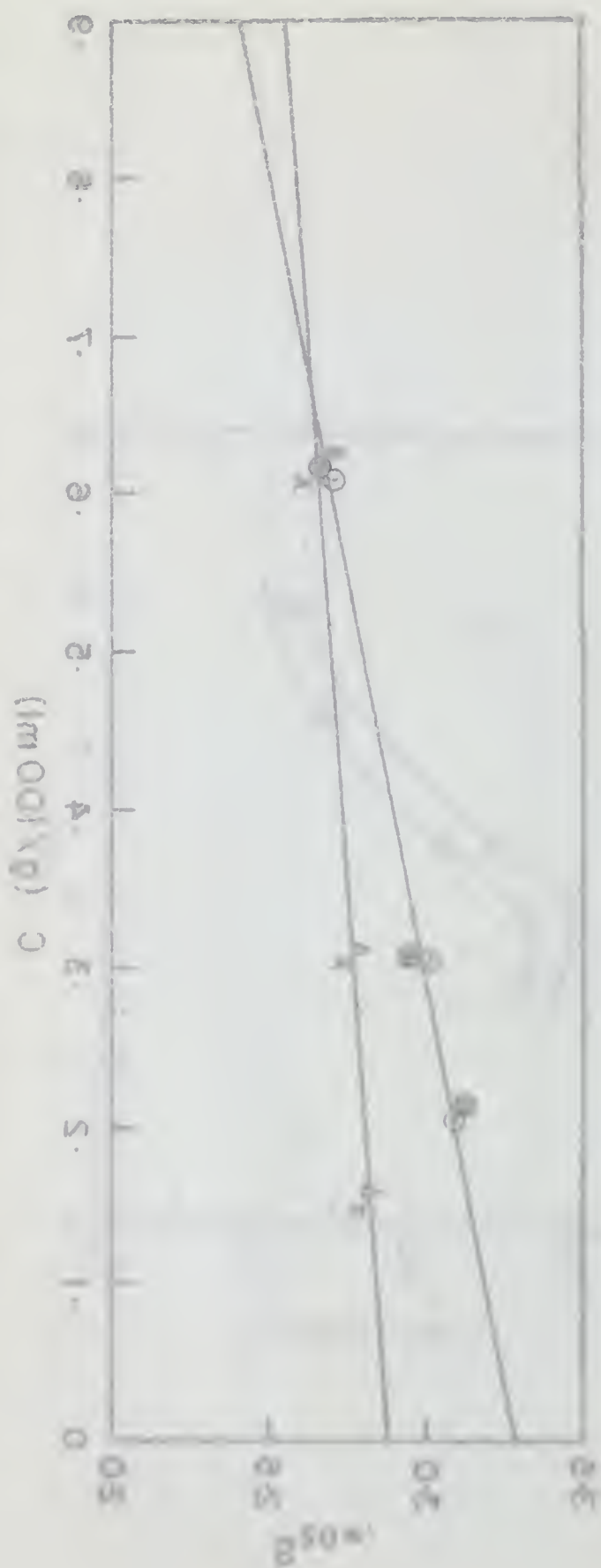
Figure 17



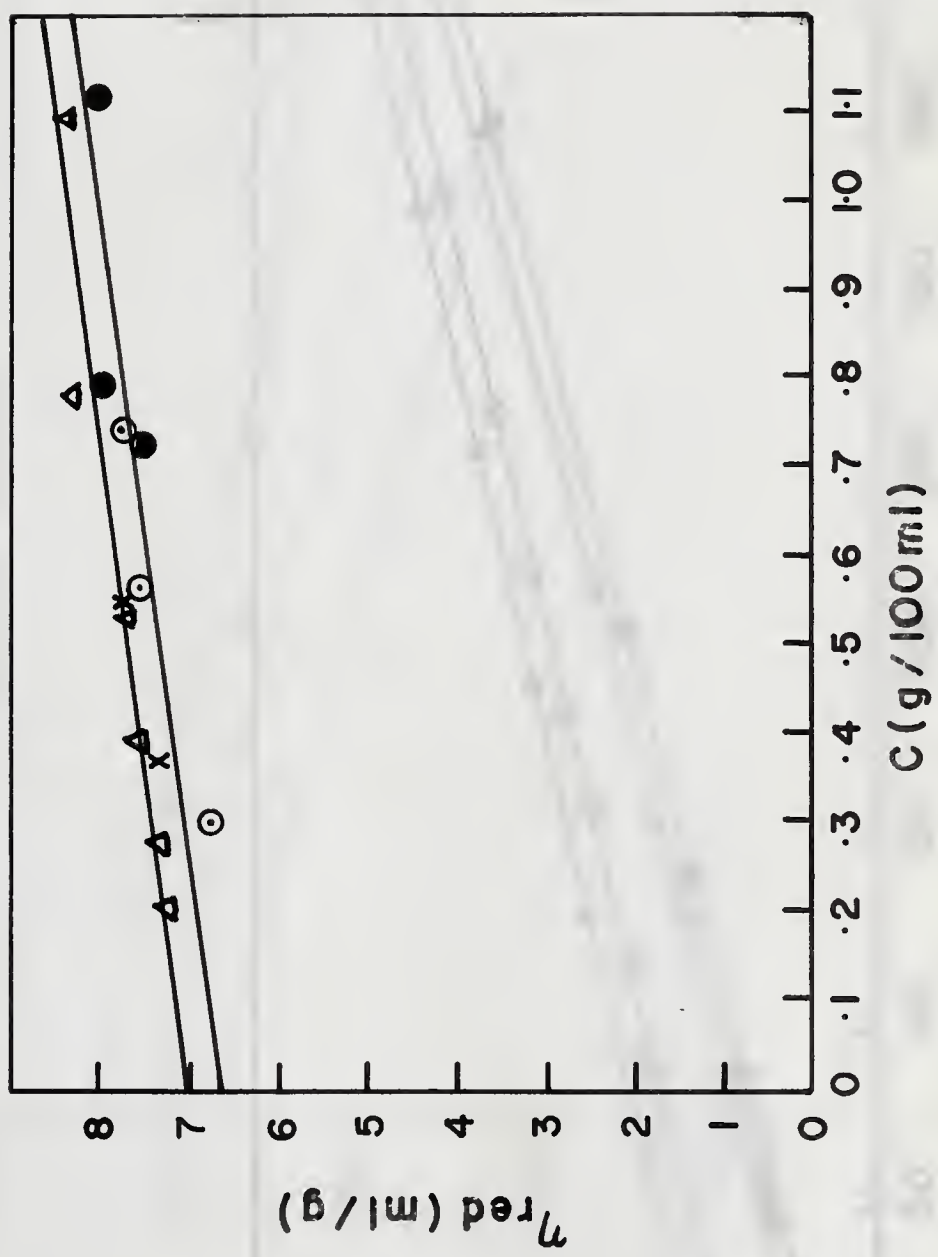


$S_{20,w}$  vs. concentration of (1) ethanol prepared fetuin #2 in phosphate buffer, pH 7.7 (x), borate buffer, pH 8.0 (o); (2) salt prepared fetuin in phosphate buffer ( $\Delta$ ), borate buffer ( $\bullet$ ), isolated from the same blood sample.

Figure 18



107101 5455000 at 20 ml. of water (1) is 10 ml. of water, (2) is 20 ml. of water, (3) is 30 ml. of water. The concentration of the solution is 0.5% and the optical density is 0.5%.



$\eta_{red}$  vs. concentration of ethanol prepared fetuin #2 in phosphate buffer, pH 8.0,  $\mu = 0.16$  ( $\Delta$ ); ethanol preparation #3 in phosphate buffer, pH 7.7 ( $\circ$ ); same as ethanol preparation #3 except 80% of ionic strength contributed by NaCl ( $\bullet$ ); ethanol preparation #3 in borate buffer + 0.1 M calcium acetate, pH 7.9 ( $\times$ ).

Figure 19



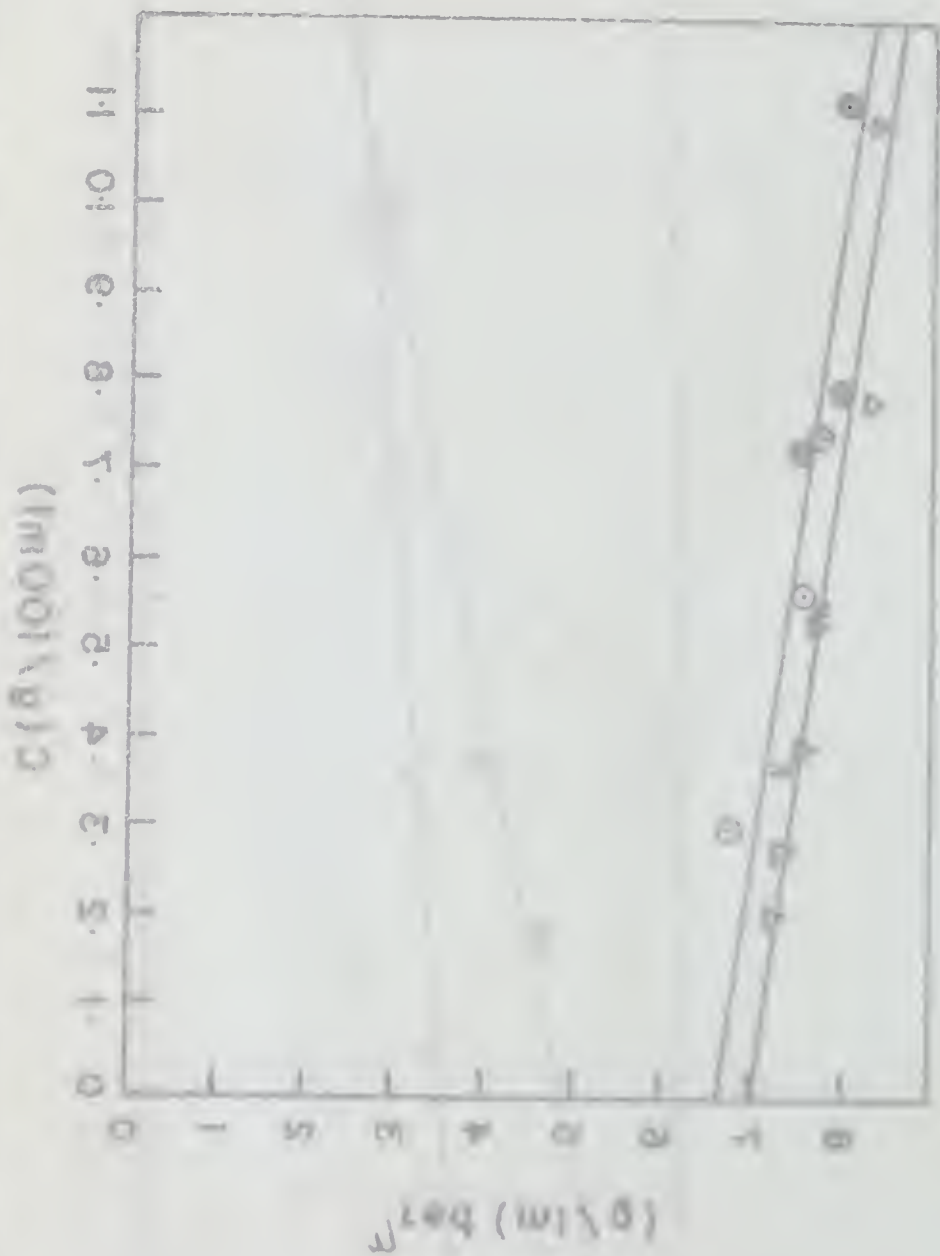
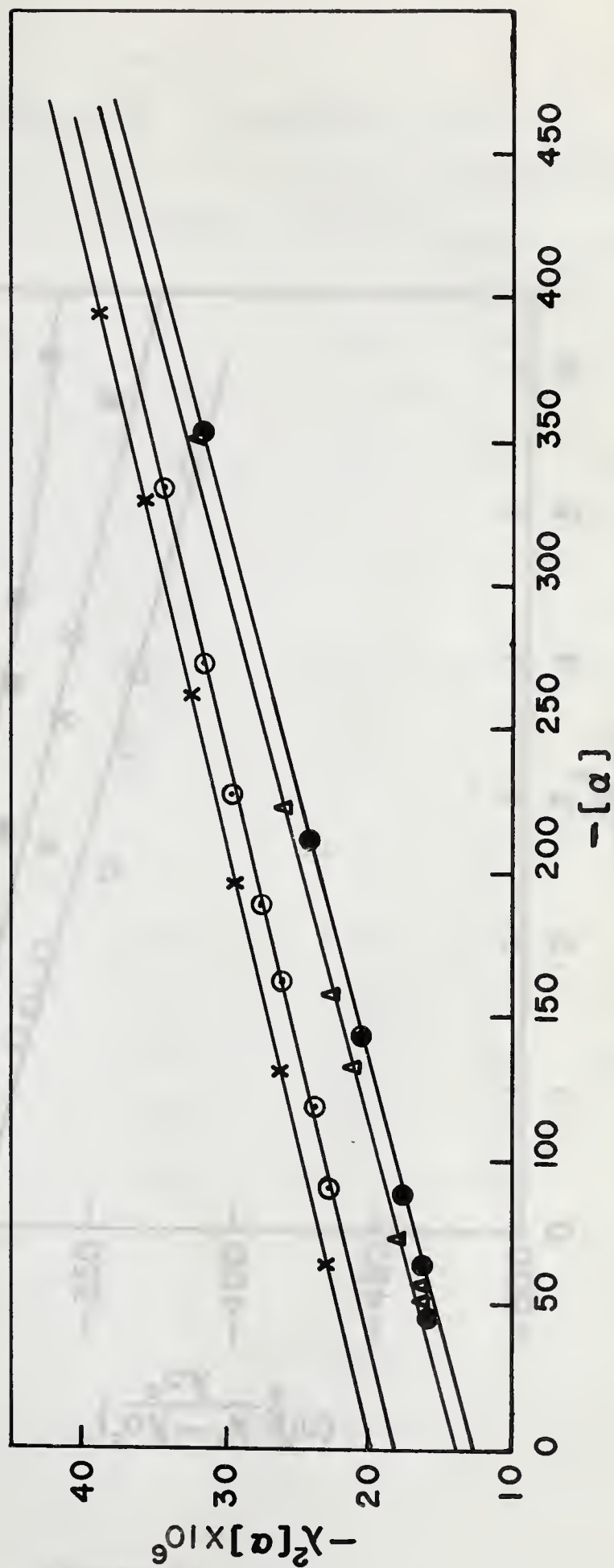


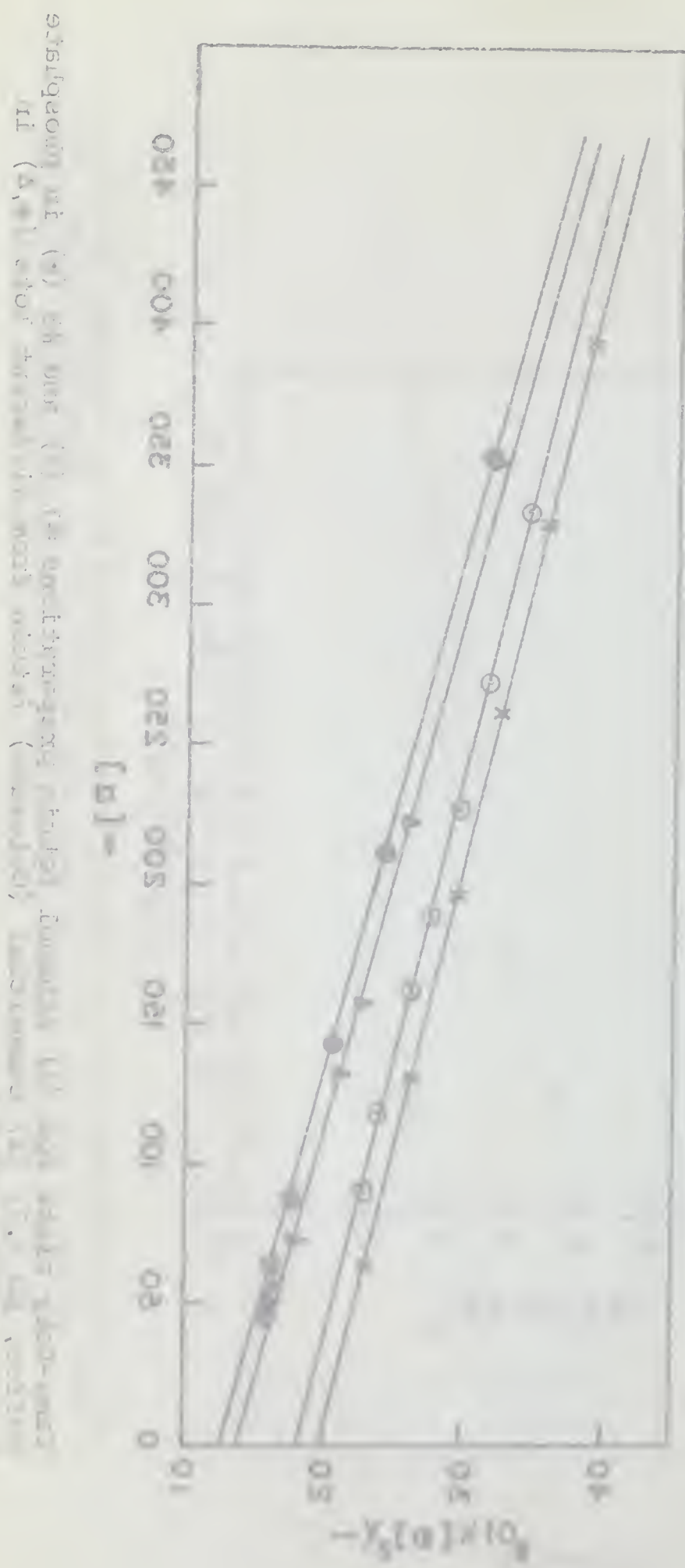
Figure 1A shows the relationship between  $\log V$  (ml) per g and  $C$  (mol/g) for a polymer solution. The data points, represented by open circles and open triangles, show a linear increase in  $\log V$  with increasing  $C$ . The upper line corresponds to a concentration of 0.01 g/g, and the lower line corresponds to a concentration of 0.02 g/g. The slope of the lines is approximately 0.015 ml/g per mol/g.

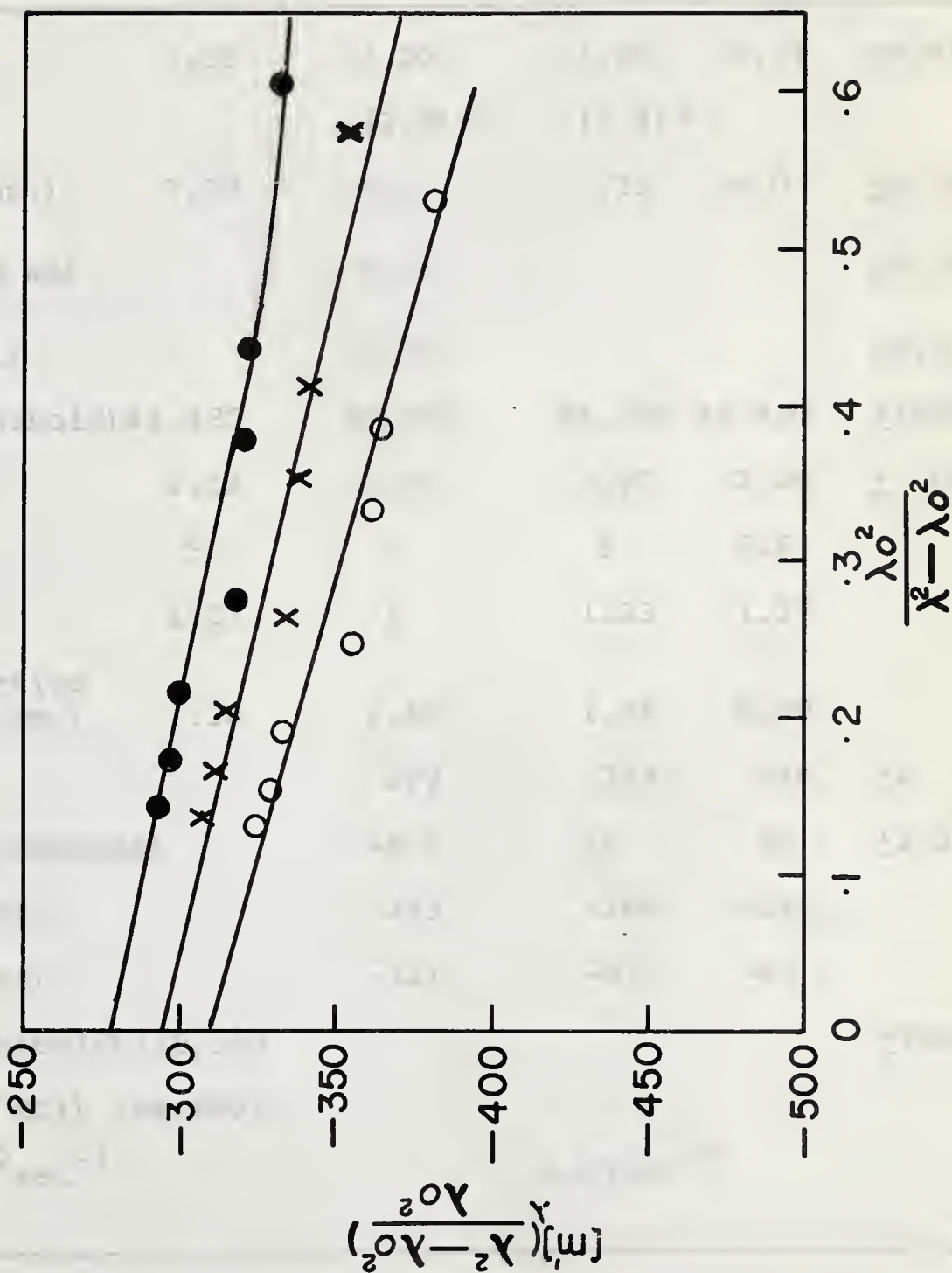


Yang-Doity plots for (1) ethanol fetuin preparations #1 (x) and #3 (○) in phosphate buffer, pH 7.7; (2) commercial (Colorado) fetuin from different lots (●, Δ) in borate buffer, pH 8.0.

Figure 20

Figure 1. Dependence of  $\log \eta$  on  $-\log a$  for the system  $\text{Pb}(\text{CH}_3\text{COO})_2$  -  $\text{Pb}(\text{CH}_3\text{COO})_2$  -  $\text{Pb}(\text{CH}_3\text{COO})_2$  at different temperatures.





Moffitt plot for 0.924% commercial (Colorado) fetuin in phosphate buffer, pH 7.7 for 3 values of  $\lambda_0$ : 209 m $\mu$  (●); 205 m $\mu$  (x); 200 m $\mu$  (○).

Figure 21

The following table gives the values of  $\frac{y_0 - y}{y_0 - y_\infty}$  for various values of  $\frac{y_0}{y_\infty}$  and  $\frac{y}{y_\infty}$ . The values are calculated from the equation  $y = y_0 e^{-kt}$  and are given to four decimal places.

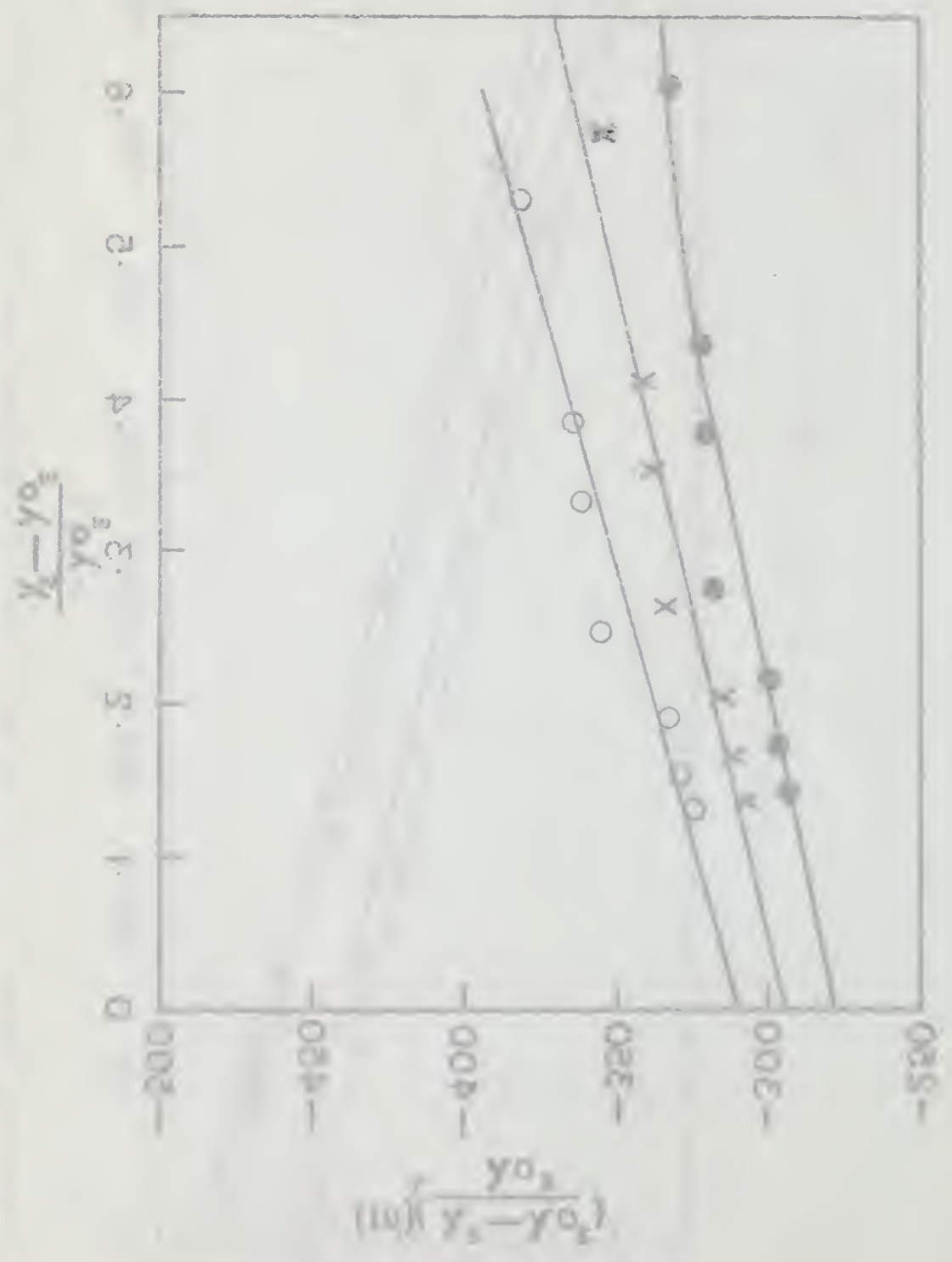


Figure 11



Table 1  
Molecular Properties of Commercial Fetuin

Parameter	Tris	Phosphate	Borate	Borate + CaAc <sub>2</sub>	Limits of Error	pH
$s_{20,w}^{\circ}$	3.30	3.20 (2.9) *	3.30 (3.3) *	3.55	$\pm 0.05$	7-8
$[\eta]$ (ml./gm.)	7.30	6.0	7.25	6.0	$\pm 0.20$	"
$E_{1cm}^{1\%}$ (278 mμ)		4.5			$\pm 0.10$	"
$\bar{v}$ (ml./gm.)		0.70			$\pm 0.01$	"
M.W. (Archibald)	43,485	45,900	44,320	43,420	$\pm 1500$	"
$\beta \times 10^{-6}$	2.22	2.02	2.22	2.24	$\pm .05$	
a/b	5	1	5	5.5		
$f/f_o$	1.23	1	1.23	1.27		
$V_e$ , effective $v_{ol.}$ (ml./gm.)	1.34	2.40	1.34	0.99		
$\lambda_c$ (mμ)		229	229	216	$\pm 2$	"
$-[\alpha]_{589}$ (degrees)		48.5	48	55	$\pm 1.0$	"
$a_o$ (degrees)		-253	-288	-326		8.0
$b_o$ (degrees)		-121	-97	-42		"
M.W. (Archibald)	118,300				$\pm 3000$	3.0
(glycine HCl) (94,850) *						3.5
$D_{20,w}^{\circ}$ cm <sup>2</sup> sec <sup>-1</sup>				$6.07 \times 10^{-7}$		



Table 2

Molecular Properties of Ethanol Fractionated Fetuin

Parameter	Phosphate	Borate	Limits of Error	pH
$s_{20,w}^{\circ}$	3.0	3.30	$\pm 0.05$	7-8
$[\eta]$ ml./gm.	6.65	7.95	$\pm 0.20$	"
$E_{1cm}^{1\%}$ (278 m $\mu$ )	4.5		$\pm 0.10$	"
$\bar{v}$ (ml./gm.)		0.70	$\pm 0.01$	"
M.W. (Archibald)	43,360	45,600	$\pm 1500$	"
$\beta \times 10^{-6}$	2.02	2.28	$\pm .05$	
a/b	1	6		
$f/f_o$	1	1.31		
$V_e$ effective vol. (ml./gm.)	2.66	1.12		
$\lambda_c$ (m $\mu$ )	220	210	$\pm 2$	"
$-\left[\alpha\right]_{589}$ (degrees)	62.5	65	$\pm 1.0$	"
$a_o$ (degrees)	-377	-471		"
$b_o$ (degrees)	-61	-36		"
M.W. (Archibald)	70,850		$\pm 3000$	3.5
(glycine/HCl)	120,300			2.6
Electrophoretic mobility (cm <sup>2</sup> volt <sup>-1</sup> sec <sup>-1</sup> )	$5.46 \times 10^{-5}$		$\pm 0.10 \times 10^{-5}$	6.85





(1)

(1) Commercial (Colorado) fetuin in phosphate buffer, pH 6.85,  $\mu=0.16$  (80% contributed by NaCl) (descending). Protein concentrations approx. 0.7%.



(2)

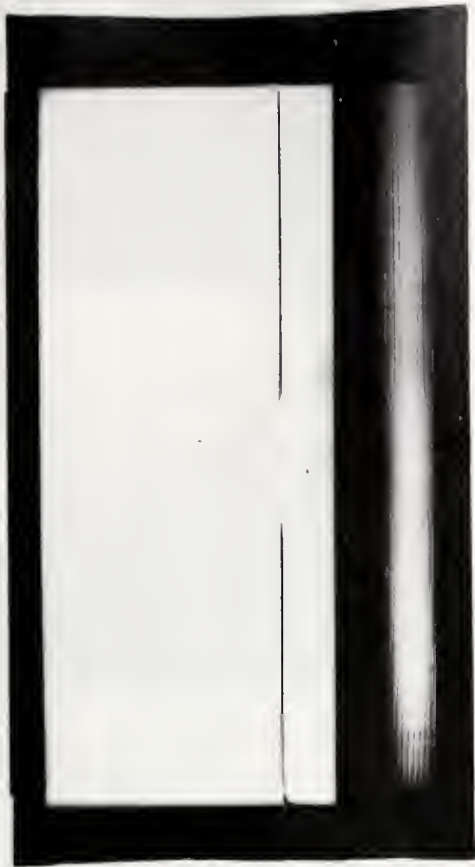
(2) Ethanol fetuin in Tris buffer, pH 8.0,  $\mu=0.1$  (ascending); (2) Ethanol fetuin in phosphate buffer, pH 6.85,  $\mu=0.16$  (80% contributed by NaCl) (descending).







(1)



(2)

(1) Commercial (Colorado) fetuin (0.6%) in borate buffer, pH 8.0,  $\mu=0.16$ , bar angle  $60^\circ$ . Time from start 21.15 hours. (2) Ethanol fetuin (1%) in phosphate buffer, pH 7.7,  $\mu=0.16$ , bar angle  $60^\circ$ . Time from start 28.43 hours.





(1)



(2)

(1) Ethanol fetuin (approx. 0.4%) in borate buffer, pH 8.0,  $\mu=0.16$ , bar angle  $50^\circ$ . Picture intervals 16 mins., speed 59,780 r.p.m. (2) Commercial (Colorado) fetuin (approx. 0.5%) in borate buffer, pH 8.0,  $\mu=0.16$ , bar angle  $50^\circ$ . Picture intervals 16 mins., speed 59,780.







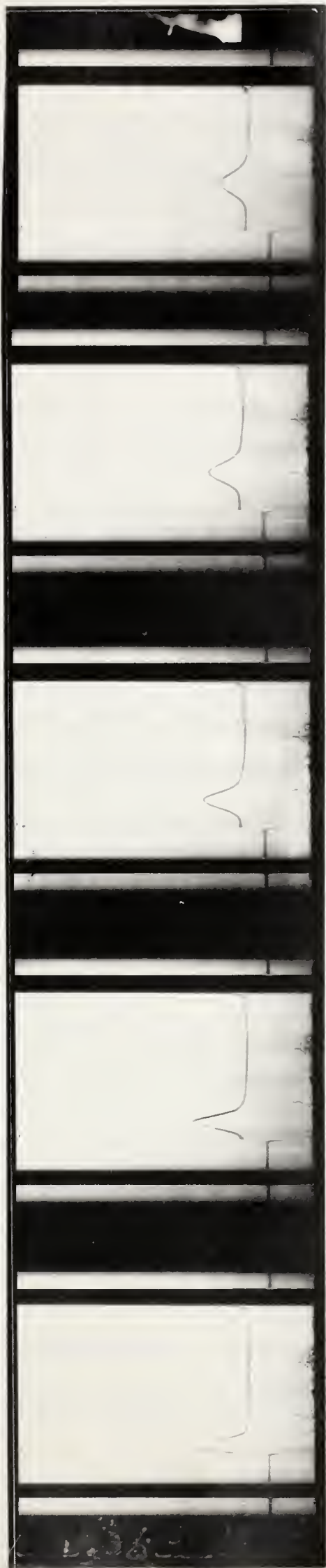
(1)



(2)

(1) Commercial (Colorado) fetuin 1% in borate buffer, pH 8.0 (+ 0.1M calcium acetate) bar angle 75°. Picture #1, speed 8,766 r.p.m., time 25 mins. Pictures #2,3,4,5, times 5, 10, 20, 45 min., speed 11,573 r.p.m. (2) Run for  $c_o$ , speed 59,780 r.p.m.





(1)

(1) Run for  $c_0$ , speed 59,780 r.p.m.



(2)

(2) Ethanol fetuin 1% in glycine/HCl buffer, pH 3.5,  $\mu=0.1$ , bar angle  $75^\circ$ .  
Pictures at 30, 45, 60, 70 mins., speed 12,590 r.p.m.





## Part II

The influence of some organic solvents on the hydrodynamic and optical rotatory properties of commercial (salt precipitated) fetuin at pH 7-8, and the pH region (ca. 2.4) where the molecule shows maximum association

In the pH range 7-8 where the molecule is monomeric, the aim was to find out whether or not changes in secondary structure could be observed, by alterations in the optical rotatory parameters  $\lambda_c$  and  $b_o$ , on the addition of organic solvents to a phosphate buffered system. As pointed out in the introduction, it is advisable to support such measurements with other techniques such as sedimentation and viscosity. This approach was adopted for a fixed concentration of protein (ca. 0.5%) using the solvents formamide, ethylene glycol and dioxane, added up to a concentration of about 30% by volume to the buffered system. In the low pH region maximum association, corresponding to a molecular weight of about 118,000, occurs close to pH 2.4, for salt prepared material, where a maximum value of  $S_{20,w} = 4.0$  is also observed for a protein concentration of 0.65%. In view of the believed heterogeneity in this region and the critical pH dependency of the associative process, this system was not considered suitable for extensive characterization. It was, however, regarded as worthwhile to see if the addition of certain denaturing agents and salts would affect the extent of association, perhaps thereby giving some insight into the nature of the linkages involved. Sedimentation was chosen since complete dissociation would be accompanied by a drop in  $S_{20,w}$  of about 1.2S, which would be readily detected by centrifugation.





### Hydrodynamic parameters of fetuin in organic solvents at pH 7-8

The effect of introducing ethylene glycol, dioxane or formamide into the phosphate system on the hydrodynamic behaviour of commercial fetuin is shown in Figures 22 and 23. The former shows the variation of  $S_{20,w}$  with solvent concentration for a fetuin concentration of approximately 0.5%. The latter shows the corresponding  $\eta_{red}$  plots as a function of the added solvent. Quantities were so arranged that a constant amount of phosphate buffer was used; in each case the solvent replaced an equal amount of water only. In this way the pH and ionic strength were maintained at constant values of 7.7 and 0.16, respectively. It is observed that the effect on the negative slope of the  $S_{20,w}$  vs.  $c$  plots is in the order: formamide > dioxane > ethylene glycol. In the case of  $\eta_{red}$  vs.  $c$  the effect on the positive slope is in the same order. Since in each instance a decrease in  $S_{20,w}$  is paralleled by an increase in  $\eta_{red}$ , a shape change is implied. Further, since the  $S_{20,w}$  and  $\eta_{red}$  for each solvent show magnitudes which vary in an inverse manner, i.e. the smallest increase in viscosity is accompanied by the smallest decrease in sedimentation and vice versa, one concludes that on a percent volume basis at least, the formamide is more effective at inducing a conformational change in this molecule than either glycol or dioxane.

### Optical rotatory dispersion measurements in organic solvents at pH 7-8

Figures 24, 26 and 28 illustrate the optical rotatory data for fetuin in the formamide, dioxane and ethylene glycol buffer systems, respectively, plotted according to the Moffitt method.



A value of 205 mμ for  $\lambda_o$  has been used throughout, as described in the previous section. As before, the Moffitt plots obtained showed good linearity. The corresponding Yang-Doty plots are shown in Figures 25, 27 and 29.

The optical rotation in terms of absolute values and slope of the plots parallels the hydrodynamic picture except that the slope of the dioxane plot instead of lying between the other two, does in fact approach more closely a value for the native molecule. For the formamide and ethylene glycol cases, however, it would appear that the solvent induced conformational change results in a decrease in helix from that of the native structure. A control for the system in phosphate, without added solvent, is also shown in Figures 24 and 25. Values of  $a_o$ ,  $b_o$  and  $\lambda_c$  for the plots shown, in addition to other data, are summarized in Table 3.

It is to be expected that any variation in the dispersion constant  $\lambda_c$  would follow the changes in slope of the Moffitt plots. The small negative slope of the plot for the protein in 20% and 30% formamide, for which  $\lambda_c = 212$  mμ is consistent with the choice of  $\lambda_o = 205$  mμ, as representative of the random coil. These results are in keeping with the view that as the molecule becomes extended, it exhibits a progressive loss in helix.

#### Sedimentation in the pH range 2.3-2.5

The values of  $S_{20,w}$  obtained in the different systems are summarized in Table 4. The data suggest that a high ionic strength of a neutral salt (0.5M  $\text{Na}_2\text{SO}_4$ ) has no effect on  $S_{20,w}$  but  $\text{CaCl}_2$  (0.1 and 0.5M) increases the sedimentation as observed





previously at pH 7-8. While formamide and guanidine do show a decrease in  $S_{20,w}$ , a molecular weight determination in the system containing 25% formamide gave a value of 116,130 which is not considered to be significantly different from its value in the absence of this reagent.

### Discussion

It is evident from the observations in the pH range 7-8 that each of the reagents added to the buffered phosphate system induces a conformational change. The inverse shift in sedimentation and viscosity is supported by no significant alteration in molecular weight in the presence of 20% formamide and 20% dioxane (see Table 3). This is paralleled by changes in  $\lambda_c$  and  $b_o$  derived from the optical rotatory measurements.

The effect of formamide as a denaturing agent is typical and supports the concept that there is partial unfolding of the native molecule when exposed to this reagent. An extended conformation is indicated by the hydrodynamic picture paralleled by a decrease in  $b_o$  and an overall increase in the levo rotation, suggesting a decrease in helical content. A similar but less dramatic effect is observed with ethylene glycol. The effect of dioxane is not entirely clear but may represent a partial reformation of helix following solvent penetration since this solvent, as a non-polar substance, is known to favour the helical form of polyamino acids (88). Although similar effects are observed with both polar and non-polar agents introduced into the aqueous system, it is probable that their action is effective at different sites and in the latter case may represent



penetration into hydrophobic regions of the molecule with consequent alterations in secondary structure. This is in keeping with the amino acid analysis of the molecule which shows that of the 329 residues present, at least 110 would contribute hydrophobic properties (72). Since an estimated 15% helix from the optical rotatory data could hardly maintain the compact form which this molecule exhibits, the hydrophobic regions could contribute a major source of stability, although as in other globular proteins, intrachain disulfide bonds doubtless limit the degree of flexibility.

The alterations in  $S_{20,w}$  observed in the pH range 2.3-2.5 emphasize the stability of the associated units. It appears that while no change in molecular weight occurs, the effect of added  $\text{CaCl}_2$  or formamide induces a shape change comparable to that observed at pH 7-8. The association does not appear to be influenced either by high ionic strength, high concentrations of polar reagents such as formamide or a non-polar reagent such as ethylene glycol. In particular, the small increase in  $S_{20,w}$  in the presence of 0.1 M  $\text{CaCl}_2$  suggests a conformational change to more compact form in the associated state, consistent with observations made on the monomer at pH 7-8, as described in Part I. Since 50% glycol produces only a drop from 4.0 to 3.70S, this too probably reflects a shape change comparable to that at pH 7-8 in the presence of this reagent. The impression is that hydrogen bonds are probably not involved and if hydrophobic groups are functional in the association process the latter are extremely strong. Electrostatic interaction seems doubtful in view of a





relative insensitivity to high ionic strength.

During association in the pH region 2-4, in the absence of additives, the  $S_{20,w}$  maxima occur at a higher pH than the maxima (see Part I). A possible explanation is as follows. As the net charge on the molecule decreases, association begins, and during this phase the asymmetry of the associating units decreases. Since the effective volume of the associated units will be larger than for the monomer, their contribution will offset the decrease in asymmetry of the associating monomer. It follows that  $\eta_{red}$  will start to increase as observed, as will  $S_{20,w}$ . Since the effective mass increases at a greater rate than the frictional resistance,  $S_{20,w}$  will increase to a maximum and the  $\eta_{red}$  will increase to a certain level. Once association is complete, the combining units are held quite strongly and as the pH is lowered beyond this point and the net charge on these units starts to increase, there is a concomitant increase in axial ratio. The associated mass remains the same and  $S$  decreases due to the increase in  $f$ , while  $\eta$  continues to rise. Once dissociation starts,  $\eta$  drops off and  $S$  continues to decrease.

Hence, on the basis of the above argument, the  $S_{20,w}$  maxima corresponds to the most compact form of the completely associated product and the  $\eta_{red}$  maxima to the most extended form of the associated product.

The effect of guanidine and formamide could then be interpreted in this pH region in similar fashion to the observations at pH 7-8. That is, although the units have associated, there is still some secondary structure which can unfold in the presence





of these reagents to give a more extended conformation. The graphs from Part I suggest that shape change for the associated product may be reflected in a concomitant variation in  $S_{20,w}$  and  $\eta_{red}$  (for a fetuin concentration of 0.65%) between the limits of (3.4-4)S and (8.5-10.4) ml./gm., respectively.



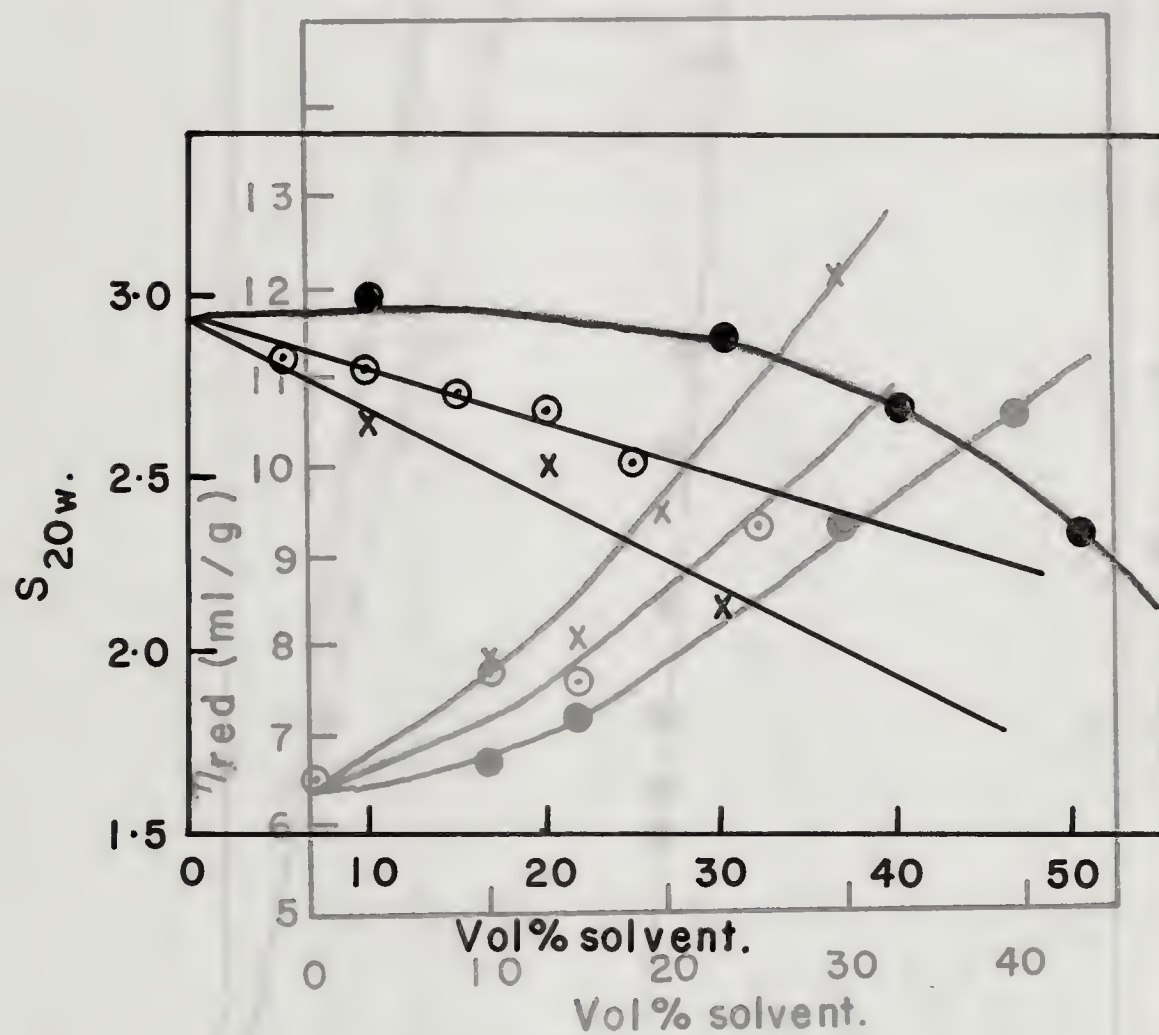
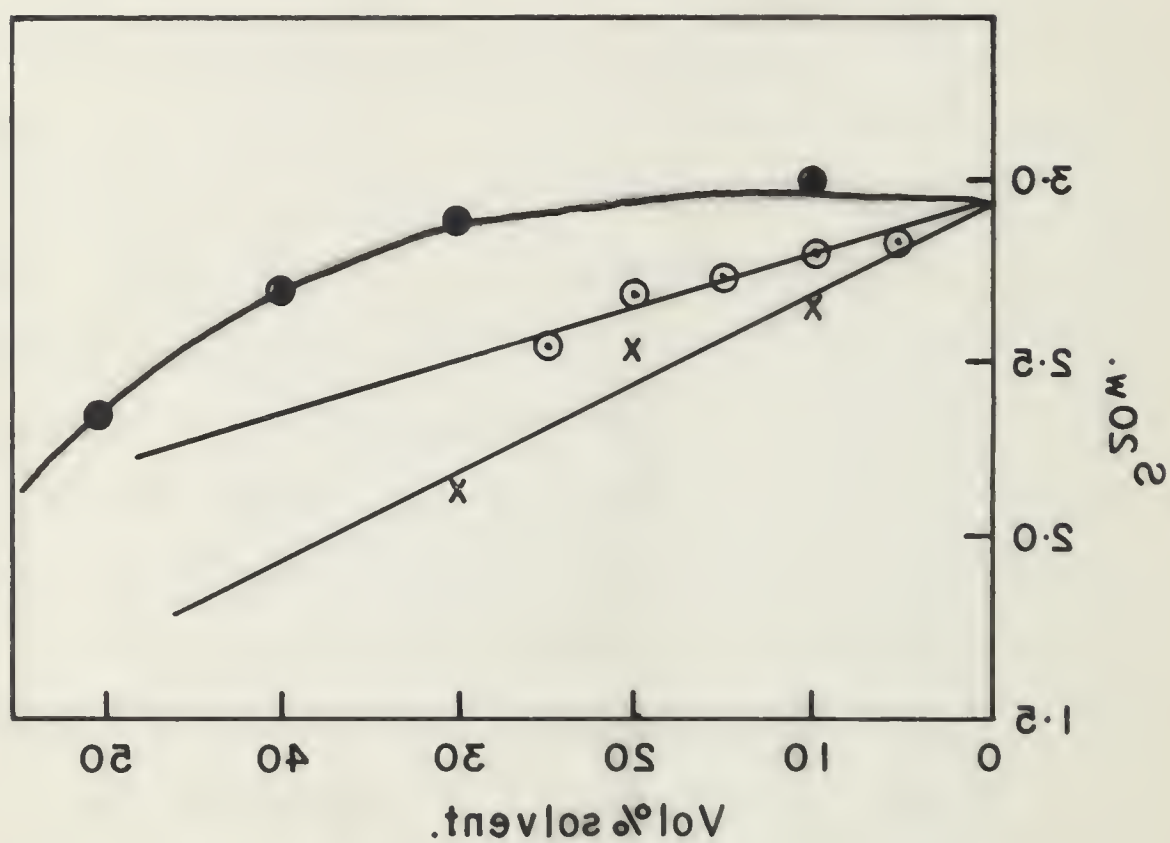


Figure 22  
Figure 23

S<sub>20,w</sub> vs. volume % solvent in phosphate buffer, pH 7.7, μ = 0.16: formamide (x); dioxane (O); ethylene glycol (●). Concentration of commercial fetuin 0.52%. (●). Concentration of commercial fetuin 0.52%.

0.52% glycol (●). Concentration of commercial fetuin  $\mu = 0.16$ : formamide (x); dioxane (○); ethylene vs. volume % solvent in phosphate buffer, pH 7.7,  $20^\circ\text{C}$

Figure 22





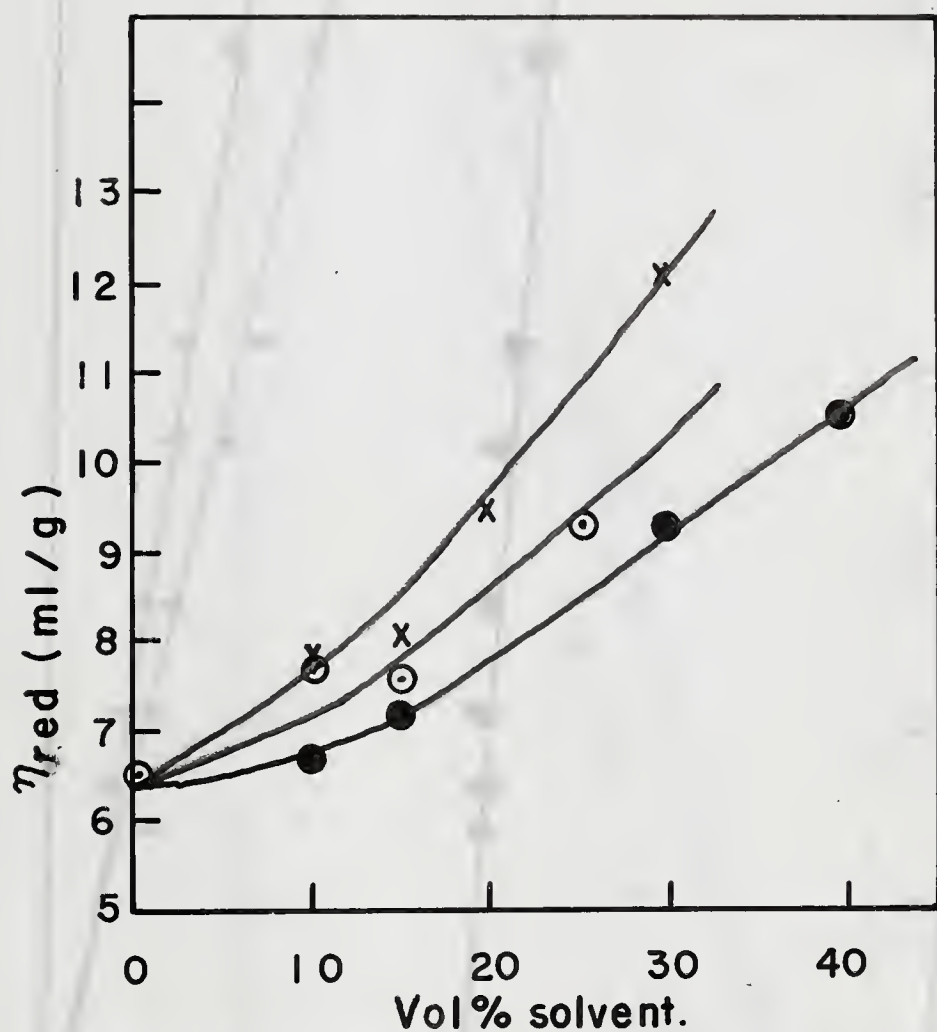


Figure 23

$\eta_{red}$  vs. volume % solvent in phosphate buffer, pH 7.7,  $\mu = 0.16$ : formamide (x); dioxane (⊙); ethylene glycol (●). Concentration of commercial fetuin 0.52%.

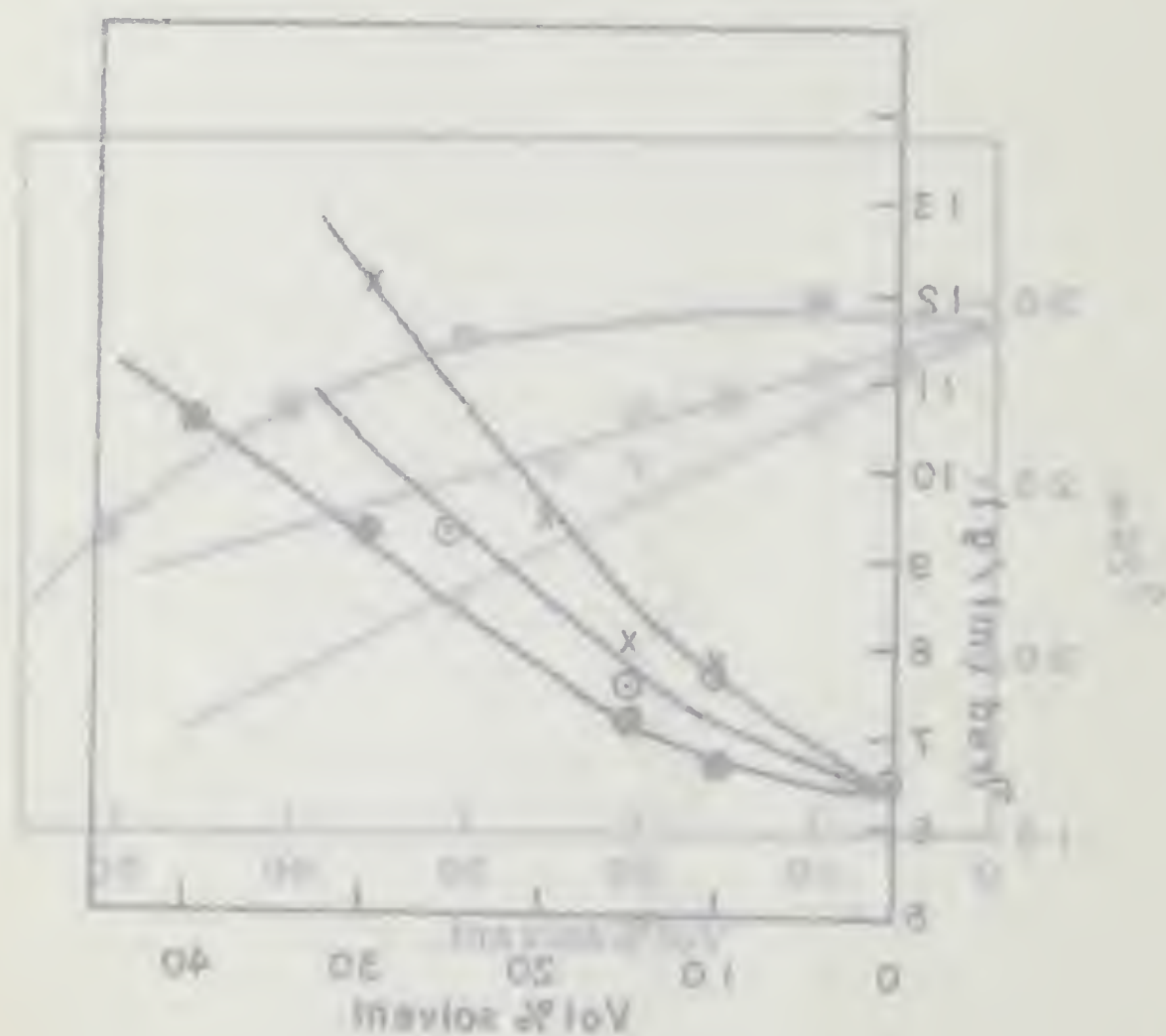
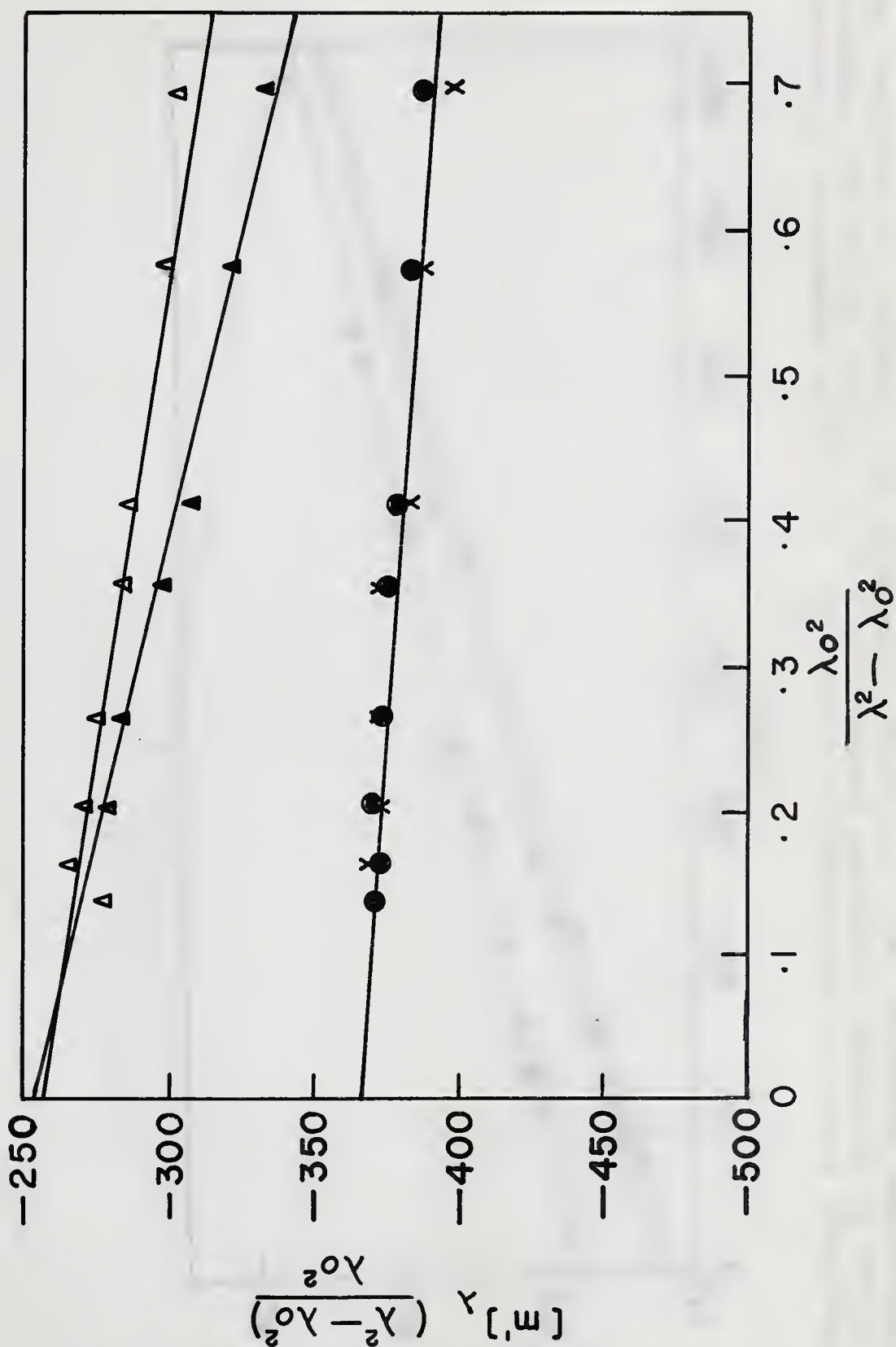


Figure 23  
 The curves show the relationship between the log unit base and the log unit for the system studied. The curves are labeled with 'x' and 'o' markers. The x-axis represents the volume percentage of solvent (0 to 100), and the y-axes represent the log unit base (0 to 13) and the log unit (0 to 10).

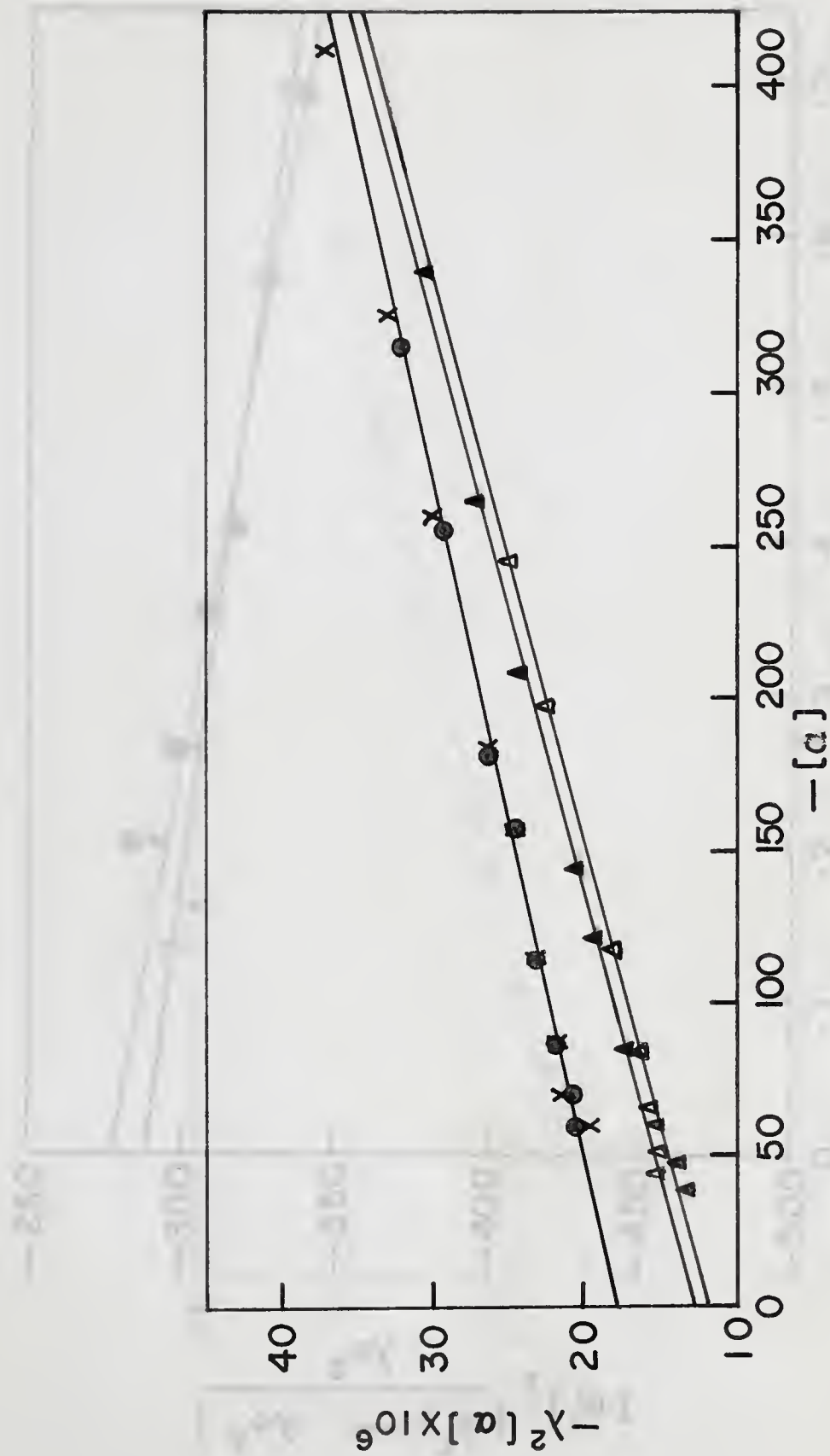


Moffitt plots for 0.515% commercial (Colorado) fetuin in formamide phosphate buffer, pH 7.9,  $\mu = 0.16$ : 30% volume formamide (x); 20% volume formamide (●); 10% volume formamide (Δ). Control in phosphate with no added solvent (Δ).

Figure 24



Fig. 1. Dependence of the dimensionless parameter  $\left(\frac{y_0}{y_s}\right)^2 (y_s - y_0)$  on the normalized time  $\frac{t - t_0}{\tau_s}$  for different values of the parameter  $\beta$ : (a)  $\beta = 0.1$ ; (b)  $\beta = 0.2$ ; (c)  $\beta = 0.3$ ; (d)  $\beta = 0.4$ . The curves are calculated for  $\gamma = 1.0$  and  $\alpha = 0.5$ .

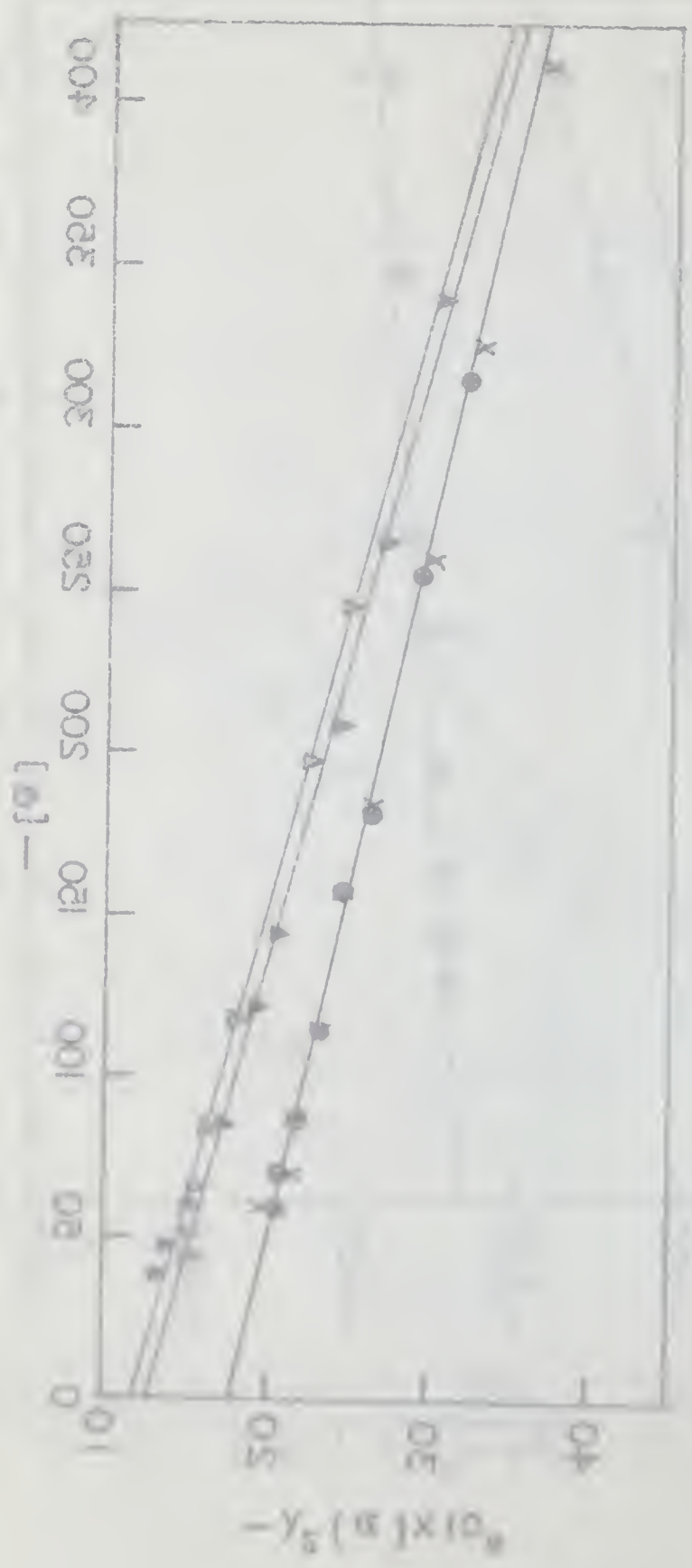


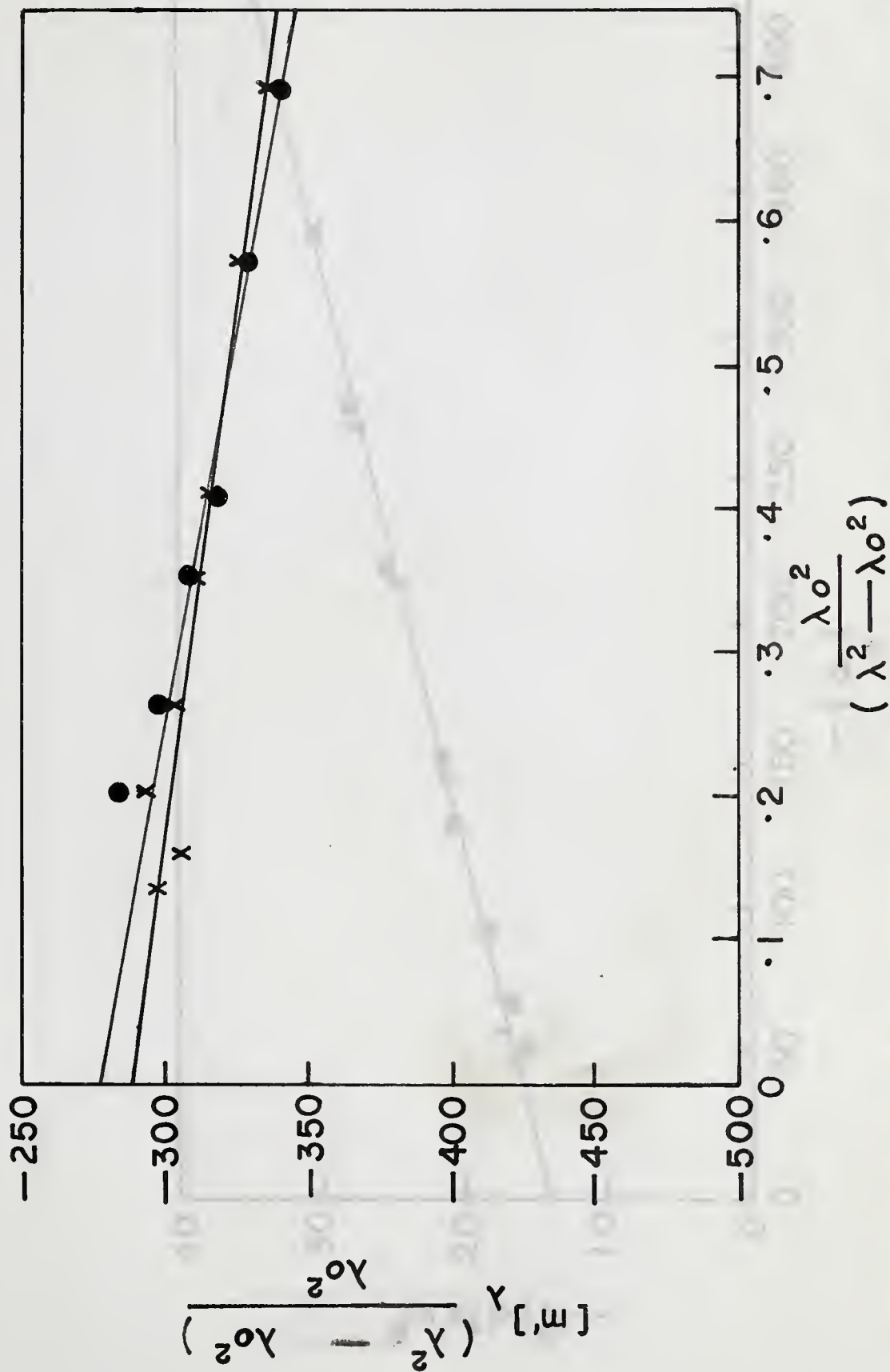
Yang-Doty plots corresponding to Figure 24, for 0.515% commercial (Colorado) fetuin in formamide phosphate buffer, pH 7.9,  $\mu = 0.16$ : 30% volume formamide (x); 20% volume formamide (●); 10% volume formamide (▲). Control in phosphate with no added solvent (▲).

Figure 25



(a)  $\gamma_2$  vs.  $[\eta]$  for 0.1% solution of polyisobutylene in benzene at 25°C. (b)  $\gamma_2$  vs.  $[\eta]$  for 0.1% solution of polyisobutylene in benzene at 35°C. (c)  $\gamma_2$  vs.  $[\eta]$  for 0.1% solution of polyisobutylene in benzene at 45°C. (d)  $\gamma_2$  vs.  $[\eta]$  for 0.1% solution of polyisobutylene in benzene at 55°C. (e)  $\gamma_2$  vs.  $[\eta]$  for 0.1% solution of polyisobutylene in benzene at 65°C.

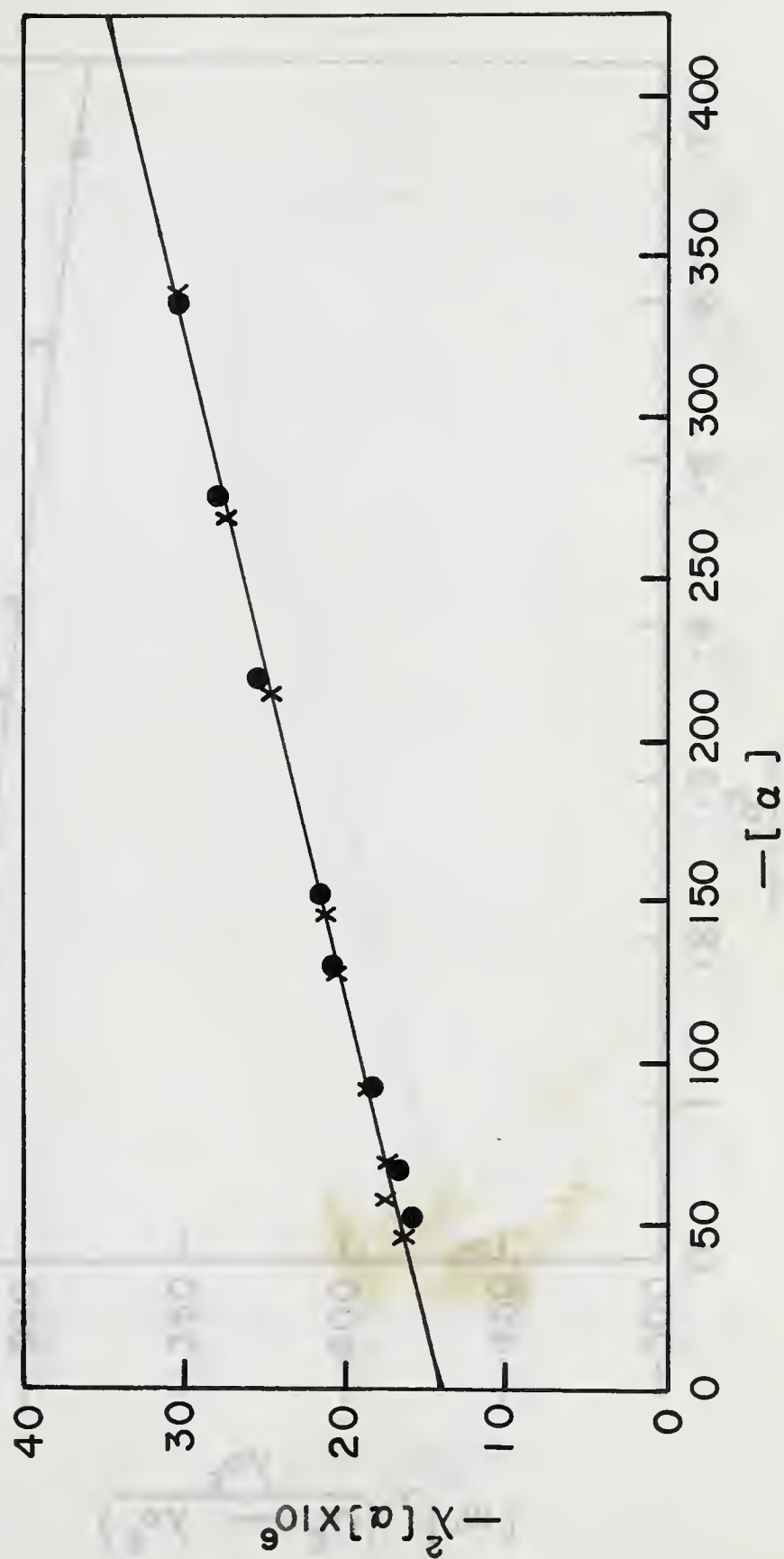




Moffitt plots for 0.53% commercial (Colorado) fetuin in dioxane phosphate buffer, pH 7.7,  $\mu = 0.16$ : 25% volume dioxane (●); 10% volume dioxane (x).

Figure 26





Yang-Doty plots corresponding to Figure 26 for 0.53% commercial (Colorado) fetuin in dioxane phosphate buffer, pH 7.7,  $\mu = 0.16$ : 25% volume dioxane (●); 10% volume dioxane (x).

Figure 27

Figure 10.

Plot of  $\chi_2 \times 10^3$  versus  $[\eta]$  for the copolymers of styrene and acrylonitrile. The data points are shown for copolymers with  $[\eta]$  values of 0.1, 0.2, 0.3, 0.4, 0.5, 0.6, 0.7, 0.8, 0.9, 1.0, 1.1, 1.2, 1.3, 1.4, 1.5, 1.6, 1.7, 1.8, 1.9, 2.0, 2.1, 2.2, 2.3, 2.4, 2.5, 2.6, 2.7, 2.8, 2.9, 3.0, 3.1, 3.2, 3.3, 3.4, 3.5, 3.6, 3.7, 3.8, 3.9, 4.0, 4.1, 4.2, 4.3, 4.4, 4.5, 4.6, 4.7, 4.8, 4.9, 5.0, 5.1, 5.2, 5.3, 5.4, 5.5, 5.6, 5.7, 5.8, 5.9, 6.0, 6.1, 6.2, 6.3, 6.4, 6.5, 6.6, 6.7, 6.8, 6.9, 7.0, 7.1, 7.2, 7.3, 7.4, 7.5, 7.6, 7.7, 7.8, 7.9, 8.0, 8.1, 8.2, 8.3, 8.4, 8.5, 8.6, 8.7, 8.8, 8.9, 9.0, 9.1, 9.2, 9.3, 9.4, 9.5, 9.6, 9.7, 9.8, 9.9, 10.0.

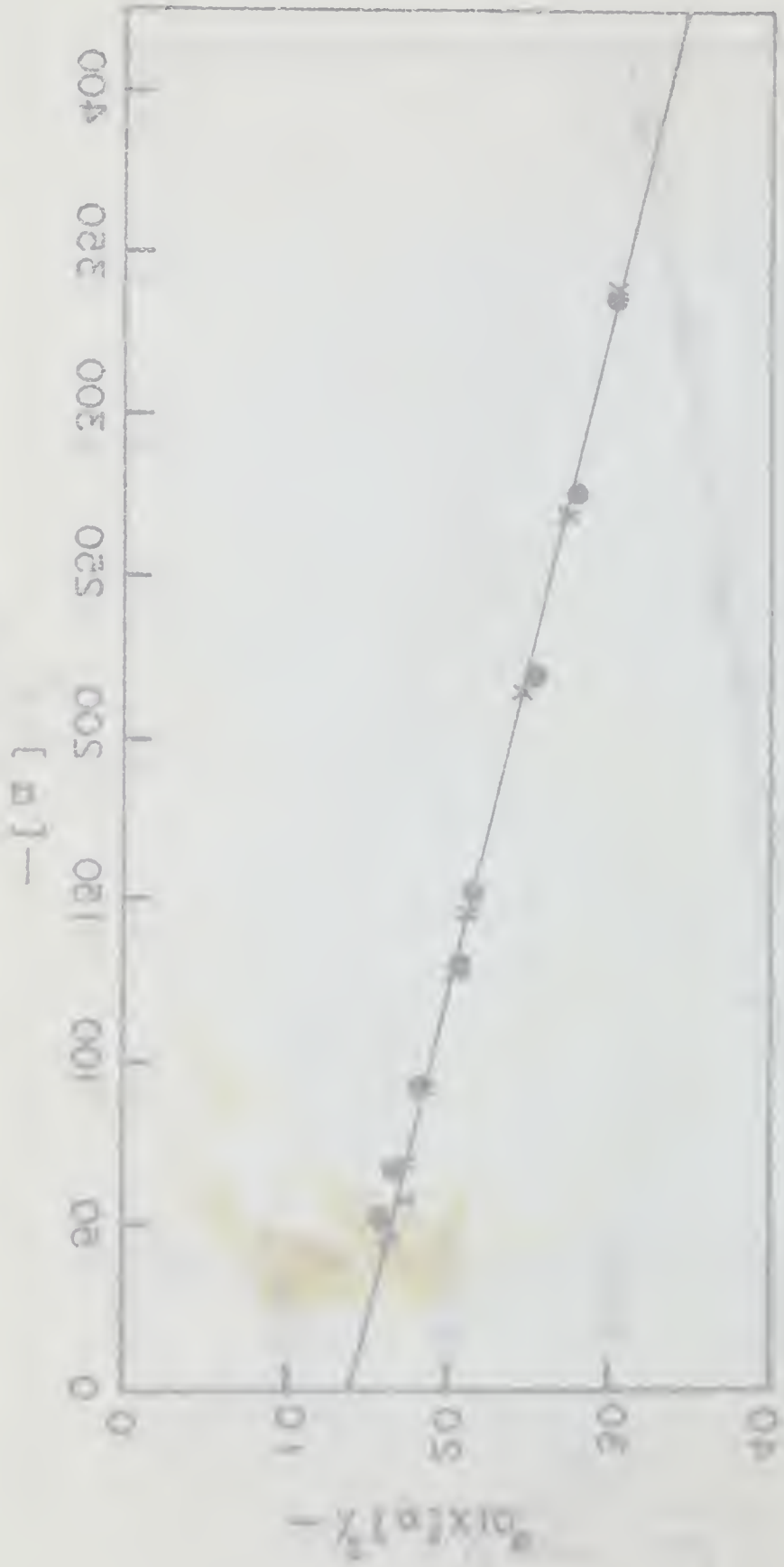
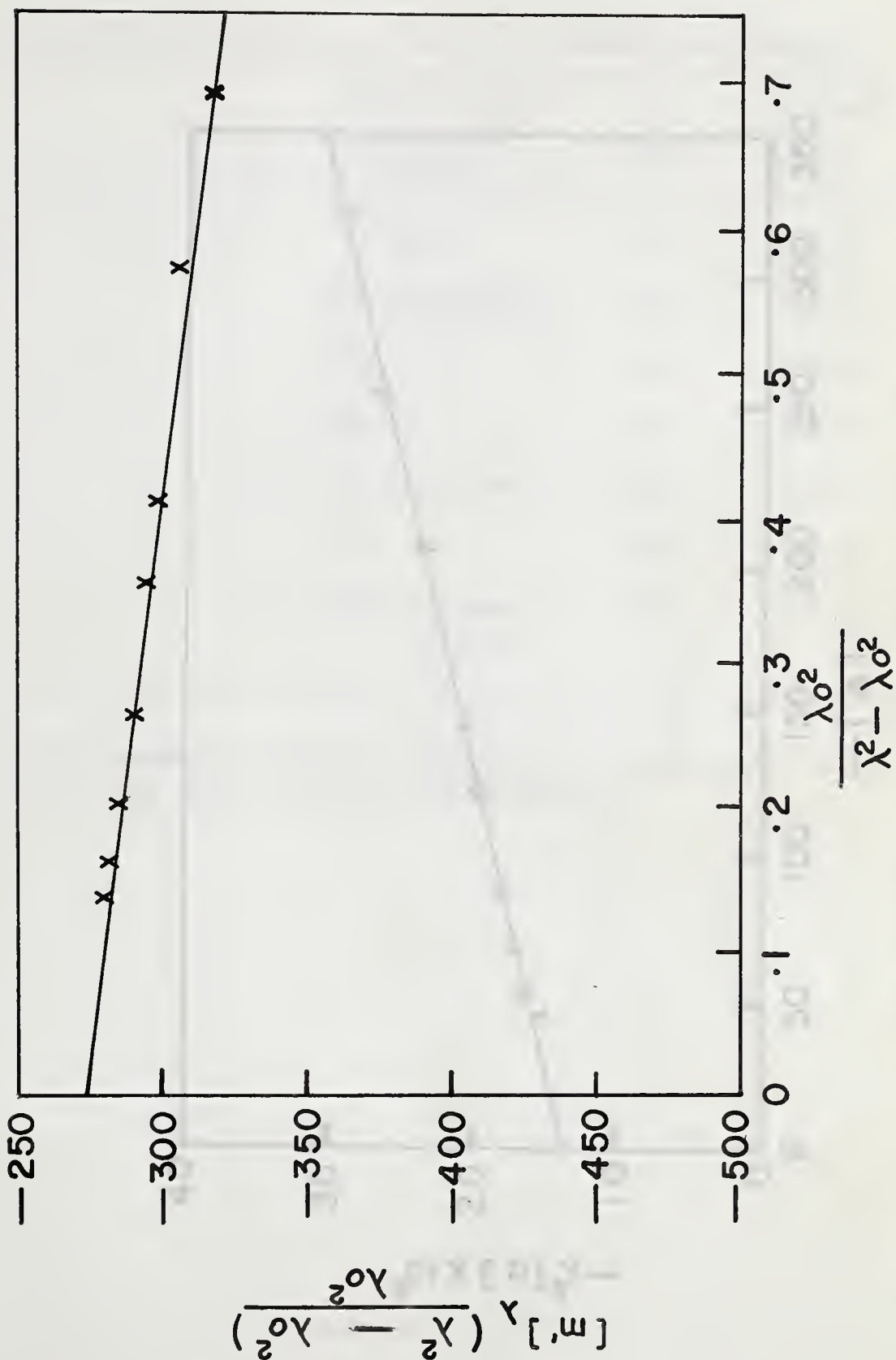


Figure 10.





Moffitt plot for 0.515% commercial (Colorado) fetuin in ethylene glycol phosphate buffer, pH 7.9,  $\mu = 0.16$  for 35% volume glycol (x).

Figure 28

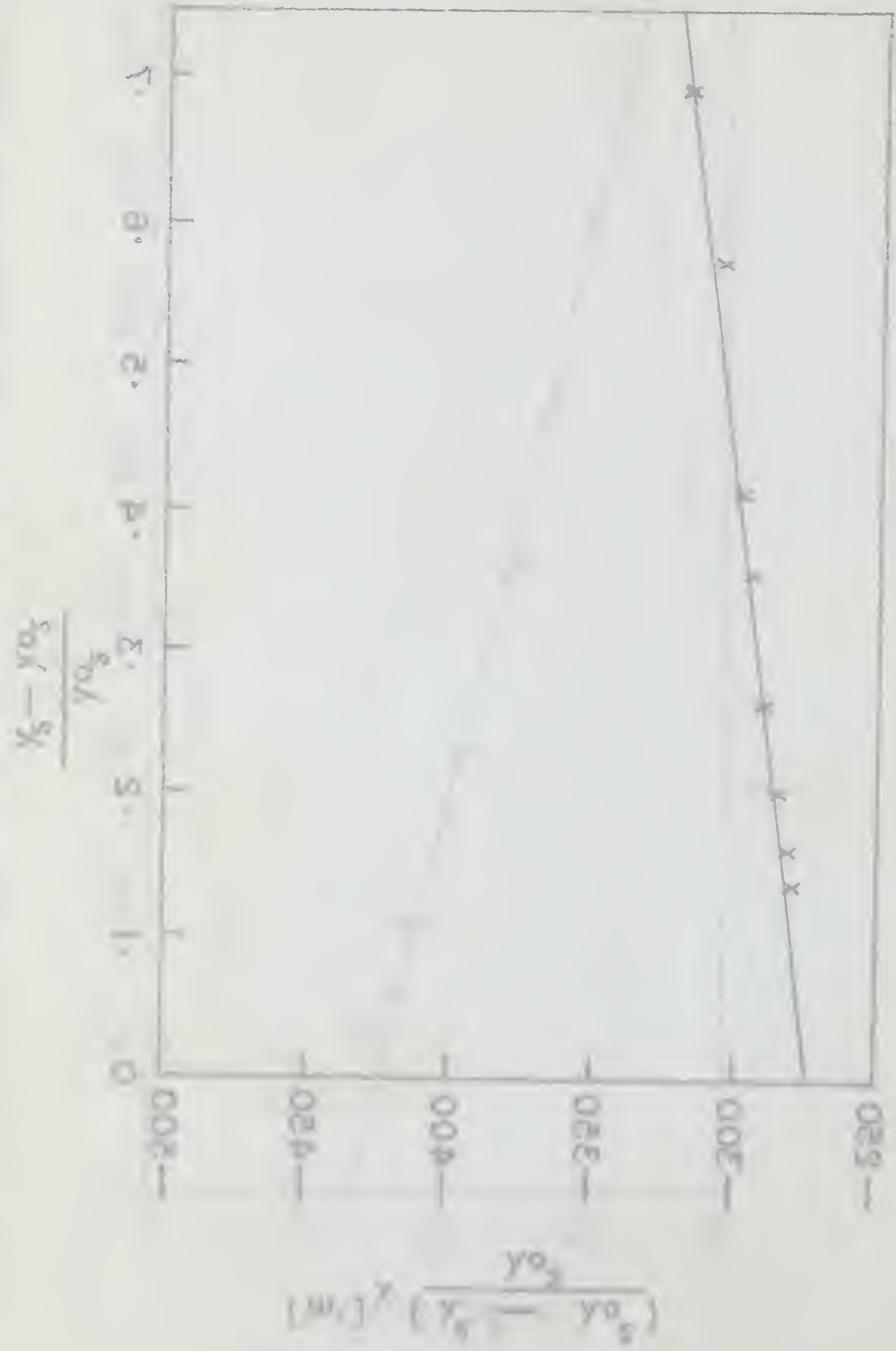
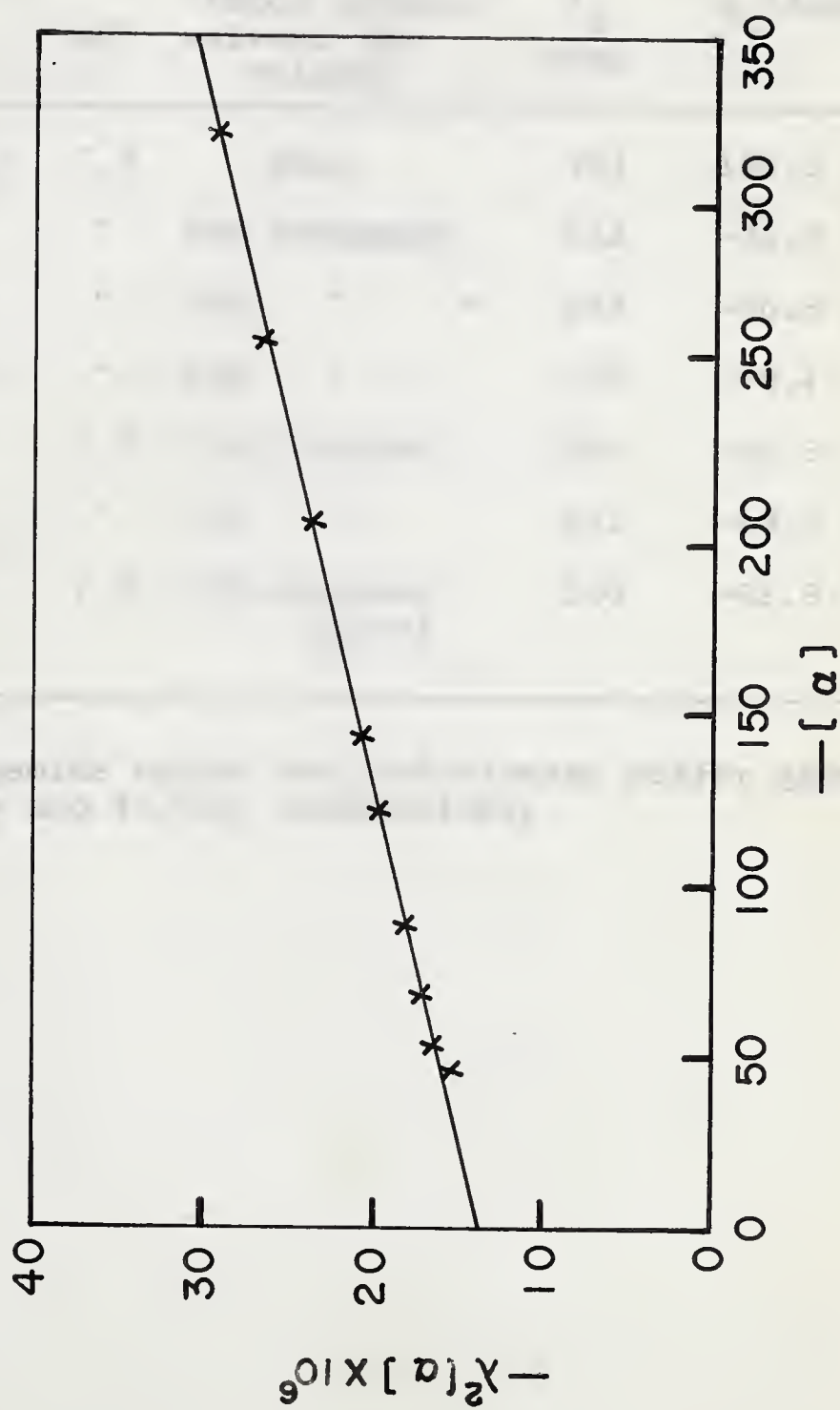


FIGURE 24

Velocity of sound,  $w_s$ , as a function of the density,  $\rho$ , for the case of a perfect gas,  $\gamma = 1.4$ , and  $y_{o_s} = 0.01$ . The curve is calculated from the equation  $w_s = \sqrt{\gamma p / \rho}$ , where  $p$  is the pressure.



Yang-Doity plot corresponding to Figure 28 for 0.515% commercial (Colorado) fetuin in ethylene glycol phosphate buffer, pH 7.9,  $\mu = 0.16$  for 35% volume glycol (x).

Figure 29



Table 3

Optical Rotatory Dispersion Data on Commercial Fetuin

Buffer	$\mu$	pH	Added organic solvent (by volume)	$\lambda_c$ $\pm 2m\mu$	$b_o$ (deg)	$a_o$ (deg)
Phosphate	0.16	7.9	None	231	-120.5	-253
"	"	"	30% formamide	212	-36.3	-366
"	"	"	20% " *	212	-36.3	-366
"	"	"	10% "	229	-78.4	-256
"	"	7.7	25% dioxane*	222	-92.5	-276
"	"	"	10% "	222	-68.5	-288
"	"	7.9	35% ethylene glycol	220	-63.8	-274

\* M.W. in 20% formamide buffer and 20% dioxane buffer gave values of 44,800 and 42,020, respectively.





Table 4

Sedimentation Values Obtained at pH 2.3-2.5 in Glycine/HCl Buffer, Ionic Strength 0.1 to which Has Been Added the Specified Salt or Organic Reagent

	Additive	pH	S <sub>20,w</sub>
0.65% commercial fetuin	None	2.3	3.95
"	25% formamide	"	3.62
"	20% "	"	3.60
"	15% "	"	4.10
"	50% glycol	2.5	3.72
"	0.5M CaCl <sub>2</sub>	"	4.35
"	0.1M CaCl <sub>2</sub>	2.3	4.13
"	0.5M Na <sub>2</sub> SO <sub>4</sub>	2.5	3.90
"	3M guanidine	"	3.23
"	3M " + 0.1M CaCl <sub>2</sub>	"	3.34



### Part III

#### A. Stability of fetuin

This part gives an account of the stability of fetuin to proteolytic attack by the enzymes trypsin and  $\alpha$ -chymotrypsin as judged by the rate at which cleavage of the protein proceeds. Measurements of molecular weight at pH values slightly acid and alkaline to pH 7.0 are used as a criterion of stability towards variation of pH. Some observations are also recorded in solutions of low ionic strength and in 80% formamide.

##### Proteolytic attack

The effect of adding trypsin to a solution of (a) salt prepared fetuin, (b) heat treated fetuin, and (c) material obtained by ethanol separation is shown in Figure 30. Noteworthy is the resistance that the salt prepared material has to trypsin while heat treatment of this material for 15 min. at 85-90°C. results in a rapid attack. It is clear from the plots that while ethanol material is not digested as rapidly as fetuin which has undergone heat treatment, it does nevertheless exhibit very little resistance to attack, as compared with native fetuin. The picture is very similar in the presence of  $\alpha$ -chymotrypsin. Salt prepared material after 3-4 min. remains inert whereas ethanol material is digested at a steady rapid rate.

##### Molecular weight studies

Table 5 summarizes some values of molecular weight obtained under the conditions listed for the second commercial preparation





of fetuin obtained from Australia. Noteworthy is the increase in molecular weight with time at pH 5.6 at normal refrigeration temperature. The apparent drop in molecular weight after 16 hrs. dialysis against deionized water and its restoration to a normal value on the addition of NaCl to 0.16 M or a phosphate buffer pair to give a pH of 7.7 and an ionic strength of 0.16 is also included. For comparative purposes, values of molecular weight for Colorado and ethanol material at pH 7.7 and at a pH corresponding to their maximum associated values in the acid region, are reproduced from Part I. Included also are their measured values of molecular weight in an 80% formamide/H<sub>2</sub>O mixture.

### Discussion

During this investigation, some stress has been placed on the comparative aspects of fetuin isolated according to two procedures, the salt fractionation of Fisher et al. (63) and the ethanol procedure using zinc and barium acetate due to Spiro (66). Both materials appear to be stable in phosphate or borate buffers at pH 7-8 under normal refrigeration temperatures. No observations have suggested that any 18S component is spontaneously produced under these conditions. While both preparations exhibit small differences, as discussed previously, either at pH 7-8 or in the isoelectric region, they both show a sensitivity to buffer composition in the first pH range and associative properties in the second. On the other hand, while salt fractionated material is resistant to attack by trypsin and chymotrypsin, ethanol material is digested quite rapidly.

This stability of salt prepared fetuin to attack by trypsin



and  $\alpha$ -chymotrypsin is in keeping with the observations on orosomucoid, which, like fetuin, contains a high content of sialic acid, removal of which, however, results in proteolytic attack (41,42). A sharp contrast is observed with material prepared according to the ethanol procedure which is attacked readily by both these enzymes as shown by Spiro (68) and confirmed in this study. In view of the fact that heat treatment of salt precipitated fetuin will destroy its tryptic resistance, this suggests that the difference probably lies in an alteration in secondary structure such as may be described in terms of a mild denaturation. This is, of course, in keeping with the differences in effective volume and optical rotatory behaviour shown by these preparations.

Another feature of interest is that while the commercial (Colorado) salt precipitated material appears to be unchanged by 80% formamide the ethanol material gave a molecular weight of 28,250 suggesting some degradation or perhaps a dissociation. This question of stability became of increasing interest when another commercial (salt fractionated) material, obtained from Australia, gave decreased sedimentation rates at low ionic strength.  $S_{20,w}$  values of about 1.7 were obtained and an apparent molecular weight of about 22,000 was recorded. The process was reversible in that 0.16 M NaCl or phosphate salts added to give a buffer solution of pH 7.7 restored the sedimentation and molecular weight values to normal. Exhaustive deionization was not necessary as dialysis overnight would produce the effect. Since, however, the ionic strength would be less than 0.01, it





appeared likely that the decrease in  $S_{20,w}$  was a reflection of the primary charge effect. Since at pH 7.0 fetuin carries a high net negative charge and the primary charge effect always results in a decrease in  $S_{20,w}$ , the observations are consistent with this effect. Viscosity measurements on exhaustively dialyzed material and the same solution to which solid NaCl was added to 0.1 M showed that the presence of NaCl caused a reduction in viscosity. This fact in conjunction with the observation that the optical rotatory data for this preparation, with and without the addition of 0.14 M NaCl, gave identical results (Figures 31, 32) ( $\lambda_c = 227$  and  $b_o = -125$ ) offers a possible explanation in terms of protein conformation. Since the secondary structure is not influenced by the presence or absence of NaCl, it seems likely that little change in shape has taken place. Also the viscosity in the absence of salt is larger and this will cause a decrease in  $S_{20,w}$  due to the increase in the frictional coefficient. As shape change is unlikely, it would seem that an additional frictional drag could result due to an increase in effective volume. This is consistent with the physical picture of the molecule as containing three carbohydrate moieties each terminating in the highly charged sialic acid groupings. As the dielectric constant of the medium is decreased the repulsion between these charged groups will increase causing the molecule to expand to a larger size. It also implies, if we accept the concept that shape does not change, that the molecule expands in a symmetrical fashion and perhaps therefore that there is in fact a spatial symmetry of the native molecule.





Since the reduced viscosity at 0.56% concentration changes from 7.36 to 10.05 ml./gm. it is unlikely that the total decrease in  $S_{20,w}$  in the absence of salt is due entirely to an increase in effective volume. It is probable that much of this decrease is due to the primary charge effect as suggested above.

Although the fetuin molecule is stable at pH 7-8, this is not true in the acid region even before a pH value is reached at which the molecule normally associates, i.e. below about pH 4.5. A sample of Australian material stored at pH 5.6 in acetate buffer at approximately 6°C. for about a week, when checked by the Archibald method gave a molecular weight of 47,950; after another two weeks this had increased to almost 53,000. Deutsch (58) suggested that association of fetuin at acid pH was accompanied by a loss of sialic acid. It is certainly true that once sialic acid is lost aggregation occurs. The sample of molecular weight 53,000 was checked for free sialic acid by the Warren method (104) and the amount measured corresponded to about 14% of the normal sialic acid content of the native protein. As control, a solution of fetuin in water liberated only 2% over a similar length of time. (See Table 6.)

While it is true that the  $S_{20,w}$  of a solution of fetuin dissolved in (say) glycine/HCl at pH 3.0 will increase from about 3S to 4S and dialysis against a suitable buffer at pH 7-8 will reverse the process, it is evident that if the solution is maintained at acid pH, slow liberation of sialic acid will occur. It follows that material thus treated, or following loss of sialic acid by any means, can be expected to show an increase in molecular



weight which is irreversible. This then raises an interesting feature of the associative properties of this molecule. Since the acid association is virtually instantaneous, by dissolving in an appropriate buffer it is presumably the loss of negative charge on the terminal sialic acid groups which permits the associating units to approach close enough that they may interact, perhaps through hydrophobic attraction, to give a product of approximately 120,000 molecular weight. If instead of lowering the pH to remove the charges on the sialic acid groups, they are removed by neuraminidase and the resulting molecule examined at pH values between about 3 and 8, other things being equal, it might be expected to associate, to the same extent as the native molecule at pH 3.0. The removal of sialic acid by neuraminidase is discussed in detail below.

B. Sialic acid content of fetuin and its removal from the two commercial preparations by neuraminidase

The sialic acid contents of commercial fetuin obtained from the Colorado Serum Company and fetuin prepared from blood obtained from the same source, by the ethanol method, are given in Table 6. Concentrations were based on the measured extinction coefficient of 4.5 for both preparations. The sialic acid content was measured by the method of Warren (104) following acid hydrolysis of the ethanol material, and on the amount liberated by neuraminidase treatment of the commercial preparation, together with the residual amount contained in the enzyme treated product. The methods are given in detail in the Experimental Section of this report.





The Australian commercial preparation appeared to be less pure than the other ones, having a distinct yellow colour which may be related to the higher extinction coefficient of 5.3 quoted by other workers using this material (78). Since concentrations based on this value gave areas for  $c_0$  in ultracentrifugal studies, very close to those for the other preparations of equal concentration, this figure was adopted for this material.

Neuraminidase treatment of commercial fetuin

(1) Colorado material. The course of the reaction was followed by measuring the amounts of sialic acid liberated according to the method of Warren. No further release of the sugar acid was observed after a 48-hour period had elapsed (see Figure 33). The amount liberated corresponded to between 9 and 10 moles of N-acetyl neuraminic acid per mole of protein. Following dialysis and lyophilization, the residual content of sialic acid, estimated by release following acid hydrolysis for 1 hour (0.1 N  $H_2SO_4$ ) in a boiling waterbath, amounted to 0.17%. If a sialic acid content for the native molecule of 6.3% is taken as representative, then about 97% of this has been removed (72).

Optical rotatory dispersion curves were run (a) on the material obtained following dialysis and prior to lyophilization, phosphate buffer salts being added to give a pH of 7.7; (b) on a solution of the solid obtained from lyophilization by dissolving in phosphate buffer, pH 7.7; and (c) on a solution of the solid obtained from lyophilization by dissolving in acetate buffer, pH 4.9. The Moffitt plots are given in Figure 34 and the Yang-Doty treatment in Figure 35.



Additional quantities of lyophilized material were dissolved in the appropriate buffer for molecular weight determinations. These results together with the dispersion parameters are summarized in Table 7. Plate F illustrates the  $c_0$  and the approach to equilibrium run on the neuraminidase treated Colorado preparation.

(2) Australian material. Although essentially the same procedure was followed as in the case of the Colorado material, the material obtained from the 48-hour treatment still contained 24% of its normal complement of sialic acid. That is, instead of almost complete removal of the sialic acid, as in the case of the Colorado material, only about 7 out of 9 moles of sialic acid were removed. The material was, however, examined for molecular weight at several values of pH. The results are shown in Table 7.

### Discussion

The measured amounts of sialic acid associated with the fetuin molecule suggest that either 9 or 10 moles per mole of fetuin are attached to the carbohydrate residues which make up the non-peptide component of this protein. These results compare with 8.5 moles obtained by Fisher et al. (72) for commercial Colorado material, 8 moles by Turner (79) for Australian material and 12 moles for Spiro (66), all based on a molecular weight of ca. 45,000. These differences may reflect the lability of the sugar acid linkages to acid pH which in turn could be influenced by collection and storage procedures and the entire past history of the blood sample, prior to isolation of the protein. As discussed in Section A of this part, the removal of 14% of the sialic acid of Australian fetuin at pH 5.6 gives a weight average





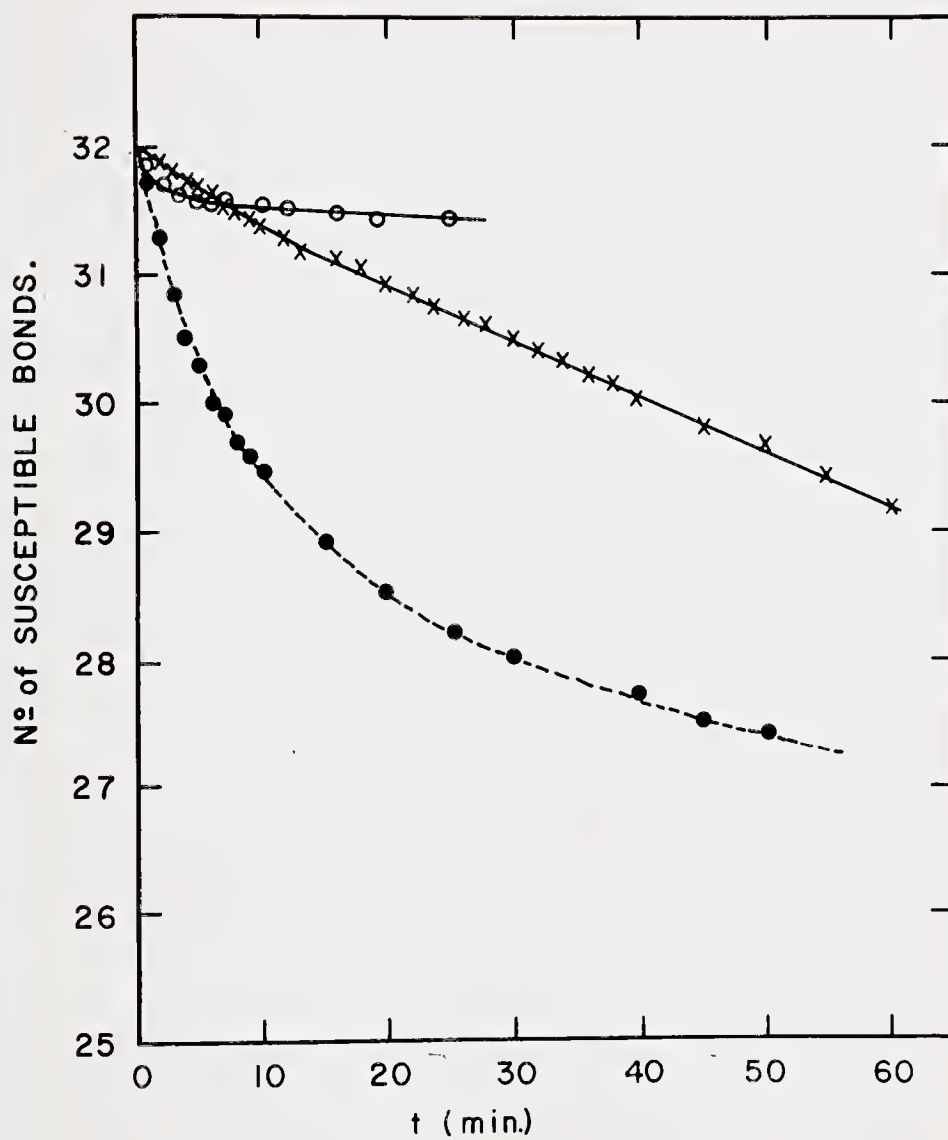
molecular weight of 52,970. It is of interest that the removal of 76% of the sialic acid by neuraminidase does not give values at either pH 5.6 or pH 7.7 appreciably different from this value. This suggests that the removal of as little as one mole of sialic acid from the fetuin molecule may be sufficient to induce association, the removal of an additional 6 or so not being critical in this regard. However, since increased association still occurs at pH 2.6, it would seem that the presence of the remaining two sialic acid groups per molecule is sufficient to prevent further aggregation, provided the pH is such that these acid groups are negatively charged. The situation in the case of neuraminidase treated Colorado fetuin, in which virtually all the sialic acid has been removed, is similar to the extent that there is an increase in weight average molecular weight, but to values closer to 60,000; however, a large increase in molecular weight at pH 2.8 did not take place. Perhaps the most interesting observation on this material was that the optical rotatory measurements indicated a complete loss of secondary structure. This could imply a stabilizing function of the sialic acid groups with regard to the overall molecular conformation of the protein. This would appear to be not entirely dependent on their charge since as discussed in Part II, the action of formamide at pH 2.3 is consistent with an additional unfolding of the associated molecule, suggesting that even in the absence of negative charge on the sialic acid groups, some secondary structure is maintained. The value of  $\lambda_c = 206.5$  obtained on the sialic acid free protein, immediately after treatment with the enzyme, supports the choice





of a  $\lambda_o = 205$  used in the Moffitt plots for the optical rotatory data. It must be borne in mind, however, that the hydrophobic groups and disulfide bridges may be a major source of stability either with or without the terminal sialic acid groups. Nevertheless, following Spiro's suggestion (68) that there are three similar carbohydrate moieties attached to the polypeptide chain of fetuin, each terminating in four sialic acid groupings, it seems possible that their interaction with parts of the molecule in close proximity may be necessary to stabilize small helical regions in the vicinity of the carbohydrate chains. Any condition leading to a modification in charge distribution would then favor a conformational change. Spiro has also offered evidence that the sialic acid groups are involved in the anion binding which this protein exhibits (66), and as such binding would necessarily modify the electric field, small conformational changes might be expected. This is in keeping with the observed sensitivity of this molecule to its ionic environment, as discussed in Part I.



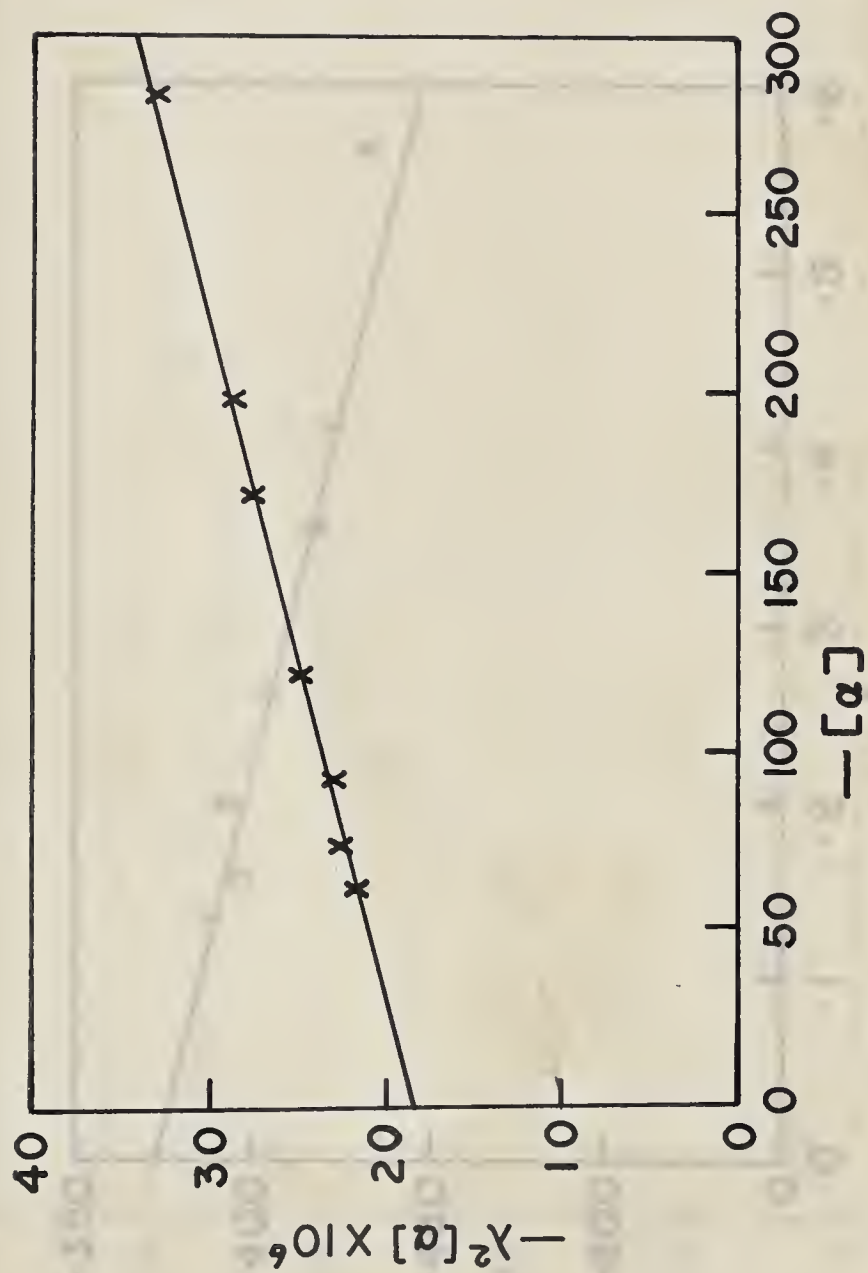


Tryptic attack on fetuin: commercial (Colorado) material (0); commercial (Colorado) heat-treated for 15 minutes at 85-90°C. (●); ethanol prepared material (x). Solvent 0.1 M NaCl, pH 8.0, 25°C. enzyme/substrate 1/45.

Figure 30



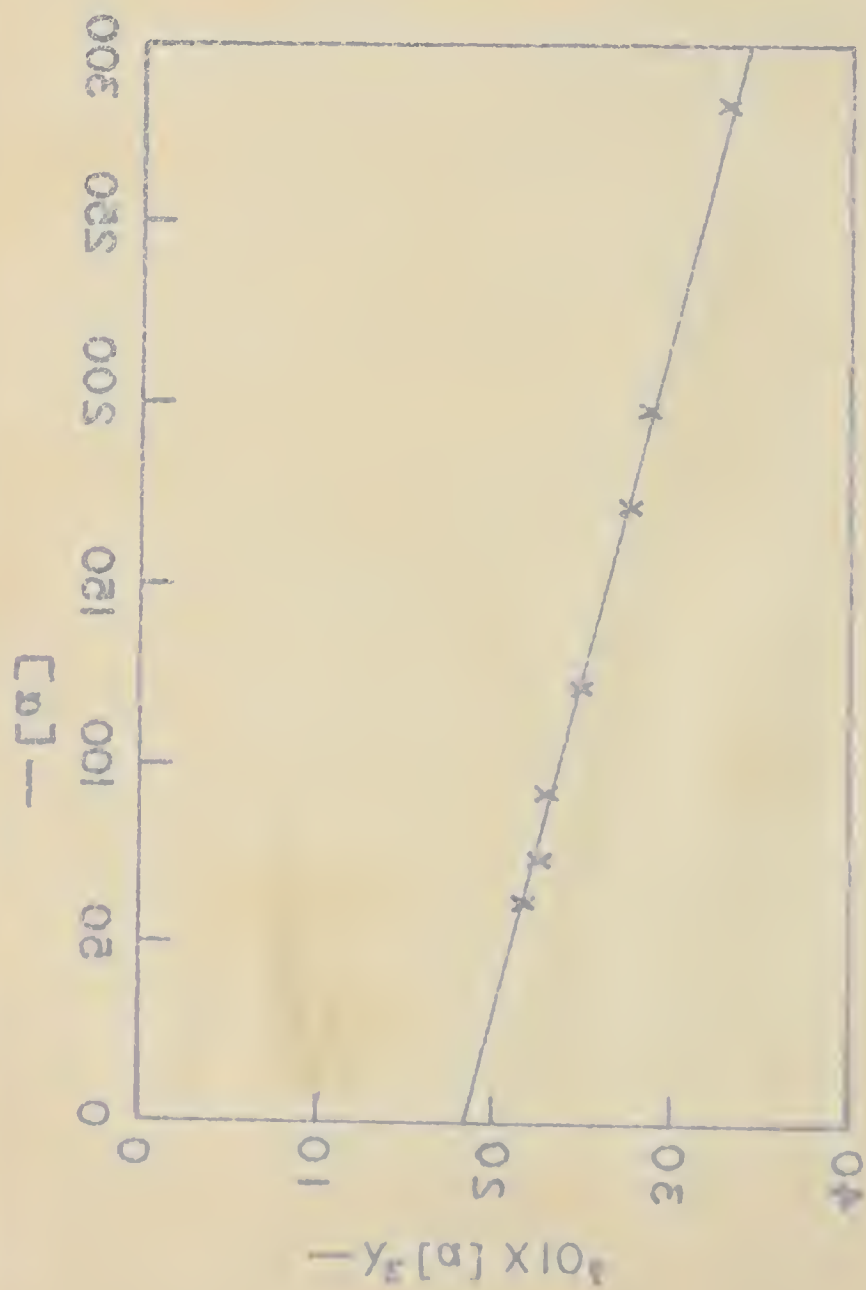




Yang-DoTy plot for commercial (Australian) fetuin following dialysis (x) and on the addition of 0.14 M NaCl (coincident plots).

Figure 31

(x)  $\alpha$  is the angle of refraction (in degrees) of the light ray at the interface between the two media.



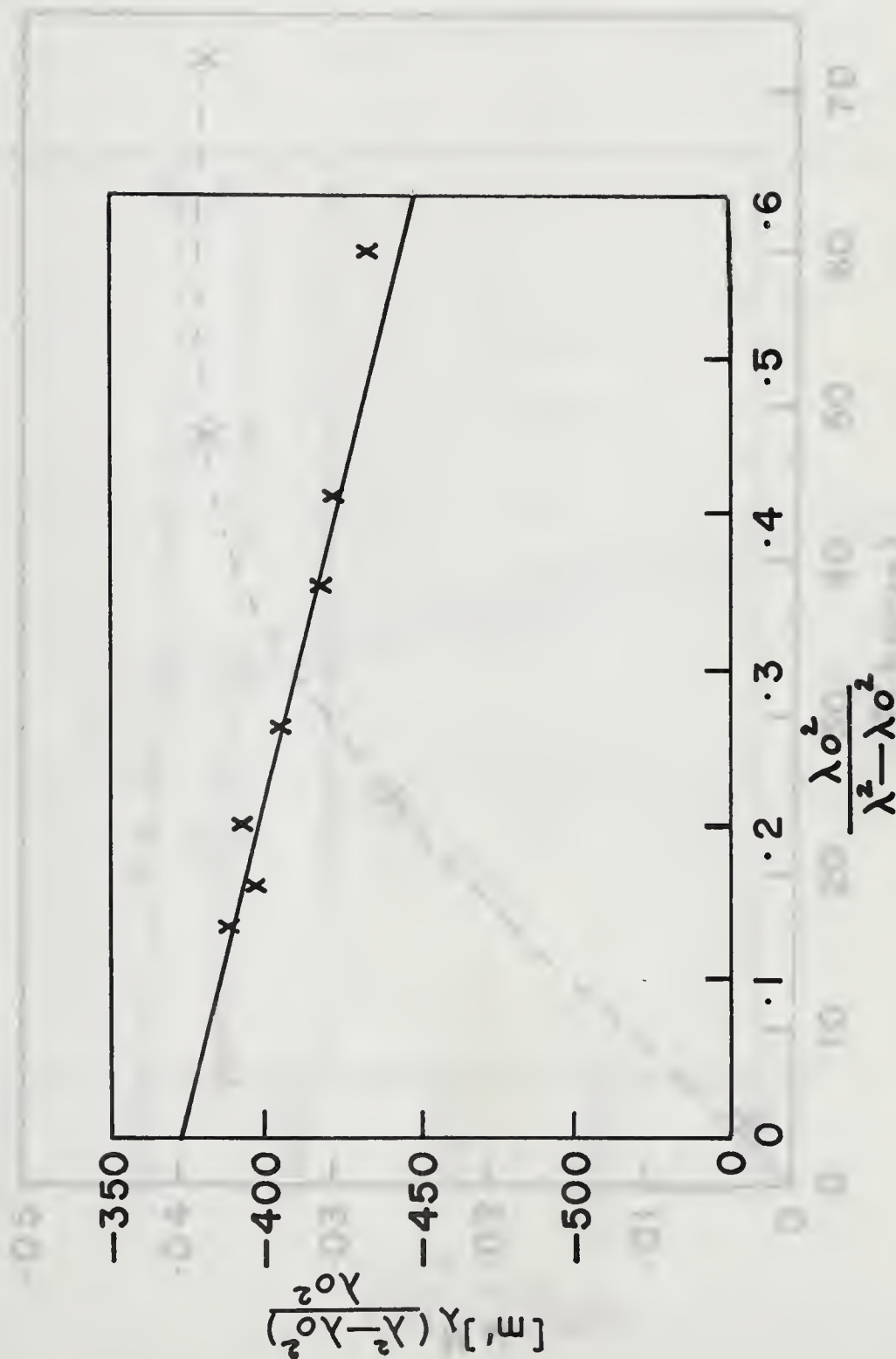


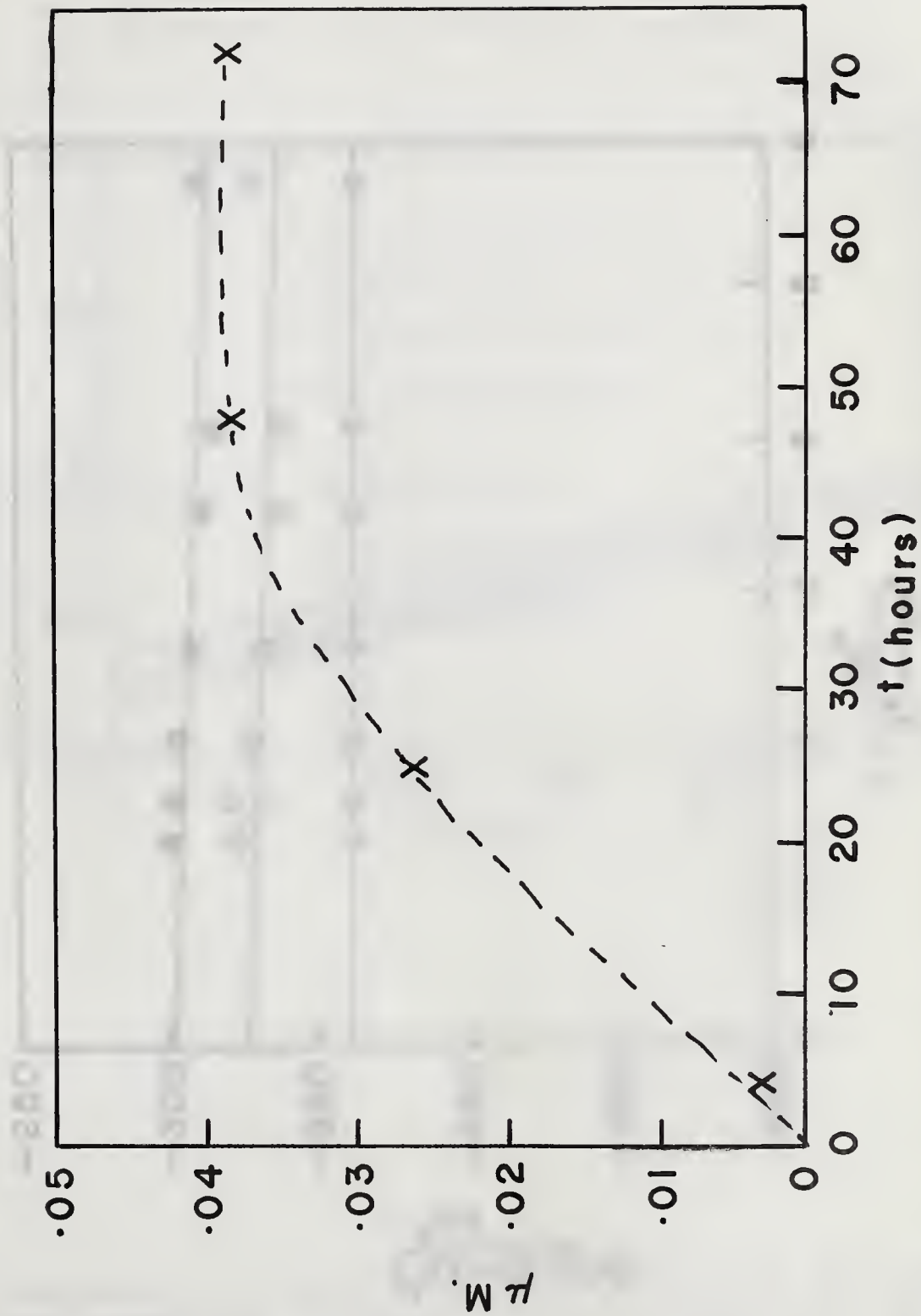
Figure 32

Moffitt plot corresponding to Figure 31 for commercial (Australian) fetuin following dialysis (x) and on the addition of 0.14 M NaCl (coincident plots).

(a)  $\frac{y_s - y_{0s}}{y_{0s}}$  vs.  $\frac{y_s - y_{0s}}{y_{0s}}$  for commercial (A) and (B) subjects.  
 (b)  $\frac{y_s - y_{0s}}{y_{0s}}$  vs.  $\frac{y_s - y_{0s}}{y_{0s}}$  for commercial (A) and (B) subjects.



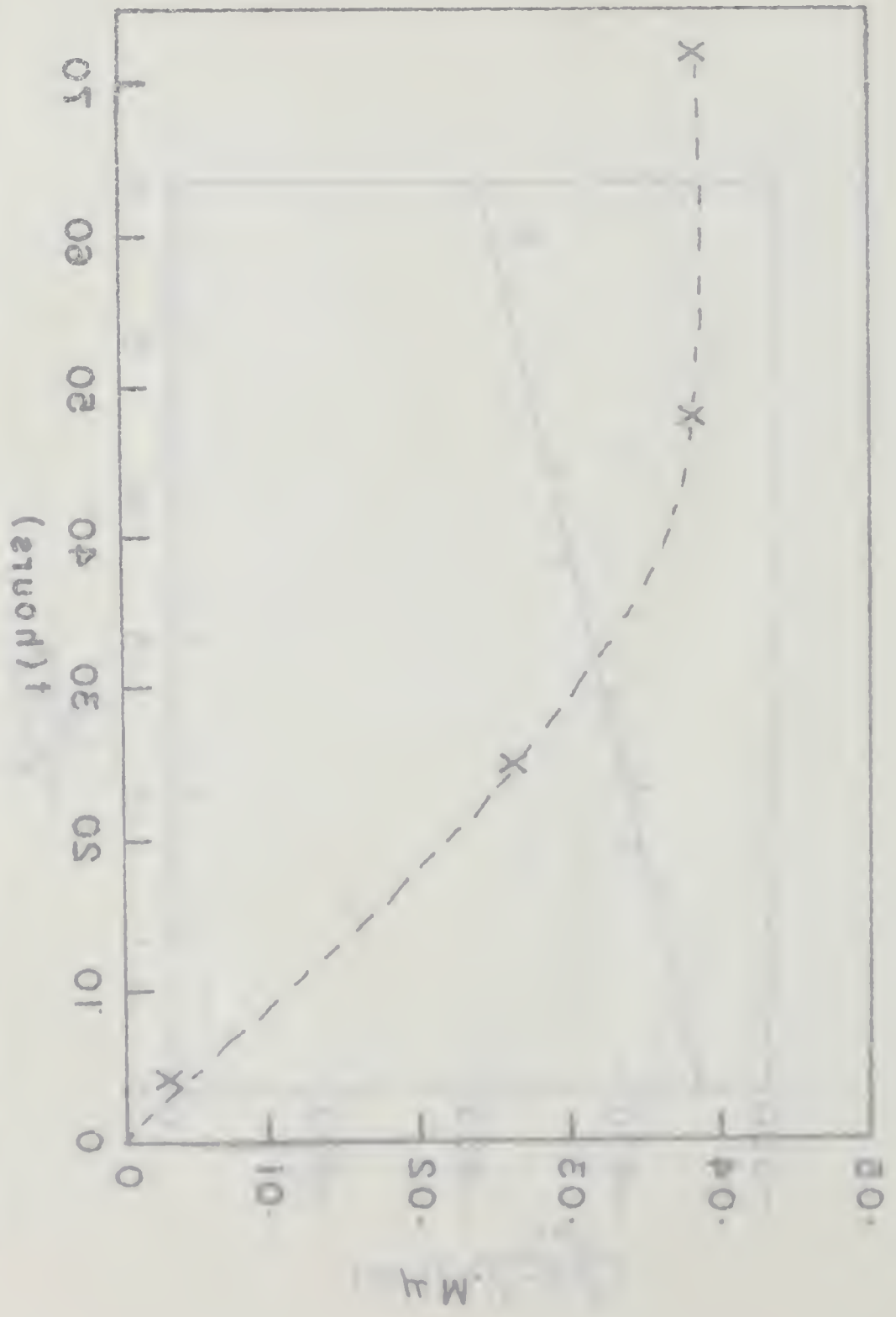
Figure 12



Rate of liberation of sialic acid during neuraminidase treatment of commercial (Colorado) fetuin (x),  $\mu M$  sialic acid vs. time. Solvent: 0.05M acetate buffer, pH 5.5 containing 0.9% NaCl and 0.1%  $CaCl_2$ . Enzyme/substrate approximately 1/100.

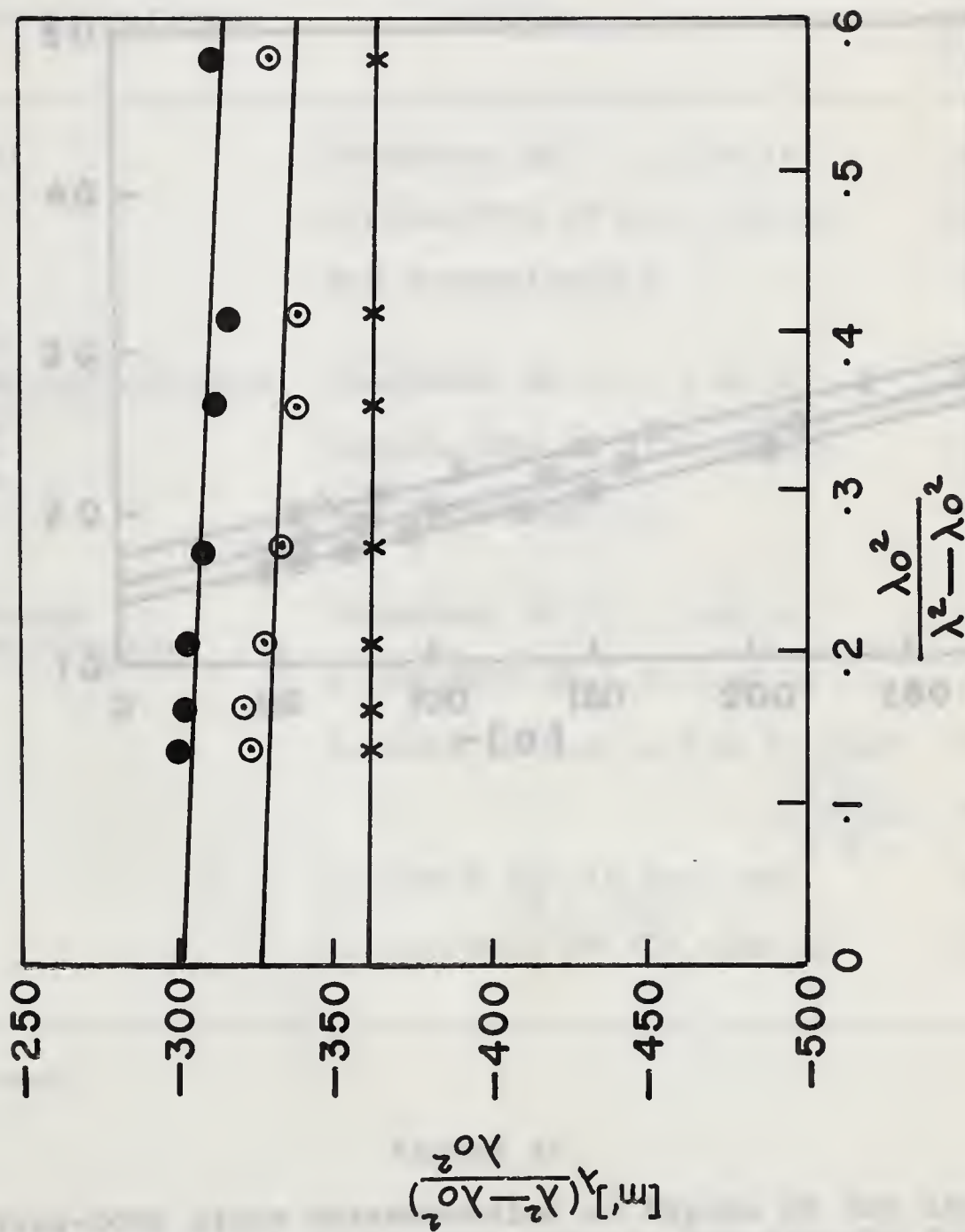
Figure 33





To determine the relationship between  $M$  and  $(\mu\text{on})^t$ , the following data were obtained from the experiment. The data points are shown in the graph above. The solid line represents the theoretical relationship, and the dashed line with 'X' markers represents the experimental data. The data points are as follows:

$(\mu\text{on})^t$	$M$
0.05	3.5
0.10	4.5
0.20	6.5
0.30	9.5
0.40	13.5
0.50	18.5
0.60	23.5
0.65	19.5



Moffitt plots for sialic acid free commercial (Colorado) fetuin: immediately following dialysis, phosphate salts added to  $\mu = 0.16$  pH (x); following freeze-drying, in phosphate,  $\mu = 0.16$ , pH (o); in acetate buffer,  $\mu = 0.2$ , pH 4.9 (•).

Figure 34

Figure 19 shows the results of the experiments for the three different values of the parameter  $\gamma_0$ . The curves are plotted for  $\gamma_0 = 0.5$ ,  $1.0$ , and  $1.5$ . The curves for  $\gamma_0 = 0.5$  and  $1.0$  are very close to each other, while the curve for  $\gamma_0 = 1.5$  is significantly higher. The curves for  $\gamma_0 = 0.5$  and  $1.0$  are also very close to the curve for  $\gamma_0 = 1.5$  at the beginning of the experiment, but they diverge significantly as the experiment progresses.

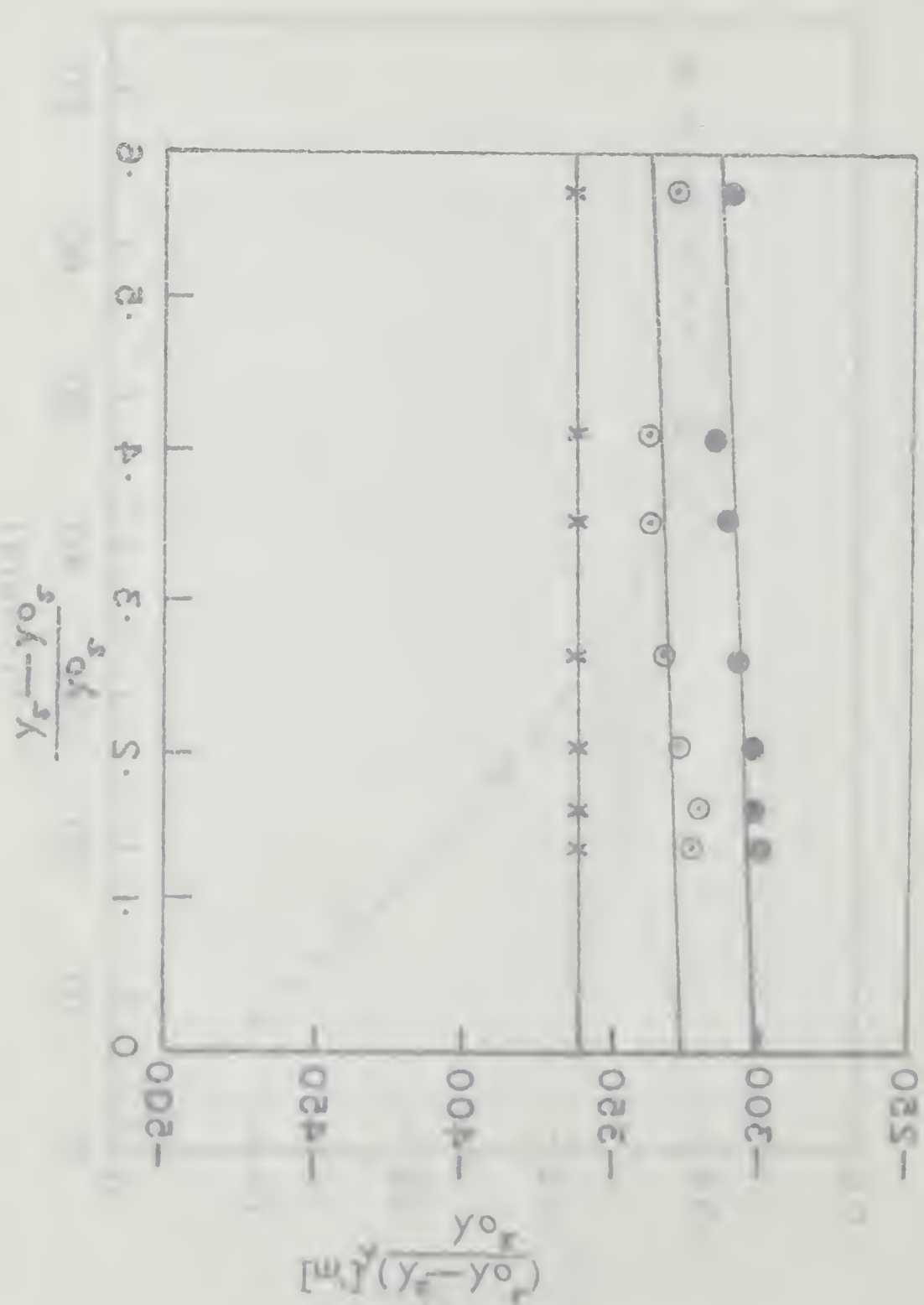
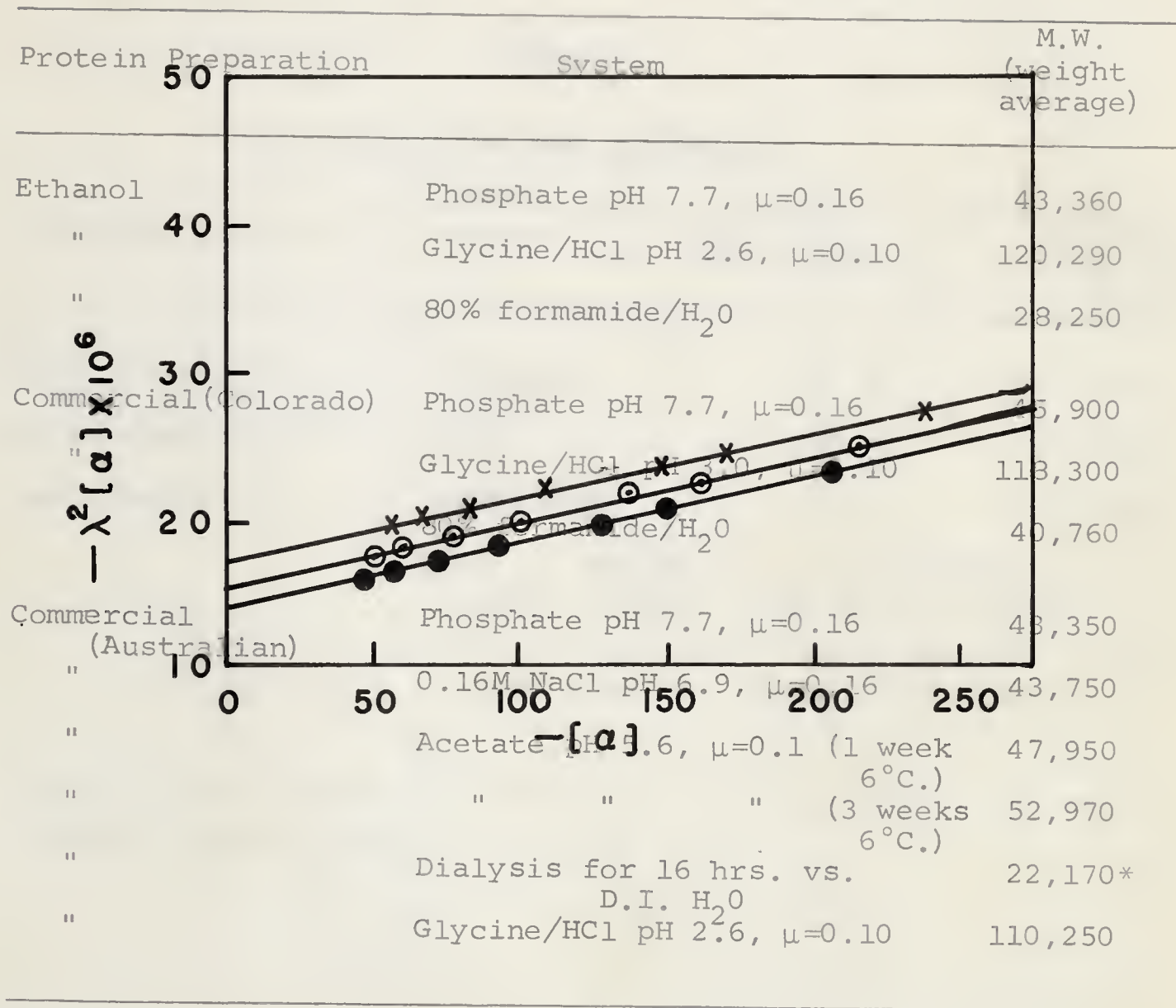


Figure 19

Table 5  
Molecular Weight Studies of Fetuin



\*See text.

Figure 35

Yang-Doty plots corresponding to Figure 34 for sialic acid free commercial (Colorado) fetuin: immediately following dialysis, phosphate salts added to  $\mu = 0.16$  pH (x); following freeze-drying, in phosphate  $\mu = 0.16$  pH (O); in acetate buffer,  $\mu = 0.2$ , pH 4.9 (●).

buffer,  $\mu = 0.2$ , pH 4.9 (●).  
 and freeze-drying, in phosphate  $\mu = 0.16$  pH (○); in acetate  
 dialysis, phosphate salts added to  $\mu = 0.16$  pH (x); follow-  
 free commercial (Colorado) tetra: immediately following  
 Yang-Doty plots corresponding to Figure 34 for stialic acid

Figure 35

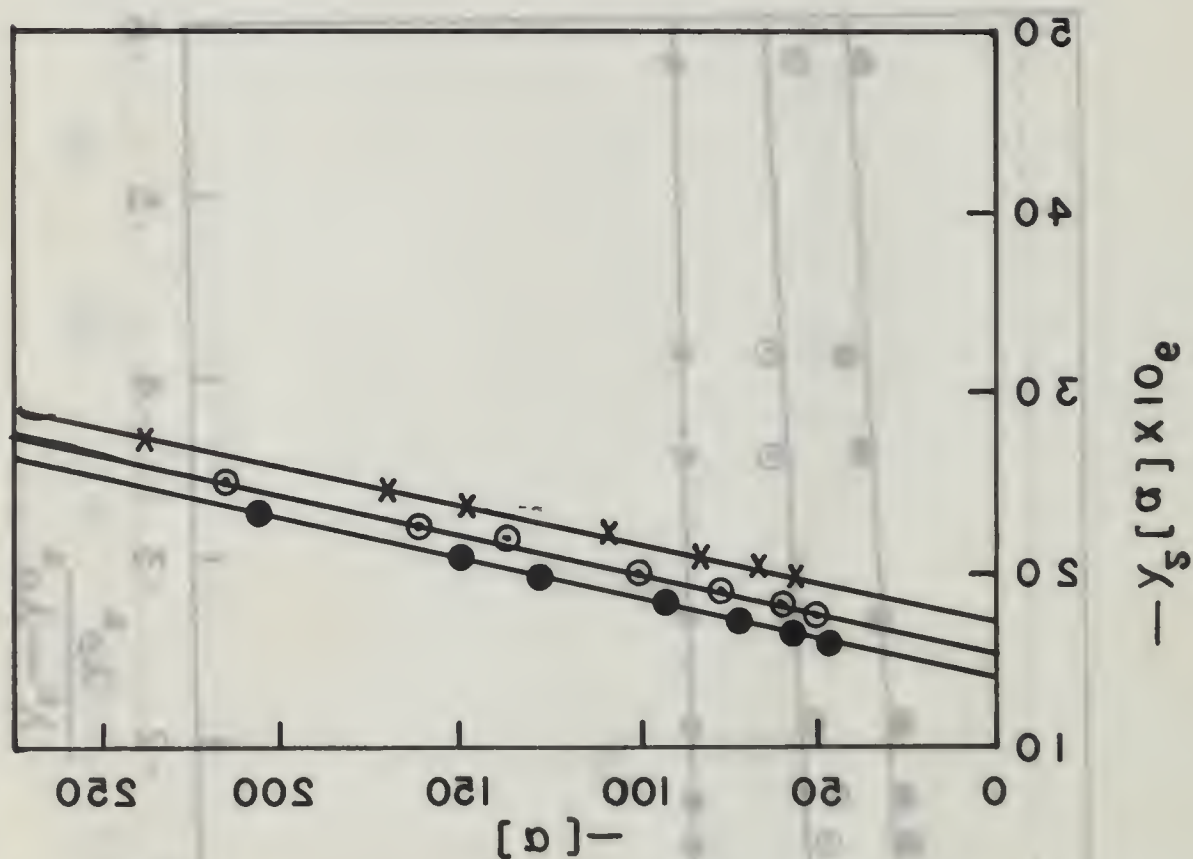




Table 5  
Molecular Weight Studies of Fetuin

Protein Preparation	System	M.W. (weight average)
Ethanol	Phosphate pH 7.7, $\mu=0.16$	43,360
"	Glycine/HCl pH 2.6, $\mu=0.10$	120,290
"	80% formamide/H <sub>2</sub> O	28,250
Commercial (Colorado)	Phosphate pH 7.7, $\mu=0.16$	45,900
"	Glycine/HCl pH 3.0, $\mu=0.10$	118,300
"	80% formamide/H <sub>2</sub> O	40,760
Commercial (Australian)	Phosphate pH 7.7, $\mu=0.16$	43,350
"	0.16M NaCl pH 6.9, $\mu=0.16$	43,750
"	Acetate pH 5.6, $\mu=0.1$ (1 week 6°C.)	47,950
"	" " " (3 weeks 6°C.)	52,970
"	Dialysis for 16 hrs. vs. D.I. H <sub>2</sub> O	22,170*
"	Glycine/HCl pH 2.6, $\mu=0.10$	110,250

\*See text.



Table 6

Sialic Acid Content of Fetuin

Isolation Procedure	Source	$\mu\text{g. sialic acid/}$ $\text{mg. fetuin}$	Moles sialic acid/mole fetuin*
Ethanol	Colorado	69.3	9.95
Salt (Commercial)	"	63.3	9.1
Salt (Commercial)	Australian	69.0	9.9
"	" (water for 3 weeks)	1.3 (liber- ated in solution)	-
"	" (pH 5.6 for 3 weeks)	7.5 (liber- ated in solution)	1.25

\*Based on M.W. 44,400.



Table 7

Neuraminidase Treated Commercial Fetuin:  
M.W. and ORD Parameters

Material	Buffer	pH	$\mu$	$\lambda_c$	$b_o$	$a_o$	M.W. (weight average)
<u>98% sialic acid removed</u>							
Colorado	Glycine/HCl	2.8	0.10	-	-	-	64,800
"	Acetate	4.9	0.10	211	-23.5	-301	61,430
"	Phosphate	7.7	0.16	206.5 211	0 -21.5	-360 -326	61,420
"	1:1 Forma- mide/H <sub>2</sub> O	-	-	-	-	-	58,190
<u>76% sialic acid removed</u>							
Australian	Glycine/HCl	2.6	0.10	-	-	-	104,100
"	Acetate	5.6	0.10	-	-	-	53,100
"	Phosphate	7.7	0.16	-	-	-	52,650







(1)

(1) Run for  $c_o$ , speed 59,780 r.p.m.



(2)

(2) Neuraminidase treated commercial (Colorado) fetuin (0.6%) in glycine/HCl buffer, pH 2.8,  $\mu=0.1$ , bar angle  $75^\circ$ . Pictures at 0, 16, 32, 48, 64 mins., speed 12,590 r.p.m.



## V. CONCLUSIONS

A summary of the features arising from this study will now be given. From these conclusions along with the results obtained by other workers, certain generalizations will be attempted.

1. The size and shape of the fetuin hydrodynamic unit is influenced by the ionic composition of the medium, as judged by changes in effective volume and axial ratio of the equivalent ellipsoid in the pH range 7-8.
2. The changes in (1) appear to be accompanied by small alterations in secondary structure, interpreted from optical rotatory measurements of  $\lambda_c$  obtained from the Yang-Doty plots and the slope term,  $b_o$ , of the generalized Moffitt treatment.
3. Both (1) and (2) depend on the method of isolation of the protein, the ethanol material giving results consistent with a less compact conformation than that of commercial (Colorado) material.
4. Confirmation of differences between ethanol and the Colorado material is shown by the resistance of the latter to trypsin and  $\alpha$ -chymotrypsin (unless heat treated) while the ethanol material is readily digested.
5. Although both preparations associate at acid pH to about 120,000 the pH dependency of  $S_{20,w}$ ,  $\eta_{red}$  and molecular weight are different in this range. Maximum  $S_{20,w}$  for





ethanol material occurs at a lower pH than for the commercial preparation.

6. The introduction of organic solvents into a buffered aqueous system of constant ionic strength, pH 7-8, causes alterations in secondary structure, to a less ordered form. The hydrodynamic data indicate an increase in frictional coefficient. Formamide is more effective than ethylene glycol.
7. Formamide and guanidine cause a decrease in  $S_{20,w}$  without change in molecular weight of the associated molecule. This could imply that even after the sialic acid groups have lost their charge and association has taken place, some secondary structure is still present.
8. While the fetuin molecule exhibits considerable stability at pH 7-8, slightly acid pH values (e.g. pH 5.6) causes release of sialic acid.
9. Neuraminidase will release the sialic acid in toto from the molecule. The content of the sugar acid appears to be either 9 or 10 molecules/molecule of fetuin.
10. The loss of sialic acid results in an increase in weight average molecular weight. The results suggest that the loss of as little as one sialic acid group/molecule of fetuin will induce aggregation. The removal of 7-8 of the sialic acid groups does not interfere with the association exhibited in the isoelectric region.
11. The complete removal of sialic acid by neuraminidase appears to be accompanied by a loss of secondary structure suggesting that these terminal groups of the carbohydrate moieties contribute to the stable conformation of the molecule. The



associative capacity at isoelectric pH also appears to be impaired.

12. As stressed in the introduction, the hydrodynamic parameters are based on the concept of the hydrodynamically equivalent ellipsoid. While the physical form of the molecule may differ from this, it is generally recognized that the folded structure of a globular protein has an overall geometry similar to that of the equivalent ellipsoid. Actual dimensions based on the model must not, of course, be interpreted too literally, but the extent to which such dimensions are consistent with other data allows the molecule to be better visualized.

From the data on commercial (Colorado) fetuin in phosphate, taking the molecular weight as 44,400 and an axial ratio of unity, the effective volume of one molecule is found to be  $177.6 \times 10^3 \text{ cu } \text{\AA}^3$  and the spherical radius  $35 \text{ \AA}$ . In tris and borate buffer where  $a/b = 5$ , the volume of the ellipsoid is  $98.8 \times 10^3 \text{ cu } \text{\AA}^3$  and the axial lengths,  $2a$  and  $2b$ ,  $170 \text{ \AA}$  and  $34 \text{ \AA}$  respectively.

#### Peptide chain length

The work of Fisher et al. (72) and Spiro (71) are mostly in good agreement. The total number of residues will be taken as 329. For a 100% helix the axial length would be  $329 \times 1.5 \text{ \AA} = 494 \text{ \AA}$ . If, on the basis of the Yang-Doty plots a helical content of 15% is taken as representative, this would contribute a length of about  $74 \text{ \AA}$ , and utilizes  $74/1.5 = 49$  residues. This will leave 280 residues for the rest of the chain. The greatest length obtainable from this would be that of the extended ( $\beta$ ) structure and an estimate is found by using the residue repeat distance of this structure, viz.  $3.5 \text{ \AA}$ ; this would involve a





total distance of  $280 \times 35 = 980 \text{ \AA}$ . It follows that the total length of a chain containing 15% helix and 85% of the  $\beta$  form would be  $74 + 980 \text{ \AA} = 1054 \text{ \AA}$ . If this is imagined to fold back and forth about eight times and assuming a chain spacing of approximately  $6 \text{ \AA}$ , the volume of the equivalent ellipsoid would readily accommodate the peptide chain. There is not at present any way of knowing the form of folding, or to what extent the believed presence of random regions will decrease the overall length of the chain. The  $\beta$  extended form has been used merely to obtain an estimate of maximum length. Since the effective volume of the spherical equivalent is larger than that of the ellipsoid there is no problem, in terms of space, in containing the chain in this model.

#### Carbohydrate moiety

Spiro (68) has suggested the presence of three distinct carbohydrate moieties, each consisting of a branched structure terminating in a sialic acid group. Taking the number of pyranose rings (i.e. total carbohydrate content) as 45, each moiety would contain fifteen such rings. If these are branched, a symmetrical distribution would consist of 5 rings in each of 3 chains branching from the point of attachment to the peptide chain. By taking the planar length of each ring as about  $3 \text{ \AA}$  and ignoring the glycoside bond length, 5 rings would extend to a maximum of about  $15 \text{ \AA}$  in the aqueous medium. The similarity between  $\alpha_1$  acid glycoprotein and native (salt precipitated) fetuin in their resistance to proteolytic attack and the readiness with which fetuin starts to associate when only one molecule of sialic acid





has been removed, suggests the stability of the native protein may be due to an effective sheath of negative charge provided by the ionized carboxyl groups of the sialic acids. With three branched chains attached at three points to the polypeptide and each extending 15 Å over a spherical contour of 35 Å radius, much of the surface would be effectively shielded. Obviously, other possibilities exist but within the crude limits implied by this approach the physical picture so far is not inconsistent with the observations drawn from primary structure and the hydrodynamic data.

### Secondary structure

Since the breakage of hydrogen and hydrophobic bonds leading to a more random conformation of the peptide chain is accompanied by changes in hydrodynamic properties, these properties are correlated with optical rotatory measurements. A point of interest arising from such correlation studies is whether or not the concentration as determined from optical density is in fact adequate in optical rotatory studies for a molecule such as fetuin containing almost 25% of a non-protein moiety. Bearing in mind that the optical rotatory dispersion is dependent on the orientation of the peptide chain, it would seem more logical to use as concentration the content of polypeptide rather than the whole molecule. The results recorded in this work are all based on total concentration and a comment on this is required. In the first place, the Yang-Doty slope will be unaffected although of course, the absolute levo rotations would increase proportionally for a lower concentration corresponding to polypeptide alone.



The Moffitt ordinate is concentration dependent and the slope will change proportionately. The use of a lower value for concentration would result in an increased (-ve) slope. Throughout this work, care has been taken to correlate the  $b_0$  term from the Moffitt with the  $\lambda_c$  of the Yang-Doty plot. Since a value of  $\lambda_0 = 205 \text{ m}\mu$  was chosen for linearity in the Moffitt treatment, this would increase the slope somewhat from that using a value of  $212 \text{ m}\mu$ . The use of the latter value and a concentration based on polypeptide content for the optical rotatory studies would tend to compensate one another. The justification for the lower value of  $\lambda_0$  chosen may have its basis in this argument.

The correlation of hydrodynamic and optical rotatory studies indicated that the ethanol preparation of fetuin differed from the (salt fractionated) commercial material. In similar fashion, the addition of calcium acetate shows a loss of secondary structure as shown by a decrease in  $\lambda_c$  and a small increase in axial ratio. In this case the increase in  $S_{20,w}$  and decrease in  $\eta_{red}$  is interpreted as due primarily to a decrease in effective volume. To interpret this in terms of molecular structure, based on the available information, is not possible. That ion binding may take place seems likely, and suggests some type of electrostatic interaction. If this is the case, and in view of the high ionic strength of the system, the interacting elements must be closely positioned in space. A possible explanation is that the carbohydrate moieties may stabilize short lengths of helix in their immediate vicinity and that if, as suggested by Spiro, the sialic acid groups have anion binding properties, their spatial alteration





might result in conformational changes of the peptide chain. This would be in keeping with the shielding effect of the sialic acid groups mentioned above, but does not preclude penetration of ions into the interior of the molecule, although somehow this seems less likely. Following this possibility, an additional significance is then attributable to the negatively charged sialic acid groups. Furthermore, their deionization or removal might be expected to produce some dramatic alteration in secondary structure. There is some indication that secondary structure exists at pH 3.0 but since the molecule has now associated and the side chain carboxyl groups will also have become deionized, it is hardly possible to draw conclusions from this region. Evidence has been given that complete removal of the sialic acid groups by neuraminidase does in fact result in loss of secondary structure.

Additional confirmation that the native molecule has some secondary structure is given by the effect of the organic solvents on the buffered systems of the protein. That formamide and ethylene glycol both give decreased values for  $\lambda_c$  and increased frictional coefficients and further, that formamide is the more effective, suggests that secondary structure is stabilized by two mechanisms other than covalent constraints such as disulfide bridges. The formamide might be expected to exert its effect on the more readily accessible hydrophilic regions while the glycol would penetrate into a hydrophobic interior. The folded nature of globular proteins lends itself to this latter feature. As pointed out earlier, one-third of the amino acids of fetuin



exhibit such properties and would confer additional stability to the molecule. On the basis of this limited evidence, an internal hydrophobic region of considerable stability is suggested. With regard to the shape change as arising from extension resulting from the disruption of helical regions, it is of interest that the full extension of the postulated 49 residues involved in the helical regions would be  $49 \times 3.5 = 172 \text{ \AA}$ . This would involve an increase of  $172 - 74 \text{ \AA} = 98 \text{ \AA}$ . Coincidentally, perhaps, the increase in dimension from a sphere of diameter  $70 \text{ \AA}$  to the major axis of an ellipsoid of length  $170 \text{ \AA}$  is  $100 \text{ \AA}$ . That commercial fetuin in borate has an axial ratio close to 5 with little loss in secondary structure from that in phosphate, restricts the usefulness of the above argument.

#### Stability and associative properties

The demonstrated lability of the sialic acid component of fetuin to mild acid, emphasizes the need to maintain mild alkaline conditions for the molecule. This is particularly important since even a small amount of sialic acid liberated, results in aggregation. The nature of the associative process is not obvious. At pH 7-8 the limiting molecular weight obtained appears to be close to 60,000 depending on how much sialic acid has been removed. Roughly speaking, these results could be explained on the basis of varying amounts of a 45,000 and a 60,000 unit, allowance being made for the drop in molecular weight as the sialic acid is removed. To progress from a 45,000 unit to one of 60,000 would require the recognition of a labile 15,000 unit in the native molecule, the continued attachment of which is





dependent in some way on sialic acid. In this regard the molecular weight corresponding to the maximum observed  $S_{20,w}$  in the acid associating region, yields values close to 120,000 for both salt precipitated and ethanol fetuin. While this is an obvious multiple of a stable 30,000 unit, it is nowhere near the value for a dimer or trimer of the original molecule. Although roughly equal amounts of a 90,000 and a 135,000 would give a value of the observed magnitude, there should be two visible components on centrifugation. This is never the case; only occasionally has a slight skew been observed. The peak is invariably single and symmetrical suggesting that if heterogeneity is present, the molecular species are close in molecular weight. This suggests that the association may involve the interchange of a 15,000 unit to a monomer to give a 60,000 unit followed by dimerization. To make a conclusive statement on this feature of the molecule will require additional characterization in the acid region and analysis of the gradient curves over the pH range of association. The concept of three carbohydrate moieties attached at different points of the peptide chain is quite consistent with a molecule consisting of three similar units, of which one might be attached differently from the other two.

#### Suggestions for further investigation

In addition to further characterization of the fetuin molecule in its associated state, directed towards a better understanding of the associative process, other lines of investigation suggest themselves. It is, of course, well-recognized that hydrophobic bonds in addition to inter- and intrachain hydrogen bonds





contribute to the conformation which a native protein molecule assumes. To what extent prosthetic groups consisting of lipid and/or carbohydrate influence conformation has not, as yet, been extensively investigated. Some of the results recorded in this study suggest that the carbohydrate moieties of fetuin may be related to the conformation which the molecule adopts under a variety of environmental conditions. By selectively removing the terminal groups of the carbohydrate chains, some insight into their function might be acquired by the hydrodynamic and optical rotatory techniques used in this initial phase of the investigation. The effect of the sugars on the rotatory properties per se of the molecule is also of importance and should be investigated. Additional information on the extent of hydrophobic bonding would be useful and a more complete hydrodynamic treatment of buffered systems in the presence of organic solvents would be a logical extension of the qualitative treatment given in Part II of this report.



## VI. BIBLIOGRAPHY

1. Ghuysen, J. M., Biochim. Biophys. Acta 47, 561 (1961).
2. Cook, G. M. W., Heard, D. H., and Seaman, G. V. F., Nature 188, 1011 (1960).
3. Patterson, M. K., and Touster, O., Biochim. Biophys. Acta 56, 626 (1962).
4. Gottschalk, A., and Murphy, W. H., Biochim. Biophys. Acta 46, 81 (1961).
5. Murphy, W. H., and Gottschalk, A., Biochim. Biophys. Acta 52, 349 (1961).
6. Bettelheim-Jevons, F. R., in Anfinsen, C. B., Anson, M. L., Bailey, K., and Edsall, J. T. (Editors), Advances in Protein Chemistry, Vol. 13, Academic Press, Inc., N. Y., 1958, p. 34.
7. Putnam, F. M. (Editor), Plasma Proteins, Vol. 1, Academic Press, Inc., N. Y., 1960, p. 339.
8. Gurin, S., Bachman, C., and Wilson, D. W., J. Biol. Chem. 133, 467 (1940).
9. Müller-Eberhard, H. J., and Kunkel, H. G., J. Exptl. Med. 104, 253 (1956).
10. Yamashina, I., Arkiv. Kemi 9, 225 (1956).
11. Tsugita, A., and Akabori, S., J. Biochem. (Tokyo) 46, 695 (1959).
12. Putnam, F. M. (Editor), Plasma Proteins, Vol. 1, Academic Press, Inc. N. Y., 1960, pp. 318-319.
13. Cunningham, L. W., Nuenke, B. J., and Nuenke, R. H., Biochim. Biophys. Acta 26, 660 (1957).





14. Johansen, P. G., Marshall, R. D., and Neuberger, A., *Nature* 181, 1345 (1958).
15. Jevons, F. R., *Nature* 181, 1346 (1958).
16. Johansen, P. G., Marshall, R. D., and Neuberger, A., *Biochem. J.* 78, 518 (1961).
17. Nuenke, R. H., and Cunningham, L. W., *J. Biol. Chem.* 236, 2452 (1961).
18. Lee, Y. C., and Montgomery, R., *Archiv. Biochem. Biophys.* 97, 9 (1962).
19. Yamashina, I., and Makino, M., *J. Biochem. (Tokyo)* 51, 359 (1962).
20. Rosevear, J. W., and Smith, E. L., *J. Am. Chem. Soc.* 80, 250 (1958).
21. Rosevear, J. W., and Smith, E. L., *J. Biol. Chem.* 236, 425 (1961).
22. Nolan, C., and Smith, E. L., *J. Biol. Chem.* 237, 446 (1962).
23. Nolan, C., and Smith, E. L., *J. Biol. Chem.* 237, 453 (1962).
24. Graham, E. R. B., and Gottschalk, A., *Biochim. Biophys. Acta* 38, 513 (1960).
25. Gottschalk, A., and Graham, E. R. B., *Biochim. Biophys. Acta* 34, 380 (1959).
26. Gottschalk, A., and Thomas, M. A. W., *Biochim. Biophys. Acta* 46, 91 (1961).
27. Bezkorovainy, A., and Doherty, D. G., *Biochim. Biophys. Acta* 58, 124 (1962).
28. Chandrasekhar, N., Warren, L., Osbahr, A., and Laki, K., *Biochim. Biophys. Acta* 63, 337 (1962).



29. Schwick, G., and Schultze, H. E., Clin. Chem. Acta 4, 26 (1959).
30. Cook, G. M. W., Heard, D. H., and Seaman, G. V. F., Nature 191, 44 (1961).
31. McKwain, H., Biochem. J. 78, 24 (1961).
32. Kimura, A., Nagai, Y., and Turumi, K. I., Nature 191, 596 (1961).
33. Sjostrand, F., Radiation Research 2, 349 (1960).
34. Biserte, G., Bull. soc. chim. biol. 39, Suppl. III, 93 (1957).
35. Stary, Z., Clin. Chem. Acta 3, 557 (1957).
36. Bundy, F. H., and Mehl, J. W., J. Biol. Chem. 234, 1124 (1959).
37. Gray, J. L., Priest, S. G., Blatt, W. F., Westphal, U., and Jensen, H., J. Biol. Chem. 235, 56 (1960).
38. Feng, C. W., and Laskowski, M., J. Biol. Chem. 235, 1680 (1960).
39. Schmid, K., Bencze, W. L., Nussbaumer, T., and Wehrmuller, J. O., J. Biol. Chem. 234, 529 (1959).
40. Popenoe, E. A., and Drew, R. M., J. Biol. Chem. 228, 673 (1957).
41. Yamashina, I., Acta Chem. Scand. 10, 1666 (1956).
42. Kuhn, R., Bull. soc. chim. biol. 40, 297 (1958).
43. Kamiyama, S., and Schmid, K., Biochim. Biophys. Acta 63, 266 (1962).
44. Schmid, K., and Kamiyama, S., Biochemistry 2, 271 (1963).
45. Schmid, K., J. Am. Chem. Soc. 75, 60 (1953).
46. Winzler, R. J., in D. Glick, Methods of Biochemical Analysis, Vol. 2, Interscience Publishers, Inc., N. Y., 1955, p. 279.



47. Got, K., Bourrillon, R., and Cornillot, P., Biochim. Biophys. Acta 58, 126 (1962) .
48. Bezkorovainy, A., Biochemistry 2, 10 (1963) .
49. Burgi, W., and Schmid, K., J. Biol. Chem. 236, 1066 (1961) .
50. Brambell, F. W. R., Biol. Revs., Cambridge Phil. Soc. 33, 488 (1958) .
51. Jameson, E., Alvarez-Testado, C., and Sortor, H., Proc. Soc. Exptl. Biol. Med. 51, 163 (1942) .
52. Hansen, R. G., and Phillips, P. H., J. Biol.Chem. 171, 223 (1947) .
53. Pierce, A. E., J. Hyg. 53, 247 (1955) .
54. Kekwick, R. A., Advances in Protein Chemistry, Vol. 14, 1959 p. 231.
55. Pedersen, K. O., Nature 154, 575 (1944) .
56. Pedersen, K. O., Ultracentrifugal Studies on Serum, Upsala, 1945.
57. Pedersen, K. O., J. Phys. Colloid Chem. 51, 164 (1947) .
58. Deutsch, H. F., J. Biol. Chem. 208, 669 (1954) .
59. Klenk, E., and Stoffel, W., Z. physiol. chem., Hoppe-Seylers 302, 286 (1955) .
60. Meyers, W. M., and Deutsch, H. F., Archiv. Biochem. Biophys. 54, 38 (1955) .
61. Oudin, J., Methods in Medical Research 5, 335 (1952) .
62. Lieberman, I., Ove, P., Biochim. Biophys. Acta 25, 449 (1957) .
63. Fisher, H. W., Puck, T. T., and Sato, G., Proc. Natl. Acad. Sci., 44, 4 (1958) .





64. Parker, R. C., Methods of Tissue Culture, P. B. Hoeber, Inc. 1950, p. 173.
65. Lieberman, I., Lamy, F., Ove, P., Science 129, 43 (1959).
66. Spiro, R. G., J. Biol. Chem. 235, 2860 (1960).
67. Kay, C. M., and Marsh, M. M., Biochim. Biophys. Acta 33, 251 (1959).
68. Spiro, R. G., J. Biol. Chem. 237, 382 (1962).
69. Neuberger, A., Biochem. J. 32, 1435 (1938).
70. Spiro, R. G., J. Biol. Chem. 237, 646 (1962).
71. Spiro, R. G., J. Biol. Chem. 237, 1507 (1962).
72. Fisher, H. W., O'Brien, D., and Puck, T. T., Archiv. Biochem. Biophys., 99, 241 (1962).
73. Spiro, R. G., J. Biol. Chem. 238, 644 (1963).
74. Porter, R. R., Biochem. J. 46, 473 (1950).
75. Schmid, K., Biochim. Biophys. Acta 14, 437 (1954).
76. Burgi, W., and Schmid, K., J. Biol. Chem. 236, 1066 (1961).
77. Schmid, K., and Burgi, W., Biochim. Biophys. Acta 47, 440 (1961).
78. Marr, A. G. M., Owen, J. A., and Wilson, G. S., Biochim. Biophys. Acta 63, 276 (1962).
79. Turner, K. J., Biochim. Biophys. Acta 69, 518 (1963).
80. Urnes, P., and Doty, P., Advances in Protein Chemistry, Vol. 16, 1961, p. 425.
81. Banford, C. H., Elliott, A., and Hanby, W. E., Synthetic Polypeptide, Academic Press, Inc., N. Y., 1956.
82. Kendrew, J. C., et al., Nature 190, 666 (1961).



83. Perutz, M. F., et al., Nature 185, 416 (1960).
84. Ambroze, E. J., and Elliott, A., Proc. Royal Soc., A, 205, 47 (1951).
85. Low, B. R., and Edsall, J. T., in D. E. Green (Editor), Currents in Biochemical Research, Interscience Publishers, N. Y., 1956, p. 378.
86. Singer, S. J., Advances in Protein Chemistry, Vol. 17, 1962, p. 1.
87. Putnam, F. W., Plasma Proteins, Vol. 1, Academic Press, Inc., N. Y., 1960, pp. 309-341.
88. Urnes, P., and Doty, P., Advances in Protein Chemistry, Vol. 16, 1961, pp. 401-536.
89. Scheraga, H. A., and Mandelkern, L., J. Am. Chem. Soc. 75, 179 (1953).
90. Scheraga, H. A., Protein Structure, Academic Press, N. Y., 1961, Chapter I.
91. Simha, R., J. Phys. Chem. 44, 25 (1940).
92. Perrin, F., J. Phys. Radium [7], 7 (1936).
93. Schachman, H. K., and Lauffer, M. A., J. Am. Chem. Soc. 72, 4266 (1950).
94. Archibald, W. J., J. Phys. and Colloid Chem., 51, 1204 (1947).
95. Kraemer, E. O., in T. Svedberg and K. O. Pedersen (Editors), The Ultracentrifuge, Clarendon Press, Oxford, 1940.
96. Schachman, H. K., in S. P. Colowick and N. O. Kaplan (Editors), Methods in Enzymology, Vol. IV, [2], 1957, p. 38.





97. Schachman, H. K., Ultracentrifugation in Biochemistry, Academic Press, Inc., N. Y., 1959, Chapter VII.
98. Kauzmann, W., Quantum Chemistry, Academic Press. Inc., N. Y., 1957.
99. Yang, J. T., and Doty, P., J. Am. Chem. Soc. 19, 761 (1957).
100. Urnes, P. J., Imahori, K., and Doty, P., Proc. Natl. Acad. Sci. (U.S.), 47, 1155 (1961).
101. Urnes, P. J., and Doty, P., Advances in Protein Chemistry, Vol. 16, 1961, p. 466.
102. Schellman, J. A., and Schellman, C. G., J. Polymer Sci. XLIX, 129 (1961).
103. Brahms, J., and Kay, C. M., J. Biol. Chem. 238, 198 (1963).
104. Warren, L., J. Biol. Chem. 234, 1971 (1959).
105. Schachman, H. K., Ultracentrifugation in Biochemistry, Academic Press, Inc., N. Y., 1959, p. 75.
106. Schachman, H. K., Ultracentrifugation in Biochemistry, Academic Press, Inc., N. Y., 1959, p. 82.
107. Kay, C. M., Biochim. Biophys. Acta 38, 420 (1960).
108. Yang, J. T., Advances in Protein Chemistry, Vol. 16, 1961, p. 327.
109. Schachman, H. K., Methods in Enzymology, Vol. IV, 1957.
110. Edsall, J. T., in H. Neurath and K. Bailey (Editors), The Proteins, Vol. I, Pt. B, 1953, p. 624.
111. Harrington, W. F., Johnson, P., and Ottewill, R. H., Biochem. J. 62, 569 (1956).



## APPENDIX I

### Helical Content of Fetuin

Estimates of helical content of proteins may be made from computations based on the  $a_o$  and  $b_o$  parameters observed from the optical rotatory dispersion treatment for partial helical content expressed in Moffitt form. It follows from equation (19) as described in the Introduction of this report that helical content is equal to  $\frac{a_o^{obs} - a_o^D}{a_o^{H-D}}$  and to  $\frac{b_o^{obs}}{b_o^H}$ .

Provided reference values  $a_o^{H-D}$  and  $b_o^H$  may be assigned for the helix itself, an estimate of % helix may be made. On the basis of polyamino acid studies, values of these parameters have been obtained. These values are dependent on the value of  $\lambda_o$  chosen, and for a value of the latter = 212 m $\mu$ ,  $a_o^{H-D}$  is quoted as equal to +650 and  $b_o^H$  as equal to -630. Fetuin shows a considerable degree of disorder in the native state and it is not to be expected that estimates of helical content will be too accurate. For this reason, only approximate values of  $a_o^{H-D}$  and  $b_o^H$  corresponding to  $\lambda_o = 205$  m $\mu$  are chosen. These are taken as +600 and -700 respectively, and reflect the increased -ve slope and lower intercept associated with the choice of a lower value of  $\lambda_o$ . The value of  $a_o^D = -360$  for fetuin is taken as that value obtained for the molecule following the removal of sialic acid and which gives a  $b_o$  value essentially zero. It is to be noted that this value is not significantly different from that obtained for the



native molecule in 30% formamide.

An alternative method for estimates of helical content for molecules which give a linear plot by the Drude equation from values of  $\lambda_c$  may also be made. As before, the reference is taken from variations in  $\lambda_c$  calculated on the basis of partial helical content and a value of  $\lambda_c$  based on the disordered chain. From such considerations, it follows that up to about 40% helix, the % helix is given by the expression  $3/4 (\lambda_c^{\text{obs}} - \lambda_c^D)$ . In this case, the justification of the choice of  $\lambda_o = 205 \text{ m}\mu$  based on linearity in the Moffitt equation is supported by the value of  $206.5 \text{ m}\mu$  ( $\pm 2 \text{ m}\mu$ ) obtained from the Yang-Doty plot of the sialic acid free protein. Since the requirement that  $\lambda_o = \lambda_c^D$  as described in the Introduction, the figure of  $205 \text{ m}\mu$  will be used.

Inherent in the estimates of helical content is the assumption that helices of opposite sense and other conformations such as the  $\beta$  structure with its associated inter-chain hydrogen bonding is absent. General considerations based on molecular volume suggest that any appreciable content of helix would give a more compact hydrodynamic unit than that observed and the relatively high levo rotations of the native molecule suggest the absence of  $\beta$  structure. With these restrictions in mind, estimates of helical content will now be given, based on the three methods outlined above.





System (Colorado)	$\frac{a_o^{\text{obs}} + 360}{+600}$	$\frac{b_o^{\text{obs}}}{-700}$	$\frac{3}{4}(\lambda_c^{\text{obs}} - 205)$
in phosphate	$\frac{-253+360}{+600} = 17.8\%$	$\frac{-121}{-700} = 17.3\%$	$\frac{3}{4}(229-205) = 18\%$
in borate	$\frac{-288+360}{+600} = 12.0\%$	$\frac{-97}{-700} = 13.9\%$	$\frac{3}{4}(229-205) = 18\%$
in borate + CaAc <sub>2</sub>	$\frac{-326+360}{+600} = 5.7\%$	$\frac{-42}{-700} = 6.0\%$	$\frac{3}{4}(216-205) = 8.2\%$
in phosphate + 30% formamide	$\frac{-366+360}{+600} = 0\%$	$\frac{-36}{-700} = 5.1\%$	$\frac{3}{4}(212-205) = 5.3\%$
in phosphate + 25% dioxane	$\frac{-276+360}{+600} = 14\%$	$\frac{-93}{-700} = 13.3\%$	$\frac{3}{4}(222-205) = 12.8\%$
in phosphate + 35% ethylene glycol	$\frac{-274+360}{+600} = 14.3\%$	$\frac{-64}{-700} = 9.1\%$	$\frac{3}{4}(220-205) = 11.3\%$
sialic acid free in phosphate	0%	0%	0%

The agreement is regarded as satisfactory within the limits of experimental error. Further, that the values of % helix evaluated from  $a_o^{\text{obs}}$  and  $b_o^{\text{obs}}$  are in reasonable agreement supports the contention that if any  $\beta$  structure is present at all, there is little of it. This follows on the basis that the  $\beta$  structure would give decreased amounts of % helix as a result of a decreased slope but that in contributing a more positive rotation the % helix based on  $a_o^{\text{obs}}$  would give an increased value. It is tentatively suggested that this could provide a general basis of distinction between right-handed



$\alpha$  helix and  $\beta$  structure in aqueous media where infra red absorption techniques are limited by absorption bands of the water present. Difference between % helix calculated from the slope and intercept of the Moffitt plot would presumably be a measure of  $\beta$  structure.





## APPENDIX II

### Molecular Charge Carried by Fetuin in the Region of pH 7.0

An estimate of charge on the protein may be made from the measured mobility of the ethanol prepared material carried out in phosphate buffer pH 7, ionic strength 0.16, with 80% contributed by NaCl. A knowledge of the frictional coefficient is required and this is readily obtained from the results of hydrodynamic measurement.

$$\text{Mobility} = \frac{\frac{dx}{dt}}{\frac{dV}{dx}} = \frac{q}{f} = 5.16 \times 10^{-5} \text{ cm}^2/\text{volt}/\text{sec.}$$

For ethanol material in phosphate  $\beta$  value

$$\frac{f}{f_0} = 1 \quad \text{and} \quad \frac{[\eta]}{V} = \frac{N}{M} V_e = 2.66 \text{ mls./gm.}$$

from which it follows that the radius of the spherical hydrodynamic unit =  $3.6 \times 10^{-7}$  cms.

The frictional coefficient  $f = 6 \times \frac{22}{7} \times 10^{-2} \times 3.6 \times 10^{-7}$ ,

from which the charge  $q$  on the molecule is given by

$$q = 6 \times \frac{22}{7} \times 10^{-2} \times 3.6 \times 10^{-7} \times \frac{5.16 \times 300}{4.8 \times 10^{-10}} \times 10^{-5} \simeq 2.5.$$

It is of interest to recall that a value for apparent molecular weight obtained in a solution of low ionic strength gave a value of 22,170.

From the relation  $\frac{M}{n+1} = M_{\text{obs}} = 22,170$ , the resultant charge on the molecule would be unity. It is likely that sufficient salt was left after dialysis to partially negate the molecular charge.



Consideration of the composition of the molecule supports the view that there would not be a high charge contributed by primary structure in this pH region. The contribution of arginine, lysine, histidine and  $\alpha$  amino would be +44. The contribution by charged glutamic and aspartic residues,  $\alpha$  carboxyl and sialic acid would be -68. However, for a molecular weight of 44,400, the analysis, according to Spiro, shows an amide content of 22 residues. This would reduce the -ve charge to -46. The residual charge would then be -2. This rather suggests at pH 7 and close to it the molecule does not exhibit strong anion binding properties or at least has little affinity for phosphate and chloride ions. This is not in keeping with the difference in isoelectric and iso-ionic points reported by Spiro and attributable to anion binding in the region where fetuin shows associative properties.















**B29814**